2038-5625

Italian Journal of Agrometeorology

Rivista Italiana di Agrometeorologia

n. 1 – 2022

FIRENZE UNIVERSITY PRESS

Cover photo by Graziano Lampa

Italian Journal of Agrometeorology

n. 1 - 2022

Firenze University Press

The ***Italian Journal of Agrometeorology*** (***IJAm - Rivista Italiana di Agrometeorologia***) is the official periodical of the Italian Association of Agrometeorology (AIAM) and aims to publish original scientific contributions in English on agrometerology, as a science that studies the interactions of hydrological and meteorological factors with the agricultural and forest ecosystems, and with agriculture in its broadest sense (including livestock and fisheries).

SUBSCRIPTION INFORMATION
IJAm articles are freely available online, but print editions are available to paying subscribers. Subscription rates are in Eur and are applicable worldwide.
Annual Subscription: € 50,00 Single Issue: € 25,00

CONTACT INFORMATION
Please contact ordini@fupress.com, if you have any questions about your subscription or if you would like to place an order for the print edition. Information on payment methods will be provided after your initial correspondence.

Published by
Firenze University Press – University of Florence, Italy
Via Cittadella, 7 - 50144 Florence - Italy
http://www.fupress.com/ijam

Italian Journal of Agrometeorology
Rivista Italiana di Agrometeorologia

Firenze University Press
www.fupress.com/ijam

Citation: J. Chmist-Sikorska, M. Kępińska-Kasprzak, P. Struzik (2022) Agricultural drought assessment on the base of Hydro-thermal Coefficient of Selyaninov in Poland. *Italian Journal of Agrometeorology* (1): 3-12. doi: 10.36253/ijam-1530

Received: December 22, 2021

Accepted: April 16, 2022

Published: July 19, 2022

Data Availability Statement: All relevant data are within the paper and its Supporting Information files.

Competing Interests: The Author(s) declare(s) no conflict of interest.

ORCID:
JC-S: 0000-0003-1612-4940
MK-K: 0000-0002-9420-4690
PS: 0000-0002-3542-4028

Agricultural drought assessment on the base of Hydro-thermal Coefficient of Selyaninov in Poland

Joanna Chmist-Sikorska*, Małgorzata Kępińska-Kasprzak, Piotr Struzik

Institute of Meteorology and Water Management, Poznań-Kraków, Poland
*Corresponding author: Joanna.Chmist-Sikorska@imgw.pl

Abstract. Climate change on the globe has been manifested over the past few decades by, among other things, an increase in the frequency of extreme weather events, such as droughts. Drought affects millions of people around the world every year. Its effects usually appear after a long period of rainfall deficit. Based on climate projections, it is emphasized that water scarcity will be one of the most important problems in the future. Due to the importance of the increasing problem of drought, the analysis of this phenomenon in Poland was undertaken in the context of agriculture. The aim of this study was to assess the course of drought in the vegetation period during years 2001-2020 for Poland based on the Selyaninov's coefficient (HTC). As shown in this study, the western and central parts of the country, dominated by arable land, are particularly vulnerable to drought. Due to the cyclic nature of periods classified by HTC as dry, it can be concluded that the problem of precipitation deficit for crops in Poland could get worse.

Keywords: climate change, drought index, growing season, yields.

INTRODUCTION

Climate change on the globe has been highlighted for several decades by, among other things, an increase in the frequency of extreme weather events, such as droughts (Kociper *et al.,* 2019; IPCC, 2021). According to research published in the United in Science 2021 report, the period from 2014 to 2020 was the warmest in the history of measurements (Christensen *et al.,* 2021). The alarming reports have increased interest in the topic of water scarcity among many researchers, including climatologists, hydrologists, and agrometeorologists. Kadbhane and Manekar (2021) and Kociper *et al.* (2019), among others, pointed out the problem that agriculture is much more impacted by climate change than any other sector, because agricultural production is highly dependent on weather. Additionally, Yeşilköy and Şaylan (2000) emphasize that water scarcity will be one of the most important problems in the future, especially due to fact that agricultural activities consume almost 70% of global water resources. Problem of droughts and water scarcity con-

cerns many countries, regardless of geographic location (Communication..., 2007). Falzoi *et al.* (2019) additionally point to the global links between the occurrence of drought in one region and the price of consumer goods in another. For example, in 2012 an increase in food price was caused by a simultaneous drought in USA and Russia. Additionally, extreme hot and dry periods in recent years, have occurred not only in summer, but also in early fall and winter. Hanel *et al.* (2018) point out that air temperatures over Europe during the autumn of 2006 and winter of 2007, were ranked as the warmest in the last 500 years. In their publication, Vlăduţ *et al.* (2017) emphasized that precipitation in Southern Europe, including Romania and Bulgaria, will decrease of about 10-20% for the 2081–2100 period, in relation to 1986-2005. Moreover, Ionita and Nagavciuc (2021) based on the analysis of the standardized precipitation index (SPI) trends from 1902-2019 showed that SPI exhibits negative, statistically significant trends (increasing drought frequency) over Central Europe region (e.g., the Czech Republic, Slovakia, Hungary, Belarus, and Poland) and over South Europe, as well as Mediterranean region (e.g., Italy, southern Spain, Albania, and Greece). The positive trend (increased frequency of wet periods) was observed only over North Europe.

Hari *et al.* (2020) further suggest in their work, that the recent Arctic warming is possibly the main factor behind more frequent extreme weather events in mid-latitude regions of the northern hemisphere. The main dynamic characteristics of the mid-latitude weather change due to arctic amplification are the position and structure of the jet stream and the activity of planetary waves. Nevertheless, studies by Barnes and Polvani (2015) indicate that the reaction of the atmospheric circulation is still largely misunderstood. Additionally, in their work, the authors indicated that the 27 state-of-the-art climate models analysed by them, often do not even agree as to the sign of the answer. Therefore, there is still great uncertainty about the correctness of these assumptions. Addressing the mechanism of the drought phenomenon itself in 2001–2020, in Poland, is a line of research that requires a comprehensive analysis and goes beyond the scope of this study.

A drought is a weather and climate-related phenomenon of complex nature. Due to that, drought usually evolves slowly but can last for months or years and its effects occur after long periods without precipitation. Therefore, it is difficult to objectively quantify its characteristics in terms of amplitude, intensity, duration, as well as spatial extent. Its complexity is reflected in the lack of a unique definition (Spinoni *et al.,* 2018). Therefore, quantification of its characteristic is difficult. However, according to Falzoi *et al.* (2019) a drought can alternatively be defined as a temporary, recurring reduction in the precipitation in an area. Despite the difficulty of quantifying its always depends on: 1) a reference (e.g., the climatic normal) and 2) on the specific vulnerability of chosen sector to drought (an agricultural sector, an economy sector etc.). Therefore, drought is classified into four general types: meteorological, agricultural, hydrological, and socioeconomic drought (Hisdal *et al.,* 1999; Spinoni *et al.,* 2018). Further complexity is difficulty with delimitation of the exact date of the beginning and the end of drought. As mentioned above, its time span varies from weeks to years, with different intensity and sensitivity to drought of the various sectors of economy. However, undoubtedly the most sensitive is agriculture where this phenomenon causes substantial reduction of crop yield. Observed climate change and variability increases the risk of serious losses in economy, especially in the countries where the agricultural production constitutes important part of income. Based on climate projections its emphasized that water scarcity, which induces drought, will be one of the most important problems in the future (Yeşilköy and Şaylan, 2020).

In the case of Poland, apart from the ongoing climate change, the high variability of its individual elements, such as air temperature and precipitation, is also influenced by the moderate nature of the climate, with both maritime and continental elements. However, in case of Poland also the orography plays a big role for the spatial extent of droughts. The northern part of the country is situated on the Baltic Sea. Therefore, the coastal areas are characterized by higher humidity. Additionally, the southern part of the country is a mountainous region with a higher precipitation than other parts of the country. The central part of the country is most vulnerable to droughts (Pińskwar *et al.,* 2020). The worse situation is observed in central-west part of Poland, especially during the growing seasons (Łabędzki, 2007; Łabędzki and Kanecka-Geszke, 2009; Mager and Kępińska-Kasprzak, 2010; Szwed, 2015). The summer water deficit and frequency of droughts is expected to increase in the future, mainly because observed increase of evapotranspiration (Bogawski and Bednorz, 2016; Pascolini-Campbell *et al.,* 2021). Moreover, the large areas of Poland are characterized by soils derived from sands, loamy sands, boulder sands as well as loose sands of different origin, which are characterized by low water holding capacity. The negative impact of droughts in agriculture will be intensified by limitation of irrigation capacity during hydrological drought, caused by rainfall deficit (Kępińska-Kasprzak and Mager, 2010).

Issues related to water scarcity have been repeatedly addressed by Polish scientists (Szyga-Pluta, 2018; Struzik *et al.,* 2016; Toulios *et al.,* 2016; Szwed *et al.,* 2010; Łabędzki, 2007; Skowera and Puła, 2004), however, due to the importance and the growing problem of drought, an analysis of this phenomenon in Poland, in the context of agriculture, was undertaken in our study. There are several methods to identify the drought phenomenon depending on the type of drought, nevertheless in this study the attention was focused on the Hydro-thermal Coefficient of Selyaninov. Its advantage is simplicity of calculation and possibility of both monthly and decadal applications. It is particularly valuable for evaluating current crop conditions and monitoring of the agricultural drought (Bokwa *et al.,* 2021). The aim of this study was to assess the course of drought in the growing periods, during years 2001-2020, for the area of Poland based on the Selyaninov's coefficient.

MATERIALS AND METHODS

This study uses data from 2001-2020 on monthly precipitation totals and monthly mean temperature values measured at two meters by 56 synoptic stations of Institute of Meteorology and Water Management – National Research Institute (IMGW-PIB), distributed throughout the country (Fig. 1). These data were used to calculate the Hydro-thermal Coefficient of Selyaninov (HTC) according to the formula (Taparauskiene and Miseckaite, 2017; Evarte-Bundere and Evarts-Bunders, 2012):

$$HTC = \frac{\sum P_{>10^{\circ}C}}{0{,}1 * \sum T_{>10^{\circ}C}}$$

where:
Σ P>10 °C - decadal/monthly sum of precipitation (calculated from periods with daily average temperature above 10 °C),
Σ T>10 °C - decadal/monthly sum of daily average air temperature (calculated from periods with daily average temperature above 10 °C).

The Selyaninov's coefficient can be calculated for periods, when the average daily temperature exceeds +10°C. In Poland, analyses of agrometeorological indices are performed during growing season, defined usually as summer season (April 1st – September 30th) and such period for analysis is applied in this article. The authors are aware of the possibility of the occurrence of cooler periods in April, however they occur much less frequently with the progressive warming of the climate. In Polish literature, due to the inclusion of April into the vegetation period, also for this month the Selyaninov's coefficient is used as a measure for assessment of the moisture deficiency in relation to cultivated plants. However, in this study, in the case of extremely low temperature (below or close to zero), such information was excluded from the analysis due to the possibility of falsification of the results.

In this paper, according to the commonly accepted classification, a division into 10 classes of the Selyaninov's coefficient was used, allowing isolation of the extreme conditions. Values of HTC as follow: extremely dry HTC <0.4, very dry HTC in range <0.4÷0.8), dry HTC in range <0.8÷1.1), quite dry HTC in range <1.1÷1.4), optimum HTC in range <1.4÷1.7), quite humid HTC <1.7÷2.1), humid HTC <2.1÷2.6), very humid HTC in range <2.6÷3.0), extremely humid HTC >3.0. The attention was focused on periods when the value of the index does not exceed 1.1. Such limit is important, because it corresponds to the minimum amount of precipitation needed for the development of selected crops (Kuś, 2016). Thus, the dry period is a potential threat to crops development and to yields reduction.

Both spatial and quantitative range of occurrence, of periods classified as dry, in April, May, June, July, August and September, which corresponds approximately to the vegetation season in Poland, was analysed. Particular attention was paid to the years, in which at least half of the analysed synoptic stations measurements indicate dry period, according to the Selyaninov's coefficient.

RESULTS

The hydrothermal Selyaninov's coefficient values shown in the maps, calculated for the growing season (2001-2020), indicate areas particularly vulnerable to crop water shortages (Fig. 2). The most drought-prone area in April was the western part of the country. The problem of precipitation deficit affected mainly Lubuskie, Wielkopolskie, Kujawsko-Pomorskie and the northern part of Dolnośląskie provinces. According to average HTC values, quite dry period concerned almost whole Poland, excluding north-eastern and southern part of the country. It is worth noting, that April is a month particularly important in agriculture, due to intensive development of crops. The highest variability of HTC values was observed in May. The areas most exposed to drought were north-western part of the country and small part of north-eastern Poland (Podlaskie province). During May, based on the Selyaninov's coefficient,

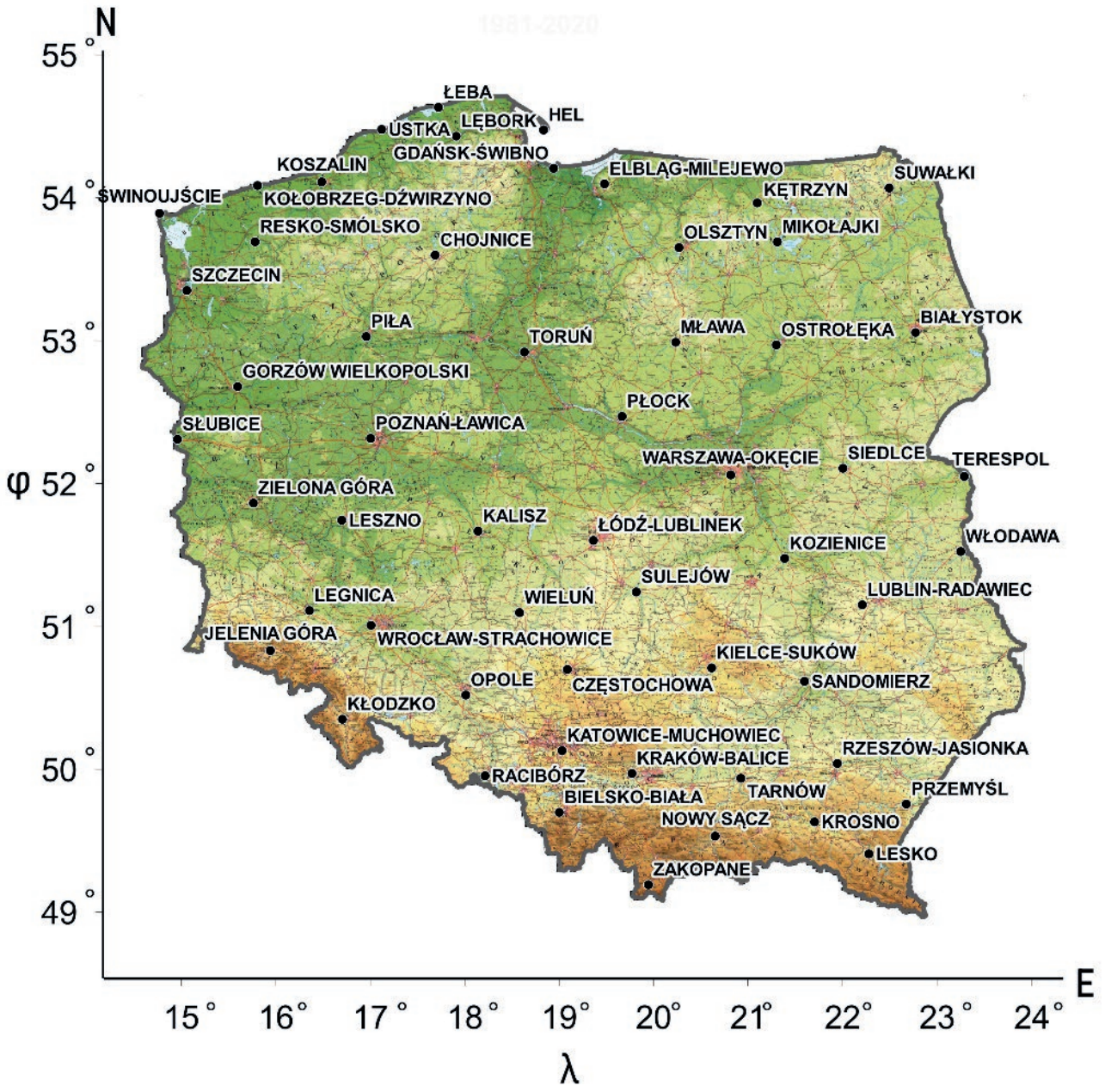

Fig. 1. Location of selected synoptic stations of IMGW-PIB.

hydrothermal conditions in the whole country were classified as humid. Extreme (extremely wet) conditions occurred especially in the northern and southern part of the country, as a direct result of orography. Increased precipitation in May improves soil moisture conditions, but their excessive amount combined with insufficient evapotranspiration and low temperatures (e.g. ground frost) may lead to the development of many fungal diseases among plants. June was another month with rather dry and barren conditions in most areas of Poland. Lack of precipitation affected mainly the western part of the country: Lubuskie and Wielkopolskie provinces. Water surpluses appeared only in the mountain areas (south Poland). In July optimal conditions prevailed, but through the centre of the country, a belt of rather dry conditions was observed. August was the month in which water deficits occurred in most parts of the country. Optimal conditions prevail only near the coast

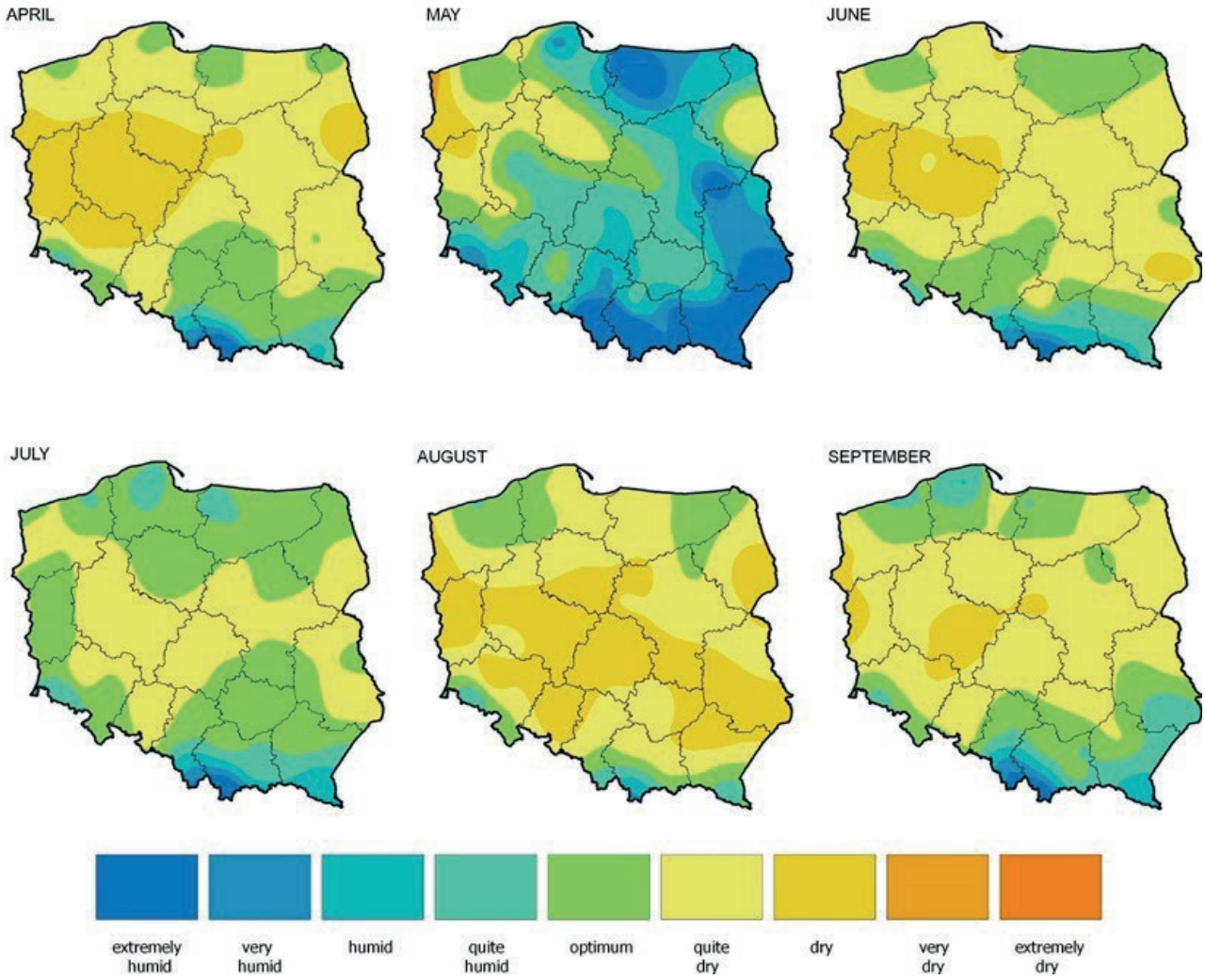

Fig. 2. Mean monthly values of HTC in Poland (2001-2020). The areas marked on the map are the province borders.

and in some mountainous areas. A similar situation occurred in September, where dry conditions prevailed in the most of central part of the country, while optimal and wet conditions prevailed in the north and south.

Due to the fact, that in Poland the north-west and west circulation is dominating, wet air masses pill up from the seaside over the windward slopes of Pomerania and Masurian Lake District on the north and over the north slopes of the mountains in the South Poland. At these places, the water vapour condenses, which cause clouds vertical development and rainfall, whereas the lowlands in central part of the country lay in the rain shadow. As a result, those mountainous and coastal areas are characterized by a higher frequency and amount of precipitation and a lower value of the potential evapotranspiration index (Fig. 3).

Described above conclusions on the areas, where low and very low values of HTC are noticed most frequently are also confirmed by the spatial distribution of Precipitation–Evapotranspiration Index (PEI) during growing season (April-September), calculated from years 2001-2020 (Fig. 3). PEI shows that the low and very low values occur in central and central-west part of the country. Totals of precipitation in the warm part of the year (April-September) are the lowest here, in comparison with other regions of the country, and the potential evapotranspiration is higher and exceeds precipitation. The spatial distribution of the greatest water shortages is quite unfavourable from the point of agriculture, because a major part of Polish agricultural potential is concentrated in those regions.

The HTC values for months and years in 2001-2020 period was presented in the form of graphs (Fig. 4). The

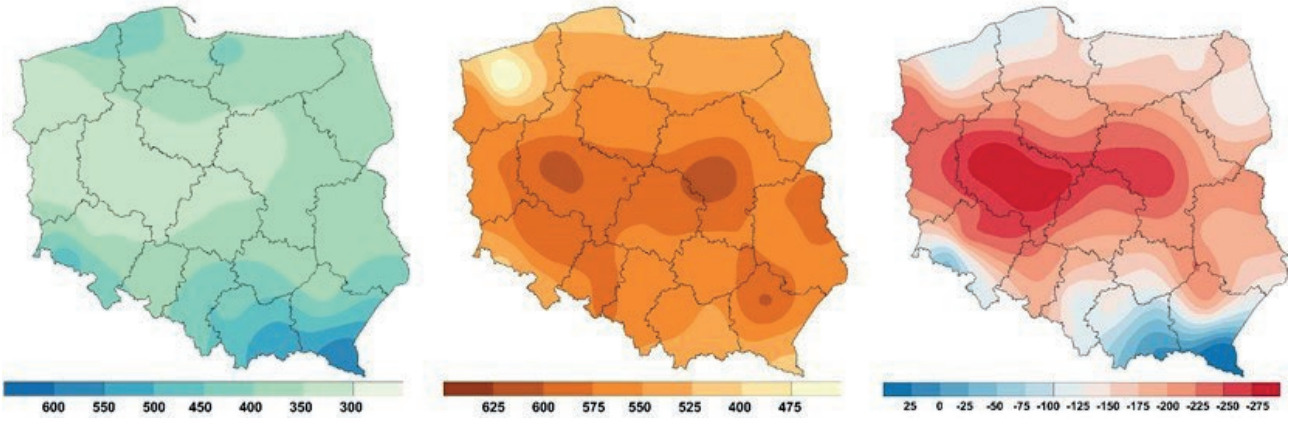

Fig. 3. Spatial distribution [in mm] of the average sums of precipitation, potential evapotranspiration and Precipitation-Evapotranspiration Index in Poland during growing season (April-September) in years 2001-2020.

thermometer mark has been placed on those years, in which at least half of analysed synoptic stations indicated minimum one of these categories the values of HTC as follow: extremely dry HTC <0.4, very dry HTC in range <0.4÷0.8) or dry HTC in range <0.8÷1.1). For the analysed multi-annual period, in April, the situation of possible water shortages occurred in nine years, twice of it occurred in the years 2009-2011 and 2018-2020. In the case of May, the dry index for at least 50% of the stations occurred in six years, among them continuously from 2016 to 2018. In June, a similar situation occurred in 10 years, of which in four cases the problem occurred year after year (2005-2006, 2010-2011, 2015-2016, 2018-2019). In July, as in May, the problem of water shortages affected six years, of which occurred in 2013-2015 and 2019 and 2020. The worst situation was in August, where the problems of water shortages appeared for five consecutive years in a row (2015-2019). Moreover, the dry period recorded by at least 50% of synoptic stations, was found 12 times in August. In September, the problem of precipitation scarcity affected 10 years, of which four years of dry periods in a row occurred from 2003 to 2006.

DISCUSSION

Based on the HTC, it has been shown that the problem of precipitation deficit leading to potential drought stress for crops, occurs during almost the entire growing season. Extremely dry periods covering the whole country occurred mainly in April, but their intensification in recent years is also seen in other months. Studies conducted by Szyga-Pluta (2018) indicated that extremely dry periods occur mainly in August and September. However, the author analysed a much longer period (1966-2015). Importantly, in the case of the very dry period, the results of the present study confirm those obtained by Szyga-Pluta. The very dry index occurs most frequently in September and August. Bartczak *et al.* (2014) found that a characteristic feature is the clustering of dry periods into periods of several or more years, which was also confirmed in the present study. In most cases, especially in the last years of the analysed 20-year period, dry months occurred cyclically.

Considering the water requirements of crops, the problem of water scarcity seems to be getting worse. Since 2011, the number of months characterized by precipitation scarcity has been increasing. At the very beginning of the twentieth century, dry months did not occur very often in succession. The last years of analysis show whole sequences of months, considered as dry according to HTC. Moreover, research conducted by Diakowska *et al.* (2018) indicated that in the near future, the highest probability of drought will occur in central part of Poland. This analysis indicates that the existing water problems in central Poland will get worse. It is important because this region is characterized by the largest share of agricultural land.

A study by Hari *et al.* (2020) found that Europe was affected by drought three times between 2001 and 2020. The first time, such a large-scale event occurred in 2003. This problem has been extensively discussed, among others, in the publication by Rebetez *et al.* (2006). The authors showed that the monthly mean temperature deviations of August 2003 reached +6°C at many meteorological stations in southwestern Germany, eastern France and western Switzerland. Also in our analysis, August 2003 was classified as very dry at more than 70% of synoptic stations. July was less extreme than

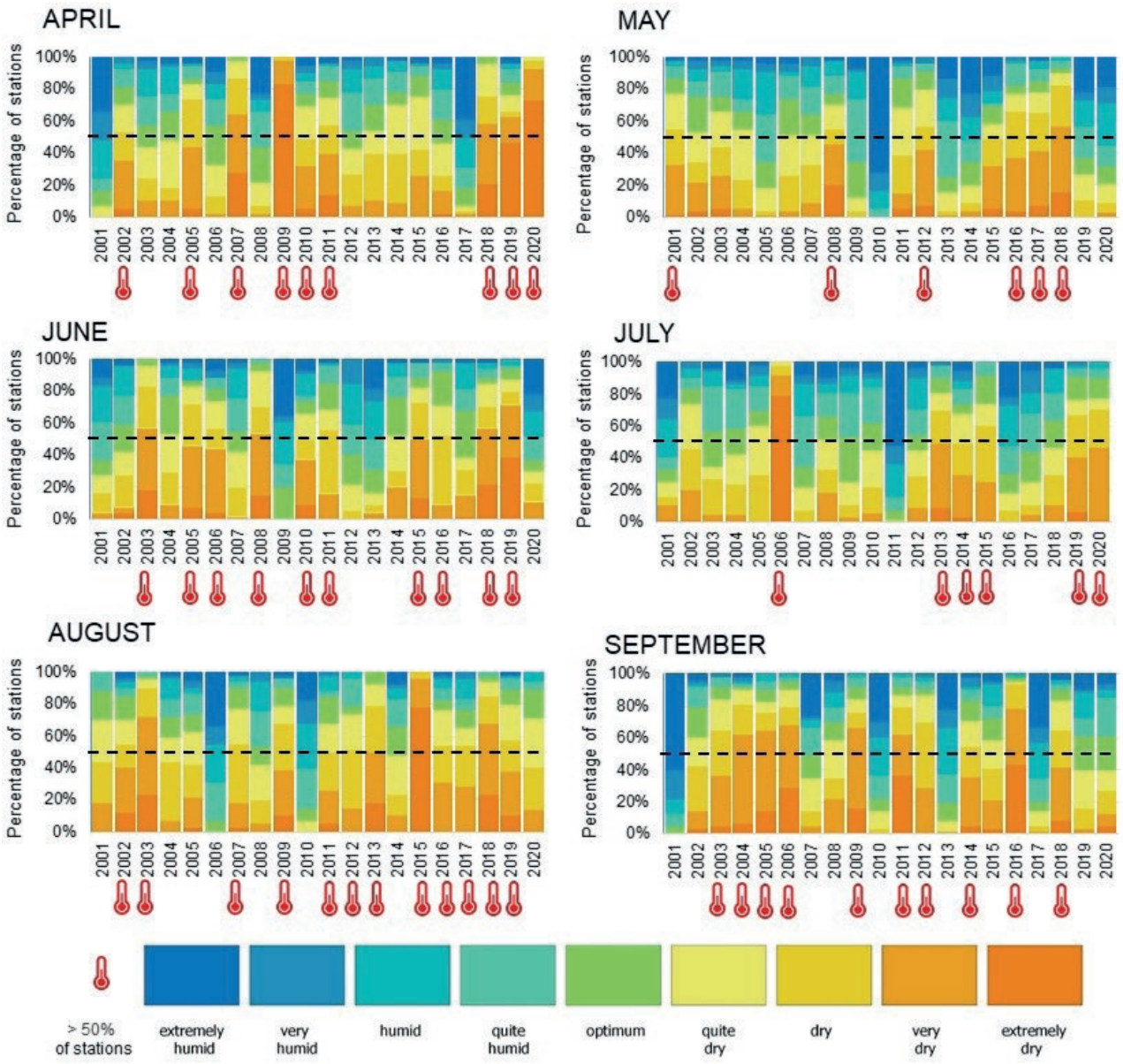

Fig. 4 Mean monthly values of HTC in Poland (2001-2020).

June and August, except in Sweden, Finland and Norway, which is also evident in our study. For 2003, from May to August, monthly minimum and maximum air temperatures were consistently above normal from Portugal to Hungary and from Great-Britain and Denmark to Sicily and Greece. In contrast, virtually all of Europe struggled with heat in 2018. Based on Hari *et al.* (2020), temperature anomalies were +2°C and precipitation anomalies showed a deficit of over 20%. Also in our study, it was shown that drought occurred in Poland for almost the entire growing season in 2018. In addition, Hari *et al.* (2020) using multi-year observations, showed that the occurrence of a summer (consecutive) drought in 2019 was unprecedented in the last 250 years. However, Ionita *et al.* (2021) have shown that the droughts, which occurred in 2003, 2018 as well as 2019 are within the historical variability and they are not unprecedented over the last millennium. Nevertheless, the combined impact of both the 2018 and 2019 droughts on vegetation activity was stronger in comparison to the 2003 European drought. Thus, determining future drought risk of in our region, droughts seem to be a key issue for many

researchers, including climatologists, hydrologists, and agrometeorologists.

Widely reported climate change is highlighted by the increasing likelihood of extreme events, including both droughts and heavy rainfalls. Based on Nikolaev (2020), the excessive rainfall in Russia causes 10 to 15% greater yield losses than rainfall deficiency in extremely dry years. Frequent occurrence of heavy rainfall in autumn makes harvesting difficult or completely impossible. Additionally, the excessive precipitation creates unsuitable conditions for winter crops. According to the climate change scenarios for East part of Europe, the further increase in annual precipitation totals, as well as annual air temperature is predicted (Nikolaev, 2020). However, predictive analyses by Hari *et al.* (2020) showed, that anthropogenic warming will lead to an intensification of droughts in Europe. Thus, the probability of biennial droughts may increase significantly. The authors highlight that such events have significant implications for many sectors, including impacts on agrophenology, crop water demand, and vegetation health activities. Nevertheless, the authors showed that the occurrence of subsequent droughts, as well as their impact on crops and pastures, can be significantly reduced if mitigation strategies are adopted that lead to changes in global warming. These observations seem to confirm the study by Ionita and Nagavciuc (2021). Authors showed that most of the countries in South Europe and Mediterranean region, as well as Central Europe show a significant trend of increasing drought frequency in the last 120 years, while countries of Northern Europe show a significant trend of increasing the frequency of wet periods. Therefore, water shortages as well as surpluses could be even more common and more severe in the future (Szwed, 2010; Ziernicka-Wojtaszek and Kopcińska, 2020).

Year by year, agriculture in Poland is becoming more and more heavily affected by climate change. Natural disasters, such as drought, are becoming more frequent and thus decrease the crop production. It seems to be necessary to improve knowledge on climate and weather, as well as to draw up plans to both identify and mitigate risk in agriculture.

CONCLUSIONS

Based on analyses of spatial and temporal distribution of Selyaninov's coefficient (HTC) for Poland in years 2001-2020, it has been found, that droughts have been noticed already in April, i.e., from the beginning of the vegetation season, at the most parts of the country. The biggest area of the country covered by dry conditions was noticed in August and September, while the smallest - in May. May was also a month, with the highest variability of HTC values in vegetation seasons of analyzed period. In July, optimal conditions prevailed in the North and South Poland, but the quite dry conditions were dominating in the belt over the center of the country.

The drought-prone area for the most of vegetation seasons of 2001-2020 was the belt of lowlands, from western to eastern border of Poland, but most often the lowest values of Selyaninov's coefficient in the western part of this area were noticed. From the economical point of view, it is unfavorable, because most of the agricultural lands are located in this area.

As this study shows, the three most dry HTC categories occur cyclically over the past two decades. Water shortages could be even more common and more severe in the future. Additionally, since 2011, the number of months characterized by precipitation scarcity has been increasing. At the very beginning of the twentieth century, dry months did not occur very often in succession, but last years of analysis show the whole sequences of months, considered as dry according to HTC. Therefore, it can be concluded that the problem of precipitation deficiency for crops in Poland could get worse.

Year by year, agriculture in Poland is becoming more heavily affected by climate change. Natural disasters, such as droughts, are becoming more frequent and thus decrease the crop production. It seems to be necessary to improve knowledge on climate and weather, as well as to draw up plans to both identify and mitigate risk in agriculture.

As shown in a study by Ionita *et al.* (2021) the occurrence of drought, year by year has much more severe effects on crops than a single event such as the drought in 2003. The results presented in this article let us believe that in the nearest future the amount of water available for plants during growing season in central Poland, may decrease even more. Published by Eitzinger *et al.* (2012) analyses, emphasize that crops, especially in the warm and dry lowland regions, will need more water to maintain their production potential. However, the similar situation may also occur in the areas like Polish lowlands, where increasingly frequent droughts are a serious problem for agriculture. Recommendation given by Eitzinger *et al.* (2012), e.g. need of efficient management of water resources used for irrigation and improved efficiency of irrigation methods, are especially necessary in the areas like Poland, where resources of surface water per capita are very low.

Due to the growing threat of negative effects of droughts, especially on agriculture, monitoring of this

phenomenon is particularly important. Among other indicators, it seems that the Selianinov's coefficient can be used for such monitoring. HTC integrates the main factors of drought: temperature and precipitation and therefore it is a useful tool in agriculture practice. The HTC is easy to calculate and is based on commonly, publicly available data. In this study were used monthly period for analyses, but HTC, in contrary to other coefficients, gives possibility to calculate for also decadal periods, important in farmers activity.

However, the indicator also has limitations. First of all, the the HTC should be calculated for periods with average daily air temperature higher than 10°C. In Polish conditions, the average values of air temperature in April are sometimes lower, so especially in mountain regions the result can be distorted by periodically occurring temperatures below zero degree Celsius. Moreover, it does not consider the water and soil balance. Therefore, this index should be interpreted with caution and in relation to other agrometeorological indices. Nevertheless, despite these limitations, the HTC can be useful for tracking the extent to which crop water needs are being met in a given area.

REFERENCES:

Barnes E. A., Polvani L. M., 2015. CMIP5 projections of Arctic amplification, of the North American/North Atlantic circulation, and of their relationship. Journal of Climate, 28(13): 5254-5271. doi: 10.1175/JCLI-D-14-00589.1.

Bartczak A., Glazik R., Tyszkowski S., 2014. Identyfikacja i ocena intensywności okresów suchych we wschodniej części Kujaw. Nauka Przyroda Technologie, 8 (4), #46. (in Polish).

Bogawski P., Bednorz E., 2016. Atmospheric conditions controlling extreme summertime evapotranspiration in Poland (central Europe). Natural Hazards, 81(1): 55-69. doi: 10.1007/s11069-015-2066-2.

Bokwa A., Klimek M., Krzaklewski P., Kukułka W., 2021. Drought Trends in the Polish Carpathian Mts. in the Years 1991–2020. Atmosphere, 12(10): 1259.

Christensen J., Kennedy J. J., Olhoff A., Liu J., Baddour O., Kappelle M.,, 2021. United In Science 2021: A multi-organization high-level compilation of the latest climate science information. doi:10.13140/RG.2.2.11238.14402.

Communication from the Commission to the European Parliament and the Council. Addressing the challenge of water scarcity and droughts in the European Union; Brussels, 18.7.2007. {COM(2007) 414 final}.

Diakowska E., Stanek P., Iwański S., Gąsiorek E., 2018. Estimation of the occurrence of drought in Poland by 2060 based on the HTC index and probability distributions. In ITM Web of Conferences (Vol. 23, p. 00006). EDP Sciences.

Eitzinger J., Trnka M., Semerádová D., Thaler S., Svobodová E., Hlavinka P., Šiška B., Takáč J., Malayinská, L., Nováková M., Dubrovský M., Žalud Z., 2012. Regional climate change impacts on agricultural crop production in Central and Eastern Europe – hotspots, regional differences and common trends. The Journal of Agricultural Science. Available on CJO doi:10.1017/S0021859612000767.

Evarte-Bundere G., Evarts-Bunders P., 2012. Using of the Hydrothermal coefficient (HTC) for interpretation of distribution of non-native tree species in Latvia on example of cultivated species of genus Tilia. Acta Biol. Univ. Daugavp., 12 (2): 135–148.

Falzoi S., Acquaotta F., Pulina M.A., Fratianni S., 2019. Hydrological drought analysis in Continental Temperate and Mediterranean environment during the period 1981-2017. Italian Journal of Agrometeorology (3): 13-23. doi: 10.13128/ijam-798.

Hanel M., Rakovec O., Markonis Y., Máca P., Samaniego L., Kyselý J., Kumar, R., 2018. Revisiting the recent European droughts from a long-term perspective. Scientific reports, 8(1): 1-11.

Hari V., Rakovec O., Markonis Y., Hanel M., Kumar R., 2020. Scientific reports, 10(1): 1-10. doi: 10.1038/s41598-020-68872-9.

Hisdal H., Tallaksen L. M., Demuth S., van Lanen H. A. J., Peters E., Stahl H., 1999. Drought Event Definition. Assessment of the Regional Assessment Impacts of Droughts in Europe (ARIDE). 19 pp.

Ionita M., Nagavciuc V., 2021. Changes in drought features at the European level over the last 120 years. Natural Hazards and Earth System Sciences, 21(5): 1685-1701. doi: 10.5194/nhess-21-1685-2021.

Ionita M., Dima M., Nagavciuc V., Scholz P., Lohmann G., 2021. Past megadroughts in central Europe were longer, more severe and less warm than modern droughts. Communications Earth & Environment, 2(1): 1-9. doi: 10.1038/s43247-021-00130-w.

IPCC, 2021. Summary for Policymakers. In: Climate Change 2021: The Physical Science Basis. Contribution of Working Group I to the Sixth Assessment Report of the Intergovernmental Panel on Climate Change [Masson-Delmotte, V., P. Zhai, A. Pirani, S.L. Connors, C. Péan, S. Berger, N. Caud, Y. Chen, L. Goldfarb, M.I. Gomis, M. Huang, K. Leitzell, E. Lonnoy, J.B.R. Matthews, T.K. Maycock, T. Waterfield, O. Yelekçi, R. Yu, and B. Zhou (eds.)]. In Press.

Kadbhane S.J., Manekar V.L., 2021. Development of agro-climatic grape yield model with future prospective. Italian Journal of Agrometeorology (1): 89-103. doi: 10.36253/ijam-406.

Kępińska-Kasprzak M., Mager P., 2010. Changes of selected climate elements and their impact on agricultural production in central-west Poland. Meteorological Journal, XIII, No 1: 3-8, Slovakia.

Kociper D., Vintar Mally K., Kajfež Bogataj L., 2019. Climate vulnerability of agriculture in statistical regions of Slovenia. Italian Journal of Agrometeorology (2): 35-48. doi: 10.13128/ijam-651.

Kuś J., 2016. Gospodarowanie wodą w rolnictwie. Studia i Raporty IUNG-PIB 47(1): 83-104. doi: 10.26114/sir.iung.2016.47.05. (in Polish).

Łabędzki L., 2007. Estimation of local drought frequency in Central Poland using the Standarized Precipitation Index SPI. Irrig. and Drain. 56: 67–77. doi: 10.1002/ird.285.

Łabędzki L., Kanecka-Geszke E., 2009. Standardized evapotranspiration as an agricultural drought index. Irrigation and Drainage. Vol. 58, Issue 5: 607-616. doi.org/10.1002/ird.421.

Mager P., Kępińska-Kasprzak M., 2010. Variability of selected climatic indices during vegetation period in Wielkopolska. Acta Agrophisica, 183: 9-21.

Nikolaev M. V., 2020. Integrated assessment of change in contribution of excessive moisture to farming risks in the humid zone of Western Russia. Meteorology Hydrology and Water Management. Research and Operational Applications, 8(1): 46-53. doi:10.26491/mhwm/111543.

Pascolini-Campbell M., Reager J.T., Chandanpurkar H.A., Rodell M., 2021. A 10 per cent increase in global land evapotranspiration from 2003 to 2019. Nature 593: 543–547. doi.org/10.1038/s41586-021-03503-5.

Pińskwar I., Choryński A., Kundzewicz Z.W., 2020. Severe Drought in the Spring of 2020 in Poland—More of the Same? Agronomy 2020, 10: 1646. doi:10.3390/agronomy10111646

Rebetez M., Mayer H., Dupont O., Schindler D., Gartner K., Kropp J. P., Menzel A., 2006. Heat and drought 2003 in Europe: a climate synthesis. Annals of Forest Science, 63(6): 569-577.

Skowera B., Puła J., 2004. Skrajne warunki pluwiotermiczne w okresie wiosennym na obszarze Polski w latach 1971-2000. Acta Agrophysica, 3(1): 171-177. (in Polish).

Spinoni J., Vogt J. V., Naumann G., Barbosa P., Dosio A., 2018. Will drought events become more frequent and severe in Europe? International Journal of Climatology, 38(4): 1718-1736. doi: 10.1002/joc.5291.

Struzik P., Kępińska-Kasprzak M., 2016. Use of conventional and satellite data for estimation of evapotranspiration spatial and temporal pattern. Meteorology, Hydrology and Water Management, Research and Operational Applications, 4(2): 3-13. doi:10.26491/mhwm/63543.

Struzik P., Kępińska-Kasprzak M., 2016. The 2015 catastrophic drought in Poland monitored by satellite products. Proc. 2016 EUMETSAT Meteorological Satellite Conf., 2016.

Szwed M., 2015. The elements of water balance in the changing climate in Poland. Advances in Meteorology, ID 149674: 1–13. doi.org/10.1155/2015/149674.

Szwed M., Karg G., Pińskwar I., Radziejewski M., Graczyk D., Kędziora A., Kundzewicz Z.W., 2010. Climate change and its effect on agriculture, water resources and human health sectors in Poland. Hazards Earth Syst. Sci., 10: 1725–1737, doi:10.5194/nhess-10-1725-2010.

Szyga-Pluta K., 2018. Zmienność występowania susz w okresie wegetacyjnym w Polsce w latach 1966-2015. Przegląd Geofizyczny, 2018(1-2): 51-67. (in Polish).

Taparauskiene l., Miseckaite O., 2017. Comparison of watermark soil moisture content with Selyaninov hydrothermal coefficient. AGROFOR, 2(2): 106-115. doi.org/10.7251/AGRENG1702106T.

Toulios L., Struzik P. (editors), 2016. How the study of the Water Footprint of agricultural crops can benefit from the use of satellite remotely sensed data. Garmond Nitra.

Vlăduţ A. Ş., Nikolova N., Licurici M., 2017. Aridity assessment within southern Romania and northern Bulgaria. Hrvatski Geografski Glasnik, 79(2): 5-26. doi:10.21861/HGG.2017.79.02.01.

Yeşilköy S., Şaylan L., 2020. Assessment and modelling of crop yield and water footprint of winter wheat by aquacrop. Italian Journal of Agrometeorology (3): 3-14. doi: 10.13128/ijam-859.

Ziernicka-Wojtaszek A., Kopcińska J., 2020. Variation in atmospheric precipitation in Poland in the Years 2001–2018. Atmosphere, 11(8): 794. doi.org/10.3390/atmos11080794.

Italian Journal of Agrometeorology
Rivista Italiana di Agrometeorologia

Firenze University Press
www.fupress.com/ijam

OPEN ACCESS

Citation: M. Ali Shahrokhnia, E. Zare (2022) Technical and economic study of irrigation scheduling devices on corn water productivity in a semi-arid region. *Italian Journal of Agrometeorology* (1): 13-22. doi: 10.36253/ijam-1513

Received: November 28, 2021

Accepted: April 16, 2022

Published: July 19, 2022

Data Availability Statement: All relevant data are within the paper and its Supporting Information files.

Competing Interests: The Author(s) declare(s) no conflict of interest.

Technical and economic study of irrigation scheduling devices on corn water productivity in a semi-arid region

Mohammad Ali Shahrokhnia[1,*], Ebrahim Zare[2]

[1] *Agricultural Engineering Research Department, Fars Agricultural and Natural Resources Research and Education Center, Agricultural Research, Education and Extension Organization (AREEO), Shiraz, Iran*
[2] *Economic, Social and Extension Research Department, Fars Agricultural and Natural Resources Research and Education Center, Agricultural Research, Education and Extension Organization (AREEO), Shiraz, Iran*
*Corresponding author. E-mail: mashahrokh@yahoo.com

Abstract. It is essential to consider water allocation control and on-farm irrigation scheduling to increase water productivity in agriculture. There are several devices used for irrigation scheduling, however the best device with the most priority is not identified yet. In the present study, the effect of using several irrigation scheduling devices on increasing water productivity in a corn field was investigated. The devices were classified technically and economically using analytic hierarchy process. The experimental farm was located in a semi-arid region in Iran, which was managed by a farmer and irrigated with drip irrigation system. Six techniques for irrigation scheduling were studied including Penman-Monteith model (T2), infrared thermometer (T3), soil moisture meter (T4), tensiometer (T5), and gypsum block (T6). The irrigation scheduling treatments were compared with the conventional treatment adopted by the farmer (T1). Economic analysis was performed. The ease of use of the devices was also evaluated. Results showed for the irrigation scheduling treatments of T3 to T6, applied irrigation water was reduced by 11 to 26% compared to T1. The corn yield in irrigation scheduling treatments was not reduced significantly compared to T1. As a result, water productivity increased by 35% from 2.0 to 2.7 kg/m^3. The best irrigation scheduling device in terms of water productivity was gypsum block. In regard to affordability and ease of use by farmers, the Penman-Monteith model had more priority. Considering all assessment criteria, tensiometer (T5) was given the first priority. The infrared thermometer (T3) and Penman-Monteith model (T2) were identified as the next priorities.

Keywords: tensiometer, gypsum block, drip irrigation, canopy temperature.

INTRODUCTION

Unsustainable use of water resources has become a global problem. This problem is especially evident in the Middle East and North Africa. Over the last few years, digging deep wells has led to a sharp increase in groundwa-

ter abstraction. One of the effective solutions for reducing applied irrigation water has been the use of modern irrigation systems such as sprinkler or drip irrigation. Singh et al. (2016) stated that the need for food products will double by the next 50 years while 85% of the world's available water will be used for agriculture. Research in water-deficient areas of the world has shown that irrigation scheduling can save up to 35% in water and energy consumption. Forecasts suggest that all groundwater may be depleted within the next 50 years. Therefore, more attention needs to be paid to irrigation scheduling. It should be possible to answer the question of what changes occur in applied irrigation water by converting traditional irrigation methods to modern methods? The results show that in very limited cases the exact effect of modern irrigation systems has been documented. These studies generally show that the development of these technologies either has no effect on water consumption or has increased applied irrigation water. Also, the water productivity has remained more or less constant. Therefore, establishing a balance between sustainable water supply and consumption needs the physical control of water resources. Therefore, reducing allocations is also necessary (Perry and Steduto, 2017). Farmers should have appropriate devices to manage irrigation in farms.

Iran is located in a semi-arid region with an annual rainfall of 250 mm. Most of the water needed for agriculture comes from groundwater resources. In the Fars province, more than 70% of agricultural water is provided from groundwater resources. Improper use of water has led to the gradual depletion of these valuable resources. If this trend continues, it will lead to various economic and social problems such as the migration of farmers to large cities. In recent decades, the Iranian government has developed modern irrigation systems over the country. Due to the low price of agricultural water in Iran, farmers have been not interested in saving applied irrigation water. Therefore, in recent years, the government has begun to build and install smart water delivery meters. When the government begin to reduce the allocated water, it is more necessary to have a suitable tool to assess the time and volume of irrigated water that is called "irrigation scheduling". Irrigation scheduling requires special devices such as a variety of soil moisture meters, tensiometers, and models for measuring plant evapotranspiration.

Iranian farmers manage irrigation according to their experience, not using irrigation scheduling devices. The type of plant also affects the amount of applied water. For example, corn is relatively sensitive to water stress, especially from flowering to grain filling stage. Farmers usually over-irrigate cornfields. Corn water productivity in different countries averages between 1.1 to 2.7 kg/m^3 and the global average is reported to be 1.8 kg/m^3 (Zwart and Bastiaanssen, 2004).

In the Fars province of Iran, the amount of applied irrigation water in cornfields with conventional irrigation management method ranges between 6700 to 28400 m^3/ha with an average of 13300 m^3/ha. Yields vary between 2800 to 15000 kg/ha with an average was 8300 kg/ha. Hence, water productivity ranges between 0.3 and 1.8 kg/m^3, with an average of 0.7 kg/m^3 (Shahrokhnia, 2015).

The application of new irrigation scheduling technologies in Iran is only limited to a few research centers. In Cyprus, low-priced tensiometers produced in the country made this device very popular among farmers. Unfortunately, due to the poor product quality, all efforts were in vain and farmers lost their desire to use it. In Jordan, the use of tensiometers allowed water-saving of 30% of applied irrigation water, and farmers were satisfied. However, farmers in Turkey were unsatisfied with the application of tensiometers due to the low quality of these devices (FAO, 2002).

Pitts and Zuzueta (2007) introduced the different devices for irrigation scheduling. Four irrigation scheduling methods (tensiometer, water balance, plant canopy temperature, and a plant model) were assessed. Results showed that all four methods can be used successfully for corn irrigation scheduling. Using irrigation scheduling methods can allow saving roughly 30% of applied irrigation water (Steele et al., 2000). Irmak et al. (2000) measured canopy temperature and water stress index for irrigation scheduling of corn. The achieved results showed that for the crop water stress index values greater than 0.22, 50% of the plant available water is consumed and the plant experiences water stress. The crop water stress index was also suggested as an appropriate indicator for irrigation scheduling. Ghinassi et al. (2003) mentioned that tensiometers decreased 30% of applied irrigation water and suggested the device as a helpful tool for corn irrigation scheduling. Tensiometers are inexpensive and simple devices to be used by farmers but need periodic maintenances. Bauder and Waskom (2003) used gypsum block for irrigation scheduling of cornfields in the fine soils of Colorado, USA, and found it as an accurate tool for irrigation scheduling. In another study, tensiometers were used in cornfields under a furrow irrigation system. Results showed that applied irrigation water decreased by 25% (Mathew and Senthilvel, 2004). Cremona et al. (2004) evaluated two methods of farm irrigation scheduling, one based on measuring plant stress index (canopy temperature) and the other based on measuring soil moisture. They con-

cluded that by measuring canopy temperature, the water productivity increases by 25%. Since canopy temperature shows the start time of irrigation, it can be used in combination with other methods to determine the end time of irrigation. Erdem et al. (2005, 2006) performed irrigation scheduling based on different levels of water stress index for watermelon and beans using an infrared thermometer. Results showed that this method was appropriate for irrigation management. Chawla and Bundela (2007) examined the advantages and disadvantages of tensiometers and gypsum blocks. They stated that these two devices may not be acknowledged by farmers for some reason. The limited range of measuring soil matric suction, inability to determine the amount of irrigation water and the duration of balancing with soil moisture, were the main reasons.

In a study in South Florida, irrigation scheduling was performed using tensiometers, based on estimation of evapotranspiration, and conventional irrigation. The amount of water used in the first two methods was equal to 31 to 36% of conventional irrigation. Plant growth and water productivity in the first two methods were better than conventional irrigation. Finally, irrigation scheduling based on tensiometer and evapotranspiration were selected as appropriate scheduling methods for irrigation (Migliaccio et al., 2010). Incrocci et al. (2014) stated that in Italy, irrigation scheduling of different plants was performed using tensiometer, soil moisture meters and estimation of evapotranspiration. Results showed that applied irrigation water decreased by 21 to 40% compared to the conventional irrigation method. Applied fertilizer also decreased by 39 to 74%. No significant decrease was observed in plant growth and crop quality (Incrocci et al., 2014). Watermelon yield increased by 30% with the use of a soil moisture meter for irrigation scheduling. This study was conducted in the sandy soils of South Carolina (Miller et al., 2014). Soulis et al. (2015) and Soulis and Elmaloglou (2018) emphasized the importance of accuracy, calibration and placement of soil moisture sensors in drip irrigation scheduling. They also stated that irrigation scheduling using soil moisture sensors plays an important role in saving water. Perea et al. (2017) scheduled strawberry irrigation in Spain using software that was installed on Android phones and used meteorological, plant and hydraulic information. The rate of water-saving was from 11 to 33%. Tensiometers were used to manage the subsurface irrigation of strawberries. Results showed that water productivity can be increased from 8 to 44% (Cormier et al., 2020). In a study in the USA, irrigation scheduling for cornfields was performed and compared using sensors that determine soil water suction and soil water balance method. Results showed that they were suitable sensors and had economically similar results to the soil water balance method (Da Cunha Leme Filho et al., 2020). Soybean irrigation was also scheduled by installing soil water suction sensors in Stoneville, USA. Results showed that irrigation scheduling did not reduce crop yield and water productivity, but increased the economic efficiency (Wood et al., 2020). Bahadur and Singh (2021) used tensiometers to schedule tomato irrigation. Results showed that the best matric suction for starting irrigation was 40 kPa with polythene block mulch.

Previous research has shown that due to water scarcity for agriculture, controlling water allocation and using different irrigation scheduling methods is necessary to increase water productivity. Irrigation scheduling requires devices that vary in accuracy, cost, and efficiency. In addition, the use of devices that do not have sophisticated technology should be recommended for illiterate farmers. Therefore, in this study, the effect of using several irrigation scheduling devices in a cornfield in a semi-arid region was investigated in terms of applied irrigation water, costs and ease of use.

MATERIAL AND METHODS

This research was conducted in a cornfield in Fasa plain in the Fars province of Iran (Figure 1). This region is located in the south of Iran and has a semi-hot and dry climate. Fasa is a fertile agricultural plain. It is cultivated with wheat in the winter and corn, tomato, cucumber, and other crops in the summer. The soil tex-

Fig. 1. Location of the study area.

ture of this area is medium to heavy (loam to clay loam) and the weather is relatively warm in summer. Average air temperature, air humidity, annual reference evaporation and annual rainfall in the region are 19.3 °C, 40%, 2756 mm and 295 mm, respectively. In recent years, the surface irrigation systems in many farms have been changed to the drip irrigation system. Despite the use of drip irrigation systems, proper management is not applied to irrigation yet. Regarding the high amount of applied irrigation water and low water productivity in cornfields in this region, it is essential to employ modern irrigation systems and implement proper water management practices.

This study was carried out in a local cornfield. Irrigation scheduling was performed using different devices. The soil texture was Silty Clay Loam (30% clay, 52% silt and 18% sand). The bulk density of the soil was 1.28 g/cm^3. The volumetric soil moisture contents at soil field capacity and permanent wilting point were 32 and 15%, respectively (measured using the pressure chamber method). Corn seeds were planted by the farmer on lines 75 cm apart. The length of planting lines was 95 meters and a strip drip irrigation pipe was placed on each line. Irrigation water was provided from the existing well in the field with no restriction on the time and amount of irrigation. The pH of soil saturated extract was 7.3 and the electrical conductivity of the irrigation water was 0.483 dS/m. To evaluate the technical, economic and ease of use of irrigation scheduling methods, 5 devices were considered as treatments of the experiment. The devices included tensiometers, gypsum blocks, an infrared thermometer, soil moisture measuring sensors and the Penman-Monteith evapotranspiration estimation model. Conventional irrigation scheduling, performed by the farmer, was also considered in the experiment as the control treatment. The experiment was performed as a randomized complete block design with 6 treatments and 3 replications:

T1 conventional irrigation managed by the farmer. The irrigation interval was approximately 5 days. No technical recommendations were given to the farmer. The amount of applied irrigation water by the farmer was measured using calibrated propeller flow meters with an accuracy of 1 l.

T2 Amount of evapotranspiration estimated by Penman-Monteith model. The irrigation frequency was 2 days.

T3 Irrigation scheduled using an infrared thermometer and the plant canopy temperature. The type of infrared thermometer used was Summit (model SIR100B) with an accuracy of 0.1 ° C.

T4 Irrigation scheduling based on soil volumetric moisture content. The irrigation scheduling was performed using a 5-cm soil moisture sensor (ECH2O, Decagon, USA). The accuracy of the device was approximately 0.1%. The critical soil moisture limit for starting irrigation was 23%. This value was calculated using the soil available water for the crop and management allowable depletion (MAD=50%).

T5 Irrigation scheduling based on soil water suction. This suction was measured by a tensiometer (Soil Moisture Co., USA) characterized by accuracy of 1 cm.

T6 Irrigation scheduling based on measurements of soil electrical resistance using a gypsum block device (Eijkelkamp). The critical limit for starting irrigation was 74 according to the device catalogue.

Each plot of the experiment consisted of four implantation lines connected to a calibrated water meter. The volume of irrigation water was measured and controlled with an accuracy of 0.1 l. In T4 to T6, device sensors (one sensor in each plot) were installed between two middle rows of each replication, about 30 centimeter from the closest emitter. The depth of sensors placement was 30 cm according to the density of plant root. Tensiometers, gypsum blocks, soil moisture sensors and canopy temperature were read every day. When the soil moisture reached the critical level (depletion of 50% of available soil moisture), the irrigation was started. Due to the limited range of measuring suction in tensiometers (80 c.bar), the management allowable depletion (MAD) was considered equal to 30% for starting irrigation in T5. The volume of irrigation water was the amount of water required to reach the soil water content corresponding to the field capacity. The volume of irrigation water per unit surface was 27 mm in T3, T4 and T6, and 16 mm in (T5). In T3, the lower and upper stress baselines, used to evaluate the crop water stress index, were adopted from the study of Irmak et al., (2000). The required meteorological data were also obtained from the automatic synoptic meteorological station of Fasa. The station was established in 1974 and it is located at 53°41' E and 28°58' N and 1288 m.a.s.l. For T5, characteristics of the soil moisture tension curve were used to convert soil suction data to soil moisture. This curve was obtained from a pressure chamber device in the laboratory. The critical soil suction limit for starting irrigation was 69 cm. The study was performed for two years. In all the six treatments, fertilizing and weeding were similar to T1 and was performed by the farmer. At the end of the growing season, the amount of crop grain yield and cumulative applied irrigation water were measured in the plots. The mean values were statistically compared using Duncan's test. The rate of applied irrigation water reduction for T2 to T6 (compared to T1) was measured.

Table 1. Saaty Spectrum table.

Interpretation	Nonsignificant	Moderately important	Very important	Very strongly important	Extremely important
Equivalent quantity	1	3	5	7	9

Water productivity was obtained by dividing the grain yield by the amount of applied water and evaluated.

Economic evaluation

Irrigation scheduling devices are different in terms of technical and economic aspects. Farmers consider different criteria when they want to decide on something. Scientifically, multi-criteria decision-making models are recommended for such issues. These models are used to select the most appropriate choice among the several available based on quantitative and qualitative indicators. The characteristics, application and results of different irrigation scheduling devices may be technically and economically different. Therefore, selecting the best device is a multi-criteria decision that justifies the use of multi-criteria decision-making models. Multi-criteria decision-making models include a wide range of methods. Analytic Hierarchy Process (AHP) method for decision making is based on qualitative indicators and it is a suitable and common tool. This method allows users to consider quantitative and qualitative indicators in their evaluations for decision making. The method is based on a pairwise comparison of criteria and options and uses a tree hierarchy structure in decision making (Benitez et al. 2011; Brunelli et al., 2013). In the AHP, two options are compared according to the desired criteria. Using a specific spectrum, the qualitative assessment of the superiority of one option over another becomes quantitative. In this study, irrigation scheduling devices were considered as an option and the desired criteria by farmers were considered as a comparison criterion. The following steps were performed to determine the weight of the options and criteria.

1 - First, the superiority of the options based on each criterion is examined in pairs. This information is collected qualitatively from farmers and experts and was quantified using the spectrum in Table 1, which is known as the Saaty spectrum (Saaty, 1987).

Intermediate values are converted to quantitative equivalents as needed using the numbers 2, 4, 6, and 8, respectively.

2 - In the next step, the matrix of options is formed. The general shape of this matrix is:

$$\mathbf{A}=\begin{bmatrix} a_{11} & a_{12} & \cdots & a_{1j} \\ a_{21} & a_{22} & \cdots & a_{2j} \\ \vdots & \vdots & \vdots & \vdots \\ a_{i1} & a_{i2} & \cdots & a_{ij} \end{bmatrix} \quad (1)$$

The method of completing matrix A is the following: considering options a_{11} and a_{12}, if option a_{12} is more important at farmer's point of view, a higher number from table 1 is given to cell a_{12}. In the same way, all the cells are completed by comparing the options.

3 - After completing the matrix cells, the matrix is normalized. For this purpose, the number in each cell is divided by the sum of the numbers in each column. Thus, the matrix R is obtained. Each cell of the matrix R is called r_{ij}, which is calculated as follows.

$$\mathbf{R}=\begin{bmatrix} r_{11} & r_{12} & \cdots & r_{1j} \\ r_{21} & r_{22} & \cdots & r_{2j} \\ \vdots & \vdots & \vdots & \vdots \\ r_{i1} & r_{i2} & \cdots & r_{ij} \end{bmatrix} \quad (2)$$

$$\mathbf{r}_{ij}=\frac{a_{ij}}{\sum_{i=1}^{n} a_{ij}} \quad (3)$$

4 - In the next step, the weight of each option and criteria are calculated. For this purpose, the cells of each row from matrix R are divided by the sum of the columns. Thus, the coefficient of importance (W_i) is determined as follows:

$$\mathbf{W}_i=\frac{\sum_{j=1}^{n} r_{ij}}{n} \quad (4)$$

Before using W_i, it is required to ensure the answers provided for pairwise comparisons are consistent. For this purpose, it is necessary to calculate the consistency rate (CR). If the CR is 0.1, the comparisons have the necessary compatibility; otherwise, the pairwise comparisons should be revised until the desired compatibility rate is reached. To calculate CR, the weighted sum vec-

tor (WSV) and consistency vector (CV) are calculated, respectively.

$$\mathbf{WSV = A.W} \quad (5)$$

$$\mathbf{CV=} \frac{WSV}{W} = \frac{A.W}{W} \quad (6)$$

The consistency index (CI) in this case is equal to:

$$\mathbf{CI=} \frac{\lambda_{max} - n}{n-1} \quad (7)$$

$$\lambda_{max} = \frac{(CV)_i}{n} \quad (8)$$

where λ_{max} is the largest eigenvalue of a'_{ij}, the perturbed value of a_{ij}. Using random numbers, a random consistency index (RI) is extracted for each matrix. After determining the random consistency index, the initial pairwise matrix is determined using the consistency ratio (CR):

$$CR = \frac{CI}{RI} \quad (9)$$

In this study, the opinions of experts and farmers were used to select the criteria, according to the factors affecting the acceptance of irrigation methods. For this purpose, 50 farmers were invited to a training class. After explaining the issue of irrigation scheduling to farmers, the most important factors that they considered in selecting irrigation scheduling tools were determined. Calculations related to pairwise comparison of options and determination of CR was performed using Expert Choice software. In addition to using the pairwise comparison method to prioritize the options, different experimental treatments were also compared economically. To compare the affordability of the choices, the following prices were considered. The price of devices, the maintenance costs, the replacement price, the time of irrigation, the number of workers used and applied irrigation water in each treatment were noted. Considering average prices and costs in the area, the difference between the costs of each treatment was calculated. To compare the affordability of the devices, the partial budgeting method was used. For this purpose, the control treatment under the farmer management was selected as the main treatment and other treatments were compared with that. The calculation method was as follows:

$$B = \Delta\pi_i - \Delta C_i \quad (10)$$

where in:

$\Delta\pi_i$ = The benefits of treatment i, compared to the farmer managed treatment

ΔC_i = The difference between the cost of treatment i, compared to the farmer managed treatment

Finally, the treatment with the highest value of B was selected as the best treatment. In the studied treatments, other costs were the same, except for irrigation and device costs. Therefore, to calculate the gross benefits of each treatment, only the sum of non-common costs of treatment was deducted from the gross income.

RESULTS AND DISCUSSION

Table 2 shows the results of irrigation scheduling treatments in the two years period of experiments. Results show that the highest and lowest applied irrigation water is related to Penman-Monteith (T2) and tensiometers (T5) with 7036 and 4763 m^3/ha. The difference of applied irrigation water between T3 and T4 was not statistically significant ($p<0.05$). The amount of water used in conventional irrigation management (T1) was 6404 m^3/ha. Therefore, the maximum amount of irrigation water saving was 26% (T5). In T2, the applied irrigation water resulted higher than T1 and no water-saving was observed. Therefore, in terms of saving applied irrigation water, priority was given to the treatment managed with the tensiometer (T5) followed by the one managed by canopy temperature measurements (T3), soil moisture meter (T4) and gypsum block (T6). The tensiometer treatment had the lowest applied irrigation water and the lowest crop yield (12387 kg/ha). The yield in T1 (12495 kg/ha) was not statistically different ($p<0.05$) from that obtained in treatment T5. The Penman-Monteith approach (T2) had the highest irrigation water, and the highest yield (16503 kg/ha). In general, with increasing the irrigation water, the yield was also increased. Therefore, in terms of water saving, the priority is represented by T5 followed by T3, T4 and T6, respectively. According to Table 2, water productivity in all irrigation scheduling treatments was significantly greater than T1 (1.96 kg/m^3). Although T6 had the highest water productivity (2.72 kg/m^3), its difference with T3 and T4 was not statistically significant. The difference between the water productivity of T2 and T6 was significant.

Table 3 shows the average productivity components of all the treatments measured within the two years of the experiment. Also, the averages for conventional surface irrigation systems in the area is presented. The average of applied irrigation water in the first and second

Table 2. Average yield, irrigation parameters and water productivity of corn in the studied farm.

Treatments	Applied irrigation water (m^3/ha)	Reduction of applied water compared to T1 (%)	Yield (kg/ha)	Water productivity (kg/m^3)	Number of irrigations	Irrigation hours
T1	6404 b	0.0	12495 c	1.96 c	14	12
T2	7036 a	-9.9	16503 a	2.35 b	28	5
T3	5334 c	16.7	13668 bc	2.56 ab	23	5
T4	5457 c	14.8	14545 ab	2.64 ab	27	5
T5	4763 d	25.6	12387 c	2.59 ab	22	5
T6	5682 c	11.3	15518 ab	2.72 a	27	5

Table 3. Average yield, applied irrigation water and water productivity of corn in two years of experiment.

Factors	First-year	Second-year	Mean	Conventional values (Shahrokhnia, 2015)
Yield (kg/ha)	15807 a	12565 b	14186	8300
Applied irrigation water (m^3/ha)	5860 a	5699 a	5780	13300
Water productivity (kg/m^3)	2.71 a	2.23 b	2.47	0.70

years was 5860 and 5699 m^3/ha, which was not significantly different. In the second year, yield and water productivity decreased significantly compared to the first year due to poor tillage and low-quality seeds used by the farmer.

Figures 2 and 3 show the relationships of yield and water productivity to irrigation water amount in the treatments. Results show that with the increase of irrigation water, the crop yield increased and water productivity decreased. The relationship of yield to applied water, and water productivity to applied water have a high determination coefficient (R^2). This study shows that tensiometers and infrared thermometers allowed to obtain better results than the other methods. The amount of applied water and crop yield using the Penman-Monteith model (T2) was higher than the other devices, however, the water productivity was lower. In the farmer-managed treatment (T1), the crop yield and water productivity were less than other irrigation scheduled treatments. This may be due to over-irrigation of the cornfield when plants needed less water, and deficit irrigation when plants needed more water.

In the region, yield, irrigation water and water productivity in conventionally managed surface irrigation systems are generally of 8300 kg/ha, 13300 m^3/ha and 0.70 kg/m^3, respectively. In the present study, using

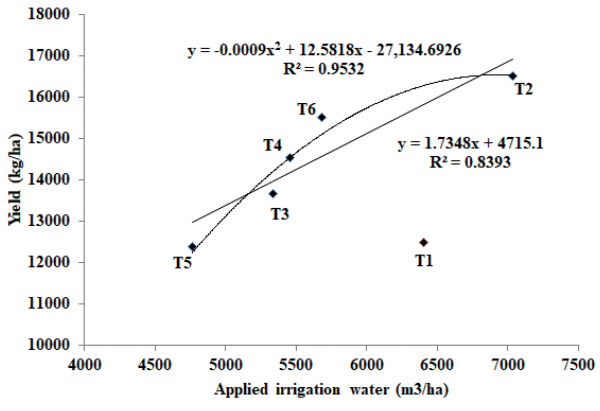

Fig. 2. Yield changes to applied water.

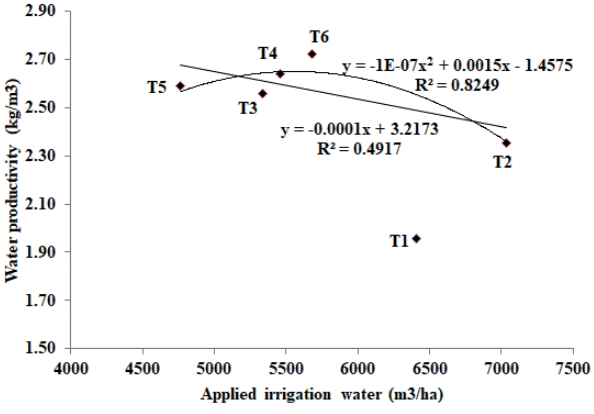

Fig. 3. Water productivity changes to applied water.

Table 4. Results of economic analysis of treatments ($/ha)

Treatments	T1	T2	T3	T4	T5	T6
Irrigation cost	168	140	115	135	110	135
Water cost	224	246	192	192	167	192
Gross income	3587	4607	3993	3993	3587	3993
Device cost	0	0	5	68	57	46
Total cost	392	387	313	395	334	373
Income compared to T1	0	1020	406	406	0	406
Cost difference compared to T1	0	-5	-80	3	-59	-19
Gross benefit compared to T1	0	1025	485	403	59	425
Priority of treatments in terms of gross benefits	6	1	2	4	5	3

irrigation scheduling and under drip irrigation system, these values reached 14524 kg/ha, 5634 m^3/ha and 2.57 kg/m^3, respectively. Therefore, improving surface irrigation system with precise scheduled irrigation using a drip system, may save up to 58% of irrigation water.

Economic analysis results

Table 4 shows the results of economic analysis of irrigation scheduling devices. The gross benefits of T2–T6 were higher than T1. Results show that all irrigation scheduling devices were economically better than the farmer management treatment. T2 and T3 have the highest economic benefit.

Prioritize treatments using the AHP method

To prioritize the treatments based on a set of factors, first, the importance coefficient of the treatments was determined. The criteria of initial price, service and maintenance cost, access to maintenance services, ease of use and accuracy in the results were selected as the most important criteria in decision making. Among the 5 important criteria in farmers' decision making, the accuracy of results was the most important factor to choose the better irrigation scheduling devices. Table 5 shows the criteria weights for selecting irrigation scheduling devices. Table 6 shows the prioritization of irrigation scheduling devices based on the pairwise comparison. After determining the importance of the criteria, their average weight was estimated. The use of tensiometer was the first priority of farmers. However, the use of infrared thermometers and the Penman-Monteith model had also high weights.

CONCLUSIONS

The results showed that the five irrigation scheduling devices in this study can be used to increase the water productivity of irrigated corn. Gypsum block allowed to achieve the maximum water productivity. Although the use of the Penman-Monteith model did not allow saving applied irrigation water, however, it increased yield and water productivity. The irrigation water requirement of corn estimated by the Penman-Monteith model was about 7,000 m^3/ha, which is much less than the volume applied in conventional irrigation systems (13,300 m^3/ha). Although the applied water in the Penman-Monteith model was 10% more than other irrigation scheduling devices, it was economically better than the other meth-

Table 5. Coefficient of importance of effective criteria in choosing irrigation scheduling method by farmers.

Criterion type	Criterion weight
Initial price of the device	0.038
The device annual service cost	0.055
Ease of use of the device	0.175
Accuracy of results	0.423
Access to maintenance services	0.309

Table 6. Priority of choosing irrigation planning method based on pairwise comparison.

Treatments	Weight of the treatment in decision making	Priority of treatments according to the weight of criteria
T2	0.221	3
T3	0.245	2
T4	0.184	4
T5	0.267	1
T6	0.083	5

ods. The water savings compared to conventional irrigation using the infrared thermometer, soil moisture meter, tensiometer and gypsum block were between 11 to 26%, which were statistically significant ($p<0.05$). The applied irrigation water in the treatment with the tensiometer was lower than in the other treatments.

In terms of ease of use, the Penman-Month model has received more attention from farmers in the region. The farmer selected the accuracy of irrigation scheduling devices in estimating required water as the most important factor. If only economic criteria are considered, the use of the Penman-Monteith model had the highest priority. However, considering all the criteria, priority is given to the use of a tensiometer, followed by the management operating with the infrared thermometer and the Penman-Monteith model. The average water productivity had increased from 2 kg/m^3 in the farmer-managed treatment to about 2.7 kg/m^3 (using gypsum block) which shows an increase of 35%.

In this study, corn applied irrigation water reached 4800-5700 m^3/ha (11-26% water saving) using both the drip irrigation system and the irrigation scheduling devices. Compared to the applied water in conventional irrigation management (13300 m^3/ha), the water-saving reaches 57 to 64% which is very significant. Water productivity of corn under conventional surface irrigation systems in the region is generally lower than 1 kg/m^3. The water productivity in the farmer-managed treatment in this study was about 1.96 kg/m^3. In other words, replacing the conventional surface irrigation systems with a well-managed drip irrigation system can significantly increase the water productivity of corn.

REFERENCES

Bahadur, A., Singh, J. (2021). Optimization of Tensiometer-Based Drip Irrigation Scheduling and Its Effect on Growth, Yield and Water Use Efficiency in Tomato (Solanum Lycopersicum). Agricultural Research, doi:10.1007/s40003-020-00529-5

Bauder, T., Waskom, R. (2003). *Best management practices for Colorado corn*. Colorado State University Cooperative Extension Bulletin XCM74A.

Benitez, J., Delgado-Galvan, X., Gutiérrez, J. A., Izquierdo, J. (2011). Balancing consistency and expert judgment in AHP. Mathematical and Computer Modelling 54: 1785-1790

Brunelli, M., Critch, A., Fedrizzi, M. (2013). A note on the proportionality between some consistency indices in the AHP. Applied Mathematics and Computation. 219: 7901-7906.

Chawla, K.L., Bundela, D.S. (2007). Irrigation scheduling techniques for higher production. National Training Course On-farm Land and Water Management, 1-7 March 2007.

Cormier, J., Depardieu, C., Letourneau, G., Boily, C., Gallichand, J., Caron, J. (2020). Tensiometer-based irrigation scheduling and water use efficiency of field-grown strawberries. Agronomy Journal, 112: 2581–2597.

Cremona, M.V., Stutzler, H., Kage, H. (2004). Irrigation scheduling of Kohlrabi (Brassica oleracea var. gongylodes) using crop water stress index. HortScience, 39(2): 276-279.

Da Cunha Leme Filho, J.F., Ortiz, B.V., Damianidis, D., Balkcom, K.S., Dougherth, M., Knappenberger, T. (2020). Irrigation Scheduling to Promote Corn Productivity in Central Alabama. Journal of Agricultural Science, 12 (9): 34-51.

Erdem, Y., Sehirali, S., Erdem, T., Kenar, D. (2006). Determination of crop water stress index for irrigation scheduling of Bean (Phaseolus vulgaris L.). Turkish Journal of Agriculture and Forestry, 30: 195-202.

Erdem, Y., Erdem, T., Orta, H., Okursoy, H. (2005). Irrigation scheduling for watermelon with crop water stress index (CWSI). Journal of Central European Agriculture, 6: 449-460.

FAO. (2002). Proceedings of the Workshop on Irrigation Advisory and Training Services in the Near East. Hammamet, Tunisia, 13-16 May 2002.

Ghinassi, G., Giacomin, A., Polil, E. (2003). Irrigation management at field level: Tensiometer utilization for performance control. Department of Agriculture and Forestry Engineering, University of Florence, Italy.

Incrocci. L., Marzialettib, P., Incroccia, G., Di Vitaa, A., Balendonckc, J., Bibbianid, C., Spagnole, S., and Pardossia, A. (2014). Substrate water status and evapotranspiration irrigation scheduling in heterogenous container nursery crops. Agricultural Water Management, 131: 30-40.

Irmak, S., Haman, D.Z., Bastug, R. (2000). Determination of crop water stress index for irrigation timing and yield estimation of corn. Agronomy Journal, 92: 1221-1227.

Mathew, A.C., Senthilvel, S. (2004). Evaluation of an automated furrow irrigation system using soil moisture sensor. Madras Agricultural Journal, 91(4-6): 215-220.

Migliaccio, K.W., Schaffera, B., Cranea, J.H., and Davies, F.S. (2010). Plant response to evapotranspiration and soil water sensor irrigation scheduling methods for papaya production in south Florida. Agricultural Water Management, 97: 1452-1460.

Miller, G.A., Farahanib, H.J., Hassellc, R.L., Khaliliand, A., Adelberge, J.W., and Wellsf, C.E. (2014). Field evaluation and performance of capacitance probes for automated drip irrigation of watermelons. Agricultural Water Management, 121: 124-134.

Perea, R.G., Garcia, I.F., Arroyo, M.M., Diaz, J.A.R., Montesinos, P. (2017). Multiplatform application for precision irrigation scheduling in strawberries. Agricultural Water Management, 183: 194-201.

Perry, C., Steduto, P. (2017). Does improved irrigation technology save water? A review of the evidence. Technical report, FAO, May 2017.

Pitts, D., Zuzueta, F. (2007). Micro irrigation scheduling. Research report, Southwest Florida Research and Education Center.

Saaty, R.W. (1987). The analytic hierarchy process, what it is and how it is used. Mathematical Modelling, 9: 161-176.

Singh, A.K., Dubey, O.P., Ghosh, S.K. (2016). Irrigation scheduling using intervention of Geomatic tools-A case study of Khedli minor. Agricultural Water Management, 177: 454-460.

Shahrokhnia, M.A. (2015). Water productivity of corn farms in Fars province. Technical report No. 47195, Agricultural Research, Education and Extension Organization, Iran.

Soulis K.X., Elmaloglou, S., Dercas, N. (2015). Investigating the effects of soil moisture sensors positioning and accuracy on soil moisture based drip irrigation scheduling systems. Agricultural Water Management, 148: 258-268.

Soulis K.X., Elmaloglou, S. (2018). Optimal soil water content sensors placement for surface drip irrigation scheduling in layered soils. Computers and Electronics in Agriculture, 152: 1-8.

Steele, D.D., Stegman, E.C., Knighton, R.E. (2000). Irrigation management for corn in the northern Great Plains, USA. Irrigation Science, 19(3): 107-114.

Wood C.W., Krutz L.J., Henry W.B., Irby T., Orlowski, J. M., Bryant C.J., Atwill R. L., Spencer G. D., Mills, B.E. (2020). Developing sensor-based irrigation scheduling that maximizes soybean grain yield, irrigation water use efficiency, and returns above irrigation costs. Crop, Forage and Turfgrass Management, 6(1), doi:10.1002/cft2.20029

Zwart, S.J., Bastiaanssen, W.G.M. (2004). Review of measured crop productivity values for irrigated wheat, rice, cotton and maize. Agricultural Water Management, 69: 115-133.

Italian Journal of Agrometeorology
Rivista Italiana di Agrometeorologia

Firenze University Press
www.fupress.com/ijam

OPEN ACCESS

Citation: F. Bakanoğulları, L. Şaylan, S. Yeşilköy (2022) Effects of phenological stages, growth and meteorological factor on the albedo of different crop cultivars. *Italian Journal of Agrometeorology* (1): 23-40. doi: 10.36253/ijam-1445

Received: November 3, 2021

Accepted: February 26, 2022

Published: July 19, 2022

Data Availability Statement: All relevant data are within the paper and its Supporting Information files.

Competing Interests: The Author(s) declare(s) no conflict of interest.

Effects of phenological stages, growth and meteorological factor on the albedo of different crop cultivars

Fatih Bakanoğulları[1,*], Levent Şaylan[2], Serhan Yeşilköy[3]

[1] *Atatürk Soil Water and Agricultural Meteorology Research Inst. Kirklareli, Turkey*
[2] *Istanbul Technical University, Faculty of Aeronautics and Astronautics, Department of Meteorological Engineering, Istanbul, Turkey*
[3] *Istanbul Directorate of Provincial Agriculture and Forestry, Istanbul, Turkey*
*Corresponding author. E-mail fbakanogullari@gmail.com

Abstract. Albedo is a key component of the atmospheric, climatologic and remote sensing studies by means of global warming, energy balance, evapotranspiration, climate models, hydrological cycle etc. For these reasons, the accurate determination of surface albedo has become more important. In this study, the variation of measured albedo values of winter wheat, barley and sunflower cultivars according to phenological stages was investigated for the first time in the northwestern part of Turkey. Additonally, influences of leaf area index as growth indicator and rainfall as meteorological variable on albedo were also analyzed. The average albedo values of winter wheat, barley and sunflower in both growing periods varied from 0.176 to 0.190 for winter wheat, from 0.171 to 0.189 for sunflower and from 0.187 to 0.214 for barley cultivars. According to phenological stages, the minimum and maximum average albedo values were found for winter wheat as 0.121 between sowing and germination and 0.247 between stem formation and head emergence; for sunflower as 0.150 between sowing and germination and 0.212 between leaf initiation and immature bud; for barley as 0.144 sowing and germination and 0.261 between head emergence and flowering stages. Additionally, significant relationships were found between albedo and leaf area index for winter wheat, barley and sunflower as r^2=0.87, r^2=0.82 and r^2=0.77, respectively.

Keywords: agrometeorology, albedo, winter wheat, barley, sunflower.

INTRODUCTION

One of the most important factors driving the climate is the absorbed energy on the surface. The energy absorption of surfaces is related to its reflection amount. Albedo, which is one of the important micrometeorological factors, indicates how much the surface reflects incoming radiation energy. Therefore, changes in albedo affect on the energy balance components of the surface (Iziomon and Mayer, 2002; Myhre and Myhre, 2003). This is because the surface albedo controls the radiative energy distribution.

Daytime net radiation is affected by the variation of albedo. Nevertheless, there is an inverse relationship between albedo and net radiation. Likewise, the decrease in net radiation causes changes in soil heat flux, sensible- and latent heat fluxes. As stated by Wie et al. (2020), shortwave radiation changes due to albedo. This affects the surface energy balance and surface temperature. The reflection amount of shortwave radiation is related to the angle of incidence of the incoming shortwave radiation during the daytime. For this reason, albedo values increase at sunrise and sunset hours. However, the low values of global solar radiation values at these times limits the effect of this increase of albedo on net radiation (Wie et al. 2020). Albedo and energy balance components such as net radiation etc. are not regularly measured meteorological variables at climatological stations by the responsible institutions in the world. There is no network to provide this kind of data for agricultural crops especially in developing countries. Therefore, collecting experimental albedo data is crucial for model development and comparing model results (Starr et al., 2020). Having actual albedo values for plants is also useful in order to validate remote sensing data too (Dexter, 2004). This is because the limited number of actual albedo measurements makes it difficult to compare remote sensing data for different crop surfaces especially where there are no ground observations. In particular, changes in vegetation affect the surface albedo, thus influence on climate patterns. Therefore, surface albedo is extremely significant in climate models. Consequently, having experimental albedo data for different plant surfaces is important for developers and users of climate models and studies of energy balance components (Myhre and Myhre, 2003).

Furthermore, cultivars with higher albedo would provide a partial mitigation of global warming and thus climate change (Henderson-Sellers and Wilson, 1983; Ridgwell et al, 2009). Doughty et al. (2011) found the effects of increases in crop albedo on the cooling of the regional climate using the model. They determined that increasing albedo values decreases the temperatures and hence the latent heat fluxes in the atmosphere, and thus cloudiness and precipitation decrease. Fuller and Ottke (2002) stated that surface albedo is an important variable for General Circulation Models (GCMs) and any changes of albedo caused a decrease in rains. Ridgewell et al. (2009) found that 0.17 °C cooling in climate models increased the surface albedo values by 0.03 - 0.09. Kala and Hirsch (2020) emphasized that the increase in plant albedo values can reduce global warming. Using the Weather Research and Forecasting (WRF) model, they simulated increases in plant albedo values from 0.02 to 0.1 in two agricultural regions of Australia. Wood et al. (2008) investigated the effects of albedo changes on climate by using a simple planetary model (Daisyworld) to show the long-term effects of coupling between life and its environment.

Plants albedo is higher than the albedo of many other natural surfaces, especially since they cover the surface completely. Leaf Area Index (LAI) expresses the plant leaf area per unit soil surface. It indicates growth of a plant and coverage of surface by leaves. For this reason there is a relationship between albedo and LAI. Albedo is critical data not only for the reduction of global warming, but also for accurately calculating net radiation (Kumar et al. 2020). It should be noted that the net radiation value also affects other energy balance components. As written by Uysal and Şaylan (2019), the ratio between soil heat flux and net radiation can be estimated using some relationships based on LAI, albedo and Normalized Difference Vegetation Index (NDVI) etc.

Surface albedo is also an extremely important input data, especially in radiation transfer models, which predict the radiation effect by changing the use of the ground surface. This situation underlines the importance of correctly detecting surface albedo. Zhou et al. (2020) determined in a model study that the reference albedo value was generally lower than the constant value of 0.23 according to seasonal and regional variations.

Furthermore, net shortwave- and net radiation values can be calculated using albedo and global solar radiation values. These data are used to make necessary calculations in agriculture, meteorology and other engineering fields. In addition, in many applications, the albedo value is taken as a constant for a crop to represent the whole growing period, but it changes during the development period. However, as Dixon (1983) and Starr et al. (2020) pointed out, albedo changes over time and many factors affect this change. So albedo is not constant. Until today, many studies have been conducted on the albedo of plants (Dexer, 2004). Breuer et al. (2003) stated that it is difficult to determine the upper and lower limits of the albedo value, which is necessary and important for many crop growth-and climate models, and these values for various plants were published by Kondratyev (1969, 1972) and Iqbal (1983). To summarize these studies; the minimum and maximum albedo values were determined for two sunflower cultivars as 0.21-0.32 and 0.23-0.29 by Gates (1980); for barley as 0.20 and 0.26 by Fritschen (1967); as 0.23 and 0.26 by Monteith and Unsworth (1990); as 0.14 and 0.36 by Piggin and Schwerdtfeger (1973); for winter wheat as 0.18 and 0.23 by Fritschen (1967); as 0.10 and 0.25 by Kondratyev (1969); as 0.13 and 0.21 by Kondratyev (1972);

as 0.16 and 0.23 by Sellers (1965), Kondratyev (1969), Pielke (1984); as 0.13 and 0.25 by Piggin and Schwerdtfeger (1973); as 0.22 and 0.26 by Monteith and Unsworth (1990) and as 0.20 and 0.23 by Song (1998). Additionally, Impens and Lemeur (1969) estimated the albedo of sunflower as 0.28.

Albedo of the land surface can be influenced by natural variability and anthropogenic impacts. Furthermore, albedo varies depending on cultivars, plant growing stages, sun angle and surface charecteristics such as color of soil, soil moisture, soil organic matter content, surface roughness etc. (Dickson, 1983; Henderson-Sellers and Wilson, 1983; Kumar et al., 2020). Piggin and Schwerdtfeger (1973), Dexer (2004) explained the seasonal trends of albedo in terms of changes in crop development and soil moisture. Furthermore, Minnis et al. (1997) and Song (1998) stated that albedo tends to decrease as the plant height and leaf, greenness, plant water status, soil moisture increase, but it tends to increase as the LAI increases. Additonally, Oguntunde and Giesen (2004) also found a strong correlation for both between albedo and LAI and between albedo and crop height for maize. Dexer (2004) also investigated the relationships between albedo and LAI for wheat. Additionally, Serban et al. (2011) investigated the albedo values of 25 winter wheat cultivars in Romania and found that each had different values and temporal changes. They determined the average albedo value for all cultivars as 0.226. Furthermore, Zhang et al. (2013) assigned that the albedo values of plants varied during the growth period due to their different pigment, size and LAI values. The same researchers found that the albedo values tended to increase from the tillering to the grain formation stage, but began to decrease after the grain formation. Again, Zhang et al. (2013) stated that the albedo value is higher in the morning and afternoon times corresponding to 40° Sun angles. In addition, Yin (1998) emphasized that the biggest obstacle that complicates the measurement of albedo in agricultural lands is the 3-dimensional area (depth, shape and surface) covered by plants. Also, some researchers found that there is a tendency to decrease in albedo values when the height of the cultivated plants increases (Jarvis et al., 1976; Rauner, 1976; Shuttleworth, 1989). Futhermore, Linacre (1992), Minnis et al. (1997), Song (1998) determined that albedo tends to decrease when humidity increases on the surface. Additionally, Wang et al. (2010) compared the albedo values measured on the surface with the albedo values calculated by remote sensing and found little differences between them. Futhermore, surface roughness is other an important parameter affecting albedo as stated by Ogilvy (1991). Likewise, Bowers and Hanks (1965) and Post et al. (1993) specified that the albedo was a function of the combination of soil color – pigment- and its spatial distribution, if the soil surface was partially smooth. Dexter et al. (2004) determined that the annual trend of wheat's albedo changed according to atmospheric and surface conditions.

64% of northwestern part of Turkey (Thrace part) is agricultural land and rainfed agriculture is dominant in that part. Wheat, barley and sunflower are generally grown in this region. However, the actual albedo values of these crops and their cultivars grown in the Thrace region of Turkey are not known. Therefore, the objectives of our study are (i) to determine for the first time the actual albedo values of different cultivars of wheat, barley and sunflower crops widely grown in Thrace part of Turkey; (ii) to examine the effect of phenological stages on these albedo values; (iii) to estimate the relationship between leaf area index as growth indicator and their albedo values; (iv) to determine the effect of rainy/dry days on crop surface albedo.

MATERIALS AND METHODS

Research Site

The experimental studies were carried out at the fields (41°41'56''N, 27°12'39'' E, 171 m asl) of Atatürk Soil, Water and Agricultural Meteorology Research Institute (ASWAM) located at the Kırklareli city in Thrace part of Turkey (Fig. 1). The measurements were made during two growing periods of winter wheat and barley (WB1: 2014/15 growing period, WB2:2016/17 growing period) and sunflower (SF1: 2016 growing period, SF2: 2018 growing period) on the experiment fields. The six experimental plots were established on the fields of the ASWAM. Fig. 2 shows the location of trial plots and measurements. Furthermore, some physical and chemical properties of the soils at the research area are given in Tab. 1.

Albedo measurements were made in the six plots. The dimensions of each plot were 35x35 m. (1225 m^2). There was a distance of 1 m between the plots.

Wheat (*Triticum aestivum*) cultivars, Gelibolu (WW_g), Selimiye (WW_s), Bereket (WW_b), Pehlivan (WW_p), Kate1A (WW_k); barley (*Hordeum vulgare*) cultivar, Bolayır (BR_b), and sunflower (*Helianthus annuus*) cultivars, Sanay (SF_s), Pioneer (SF_p), Tunca (SF_t) widely grown in Thrace part of Turkey were used for albedo measurements. Wheat-sunflower rotation applied in the trial plots.

Sunflower fertilization was performed with 100 kg ha^{-1} diammoniumphosphate (18-46-0) as base fertilizer

Fig. 1. Location of experiment field (The map is rearranged from the Google Earth).

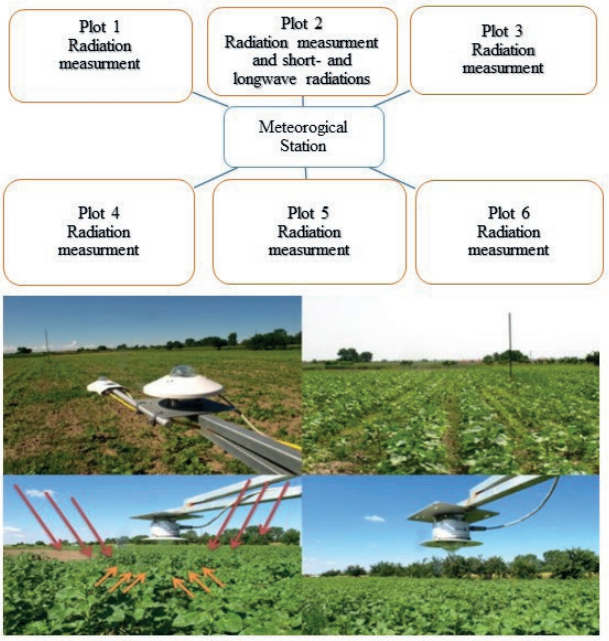

Fig. 2. Trial plots and radiation measurements.

and 100 kg ha^{-1} urea in hoeing. 150 kg ha^{-1} diammoniumphosphate (18-46-0) as base fertilizer, 150 kg ha^{-1} urea in tillering period and 100 kgha^{-1} urea fertilizers were applied for wheat and barley during the growing period.

Observations and measurements

The experiemental studies were carried out at six plots. In only one of these plots, incoming radiation was measured by using the upward-facing pyranometer (Kipp&Zonen, CMP6). At the same plot, incoming and outgoing short- and longwave radiations were measured using the four components radiation sensor (Kipp&Zonen, CNR4). In the other plots, the reftected radiations from the surfaces were measured using inverted (downward) pyranometers (Kipp&Zonen, CMP6). Surface albedo is calculated as the ratio of outgoing and incoming radiations. Data from all sensors were recorded by a datalogger at the agrometeorological station in a tower placed between the plots. The measurement system consisted of the temperature and relative humidity meter (Hygromer MP100A, Rotronic Instr. Corp., at 2 m), the rain gauge (TE525 Tipping Bucket Rain Gauge, Campbell Sci., at 1 m), the four component radiation sensor (Incoming-Outgoing Short and Longwave Radiation; CNR4, Kipp&Zonen), seven pyranometers (Kipp&Zonen, CMP6), the anemometer (#NRG40C, at 2 m) and wind vane sensor (#NRG200P, NRG Systems, at 2 m), the soil water content sensor (TDR, Campbell Sci. at 30 cm depth), the soil temperature sensors (at 5, 10, 20 cm depths), the data logger (CR1000, Campbell Sci.), the multiplixer (Campbel Sci.). Albedo measurements were installed at 1.75 m above soil surface for winter wheat, barley and 2.25 m for sunflower. Additionally, LAI was measured using the radiation-based Plant Canopy Analyzer (LI-COR, 2200C) in an interval of two weeks. Phenological stages (BBCH scale) of crops were observed and recorded during the growing periods. Furthermore, all meteorological data were measured in an interval of 1 s and recorded every 30 min.

Table 1. Physical and chemical properties of the soil in the experiment field.

Soil Depth (cm.)	Saturation (%)	pH	Total Salt (%)	Lime ($CaCO_3$) (%)	Organic Matter (%)	P_2O_5 ($kgha^{-1}$)	K_2O ($kgha^{-1}$)	Soil Structure			Soil Type	Field Capacity (%)	Wilting Point (%)
								Clay (%)	Silt (%)	Sand (%)			
0-30	40	7.20	0.03	6.0	0.77	186.9	670.3	22.92	35.42	41.67	Loam	25.31	15.31
30-60	49	7.50	0.03	6.0	0.54	207.7	350.4	20.83	22.92	56.25	Sandy-Clay-Loam	22.31	14.27
60-90	44	7.49	0.03	5.0	0.45	282.7	227.6	12.50	20.83	66.67	Sandy-Loam	17.91	10.78

RESULTS AND DISCUSSION

In this study, the changes in the actual albedo values of different winter wheat, barley and sunflower cultivars grown in the Thrace region of Turkey under the conditions (climate, soil, crop) during the development period were determined by field measurements for the first time. In addition to the albedo measurements, the LAI values of the crops were also measured. After that, first, the albedo differences between crop cultivars; then, the change of albedo values according to phenological stages and finally the relationships between albedo and other factors such as LAI, precipitation were determined.

Development of crops

Information on the phenological stages observed in the development period of the crops are given below in the Tab. 2. Additionally, SF_t cultivar could not provide homogeneous and sufficient emergence during the germination period at the beginning of the SF1 period. Therefore, SF_t was planted again and late in this period. In this context, the phenological stages and growth of SF_t in the SF1 period were different from the other cultivars.

Meteorological variables

The temporal variations of meteorological variables measured on the field during WB1 period for winter wheat and barley cultivars are given in Fig. 3. In WB1 (between 14 November 2014 and 17 June 2015), the average, maximum and minimum temperatures were 9.9, 25.2 and -6.8 °C, respectively. The total precipitaion amount during that period was 460.4 mm with a daily maximum of 61.2 mm. Furthermore, the average volumetric soil water content between 0 and 30 cm depths was 19 % with a maximum of 24.7 % and with a minimum of 11.4 %. Additionally, net radiation in WB1 ranged from -62.2 to 195.4 W m^{-2} with an average value of 65.8 W m^{-2}. The average global solar radiation was 142.2 W m^{-2} and changed between 9.6 and 355.2 W m^{-2} throughout WB1. The average relative humidity in WB1 was 76.2%.

The amount of precipitation (366. 3 mm) during WB2 was 20.44% less than the total precipitation amount of WB1 (Fig. 4). Therefore, WB2 period was drier than WB1 period. The average daily precipitation amount was 1.5 mm throughout the WB2 period and the daily maximum precipitation was measured as 51.0 mm. Due to the scarcity of rainfall in the WB2 period,

Table 2. Phenological stages of crops.

Plants Stage	Phenological Stages (Date)								
	S	*G*	*TL*	*T*	*SF*	*HE*	*F*	*M*	*H*
WB1	14 Nov.	24 Nov	08 Dec.	10 Feb.	27 Mar.	08 May	18 May	04 June	17 June
WB2	26 Oct.	11 Nov.	02 Dec.	23 Feb.	23 Mar.	03 May	20 May	05 June	29 June
	S	*G*	*L*	*I*	*F*	*M*	*H*		
SF1 (SF_s SF_p)	08 Apr.	14 Apr.	16 May	17 Jun.	24 Jun.	14 Jul.	05 Sep		
SF1 (SF_t)	31 May	10 Jun.	24 Jun	14 Jul.	05 Aug.	18 Aug.	24 Sep.		
SF2	25 Apr.	04 May	18 May	19 Jun.	28 Jun.	23 Jul.	04 Sep.		

S: Sowing; ***G***: Germination; ***TL***: Third leaf; ***T***: Tillering; ***SF***: Stem formation; ***HE***: Head Emergence; ***F***: Flowering; ***M***: Maturity; ***H***: Harvest, ***L***: Leaf initiation; ***I***: Immature bud; ***F***: Flowering; ***M***: Maturity; ***H***: Harvest.

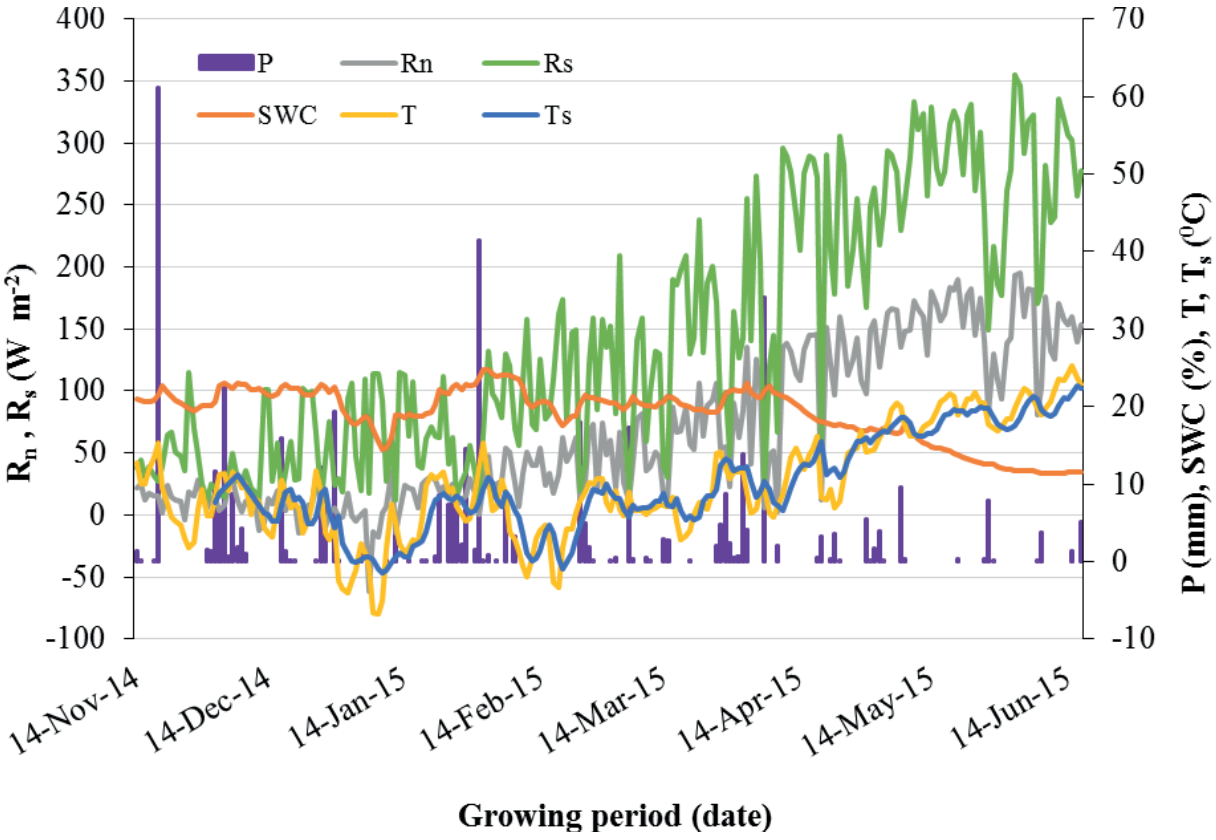

Fig. 3. Time series of meteorological variables during WB1 growing period.

the soil water content was also lower than in the WB1 period. Average soil water content was 17% in WB2. Soil water content varied between 13.5% and 21.2% during this period. Less precipitation led to a decrease in cloudiness and more net radiation in the WB2 period. Therefore, the average net radiation in the WB2 period was determined as 71.9 W m^{-2}. Daily average net radiation varied between -24.3 and 211.3 W m^{-2} during this period. In WB2, the daily average temperature was 9.8, and the maximum and minimum temperatures were 29.7 and -8.4 °C, respectively. The daily average soil temperature was determined to be slightly higher than the air temperature (10.3 °C). During the WB2, the minimum and maximum soil temperatures varied between -17.3 and 36.3 °C. Furthermore, global solar radiation was also higher in WB2 period than WB1. Average global solar radiation in WB2 was measured as 155.4 W m^{-2} varied between 11.1 and 348.1 W m^{-2}. The time series of the measured daily average relative humidity in the WB2 period were 75.9%, respectively. As can be seen in the Fig. 3 and 4, the average air temperature of wheat and barley in the first growing period (WB1) was slightly higher than in the second period (WB2). Furthermore, total rainfall in the WB1 was 25.7% more than WP2 measured rainfall. Additionally, the average soil water content in the WB1 was 2 % more than WB2. In contrast, average global solar radiation in the WB1 was about 9.3 % less than WB2.

The first growing period of sunflower (SF1) was in 2016 and the second (SF2) was in 2018. During the SF1 period, the total amount of precipitation was 146.7 mm. The temporal distributions of meteorological variables are shown in Fig. 5. In SF1, the average and maximum of the daily total precipitation amounts were 0.9 and 30.2 mm, respectively. The average soil water content was 11.3% in the SF1 period changed between 7 and 24.5%. This situation shows that the crop was under water stress in different phenological stages. The average of daily net radiation was 120.4 W m^{-2} during this period and varied from 15.4 to 183.3 W m^{-2}. During the SF1 period, the average air- and soil temperatures were 21.3 and 20.9 °C, respectively. Additionally, the average of the global solar radiation in SF1 was 248.3 W m^{-2} and varied between 62.1 and 344.4 W m^{-2}.

The total amount of precipitation was 210 mm during the SF2 and this period was more humid compared

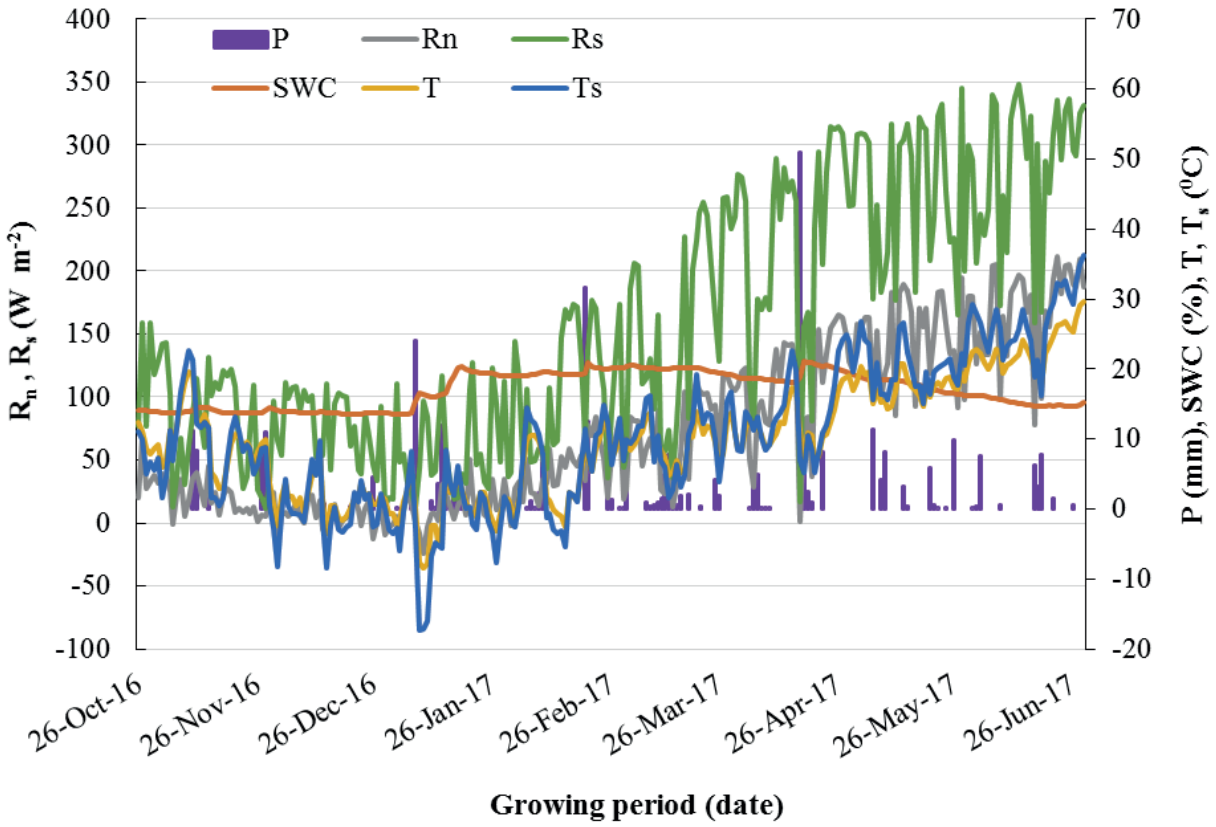

Fig. 4. Time series of meteorological variables during WB2 growing period.

to SF1. In the SF2 'period, the average of daily total precipitation was 1.6 mm and it was 0.7 mm day^{-1} more than SF1. During this period, the maximum total precipitation per day was recorded as 23.5 mm. The temporal distributions of meteorological variables are given in Fig. 6. The average soil water content (18.5%) in this period was considerably higher than in the SF1 period. Additionally, average net radiation during SF2 period was about 28% more than SF1. The lowest daily average net radiation was measured as 35.8 and the maximum value was 230.0 W m^{-2}. Average air- and soil temperatures in SF2 period were higher than in SF1 period. Therefore, SF2 period was a warmer period than SF1. In addition to these, the average, minimum and maximum values of the global solar radiation value during the SF2 period were determined as 266.1, 75.4 and 356.4 W m^{-2}, respectively.

Albedo of winter wheat and barley

It was necessary to determine how albedo values chance in our country by making measurements for different cultivars. In both development periods (WB1 and WB2), one barley and five wheat cultivars were grown in the trial plots. The distribution of the measured albedo values during the day in both growing periods was examined. Although the same cultivars of wheat and barley were grown in both growing periods, hourly averages of albedo values were not the same. Hence, it was determined that the barley had higher albedo values than the wheat cultivars in both periods.

In both periods, albedo had higher values at sunrise and sunset hours compared to midday. This was related to the angle of incidence of the sun. Similar relationships to the temporal change of the albedo found in this study during the day were also emphasized by Impens and Lemeur (1969).

The average albedo values of cereal crops for the WB1 were determined as 0.190 for WW_g, 0.203 for WW_s, 0.183 for WW_b, 0.171 for WW_p, 0.181 for WWk and 0.214 for BR_b cultivars. In the Tab. 3, the albedo values in WB1 are given according to their phenological stages during the growing period from sowing to harvest. Low albedo values were observed on the bare soil surface during the planting of the crops. Additionally, it was

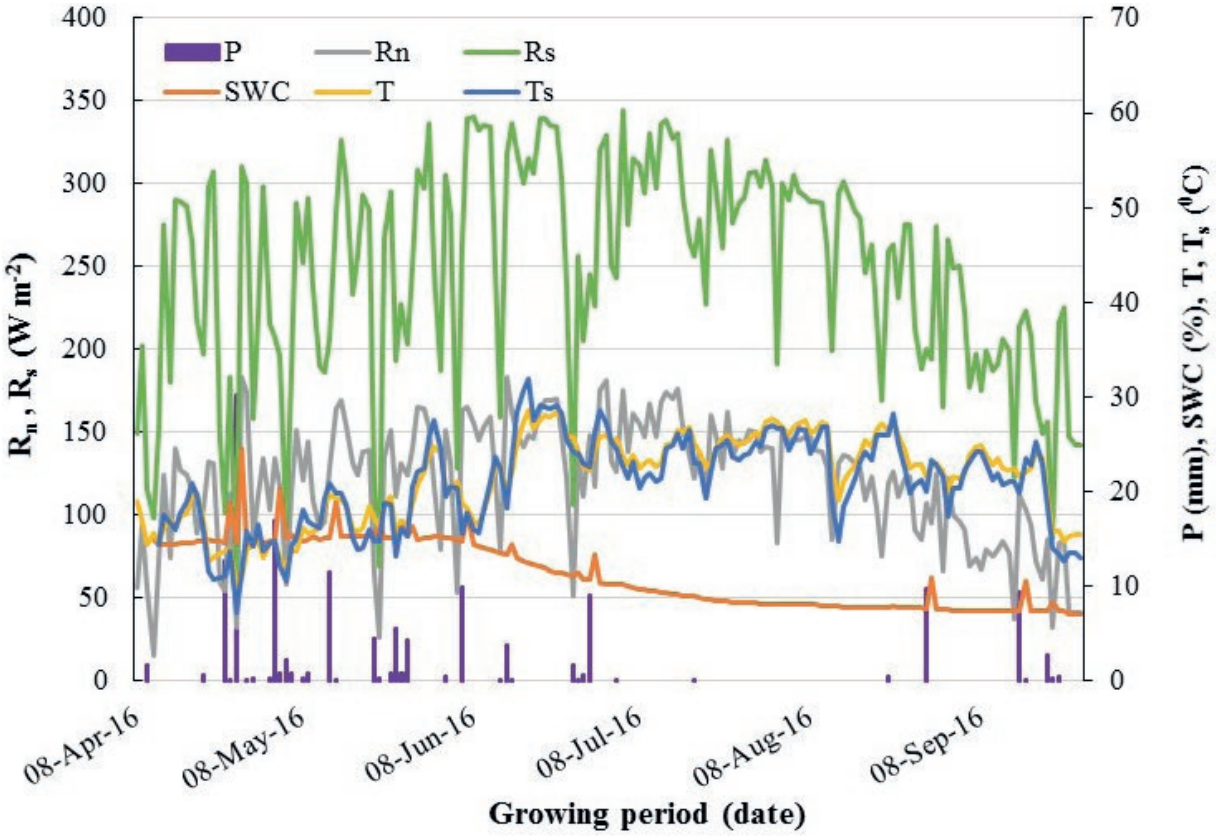

Fig. 5. Time series of meteorological variables during SF1 growing period.

determined that the albedo values increasing with the emergence of the crops have different values according to their phenological stages.

Additonally, it was determined that the average albedo values of wheat cultivars ranged from 0.171 to 0.203 throughout WB1 (Fig. 7). Furthermore, the average albedo for five cultivars of wheat was 0.185 for all days (rainy and non-rainy (dry) days). Simularly, average barley's albedo changed between 0.144 and 0.261. As can be seen from the values, the average albedo values differ between wheat and barley cultivars during the growing stages.

Fig. 7. Time series of daily average albedo and daily total precipitation during WB1.

In order to understand the effect of rainy and dry days on the albedo of crop cultivars, the albedo values on rainy (≥1 mm d^{-1}) and dry days (<1 mm d^{-1}) were determined. On the rainy days, average albedo values for five cultivars of winter wheat was 8.4 % less than the average albedo in the dry days in WB1. On the rainy days, albedo values of wheat were a little bit decreased and average albedo of all wheat cultivars changed from 0.165 to 0.190. The average barley's albedo was 0.199 on rainy days in WB1. On dry days, average albedo varied from 0.171 to 0.205 for all wheat cultivars and it was 0.221 for barley in WB1. The average albedo value of barley for all data was determined to be about 13.1 % higher than the average of wheat cultivars.

The effect of bare soil on albedo decreased as the plant's surface coverage increased in WB1. During sowing (S) and germination (G) stage in WB1, the surface albedo changed between 0.121 and 0.152 for all wheat cultivars for all data when it varied from 0.087 to 0.112 with the effect of soil water content on the rainy days. This value was 0.106 in barley variety on rainy days during S-G stage. With the emergency of the wheat to the surface, albedo of winter wheat and barley increased. Between S and G stages in the WB1 period, the maximum albedo value was determined as 0.152 for WW_s and the minimum albedo was 0.121 for WW_p. In all wheat cultivars except WW_k and WW_g, the maximum albedo value occurred between stem formation (SF) and heat emergence (HE) phenological stage. In this period, the maximum average albedo in the period of SF-HE

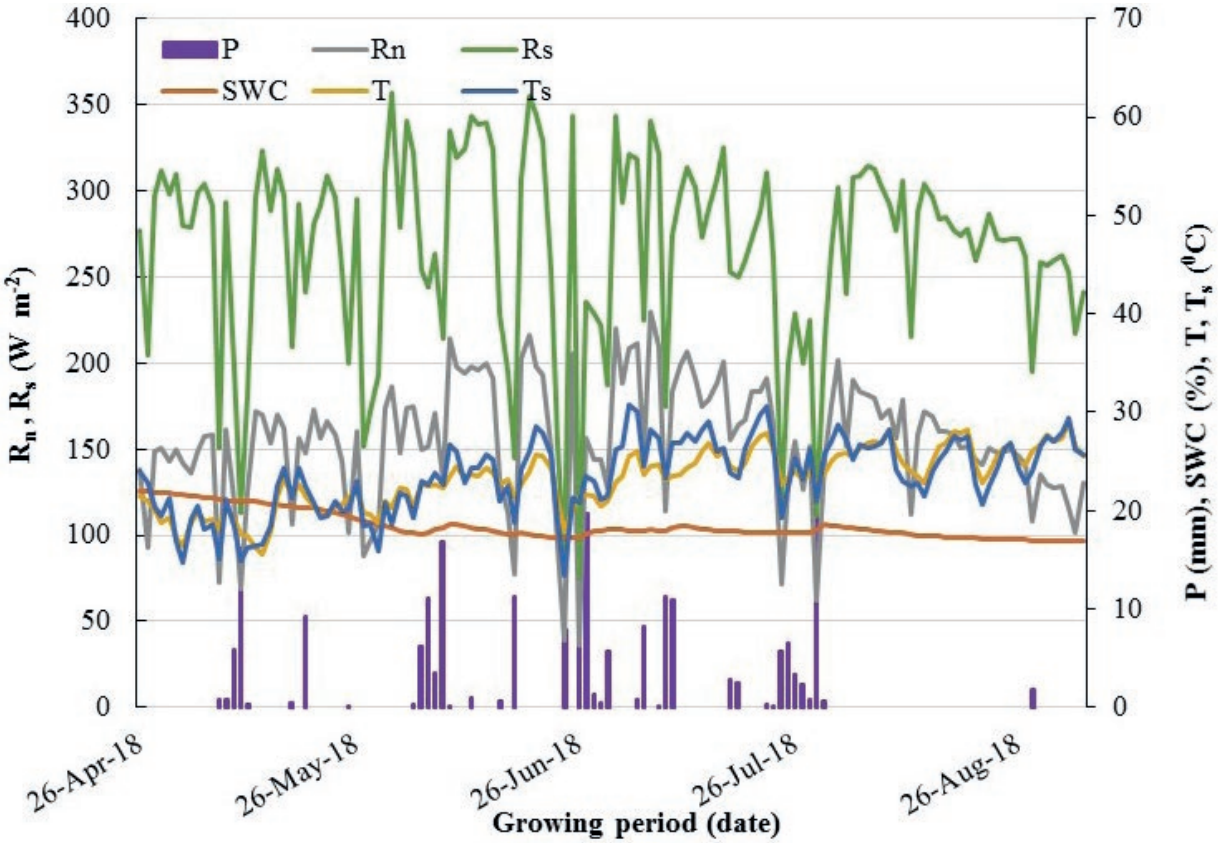

Fig. 6. Time series of meteorological variables during SF2 growing period.

Table 3. Albedo values of winter wheat and barley cultivars in WB1 according to phenological stages.

	S-G	*G-TL*	*TL-T*	*T-SF*	*SF-HE*	*HE-F*	*F-M*	*M-H*	Average
WW_g	0.136	0.164	0.176	0.184	0.219	0.223	0.216	0.199	0.190
WW_s	0.152	0.181	0.194	0.206	0.247	0.236	0.207	0.204	0.203
WW_b	0.134	0.162	0.180	0.198	0.227	0.217	0.181	0.164	0.183
WW_p	0.121	0.144	0.160	0.170	0.200	0.196	0.194	0.181	0.171
WW_k	0.125	0.144	0.157	0.182	0.210	0.212	0.218	0.198	0.181
BR_b	0.144	0.183	0.203	0.220	0.258	0.261	0.225	0.214	0.214

was determined as 0.247 for WW_s. For WW_k, the maximum average albedo value was determined as 0.218 in the period from flowering (F) to maturity (M). Furthermore, for Barley (BR_b) in WB1 period, the maximum average albedo value was measured as 0.261 between HE and F phenological stages. The maximum albedo of barley was higher than the wheat cultivars. Additionally, albedo values measured on dry days were determined to be higher than those on rainy days. On dry days in WB1, the highest albedo value was determined as 0.252 between SF-HE stage for WW_s, while the lowest albedo value was determined as 0.127 for the WW_p. Furthermore, increasing soil water content with the effect of rainfall and wetting of the crop surface caused the albedo value to decrease as expected.

The average albedo values for WB2 were calculated as 0.180 for WW_g, WW_b, 0.176 for WW_s, 0.181 for WW_p, WW_k and 0.187 for BR_b (Tab. 4). The average albedo (0.180) of the wheat cultivars in WB2 was less than the average albedo (0.185) in WB1. During the WB2, the average wheat albedo varied from 0.176 to 0.187 (Fig. 8). Most of the wheat cultivars reached their maximum in the WB2 period between HE and F stage except WW_p. However, this time the maximum wheat albedo was determined as 0.227 for WW_p. The same maximum value for BR_b was measured between SF and HE phenological phase.

In the WB2 period, the average albedo on rainy days (for all wheat cultivars) was determined as 7.87% less than the average albedo on dry days. This is because the albedo of the water is less than the albedo of the plants. In addition, the fact that the amount of rainfall in the WB2 period is less than in the WB1 period

Table 4. Albedo values of winter wheat and barley cultivars in WB2 according to phenological stages.

	S-G	*G-TL*	*TL-T*	*T-SF*	*SF-HE*	*HE-F*	*F-M*	*M-H*	Average
WW_g	0.151	0.156	0.156	0.166	0.214	0.218	0.197	0.181	0.180
WW_s	0.140	0.148	0.152	0.172	0.219	0.221	0.194	0.158	0.176
WW_b	0.154	0.159	0.160	0.173	0.221	0.221	0.202	0.153	0.180
WW_p	0.148	0.150	0.153	0.181	0.227	0.222	0.203	0.166	0.181
WW_k	0.148	0.154	0.154	0.168	0.216	0.224	0.210	0.174	0.181
BR_b	0.144	0.154	0.157	0.178	0.227	0.226	0.222	0.188	0.187

might be one of the reasons why the albedo values in dry days were high in WB2. This was because increasing soil moisture, cloudiness can lead to decrease the albedo of surface. Approximately 24% of the WB1 and 20% of the WB2 consisted of rainy days. In WB2, the average albedo values of all wheat cultivars with growth stages were calculated as 0.148 for S-G; 0.153 for G and third leaf (TL); 0.155 for TL-tillering (T); 0.172 for T-SF; 0.219 for SF-HE; 0.221 for HE-F; 0.201 for F-M and 0.166 for M-Harvest (H) phenological stages.

As a result, it has been determined that the albedo values of five wheat cultivars were different in the phenological stages of WB1 and WB2. The reason for the low albedo that occurs during periods of rainfall can be explained by the increase in the water content of the soil with the rainfall and the fact that the soil reflects less radiation and its color turns dark. It was observed that the albedo of wheat and barley suddenly decrease on the days when there was precipitation in both growing periods. For this reason, deviations of albedo values from the mean were high in phenological stages when the number of rainy days was high. Barley and wheat cultivars attained the highest reflectance values in both periods during SF and F. The reason for this was the increase in canopy development, LAI and soil coverage in this period. In addition, as well as color changes of plant organs expecially leaves caused an increase in albedo values. In general, there was a trend towards a decrease in albedo values after HE stage. Likewise, the albedo value has an increasing trend from G to HE phases.

Although Oguntunde and Van de Giesen (2004) found different albedo values for six different cereal cultivars according to phenological periods, they could not detect a significant difference between the albedo coefficients. However, unlike Oguntunde and Van de Giesen (2004), in this study, albedo differences were determined between wheat and barley culitivars. The differences between determined albedo values in WB1 and WB2 periods (WB1-WB2) for wheat and barley are given in the following Fig. 9. When we anayzed the differences in the measured albedo values of winter wheat in different phenological stages in both development periods (WB1-WB2), it was determined that the greatest albedo difference for WW_p and WW_k cultivars was in the S-G period. For WW_g, WW_s and BR_b, the highest differences were detected in TL-T stage. As can be seen in Fig. 9, the albedo values measured in the WB1 period are generally higher than the albedo in WB2 except between the S and G phenological stage.

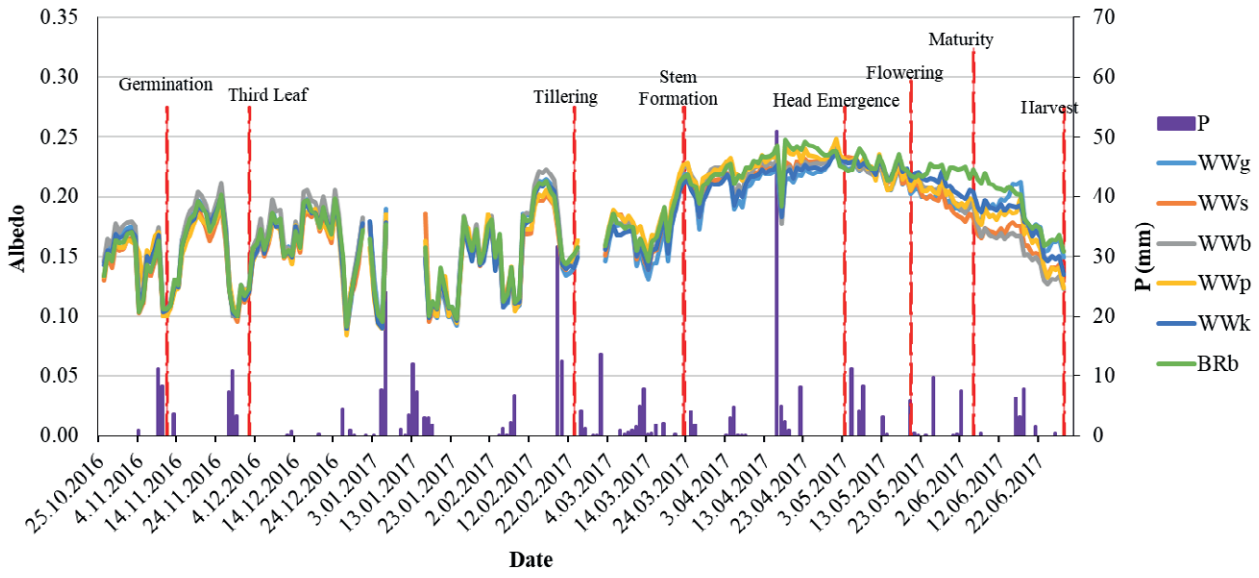

Fig. 8. Time series of daily average albedo and daily total precipitation during WB2.

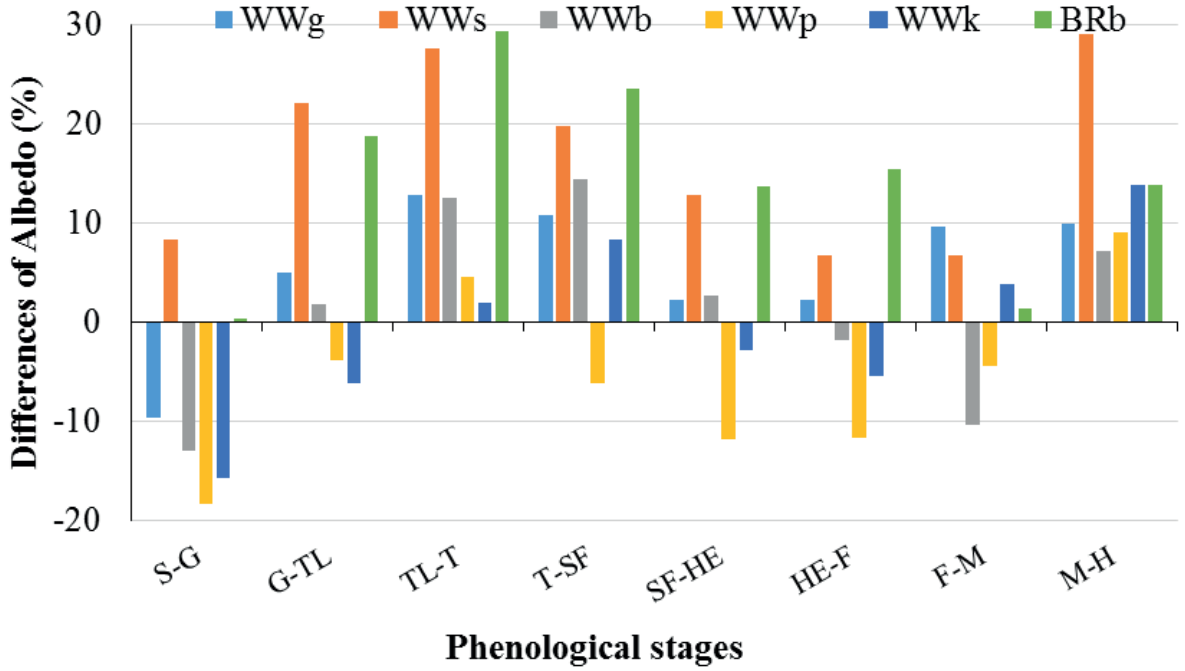

Fig. 9. Differences (WB1-WB2) in albedo values of winter wheat and barley cultivars.

Albedo of sunflower

The albedo values during the SF1 and SF2 growing periods changed asymmetrically during the daytime. The reason for the increase in the albedo at sunrise and sunset hours is the angle of incidence of the sun. The albedo values of sunflower cultivars with growth stages from the sowing to the harvest of SF1 and SF2 are shown in Tab. 5 and 6. Low albedo values were observed on the bare soil surface during the planting of the crops. It was determined that the albedo values increasing with the emergence of the crops. Considering the phenological development periods, although three cultivars of sunflower had different albedo values, they had a similar trend. The average albedo values of sunflower for the SF1 period were measured as 0.186 for SF_s, 0.189 for SF_t and 0.187 for SF_p (Tab. 5). The average albedo values of sunflower cultivars in SF2 period were determined as 0.172 for SF_s, 0.178 for SF_p and 0.164 for SF_t (Tab. 6). There was no significant difference between albedo values except SF_t. Futhermore, albedo values in SF2 were determined to be slightly lower than SF1 period albedo. This might be due to the fact that the SF2 development period was more rainy (210 mm) compared to the SF1 period (147.6 mm) and consequently the soil water content was higher.

Albedo values were determined according to the phenological stages of the sunflower, too. It has been determined that the sunflower had different albedo values in different phenological stages. Time series of daily average values of albedo measurements in SF1 and SF2 are shown in Fig. 10 and 11. The reason for the low albedo occurring during the rainy periods in SF2 can be explained by the increase in the water content of the soil as a result of the rainfall and the less reflection of the incoming energy.

Table 5. Average albedo values in different phenological stage in SF1.

	S - G	*G - L*	*L - I*	*I - F*	*F - M*	*M - H*	Average
SF_s	0.159	0.181	**0.212**	0.200	0.185	0.180	0.186
SF_p	0.164	0.184	**0.210**	0.200	0.186	0.176	0.187
SF_t	0.164	0.197	**0.199**	0.197	0.196	0.178	0.189

Table 6. Average albedo values in different phenological stage in SF2.

	S - G	*G - L*	*L - I*	*I - F*	*F - M*	*M - H*	Average
SF_s	0.157	0.160	0.186	**0.189**	0.177	0.156	0.171
SF_p	0.168	0.170	**0.196**	0.191	0.187	0.157	0.178
SF_t	0.150	0.157	0.179	**0.181**	0.171	0.146	0.164

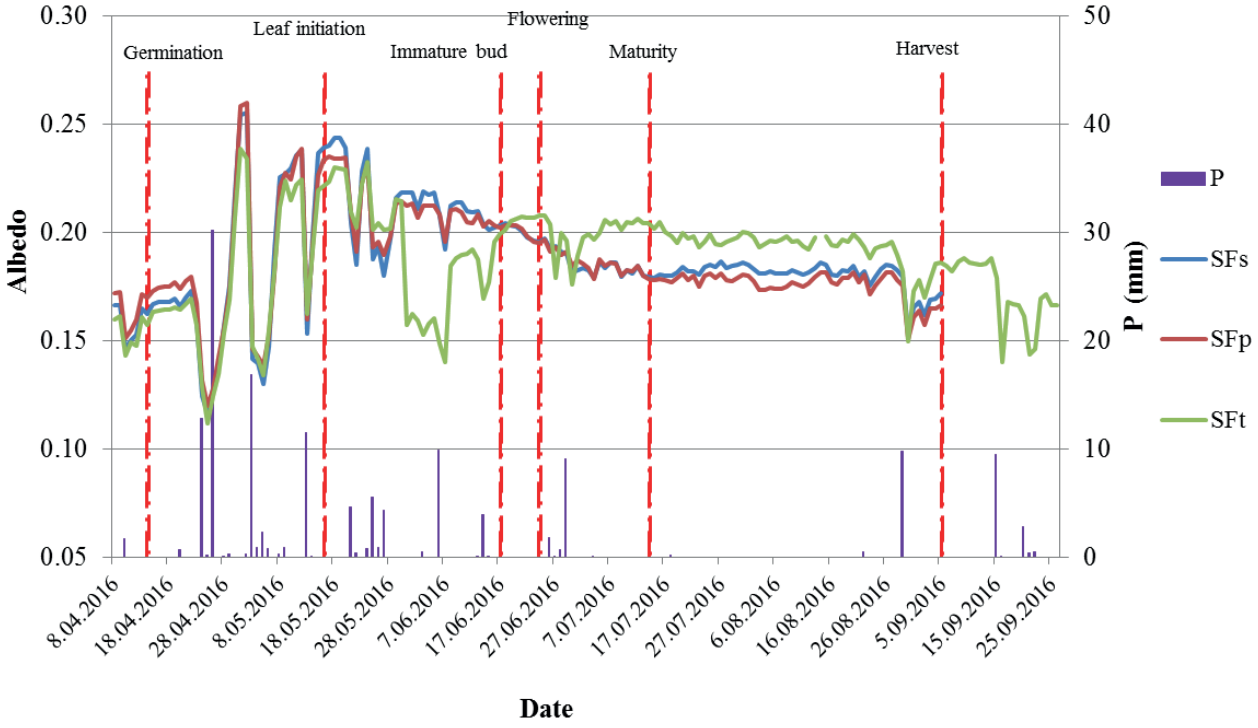

Fig. 10. Time series of daily average albedo and daily total precipitation during SF1.

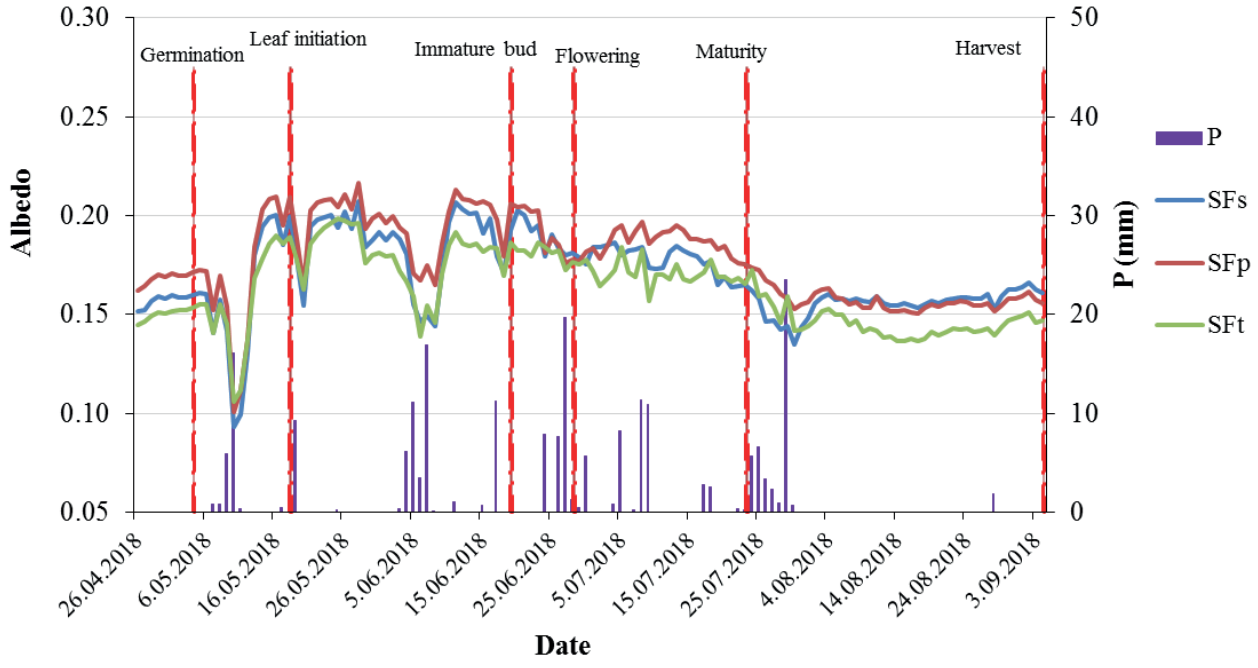

Fig. 11. Time series of daily average albedo and daily total precipitation during SF2.

In SF1, the albedo varied from 0.159 to 0.212 for SF_s; from 0.164 to 0.210 for SF_p and from 0.164 to 0.199 for SF_t. Maximum albedo value in SF1 was determined between leaf initiation (L) and immature bud (I) phenological stage for all three sunflower cultivars. Although the highest albedo was determined for SF_s, there were

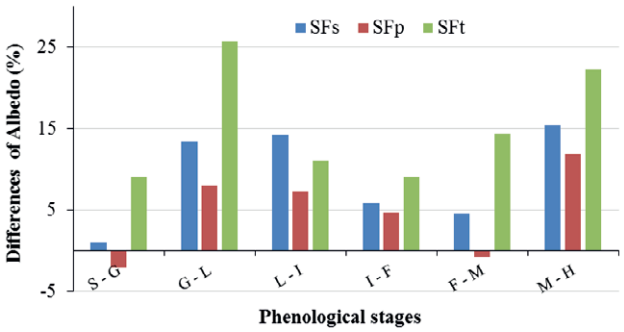

Fig. 12. Differences (SF1-SF2) in albedo values of sunflower cultivars.

minor differences between the maximum values of the cultivars. They changed between 0.199 and 0.212 for sunflower cultivars. The average albedo of sunflower on rainy days in the SF1 period was about 7.5% lower than the albedo for all the data (rainy and dry days). When the albedo values in SF1 on dry days were analyzed, albedo values increased in all cultivars and the average albedo value was calculated as 0.189.

In SF2, the albedo varied from 0.157 to 0.189 for SF_s; between 0.168 and 0.196 for SF_p and between 0.150 and 0.181 for SF_t. The average albedo of all three cultivars in the SF2 period was 0.171 for all data, 0.173 for dry days (low soil moisture) and 0.162 for rainy days (high soil moisture). The maximum albedo of sunflower determined between immature bud (I) and flowering (F) stage except for SF_p (L-I). In SF2 period, similar to SF1; albedo values on rainy days were about 5.3% lower. On dry days, the average albedo value rised up to 0.173. As seen in Tab. 6, during the SF2, maximum albedo values varied between 0.181and 0.196 for all cultivars. It was determined the highest albedo for SF_p variety in SF2.

Comparing the albedo values obtained in two growing periods for all sunflower cultivars in different phenological stage, the biggest difference in the albedo occurred in the G-L phase. The difference between the albedo values of SF_s and SF_t cultivars determined in both periods was minimum on S-G stage. The difference between the albedo values of both growing periods was calculated as the smallest (4.83%) for the SF_p and the highest (15.25%) for the SF_t (Fig. 12).

The average albedo was 0.179 for SF_s, 0.183 for SF_p and 0.177 for SF_t, when the average values of both periods for all three cultivars were analyzed. Additionally, considering the average albedo values in both periods, they ranged from 0.157 to 0.212 for SF_s; from 0.164 to 0.210 for SF_p and from 0.150 to 0.199 for SF_t. For all the albedo values of cultivars measured in both periods; average albedo was calculated as 0.160 in S-G; 0.175 in G-L; 0.198 in L-I; 0.193 in I-F, 0.184 in F-M and 0.166 in M-H stages.

Although the average albedo values determined for all growing periods of different cultivars did not change much, differences were determined in albedo values according to phenological periods.

Average albedo values of all growing periods of winter wheat, barley and sunflower cultivars were found as 0.185 for WW_g, 0.189 for WW_s, 0.182 for WW_b, 0.176 for WW_p, 0.181 for WW_k, 0.200 for BR_b, 0.179 for SF_s, 0.176 for SF_t and 0.182 for SF_p, respectively. The variation of average, maximum and minimum albedo values of all periods for all crops are given in Fig. 13-15.

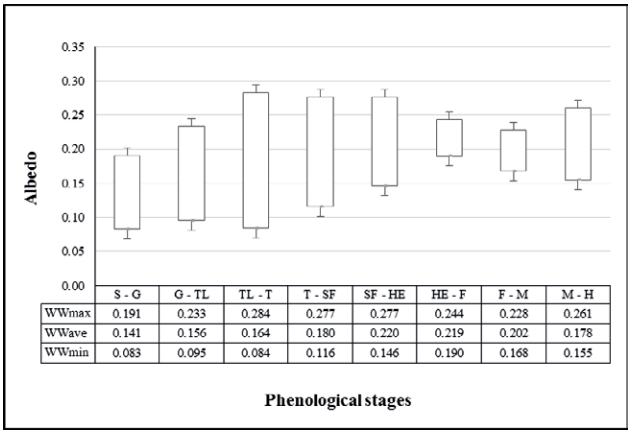

	S - G	G - TL	TL - T	T - SF	SF - HE	HE - F	F - M	M - H
WWmax	0.191	0.233	0.284	0.277	0.277	0.244	0.228	0.261
WWave	0.141	0.156	0.164	0.180	0.220	0.219	0.202	0.178
WWmin	0.083	0.095	0.084	0.116	0.146	0.190	0.168	0.155

Fig. 13. Variation of average (WW_{ave}), maximum (WW_{max}) and minimum (WW_{min}) albedo values of all wheat cultivars for WB1 and WB2 periods.

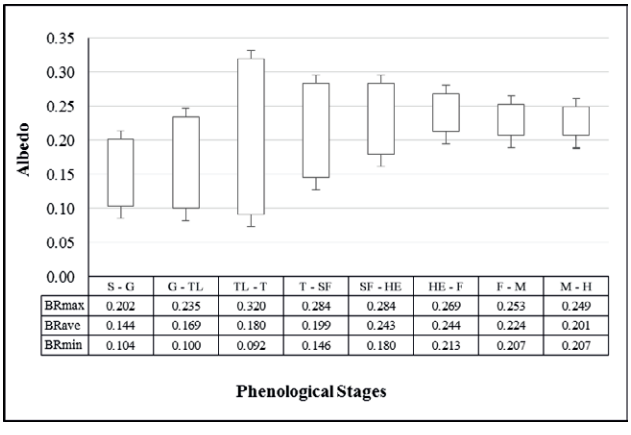

	S - G	G - TL	TL - T	T - SF	SF - HE	HE - F	F - M	M - H
BRmax	0.202	0.235	0.320	0.284	0.284	0.269	0.253	0.249
BRave	0.144	0.169	0.180	0.199	0.243	0.244	0.224	0.201
BRmin	0.104	0.100	0.092	0.146	0.180	0.213	0.207	0.207

Fig. 14. Variation of average (WW_{ave}), maximum (WW_{max}) and minimum (WW_{min}) albedo values of barley for WB1 and WB2 period.

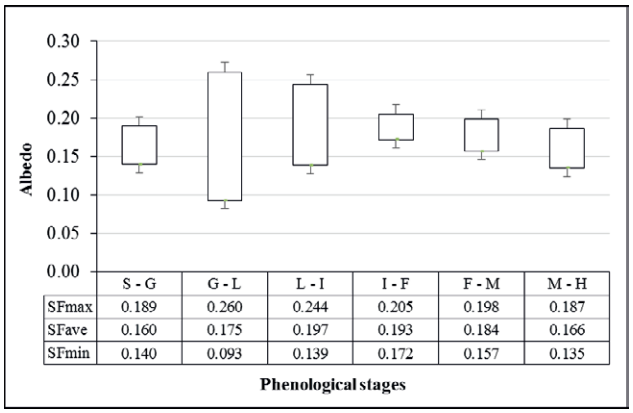

	S - G	G - L	L - I	I - F	F - M	M - H
SFmax	0.189	0.260	0.244	0.205	0.198	0.187
SFave	0.160	0.175	0.197	0.193	0.184	0.166
SFmin	0.140	0.093	0.139	0.172	0.157	0.135

Fig. 15. Variation of average (SF_{ave}), maximum (SF_{max}) and minimum (SF_{min}) albedo values of all sunflower cultivars for SF1 and SF2 period.

Relationship between albedo and LAI

Relationship between albedo and LAI for Winter Wheat and Barley

LAI values of winter wheat and barley cultivars were measured periodically during both growing periods. Although there were differences between the LAI values of the crops, they had a similar time series (Fig. 16 and 17).

The highest LAI was determined in WB1 for BR_b with a value of approximately 4.91 between HE and F phase. In other wheat cultivars, LAI reached its maximum in the same phenological stage, too. The average LAI values in WB1 were 2.11 for WW_g, 2.01 for WW_s, 2.20 for WW_b, 2.17 for WW_p, 2.14 for WW_k and 2.06 for BR_b. Additionally, maximum LAI for WW_g, WW_s, WW_b, WW_p, WW_k and BR_b cultivars were measured as 4.57, 4.48, 4.77, 4.78, 4.44 and 4.91, respectively. Although there were very small differences between LAI of cultivars in the WB2 period, the general LAI pattern showed similar characteristics for all cultivars (Fig. 17). LAI values in this period increased to a maximum of 7.1. All wheat and barley cultivars had similar tendencies and values. In WB2 period, the highest values were detected between HE and F phenological stage, too. Fig. 18 shows the relationships between measured albedo values of wheat, barley cultivars and LAI values for both growing periods.

Statistically significant and strong relationships, which were r^2=0.85 and r^2=0.83, respectively, were found between LAI and albedo for wheat and barley in WB1. Similarly, determination coefficients for both crops in WB2 were calculated as 0.89 and 0.81, respectively. This showed us that even if only LAI value was used as input, the albedo values of these crops can be determined to a great extent.

Relationship between albedo and LAI for Sunflower

LAI values were measured periodically throughout the growing period of SF1, too. However, LAI can not be measured in SF2 because of technical problems. Although there were differences between the LAI of the sunflower cultivars, they had similar characteristics except SF_t. The albedo value of the sunflower, which was approximately 0.15 in the planting stage, increased by maximum 2.7% with the emergence. The highest albedo values varied from 0.21 to 0.232 within three cultivars during the leaf initiation stage (Fig. 19). When the LAI values of sunflower cultivars were examined, it reached the maximum LAI value (up to 3) for the SF_s cultivar and the lowest LAI value was approximately 1.1 in the late planted SF_t cultivar.

Fig. 20 shows the relationship between albedo and LAI of sunflower cultivars grown in SF1. As can be seen in Fig. 20, the determination coefficients between LAI and albedo for SF_p and SF_s cultivars were the same

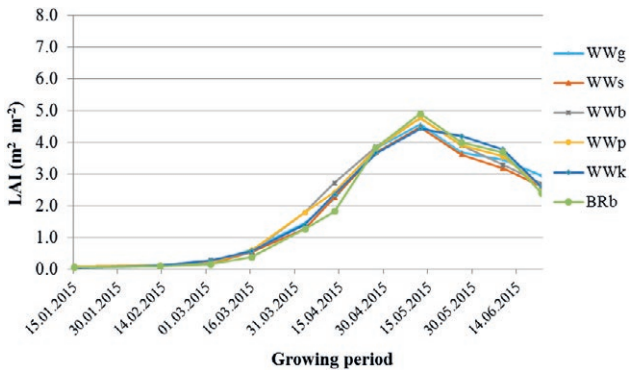

Fig. 16. LAI values of winter wheat and barley cultivars in WB1.

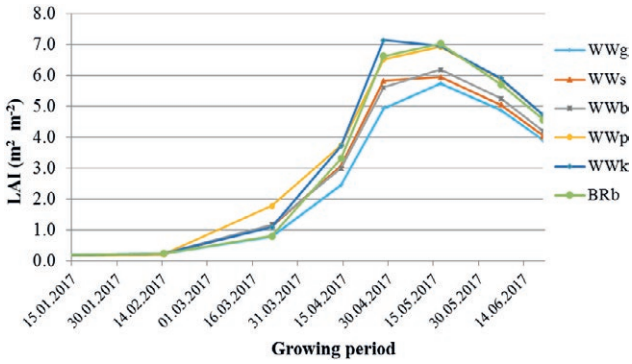

Fig. 17. LAI values of winter wheat and barley cultivars in WB2.

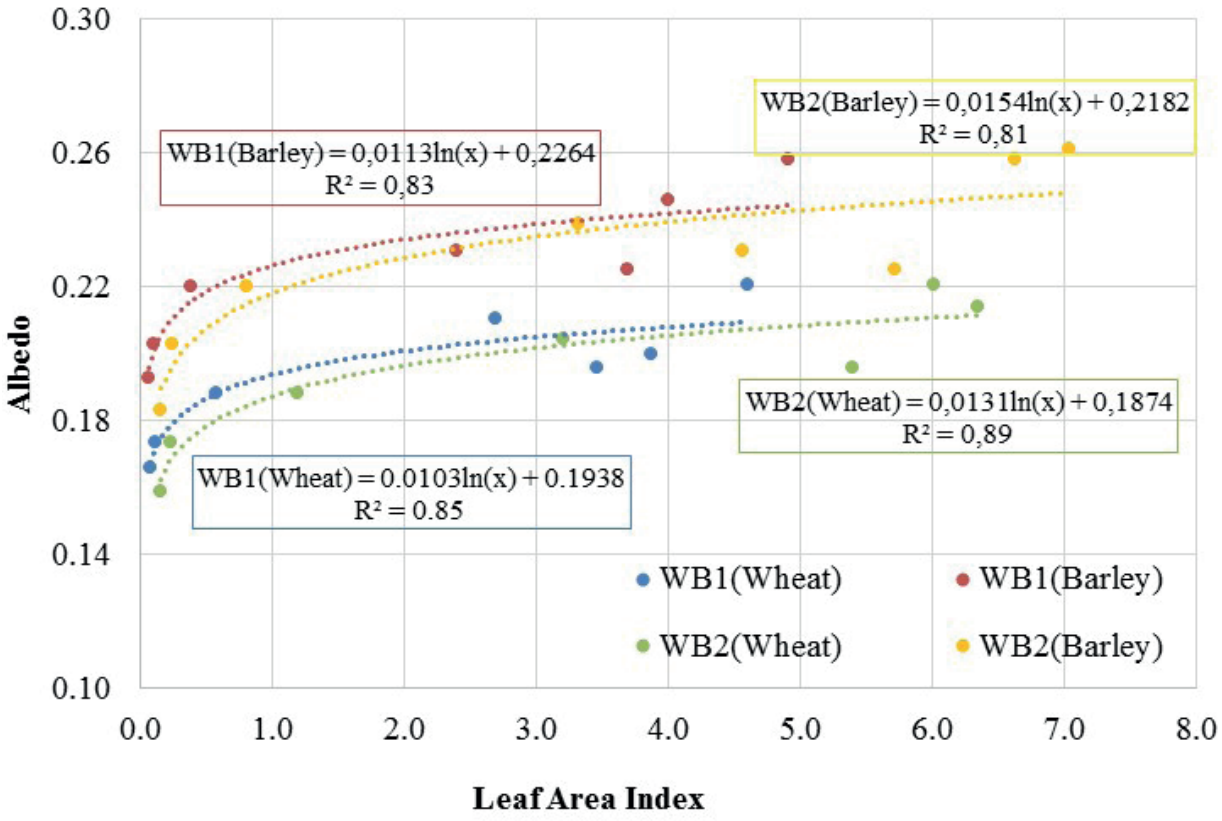

Fig. 18. Relationships between albedo and LAI values for winter wheat and barley cultivars in WB1 and WB2.

as 0.77. However, the weak relationship was estimated between the albedo and LAI for SF_t.

CONCLUSION

In this study, the variation of albedo with growth stages and its relationships with LAI and precipitation (rainy and dry days) were investigated by measuring albedo for winter wheat, sunflower and barley cultivars in Thrace part of Turkey. Other aim of this study was to fill the lack on about the ground albedo observations for widely grown crop cultivars in Thrace part.

Consequently, significant relationships were found between albedo and LAI for wheat and barley cultivars (wheat r^2=0.87, barley r^2=0.82) for whole growing periods. In general, the decrease in the incoming radiation and the high soil water content values caused a decrease in the albedo values on rainy days. Our average albedo values for the growing periods of the five-winter wheat cultivars considered in this study varied from 0.176 to 0.190. These values are similar to Sellers (1965), Kondratyev (1969, 1972), Fritshen (1967), and Pielke (1984); however, it is less than the values specified by Song (1998), Monteith and Unsworth (1990) and Şerban et al. (2011). The reason for these differences might be the diversity in crop cultivars, climatic and soil conditions etc. Similarly, our average albedo value determined for the two growth periods of barley is within the values determined by Frithschen (1967), but it is smaller than the values determined by Monteith and Unsworth (1990). The values determined for sunflower in this study are less than those determined by Gates (1980) and Impens and Lemeur (1969).

As known, many factors influence on the surface albedo. For this reason, determination of the variations of surface albedo with growth stage of crops are important in crop growth, eco-hydrological and climate models. However, it should be noted that all approaches developed for the determination of albedo in models should be based on ground-based observation. For this reason, ground based albedo observation is also necessary for the development of models, too. Furthermore, validation of the albedo values determined by remote sensing with the ground-based observations is extremely important for the comparison of the models of albedo.

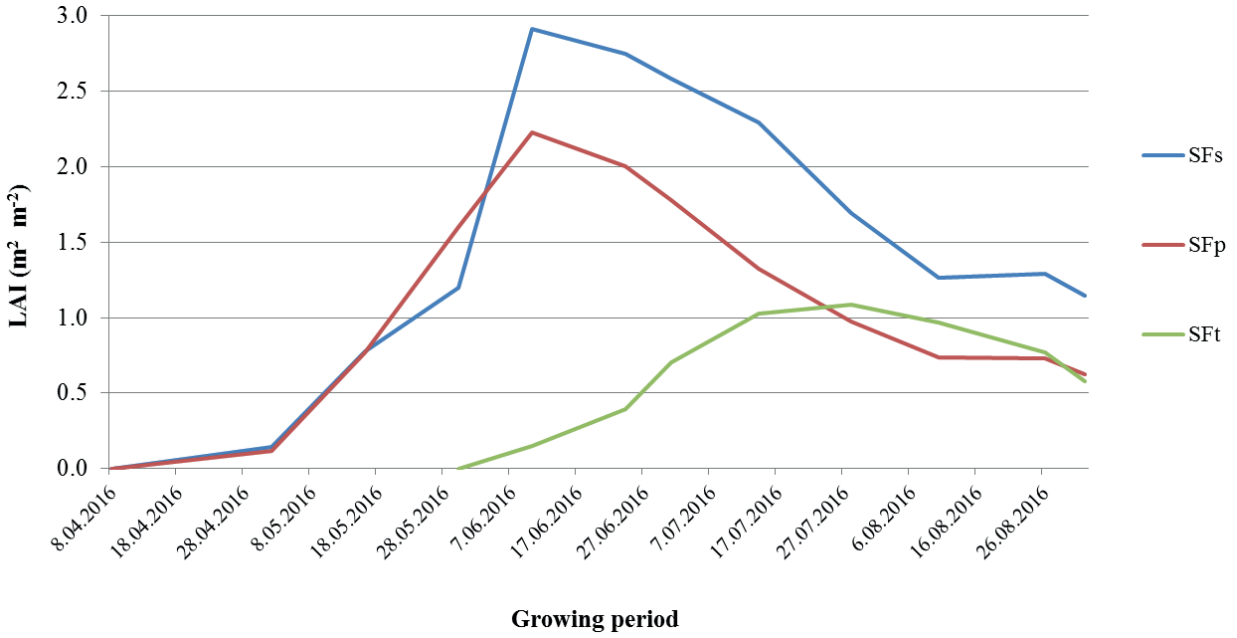

Fig. 19. Time series of the Leaf Area Index during SF1.

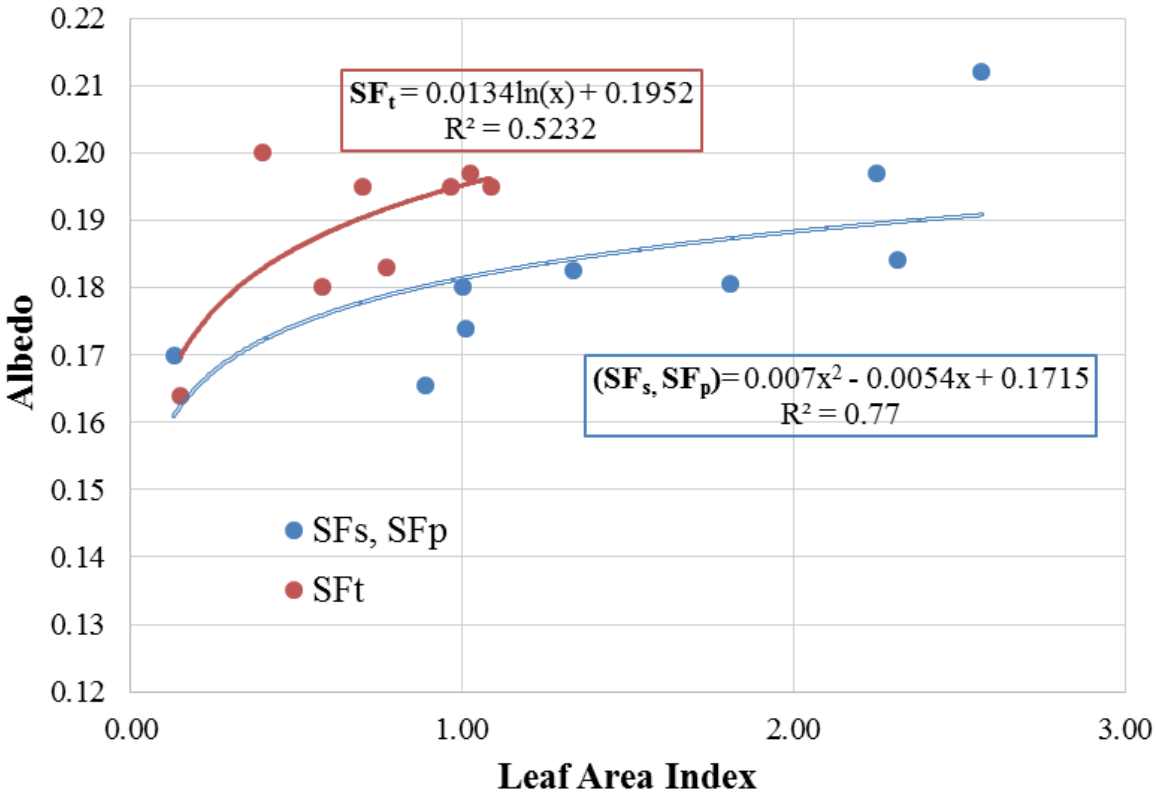

Fig. 20. Relationship between albedo and LAI of sunflower cultivars grown in SF1.

Therefore, ground based albedo observation is very helpful for model studies to enhance the temporal resolution of surface albedo.

As stated before, albedo is a micrometeorological data that is effective in energy balance of the surface, climate change, climate models, remote sensing and many sectors (agriculture, etc). For this reason, this study is going to be useful for researchers and engineers who need albedo data. In addition, it was revealed that the albedo data, which is one of the hypotheses of this study, was not a constant during the whole growing period, but changed with phenological- and growth stages and weather conditions.

We hope that the results of this study will be a reference to experts working in this field and needing this data, both in our country and around the world. In this study, only precipitation and LAI are considered as meteorological and plant growth factors in terms of their effect on albedo. In future studies, it would be useful to consider other factors and/or energy balance components and include remote sensing and climate models.

ACKNOWLEDGEMENTS

This paper was prepared based on certain outcomes by the project (TAGEM/TSKAD/14/A13/P01/06) which was supported by TAGEM (General Directorate of Agricultural Research and Policy), Ministry of Agriculture and Forest, Turkey. We thank to Assoc. Prof. Dr. Barış Çaldağ. Moreover, thanks to Cantekin Kıvrak and Ozan Öztürk for their efforts during the field studies.

REFERENCES

Bowers, S.A., Hanks, A.J. 1965. Reflection of radiant energy from soil. Soil Science, 100: 130-138.

Breuer, L., Eckhardt, K., Frede, H.G. 2003. Plant parameter values for models in temperate climates. Ecological Modelling, 169: 237–293 doi: 10.1016/S0304-3800(03)00274-6.

Dexter, R. 2004. Diurnal and seasonal albedo trends of wheat at the Bratt's Lake observatory, Saskatchewan. Dissertation, Simon Fraser University.

Doughty, C.E., Field, C.B., McMillan, A.M.S. 2011. Can crop albedo be increased throughy the modification of leaf trichomes, and could this cool regional climate. Climatic Change, 104: 3379-387.

Fritschen, L.J. 1967. Net and solar radiation relations over irrigatedfield crops. Agric. Met. 4: 55–62.

Fuller, D.O., Ottke, C. 2002. Land cover, rainfall and land-surface albedo in West Africa. Climatic Change, 54(1-2): 181-204.

Gates, D.M. 1980. Biophysical Ecology. Springer, New York, 611 pp.

Henderson-Sellers, A., Wilson, M. 1983. Surface albedo data for climate modeling. Rev. Geophys. Space Phys., 21: 1743–1778.

Iqbal, M. 1983. An introduction to solar radiation. Academic Press, Toronto, 390 pp.

Impens, I., Lemeur, R. 1969. The radiation balance of several field crops. Archiv für Meteorologie, Geophysik und Bioklimatologie, Serie B, 17(2-3): 261-268.

Iziomon, M.G., Mayer, H. 2002. On the variability and modelling of surface albedo and longwave radiation components. Agricultural and Forest Meteorology, 111: 141-152.

Jarvis, P.G. 1976. Coniferous forest. Vegetation and the Atmosphere, 2: 171-240.

Kala, J., Hirsch, A.L. 2020. Could crop albedo modification reduce regional warming over Australia? Weather and Climate Extremes, 30. https://doi.org/10.1016/j.wace.2020.100282.

Kondratyev, K.Y. 1969. Radiation in the atmosphere. Academic Press, New York, 912 pp.

Kondratyev, K.Y. 1972. Radiation processes in the atmosphere. World Meteorological Organization, Geneva, 214 pp.

Kumar, S., Mocko, D., Vuyovich, C., Peters-Lidard, C. 2020. Impact of surface albedo assimilation on snow estimation. Remote Sensing, 12(4): 645.

Linacre, E. 1992. Climate data and resources: a reference and guide. London: Routledge. doi.org/10.1177/030913339401800122, ISBN: 0 415 05702 7.

Minnis, P., Mayor, S., Smith, W.L., Young, D. F. 1997. Asymmetry in the diurnal variation of surface albedo. IEEE Transactions on Geoscience and Remote Sensing, 35(4): 879-890.

Monteith, J.L., Unsworth, M.H. 1990. Principles of environmental physics. Edward Arnold, London, 291 pp.

Myhre, G., Myhre, A. 2003. Uncertainties in radiative forcing due to surface albedo changes caused by land-use changes. *Journal of Climate*, **16**(10), 1511-1524.

Ogilvy, J.A., Merklinger, H.M. 1991. Theory of wave scattering from random rough surfaces. J. Acoust. Soc. Am. 90: 33-82.

Oguntunde, P.G. Van de Giesen, N. 2004. Crop growth and development effects on surface albedo for maize and cowpea fields in Ghana, West Africa. International Journal of Biometeorology, 49(2): 106-112.

Pielke, R.A. 1984. Mesoscale meteorological modeling. Academic Press, 612 pp.

Piggin, I., Schwerdtfeger, P., 1973. Variations in the albedo of wheat and barley crops

Variationen der Albedo von Weizen- und Gerstenfeldern. Archiv für Meteorologie, Geophysik und Bioklimatologie, Serie B, 21, 365–391.

Post, D.F., Bryant, R.B., Batchily, A.K., Huete, A.R., Levine, S.J., Mays, M.D., Escadafal, R. 1993. Correlations between field and laboratory measurements of soil color. Soil Color, 31: 35-49.

Rauner, J.L. 1976. Deciduous forests. In vegetation and the atmosphere, 2: 241-264.

Ridgwell, A., Singarayer, J.S., Hetherington, A.M., Valdes, P.J. 2009. Tackling regional climate change by leaf albedo bio-geoengineering. Current Biology, 19(2): 146-150.

Sellers, W.D. 1965. Physical climatology. Chicago. University of Chicago Press, 272 pp. doi. org/10.1177/0309133308096757.

Shuttleworth, W.J. 1989. Micrometeorology of temperate and tropical forest. Philosophical Transactions of the Royal Society of London. B, Biological Sciences, 324(1223): 299-334.

Song, J. 1998. Diurnal asymmetry in surface albedo. Agric. For. Meteorol. 92: 181–189.

Starr J, Zhang J, Reid J.S., Roberts D.C. 2020. Albedo impacts of changing agricultural practices in the United States through Space-Borne analysis. Remote Sensing; 12(18):2887. https://doi.org/10.3390/rs12182887

Şerban, G., Cotfas, D.T., Cotfas, P.A. 2011. Significant differences in crop albedo among Romanian winter wheat cultivars. Romanian Agricultural Research, 28: 11-15.

Uysal, S.K., Şaylan, L. 2019. Assessment of soil heat flux equations for different crops under semi humid conditions. Italian Journal of Agrometeorology (2): 49-61.doi: 10.13128/ijam-652

Yin, X. 1998. The albedo of vegetated land surfaces: systems analysis and mathematical modeling. Theoretical and applied climatology, 60(1-4): 121-140.

Wang, K., Liang, S., Schaaf, C.L., Strahler, A.H. 2010. Evaluation of moderate resolution imaging spectroradiometer land surface visible and shortwave albedo products at FLUXNET sites. Journal of Geophysical Research: Atmospheres, 115: D17107. https://doi.org/10.1029/2009JD013101

Wie, J., Hong, S.O., Byon, J.Y., Ha, J.C., Moon, B.K. 2020. Sensitivity analysis of surface energy budget to albedo parameters in Seoul Metropolitan Area using the unified model, Atmosphere, 2-12.

Wood, A.J., Ackland, G.J., Dyke, J.G., Williams, H.T.P., &. Lenton, T.M. 2008. Daisyworld: A review, Rev. Geophys., 46, RG1001, doi:10.1029/2006RG000217

Zhang, Y.F., Wang, X.P., Pan, Y.X., Hu, R. 2013. Diurnal and seasonal variations of surface albedo in a spring wheat field of arid lands of Northwestern China. International journal of Biometeorology, 57(1): 67-73.

Zhou, M., Chen, G., Dong, Z., Xiea, B., Gua, S., Shi, P. 2020. Estimation of surface albedo from meteorological observations across China. Agricultural and Forest Meteorology, 281**,** doi.org/10.1016/j.agrformet.2019.107848.

Italian Journal of Agrometeorology
Rivista Italiana di Agrometeorologia

Firenze University Press
www.fupress.com/ijam

OPEN ACCESS

Citation: T. Pogačar, L. Kafež Bogataj, R. Kuk, Z. Črepinšek (2022) Effects of heat waves on soil temperatures in Slovenia. *Italian Journal of Agrometeorology* (1): 41-48. doi: 10.36253/ijam-1388

Received: September 2, 2021

Accepted: January 24, 2022

Published: July 19, 2022

Data Availability Statement: All relevant data are within the paper and its Supporting Information files.

Competing Interests: The Author(s) declare(s) no conflict of interest.

ORCID:
TP: 0000-0003-1047-0121
ZČ: 0000-0001-8000-6477

Effects of heat waves on soil temperatures in Slovenia

Tjaša Pogačar[1,*], Lučka Kafež Bogataj[1], Rok Kuk[2], Zalika Črepinšek[1]

[1] *Department of Agronomy, Biotechnical Faculty, University of Ljubljana, Jamnikarjeva 101, 1000 Ljubljana, Slovenia*
[2] *Faculty of Mathematics and Physics, University of Ljubljana, Jadranska 19, 1000 Ljubljana, Slovenia*
*Corresponding author. E-mail: tjasa.pogacar@bf.uni-lj.si

Abstract. Soil temperature regulates the rate of plant growth and tells us much about the climatic characteristics of a particular site. Climate variability and extremes need to be studied and there is a large gap in knowledge about soil temperature during heat waves. Agricultural land is highly dependent on heat waves, which are becoming longer, more intense and more frequent, and it is important to monitor soil temperatures in situ to understand their changes during heat waves. Therefore, the aim of this work was to investigate how soil temperatures change at different depths during and after heat waves. Average daily air and soil temperature data for the 25-year period 1992-2016 were evaluated at four agrometeorological stations in three climate zones in Slovenia and analyzed during heat waves determined according to the Slovenian definition. During the period 1992-2016, 53 (Lesce) to 76 (Ljubljana) heat waves were identified. Analysis of average air and soil temperatures before, during and after heat waves showed higher responsiveness of the upper part of the soils and an increase in the time lag between maximum air temperature and maximum soil temperature with depth. The maximum temperature during the heat wave was reached on average in three to nine days, depending on the depth. Only in Moderate climate of the hilly region, the average daily temperatures at a depth of 100 cm remained below 20°C during and after the heat wave. The temperature rise in the deeper layers of the soil lasts longer than in the shallower layers.

Keywords: soil temperature, heat wave, air temperature, climate change.

1. INTRODUCTION

Soil temperature is of great importance for soil decomposition, regulates various processes including the rate of plant growth, and as such is a very sensitive climate indicator (Jebamalar et al., 2021; Onwuka and Mang, 2018). In soils, carbon mineralization and sequestration can be severely affected by heat. Above a critical threshold of heat wave duration, biomass can be drastically depleted and soil microbial communities restructured, associated with a shift in physiological properties (Berard et al., 2011). Soil organic matter decomposition is controlled primarily by soil temperature during wet periods

and by the combined effect of soil water and soil temperature during dry periods (Yuste et al., 2007). Heat stress itself is a complex function of intensity, duration, and the rate of increase in air temperature.

As shown in a previous study, air temperatures in Slovenia were strongly correlated with upper soil temperatures, with coefficients decreasing rapidly with depth (Pogačar et al., 2018). Moreover, the effect of an increase in soil temperature may be even stronger if accompanied by a decrease in soil water content. The frequency of very hot days increases in summers with dry soils (Fischer et al., 2007a, 2007b; Hirschi et al., 2011). In addition to the well-known influence of soil moisture on heat wave intensity, it also plays the key role in the persistence of heat wave events (Lorenz et al., 2010). Case studies of selected large summer heat waves show that intraseasonal and interannual variability in soil moisture accounts for 5-30% and 10-40% of the simulated heat wave anomaly, respectively (Jaeger and Seneviratne, 2011). When soil temperatures are higher, soil water evaporation also increases (Aguilera et al., 2015). When soils are moist, heat transport is rapid, but more energy is required to change temperature (Manfredi et al., 2015). Increased soil surface temperature can lead to loss of subsoil carbon stocks, more carbon release to the atmosphere, increased soil respiration, and extended potential growing season (Soong et al., 2021; Zhang et al., 2016). Therefore, soil temperature with its influence on plant development is very important and should be monitored or analyzed if it is above a certain critical threshold (Mueller et al., 2010; Sviličić et al., 2016). Extreme air and soil temperature can alter the water transport rate due to reduced plant stomatal conductance, which reduces transpiration rate and consequently also yields (Irmak and Mutiibwa, 2010). Many agricultural crops are sensitive and vulnerable to changes in soil temperature. Research of Liao et al. (2016) showed that the temperature at the surface soil (20 cm soil depth), and the soil moisture content at 20–30 cm depth were the significant factors that affected potato yields. High soil temperatures negatively affected the photosynthesis of the maize plants due to decreased carboxylation rates (Nóia Júnior et al., 2018). The same research showed that short-term exposure to extreme soil temperatures affects the root system growth, leading to lower shoot dry mass accumulation. In addition, high soil temperatures reduced the relative water content of the leaves, causing an increased leaf temperature and cells rupture.

All over the world, the latest scenarios show increased uncertainty in climate conditions, which are important for agriculture (Parisse et al., 2020). The increasing duration of extreme heat waves is having a major impact on agricultural land (Hansen et al., 2018). For example, row crops are particularly susceptible to heat stress under hot and dry conditions because of excessive heating due to heat fluxes in the soil and very limited capacity for leaf cooling (Costa et al., 2019). Mortality due to drought is far more likely for trees than mortality due to heat stress, but its severity and rate of development, is greatly increased at high temperatures (Teskey et al., 2015). In the Mediterranean region, extreme events caused by climate change, such as prolonged and more intense heat waves, have an impact on soils and their functions through changes in the biomass, composition and activities of edaphic microbial communities (Berard et al., 2011).

In Slovenia, soil temperatures at all stations showed a positive trend in the period 1971-2015, with the strongest warming in summer (Pogačar et al., 2018). Average annual air temperatures have already increased by 2°C since 1961, and projections show an average increase of 1 to 4°C (with the 1981-2010 reference period) for the average summer air temperature by the end of the century. The projected increase in average soil temperatures from July to September is even slightly higher, by 2 to 4.5°C (ARSO, 2020).

Average values give us only a superficial idea of warming, as it is difficult to translate them into real change. In addition, climate variability and extremes need to be studied and there is a large gap in our knowledge of soil temperature during heat waves. Therefore, the intent of this paper is to investigate how soil temperatures change at different depths during and after heat waves.

2. MATERIALS AND METHODS

Four standard agrometeorological stations, namely Bilje, Ljubljana, Lesce and Novo mesto from three different climatic zones and on three different soils were selected (Tab. 1). All four stations belong to the official meteorological network from the Slovenian Environment Agency (ARSO: http://www.meteo.si/).

Average daily soil temperature data and average air temperature data at 2 m above sea level were evaluated for the 25-year period 1992-2016. Data were retrieved from ARSO and for soil temperatures the calculation of daily averages was performed using the climatological standard. The period was chosen because the number of days with fulfilled criteria for dangerous heat-related conditions due to the meteoalarm has especially increased since 1990 (Pogačar et al., 2020), and after

Table 1. Description of four measurement sites: altitude, geographical coordinates, surrounding land use and climatic zone.

Station	Altitude (m a.s.l)	Geographical coordinates (longitude, latitude)	Area description	Soil type	Climate
Ljubljana	299	14°31', 46°4'	Urban	Antroposols	Subcontinental
Novo mesto	220	15°11', 45°48'	Urban/peri urban	Antroposols	Subcontinental
Lesce	515	14°11', 46°22'	Rural/peri-urban	Rendzina	Moderate climate of hilly region
Bilje	55	13°38', 45°54'	Rural	Eutric fluvisol	Submediterranean

2000 heat waves in Slovenia are much more frequent, intense and longer than before (Pogačar et al., 2019). The upper year was set to 2016, because since 2017 there are no more measurements of soil temperatures at depths of 2 and 100 cm in Slovenia.

The Slovenian definition of heat wave was used, where the average daily air temperature must be higher than or equal to the threshold (in graphs marked with the red line) for at least three consecutive days. For Subcontinental climate (Ljubljana, Novo mesto) the threshold is 24°C, for Moderate climate of hilly region 22°C (Lesce) and for Submediterranean climate 25°C (Bilje) (Ključevšek et al., 2018). First, periods in heat waves were identified based on the definition using air temperatures. The first day of each heat wave was identified. Then, soil temperatures at a given depth of 2, 5, 10, 20, 30, 50 and 100 cm were averaged for each consecutive day before, during and after the heat wave. There is quite some missing data of soil temperatures, so we checked it carefully and eliminated these days (only for specific depths) from averages: at Bilje days around 24.6.2005 (20 cm), 9.7.2016 (10 cm); at Ljubljana around 14.7.2007 (30 cm), 11.8.2013 (5 and 10 cm); at Lesce around 3.8.1993 (2 cm), 27.7.2006, 22.6.2008, 26.7. and 29.8.2009 (2, 5, 10, 20, 30, 50 cm); and at Novo mesto around 2.7. and 30.7.2006 (100 cm). According to a sensitivity analysis, these specific dates do not change the averages significantly.

3. RESULTS

Soil temperatures during heat waves have never been analyzed in Slovenia. In the period 1992-2016, 76 heat waves were identified in Ljubljana, 56 in Novo mesto, 55 in Bilje, and 53 in Lesce. As an example of temperature distribution on days before, during and after a heat wave, we took the case of a heat wave in Bilje in June 2003 (Fig. 1). It can be seen that the heat threshold (marked with red line) was reached on 8 June and the heat wave lasted until 17 June. Only the soil temperatures at a depth of 100 cm were lower than the air temperatures throughout the heat wave and higher only for two days after the heat wave. Temperatures at a depth of 50 cm were very similar to air temperatures, but remained high longer after the air had already cooled. At shallower depths, temperatures rose higher, reaching over 30°C, although average air temperatures did not. The highest maximum average daily soil temperature was at a depth of 2 cm, about 5°C higher than the highest maximum average daily air temperature.

Average air and soil temperatures (1992-2016) before, during and after heat waves at 4 sites (Fig. 2) showed similar characteristics, in Bilje especially similar as in the heat wave shown above. At other sites, air temperatures exceeded soil temperatures for a short time at depths greater than 10 cm. The upper part of the soils was more sensitive to air temperature changes, and the time interval between maximum air temperature and maximum soil temperature increased with depth. The maximum temperature during the heat wave was reached on average in three days for air temperature and soil temperatures at shallower depths below 10 cm, in three to four days at a depth of 20 to 30 cm, in four to five days at a depth of 50 cm, and in six to nine days at a depth of 100 cm.

The smallest difference between the maximum average air and soil temperature was in Novo mesto, less than 2°C, followed by Ljubljana, both of Subcontinental climate. In Lesce the difference was about 3.5°C and in Bilje about 5°C. Only in Lesce, due to Moderate climate of hilly region, the average daily temperatures remained below 20°C at the depth of 100 cm, maintaining an adequate environment for drinking water quality, as water pipes are usually installed at this depth.

In Novo mesto and Ljubljana, soil temperatures after the heat wave averaged just above 20°C at the 100 cm depth and about 22°C at the 50 cm depth. In Bilje (Sub-Mediterranean climate) the situation was most critical, with average soil temperatures after the heat wave at the depth of 100 cm reaching above 24°C, and at the depth of 50 cm even up to almost 28°C. For an average heat wave that lasted 5 days, the elevated soil temperatures

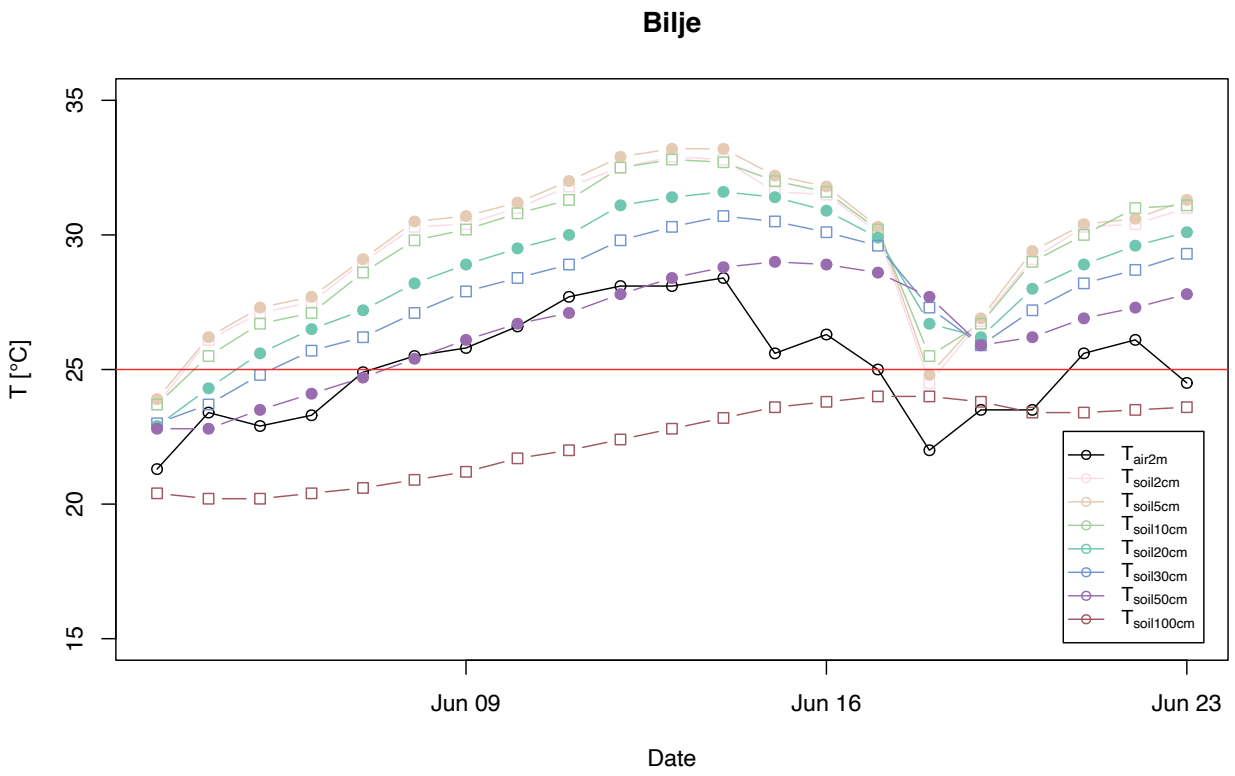

Fig. 1. An example of the time course of the daily average air and soil temperature at different depths before, during and after the heat wave (threshold – red line) in June 2003 at the Bilje station.

lasted only a few more days at shallower depths, and even more than 15 days at greater depths.

Further analysis of the slopes between the points in the graphs in Fig. 2 showed that the temperature in the upper soil layers and in the air increased the fastest (large positive slope) and decreased the fastest (large negative slope) (Fig. 3). It can also be seen that the zero slope, where the maximum temperature is reached, moves to the right with depth. Thus, the temperature rise in the deeper layers of the soil takes longer than in the shallower layers.

4. DISCUSSION

Changes in soil temperature affect many agricultural practices, so we wanted to examine changes during heat waves. The similar number of heat waves at 3 sites (except Ljubljana as an urban heat island) over the 25-year period confirms that the thresholds are appropriately set because in different climates all living organisms are acclimated to their usual conditions, so the threshold may not be the same everywhere (Wang et al., 2020). Air temperatures are strongly correlated with upper soil temperatures, and in Slovenia warming was observed at all depths in all seasons, but the threshold of 45°C was not (yet) reached at any depth (Pogačar et al., 2018).

We have shown how the time lag of a heat wave is longer when going deeper, with the maximum temperature delayed by as much as four to five days. With slower responses and less influence of air temperature changes, the highest average annual soil temperatures are measured at a depth of 50 or 100 cm (Pogačar et al., 2018). Soil warming is more pronounced in summer, as also shown in a study for the Mediterranean region (Aguilera et al., 2015), which means more heat stress during heat waves that negatively affect crop production (Lasram and Mechlia, 2015; Melkonyan, 2015), as well as more changes in soil microbial community composition (Acosta-Martinez et al., 2014). It is important to monitor as early as the first seasonal heat waves that may occur in early June, as soil surface temperature is the dominant factor influencing vegetation variation in March-July (Xu et al., 2011), as well as throughout the summer, as soil water content must be maintained at appropriate levels during extreme heat periods to ensure plant uptake and minimize the effects of heat stress.

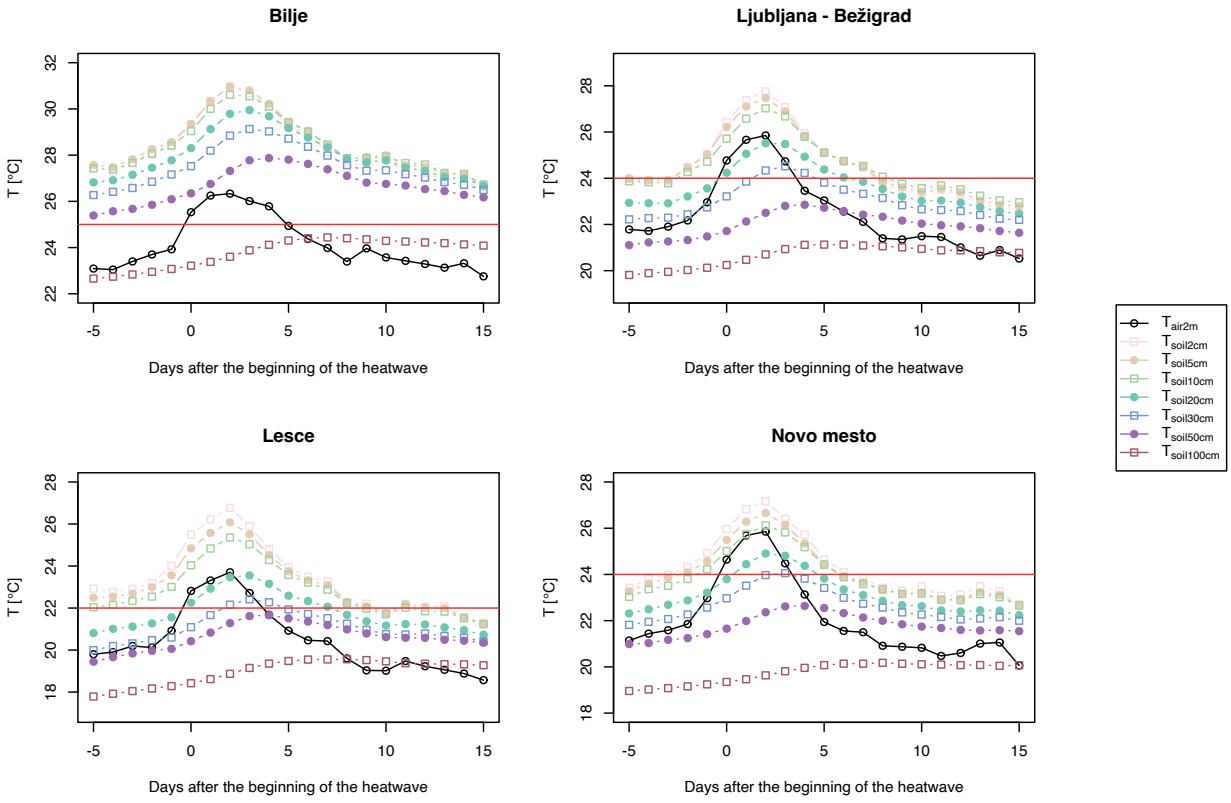

Fig. 2. The courses of average air and soil temperature at four sites in Slovenia. Temperature per individual day is the average value for all heat waves in the period 1992–2016, negative days meaning days before the start of the heat wave.

One way to reduce soil temperature during heat waves is to provide additional residue on the soil surface in reduced and no-till fields, which can minimize radiation interception on the soil surface, which lowers soil temperature and is beneficial for improving root growth and water and nutrient uptake during heat wave periods (Lipiec et al., 2013).

Since the altered contributions of circulation and soil moisture to temperature anomalies include enhanced feedbacks in the surface energy budget (Gessner et al., 2021), which increase sensible heat fluxes and reduce latent cooling over dry soils (Miralles et al., 2014; Seneviratne et al., 2006), the latter should also be investigated in additional studies for Slovenia to better plan agrotechnical measures in the near future.

The limitation of the study is only a small number of sites, however these four are good representatives of three different climatic zones in Slovenia and as such suitable to use. Due to the large amount of data over a period of 25 years, average daily values were studied, but they give us an insight into the usual spread of heat in the soils.

4. CONCLUSIONS

During more than 50 heat waves over a 25-year period, at 4 sites, on average, the time interval between maximum air temperature and maximum soil temperature increased with depth. We have shown that the upper part of the soil is the most sensitive, reaching maximum temperatures within three days after the onset of the heat wave. At greater depths, up to 100 cm, the maximum was reached in up to nine days. Moreover, the temperature rise lasted longer in the deeper layers and only in Moderate climate of hilly region the average daily temperatures at the depth of 100 cm remained below 20°C during and after heat waves. Maize and potato are widely grown in the regions of our studied agrometeorological stations (SURS, 2021). Both crops are sensitive and vulnerable to changes in soil temperature, as the temperature at the upper soils is the significant factor that affects potato yields, and high soil temperatures negatively affect the photosynthesis of the maize, lead to lower shoot dry mass accumulation and reduce relative water content of the leaves. Due to the strong influence of soil temperatures on agricultural production, it is of great importance

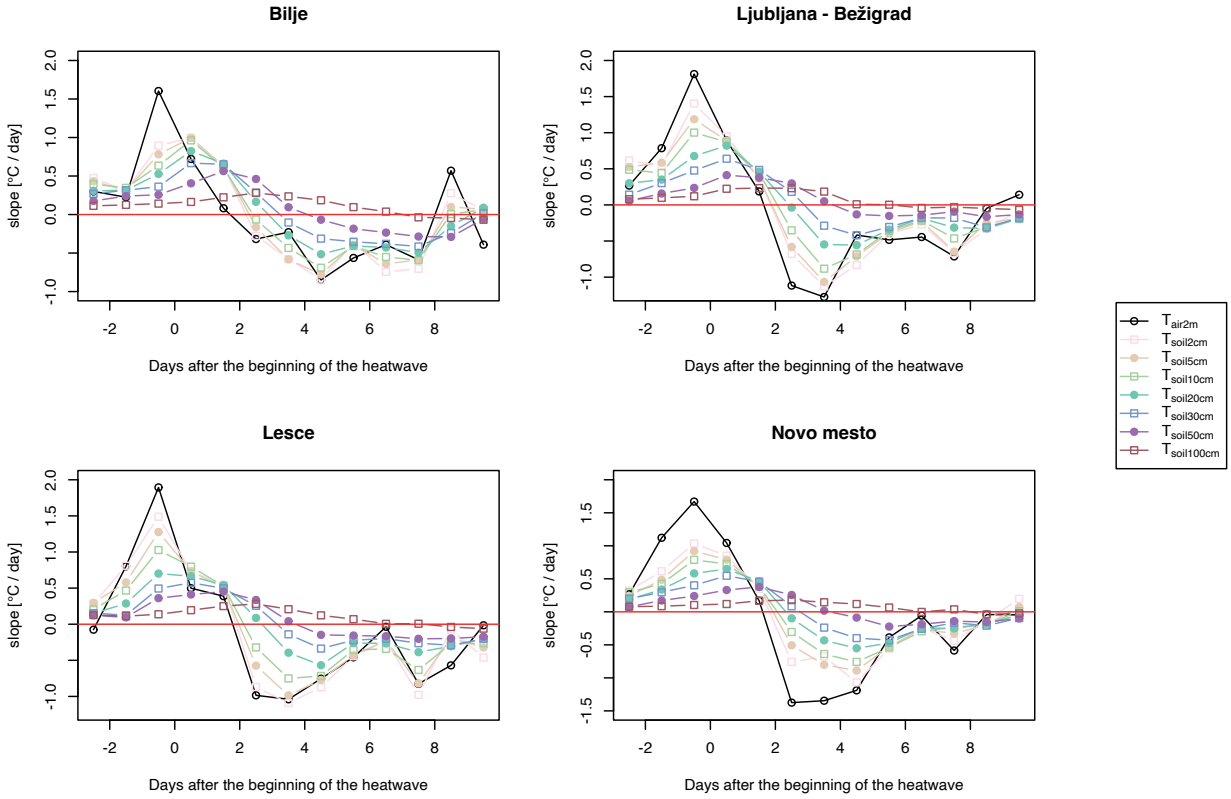

Fig. 3. The slopes of the lines between the points on Fig. 2.

to understand their evolution during heat waves. We recommend monitoring them in situ if only possible.

ACKNOWLEDGEMENTS

This work was supported by the Slovenian Research Agency, Research Program P4–0085.

REFERENCES

Acosta-Martínez V., Cotton J., Gardner T., Moore-Kucera J., Zak J., Wester D., Cox S., 2014. Predominant bacterial and fungal assemblages in agricultural soils during a record drought/heat wave and linkages to enzyme activities of biogeochemical cycling. Applied Soil Ecology, 84: 69-82. doi:10.1016/j.apsoil.2014.06.005.

Aguilera F., Orlandi F., Oteros J., Bonofiglio T., Fornaciari M., 2015. Bioclimatic characterisation of the Mediterranean region: future climate projections for Spain, Italy and Tunisia. Italian Journal of Agrometeorology, 1: 45-58.

ARSO, 2020. Atlas podnebnih projekcij. https://meteo.arso.gov.si/uploads/probase/www/climate/OPS21/Priloge-app/#/izbor

Bérard A., Bouchet T., Sévenier G., Pablo A.L., Gros R., 2011. Resilience of soil microbial communities impacted by severe drought and high temperature in the context of Mediterranean heat waves. European Journal of Soil Biology, 47(6): 333-342. doi: 10.1016/j.ejsobi.2011.08.004.

Costa J.M., Egipto R., Sánchez-Virosta A., Lopes C.M., Chaves M.M., 2019. Canopy and soil thermal patterns to support water and heat stress management in vineyards. Agricultural Water Management, 216: 484-496. doi: 10.1016/j.agwat.2018.06.001.

Fischer E.M., Seneviratne S.I., Lüthi D., Schär C., 2007a. Contribution of land-atmosphere coupling to recent European summer heat waves. Geophys. Res. Lett., 34: L06707. doi.org/10.1029/2006GL029068.

Fischer E.M., Seneviratne S.I., Vidale P.L., Lüthi D., Schär C., 2007b. Soil moisture–atmosphere interactions during the 2003 European summer heat wave. J Climate, 20: 5081–5099. doi: 10.1175/JCLI4288.1.

Gessner C., Fischer E.M., Beyerle U., Knutti R., 2021. Very Rare Heat Extremes: Quantifying and Under-

standing Using Ensemble Reinitialization. Journal of Climate, 34(16): 6619-6634. doi: 10.1175/JCLI-D-20-0916.1.

Hansen L.D., Barros N., Transtrum M.K., Rodríguez-Añón J.A., Proupín J., Piñeiro V., Arias-González A., Gartzia N., 2018. Effect of extreme temperatures on soil: A calorimetric approach. Thermochimica Acta, 670: 28-135. doi: 10.1016/j.tca.2018.10.010.

Hirschi M., Seneviratne S., Alexandrov V., Boberg F., Boroneant C., Christensen O.B., Formayer H., Orlowsky B., Stepanek P., 2011. Observational evidence for soil-moisture impact on hot extremes in southeastern Europe. Nature Geoscience, 4: 17-21. doi: 10.1038/ngeo1032.

Irmak S., Mutiibwa D., 2010. On the dynamics of canopy resistence: Generalized-linear estimation and its relationships with primary micrometeorological variables. Water Resources Research, 46: 1-20. W08526. doi:10.1029/2009WR008484.

Jaeger E.B., Seneviratne S.I., 2011. Impact of soil moisture–atmosphere coupling on European climate extremes and trends in a regional climate model. Clim Dyn, 36: 1919-1939. doi: 10.1007/s00382-010-0780-8.

Jebamalar S., Christopher J.J., Ajisha M.A.T., 2021. Random input based prediction and transfer of heat in soil temperature using artificial neural network. Materials Today: Proceedings, 45(2): 1540-1546. doi:10.1016/j.matpr.2020.08.091.

Ključevšek N., Hrabar A., Dolinar M., 2018. Podnebne podlage za definicijo vročinskega vala. Vetrnica, 10, 44-53.

Lasram A., Mechlia N.B., 2015. Effects of thermal stress on the pre-heading duration and grain production for Mediterranean irrigated durum wheat. Italian Journal of Agrometeorology, 3: 25-34.

Liao X., Su Z., Liu G., Zotarelli L., Cui Y., Snodgrass C., 2016. Impact of soil moisture and temperature on potato production using seepage and center pivot irrigation. Agricultural Water Management, 165: 230-236. https://doi.org/10.1016/j.agwat.2015.10.023.

Lipiec J., Doussan C., Nosalewicz A., Kondracka K., 2013. Effect of drought and heat stresses on plant growth and yield: A review. Int. Agrophys., 27: 463-477. doi: 10.2478/intag-2013-0017.

Lorenz R., Jaeger E.B., Seneviratne S.I., 2010. Persistence of heat waves and its link to soil moisture memory. Geophys. Res. Lett., 37: L09703. doi: 10.1029/2010GL042764.

Manfredi P., Cassinari C., Trevisan M., 2015. Soil temperature fluctuations in a degraded and in a reconstituted soil. Italian Journal of Agrometeorology, 3: 63-72.

Melkonyan A., 2015. Climate change impact on water resources and crop production in Armenia. Agricultural Water Management, 161: 86-101. doi. org/10.1016/j.agwat.2015.07.004.

Miralles D.G., Teuling A.J., van Heerwaarden C.C., de Arellano J.V., 2014. Mega-heatwave temperatures due to combined soil desiccation and atmospheric heat accumulation. Nat. Geosci., 7: 345-349. doi: 10.1038/ngeo2141.

Mueller L., Schindler U., Mirschel W., Shepherd G.T., Ball B.C., Helming K., Rogasik J., Eulenstein F., Wiggering H., 2010. Assessing the productivity function of soils. A review. Agronomy for Sustainable Development, 30: 601-614. doi: 10.1051/agro/2009057.

Nóia Júnior R.S., do Amaral G.C., Pezzopane J.E.M., Toledo J.V., Xavier T.M.T., 2018. Ecophysiology of C3 and C4 plants in terms of responses to extreme soil temperatures. Theor. Exp. Plant Physiol., 30: 261-274. https://doi.org/10.1007/s40626-018-0102-7.

Onwuka B., Mang B., 2018. Effects of soil temperature on some soil properties and plant growth. Adv Plants Agric Res., 8(1): 34-37. doi: 10.15406/apar.2018.08.00288.

Parisse B., Pontrandolfi A., Epifani C., Alilla R., De Natale F., 2020. An agrometeorological analysis of weather extremes supporting decisions for the agricultural policies in Italy. Italian Journal of Agrometeorology, 3: 15-30. doi: 10.13128/ijam-790.

Pogačar T., Žnidaršič Z., Kajfež Bogataj L., Črepinšek Z., 2020. Steps Towards Comprehensive Heat Communication in the Frame of a Heat Health Warning System in Slovenia. Int. J. Environ. Res. Public Health, 17: 5829. doi: 10.3390/ijerph17165829.

Pogačar T., Žnidaršič Z., Kajfež Bogataj L., Flouris A.D., Poulianiti K., Črepinšek Z., 2019. Heat Waves Occurrence and Outdoor Workers' Self-assessment of Heat Stress in Slovenia and Greece. Int. J. Environ. Res. Public Health, 16: 597. doi: 10.3390/ijerph16040597.

Pogačar T., Zupanc V., Kajfež Bogataj L., Črepinšek Z., 2018. Soil temperature analysis for various locations in Slovenia. Italian Journal of Agrometeorology, 23(1): 25-34. doi: 10.19199/2018.1.2038-5625.025.

Seneviratne S.I., Lüthi D., Litschi M., Schär C., 2006. Land–atmosphere coupling and climate change in Europe. Nature, 443: 205-209. doi: 10.1038/nature05095.

Soong J.L., Castanha C., Hicks Pries C.E., Ofiti N., Porras R.C., Riley W.J., Schmidt M., Torn M.S., 2021. Five years of whole-soil warming led to loss of subsoil carbon stocks and increased CO_2 efflux. Science advances, 7(21), eabd1343. https://doi.org/10.1126/sciadv.abd1343.

SURS, Statistični urad republike Slovenije, 2021. Kmetijstvo, gozdarstvo, ribištvo, rastlinska pridelava, pridelki in površina. https://www.stat.si/StatWeb/Field/Index/11

Sviličić P., Vučetić V., Filić S., Smolić A., 2016. Soil temperature regime and vulnerability due to extreme soil temperatures in Croatia. Theor Appl Climatol, 126: 247-263. doi: 10.1007/s00704-015-1558-z.

Teskey R., Wertin T., Bauweraerts I., Ameye M., McGuire M.A., Steppe K., 2015. Tree response to extreme heat. Plant cell environ, 38: 1699-1712. doi: 10.1111/pce.12417.

Wang X., Chen R., Han C., Yang Y., Liu J., Liu Z., Guo S., Song Y., 2020. Soil temperature change and its regional differences under different vegetation regions across China. International Journal of Climatology, 41(Suppl.1): E2310-E2320. doi: 10.1002/joc.6847.

Xu W., Gu S., Zhao X.Q., Xiao J., Tang Y., Fang J., Zhang J., Jiang S., 2011. High positive correlation between soil temperature and NDVI from 1982 to 2006 in alpine meadow of the Three-River Source Region on the Qinghai-Tibetan Plateau. International Journal of Applied Earth Observation and Geoinformation, 13(4): 528-535. doi:10.1016/j.jag.2011.02.001.

Yuste Y.C., Baldocchi D.D., Gershenson A., Goldstein A., Misson L., Wong S., 2007. Microbial soil respiration and its dependency on carbon inputs, soil temperature and moisture. Glob. Change Biol., 13: 2018-2035.

Zhang H., Wang E., Zhou D., Luo Z., Zhang Z., 2016. Rising soil temperature in China and its potential ecological impact. Scientific Reports, 6: 35530. doi.org/10.1038/srep35530.

Italian Journal of Agrometeorology
Rivista Italiana di Agrometeorologia

Firenze University Press
www.fupress.com/ijam

OPEN ACCESS

Citation: V.H. Quej, C. De La Cruz Castillo, J. Almorox, B. Rivera-Hernandez (2022) Evaluation of artificial intelligence models for daily prediction of reference evapotranspiration using temperature, rainfall and relative humidity in a warm sub-humid environment. *Italian Journal of Agrometeorology* (1): 49-63. doi: 10.36253/ijam-1373

Received: August 3, 2021

Accepted: May 30, 2022

Published: July 19, 2022

Data Availability Statement: All relevant data are within the paper and its Supporting Information files.

Competing Interests: The Author(s) declare(s) no conflict of interest.

ORCID:
VHQ: 0000-0002-9356-6251
CCC: 0000-0001-7707-505X
JA: 0000-0003-1523-0979
BRH: 0000-0003-1713-4710

Evaluation of artificial intelligence models for daily prediction of reference evapotranspiration using temperature, rainfall and relative humidity in a warm sub-humid environment

Victor H. Quej[1], Crescencio De La Cruz Castillo[1], Javier Almorox[2], Benigno Rivera-Hernandez[3,*]

[1] *Colegio de Postgraduados. Campus Campeche. Carretera Haltunchen – Edzná, km 17.5, 24450, Sihochac. Champotón, Campeche, Mexico.*
[2] *Departamento de Producción Agraria ETSI Agrónomos, Universidad Politécnica de Madrid, UPM, Avd. Puerta de Hierro, 2, 28040-Madrid, Spain.*
[3] *Universidad Popular de la Chontalpa, Carretera Cárdenas-Huimanguillo km 2.0, 86500, Cárdenas, Tabasco, Mexico.*
*Corresponding author. E-mail: benigno.rivera@upch.mx

Abstract. Accurate estimation of reference evapotranspiration is essential for agricultural management and water resources engineering applications. In the present study, the ability and precision of three artificial intelligence (AI) models (i.e., Support Vector Machines (SVMs), Adaptive Neuro-Fuzzy Inference System (ANFIS) and Categorical Boosting (CatBoost)) were assessed for estimating daily reference evapotranspiration (ET_0) using limited weather data from five locations in a warm sub-humid climate in Mexico. The Penman–Monteith FAO-56 equation was used as a reference target for ET_0 values. Three different input combinations were investigated, namely: temperature-based (minimum and maximum air temperature), rainfall-based (minimum air temperature, maximum air temperature and rainfall), and relative humidity-based (minimum air temperature, maximum air temperature and relative humidity). Extraterrestrial radiation values were used in all combinations. The temperature-based AI models were compared with the conventional Hargreaves–Samani (HS) model commonly used to estimate ET_0 when only temperature records are available. The goodness of fit for all models was assessed in terms of the coefficient of determination (R^2), Nash–Sutcliffe model efficiency coefficient (NSE), root mean square error (RMSE) and mean absolute error (MAE). The results showed that among the AI models evaluated, the SVM models outperformed ANFIS and CatBoost for modeling ET_0. Further, the influence of relative humidity and rainfall on the performance of the models was investigated. The analysis indicated that relative humidity significantly improved the accuracy of the models. Finally, the results showed a better response of the temperature-based AI models over the HS method. AI models can be an adequate alternative to conventional models for ET_0 modeling.

Keywords: reference evapotranspiration, FAO56-PM, artificial intelligence, warm sub-humid environment, Yucatán Peninsula.

1. INTRODUCTION

Evapotranspiration (ET) refers to the physical processes of transferring water from the soil surface (evaporation) and plants (transpiration) to the atmosphere (Allen et al., 1998). ET is a critical component of the water balance at plot, field, farm, catchment, basin and global levels. The measurement of evapotranspiration under normal conditions is of great importance in the estimation and management of present and future water resources and for solving many theoretical problems in the fields of hydrology, climatology and meteorology. In irrigation planning, evapotranspiration data are used for estimating the acreage of various crops or combinations of crops that can be irrigated with a given water supply or as a basis for estimating the amount of water that will be required to irrigate a given area. A lysimeter can be used to directly and accurately measure crop evapotranspiration (ET_c) from a well-watered agricultural crop. However, its widespread application is restricted by costly and time-consuming operations for data management (Wang et al., 2014). Therefore, in practice, the most common approach used for estimating crop evapotranspiration (ET_c) is the crop coefficient (K_c) approach, which consists of multiplying reference evapotranspiration (ET_0) with the crop coefficient (Allen et al., 1998). ET_0 is "the rate at which water, if available, would be removed from the soil and plant surface of a specific crop, arbitrarily called a reference crop" (Jensen et al., 1990). The reference crop is typically grass or alfalfa under well-watered conditions. Numerous equations, classified as temperature-based, radiation-based, pan evaporation-based and combination-type have been developed for estimating ET_0. They vary in terms of data requirements and accuracy. The adapted FAO-56 Penman–Monteith equation (FAO56-PM) was recommended as the standard equation for estimating ET_0 and calibrating other ET_0 equations (Allen et al., 1998; Jensen et al., 1990; Kisi, 2013; Wang et al., 2014). FAO56-PM can be used in a wide variety of climate conditions, at different time steps and needs no local calibration because of its physical basis.

In the recent years, artificial intelligence (AI) techniques such as Artificial Neural Network (ANN), Generalized Regression Neural Network (GRNN), Adaptive Neuro-Fuzzy Inference System (ANFIS), Support Vector Machines (SVMs), Gene Expression Programming (GEP), Genetic Programming (GP), Extreme Learning Machine (ELM), Random Forest (RF), Categorical Boosting (CatBoost), Multilayer Perceptron (MLP) and Cascade Correlation Neural Network (CCNN) have been accepted as effective tools for estimating reference evapotranspiration (ET_0). Artificial intelligence methods are an alternative and emerging method, and can be used as innovative approaches because they offer benefits such as no required knowledge of internal variables, simpler solutions for multi-variable problems and accurate calculation (Gocić et al., 2015). In several studies, the accuracy of these techniques has been improved by using algorithms [e.g., Fire Fly Algorithm (FFA), Genetic Algorithm (GA), Particle Swarm Optimizer (PSO), Grey Wolf Optimizer (GWO), Multi-Verse Optimizer (MVO), Whale Optimization Algorithm (WOA) and Ant Lion Optimizer (ALO)] to tune the model's parameters and by the use of wavelet transform (WT) techniques to transform data series into sub-series. Reis et al. (2019) examined the accuracy of ANN and ELM techniques for estimating ET_0 based on temperature data in a semi-arid region of Brazil and compared them with the Hargreaves–Samani (HS) empirical equation. They found that ANN and ELM models provide further accuracy compared to the HS equation. In recent years, the company Yandex has proposed a novel AI algorithm called CatBoost, capable of solving problems with heterogeneous features, noisy data and complex dependencies (Dorogush et al., 2018). Among its main features is the ability to avoid overfitting of trained models (Prokhorenkova et al., 2018). Huang et al. (2019b) employed CatBoost, RF and SVMs to predict ET_0 in a humid region of China. The results showed that the SVM technique offered the best accuracy when an incomplete combination of meteorological parameters was used, while CatBoost performed best with the complete combination of meteorological parameters. Tikhamarine et al. (2019) used five ANN models optimized by GWO, MVO, PSO, WOA and ALO algorithms to estimate monthly ET_0. The results of the comparison showed that the ANN-GWO model's performance was superior to that of the other models. Raza et al. (2020) investigated the potential of SVM, MLP, GRNN and CCNN machine learning models to estimate ET_0 in four climatic regions. They found that the accuracy of the SVM model was better than the others for all evaluated climatic zones. Zhang et al. (2020) compared the performance of three artificial intelligence methods (i.e., CatBoost, GRNN and RF) for estimating daily ET_0 using limited meteorological data in an arid and semi-arid region of Northern China. CatBoost was found to perform better than GRNN and RF models. Tikhamarine et al. (2020) developed an optimized SVM model using the WOA algorithm for monthly ET_0 estimation and compared it with other two SVM-hybrid models named SVM-MVO and SVM-ALO. Their results indicated that the SVM-WOA model was more accurate at predicting ET_0 compared to the other

models. Furthermore, prior studies have also proved the usability and potential of the ANFIS method for ET_0 modeling (Alizamir et al., 2020; Rezaabad et al., 2020; Roy et al., 2020).

In more recent years, a special class of AI algorithms known as Deep Learning (DL) has been successfully applied for estimating ET_0, as in the case of Chen et al. (2020), who evaluated three DL models named Deep Neural Network (DNN), Temporal Convolution Neural Network (TCN) and Long Short-Term Memory Neural Network (LSTM) using limited meteorological data. Their results were compared with classic Machine Learning (ML) and empirical models, and the results indicated that both DL and ML techniques performed better than empirical models. In another study, Granata and Di (2021) examined two types of DL models called LSTM and NARX (Nonlinear Autoregressive Network with Exogenous input) for estimating actual evapotranspiration (ETa) in two different climatic conditions of the United States. The results revealed that both models can provide very accurate predictions of ETa, although the performance of the models can be affected by local climatic conditions.

The objectives of this study were to: (1) investigate the capability of three artificial intelligence techniques, i.e., ANFIS, SVMs and CatBoost, for modeling daily ET_0 in a sub-humid region based on limited climate data, (2) to compare the accuracy of the ANFIS, SVM and CatBoost techniques with the Hargreaves–Samani model when only temperature data are available, and (3) to examine the effect of using relative humidity and rainfall as input variables on the artificial intelligence model's prediction precision in a warm sub-humid region.

2. MATERIALS AND METHODS

2.1. Case study site and data collection

This study was performed using weather data from five meteorological stations located in the Yucatán Peninsula, Mexico (Fig. 1). The climatic data were provided by the Mexican National Meteorological Service (SMN; Servicio Meteorológico Nacional) and Mexico's National Institute for Forestry, Agriculture and Livestock Research (INIFAP; Instituto Nacional de Investigaciones Forestales Agrícolas y Pecuarias). Continuous and long-term series of observed daily weather data including minimum and maximum air temperature (T_{min}, T_{max}, °C), mean wind speed (u_2, ms^{-1}), mean relative humidity (RH, %), precipitation (W) and global solar radiation (R_s, MJ $M^{-2}day^{-1}$) were collected from five meteorological stations. The geographic information and annual meteorological conditions of these stations during the period under study are presented in Tab. 1. All stations studied were identified as moist sub-humid (annual P/ET_0 ratio between 0.65 and 1.0) according to the global aridity index (Tab. 1) developed by the United Nations Convention to Combat Desertification (Middleton and Thomas, 1997).

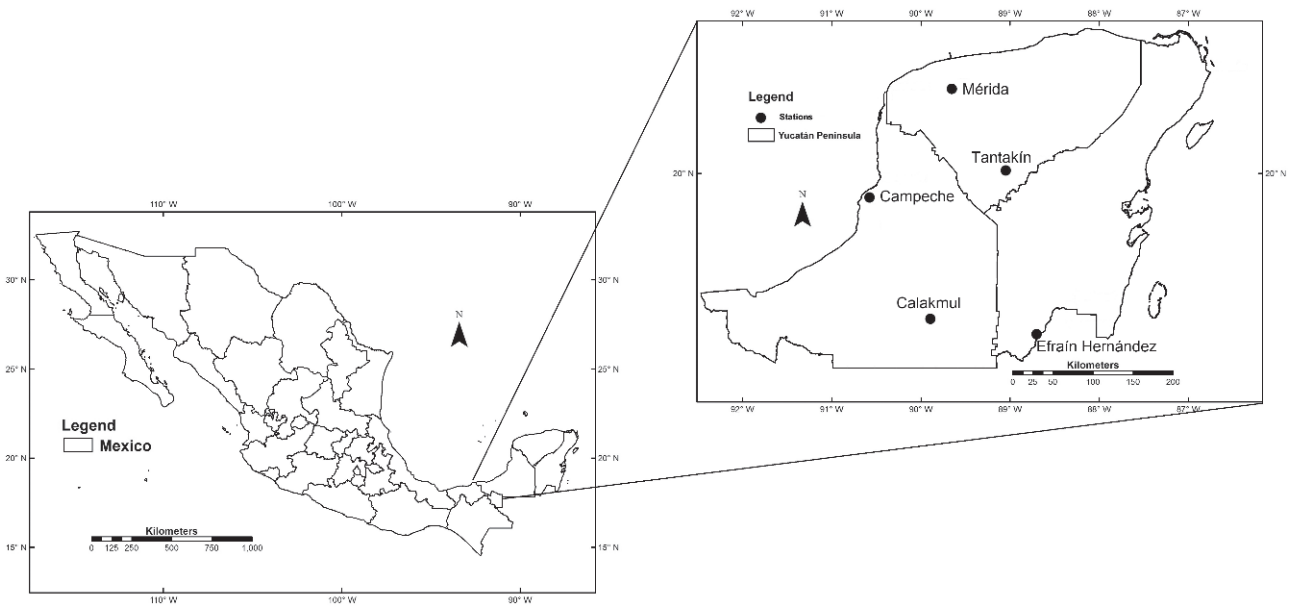

Fig. 1. Locations of the weather stations in the Yucatán Peninsula, Mexico used in this study.

Table 1. Geographic information and annual meteorological conditions during the period under study.

Station	LON (°W)	LAT (°N)	TP	ALT (m)	Annual Average				P/ET_0Ratio	CZ
					T (°C)	P (mm)	U_2 (m/s)	ET_0 (mm)		
Campeche	-90.507	19.836	2000-2018	11	26.8	1279	1.8	1555	0.82	Moist sub- humid
Efraín Hernández	-89.892	18.193	2006-2014	90	25.9	1336	2.6	1361	0.98	Moist sub-humid
Mérida	-89.651	20.946	2000-2006	18	27.4	1123	2.9	1690	0.66	Moist sub-humid
Tatankín	-89.047	20.030	2003-2011	30	26.5	1154	1.6	1515	0.76	Moist sub-humid
Calakmul	-89.893	18.365	2003-2014	28	26.2	1357	1.2	1580	0.85	Moist sub-humid

LON longitude, LAT latitude, TP time period, ALT altitude, T temperature, P precipitation, U_2 wind speed, ET_0 reference evapotranspiration, CZ climate zone.

The climate in the Yucatán Peninsula can be described as tropical savanna (Aw) according to the Köppen system (Köppen, 1936), with a rainy summer and dry winter. The maximum and minimum daily air temperature is 36 °C and 16 °C respectively. The rainfall occurs in summer and autumn with a gradient of minimum rainfall in the northwest (600 mm/year) to higher quantities toward the southeast (1400 mm/year).

The database was checked to find missing or inconsistent records of air temperature, relative humidity and precipitation. In cases where less than five consecutive missing or incorrect records were found within a period of one month, the Piecewise Cubic Hermite Interpolating Polynomials (PCHIPs) interpolation method (Fritsch and Carlson, 1980; Torrente Cantó, 2018) was used to fill in missing values or replace inconsistent values. Otherwise, these values were removed from the database. Overall, deleted and missing data, which accounted for approximately 2% of the database, were replaced with values estimated by interpolation.

2.2. Targets used for training and testing

In this paper, the FAO56-PM equation (Allen et al., 1998) was used to provide the daily ET_0 estimates for training and testing the models. This is a very common practice, because lysimetric or other experimental ET measurements are not available in most cases.

$$ET_0 = \frac{0.408\Delta(R_n - G) + \gamma\frac{900}{T+273}u_2(e_s - e_a)}{\Delta + \gamma(1 + 0.34u_2)} \quad (1)$$

where ET_0 is reference evapotranspiration (mm day^{-1}), Δ is the slope of the saturation vapor pressure (kPa $°C^{-1}$), γ is the psychrometric constant (kPa $°C^{-1}$), R_n is net radiation at the crop surface (MJ m^{-2} day^{-1}), G is soil heat flux density (MJ m^{-2} day^{-1}), which may be ignored as the magnitude of the day soil flux is small, T is mean daily air temperature (°C), u_2 is average wind speed at 2 m height (m s^{-1}), e_s is saturation vapor pressure (kPa), e_a is actual vapor pressure (kPa), and e_s - e_a is saturation vapor pressure deficit (kPa). The computation of all data required for calculating ET_0 followed the method and procedure given in Chapter 3 of FAO-56.

In this study, the ET_0-FAO56PM equation was used to evaluate multiple linear regression and artificial intelligence methods.

2.3. Adaptive neuro fuzzy inference system (ANFIS)

ANFIS is a multilayer model initially proposed by Jang (1993). It is a hybrid model where the nodes in the different layers of a feed-forward network handle fuzzy parameters. This is equivalent to a fuzzy inference system (FIS) with distributed parameters. The technique splits the representation of prior knowledge into subsets, in order to reduce the search space, and uses the backpropagation algorithm to adjust the fuzzy parameters. The resulting system is an adaptive neural network functionally equivalent to a first-order Takagi–Sugeno inference system, where the input-output relationship is linear.

In a first-order Sugeno system, a standard rule set with two fuzzy IF/THEN rules can be expressed as:

- Rule 1. If x is A_1 and y is B_1, then $f_1 = p_1 x + q_1 y + r_1$ (2)
- Rule 2. If x is A_2 and y is B_2, then $f_2 = p_2 x + q_2 y + r_2$ (3)

where A_1 and B_1 are the fuzzy sets in the antecedent, f_i is the output within the fuzzy region specified by the fuzzy rule; and pi, q_i and r_i are the design parameters that are determined during the training process.

The ANFIS architecture consists of five layers, namely: fuzzy layer, product layer, normalized layer, defuzzy layer and total output layer. The inputs for two of them are shown in Fig. 2. Each layer performs a specific function in the fuzzy inference system. For identification, the adaptive nodes are represented by squares and fixed nodes are portrayed as circles.

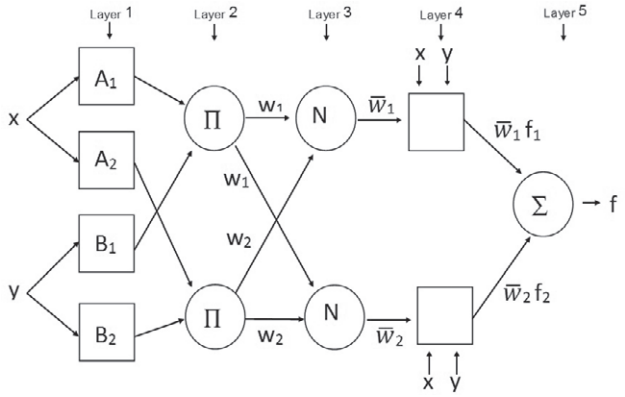

Fig. 2. Topological structure of ANFIS.

Layer 1 (Fuzzy layer): each node *i* in this layer (indicated with a square) represents a node function:

$$O_{1,i} = \mu_{Ai}(x), \text{ for } i = 1,2,\ldots,n$$
$$O_{1,i} = \mu_{Bi-2}(y), \text{ for } i = 1,2,\ldots,n \quad (4)$$

where x (or y) is the input to node *i*, and A_i or (B_{i-2}) is the linguistic label (small, large, etc.) characterized by appropriate membership functions (MFs) $\mu_{Ai}(x)$ and $\mu_{Bi-2}(y)$. In this study, bell-shaped MFs (Eq. 5) were used (Petković et al., 2015).

$$f(x;a,b,c) = \frac{1}{1+\left|\frac{x-c}{a}\right|^{2b}} \quad (5)$$

where x is the input to the node and ({a,b,c}) are the premise parameters set that changes the shapes of the MFs with a maximum of 1 and a minimum of 0.

Layer 2 (Product layer): The circle nodes represented with Π in Fig. 2 denote a fuzzy operator, e.g., product t-norm, which multiplies the incoming signals, such as:

$$O_{2,i} = w_i = \mu_{Ai}(x) * \mu_{Bi}(y), \text{ for } i=1,2. \quad (6)$$

where $O_{2,i}$ is the output of layer, and the output signal w_i indicates the firing strength of the rule.

Layer 3 (Normalized layer): The nodes in this layer are represented with ***N*** and they calculate the ratio of the *i*-th rule's firing strength to the sum of firing strengths of all rules by:

$$O_{3,i} = \overline{w} = \frac{w_i}{w_1 + w_2}, \text{ for } i=1,2. \quad (7)$$

where the $O_{3,i}$ is the output of Layer 3. The quantity $\overline{w}$ is referred to as the normalized firing strength.

Layer 4 (De-fuzzy layer): The nodes in this layer are represented with a square and they calculate the weighted output of each linear function:

$$O_{4,i} = \overline{w_i}.f_i = w_i\ (p_i\, x + q_i\, y + r_i), \text{ for } i=1,2. \quad (8)$$

where $\overline{w}$ is the output of layer 3, and $\{p_i\, x + q_i\, y + r_i\}$ is the parameter set, referred to as the consequent parameters.

Layer 5 (Total output layer): The single node denoted with a Σ computes the overall output as follows:

$$O_{5,i} = \sum \overline{w_i}.f_i = \frac{\sum_i w_i.f_i}{\sum_i w_i} = fout = \text{Estimated overall output} \quad (9)$$

A hybrid learning algorithm was used to determine the premise and consequent parameters. The hybrid learning algorithm procedure calculates the consequent parameters in a forward pass and the premise parameters in a backward pass. In the forward phase, the information is transmitted forward to layer 4, where the consequent parameters are calculated using the least squares regression algorithm. In the backward phase, the error signals propagate backwards and the premise parameters are estimated by the gradient descent (GD) algorithm (Jang et al., 1997). This error measure is generally defined by the sum of the squared differences between actual and desired outputs.

In the present study, a bell-shaped function (Eq. 5) was used for the MFs. On the other hand, two MFs were used for each input variable, considering that the best results were obtained with this value, achieved through an iterative process. The clustering method called grid partitioning was used to create the Takagi–Sugeno FIS structure (Cobaner, 2011; Shiri et al., 2012).

2.4. Support Vector Machines (SVMs)

Support vector machines (SVMs) is a supervised learning method from the field of machine learning theory and structural risk minimization, applicable to classification or regression analysis, and was presented by Vapnik (2013). In addition to its strong mathematical foundation in statistical learning theory, SVMs have proven to have highly competitive performance in several real-world applications. Originally developed for solving classification problems, the SVM procedure can also be effectively applied to regression problems as follows. Given a data set $\{(x_i,y_i)\}^N_{i=1}$, where x_i is the input vector, y_i is the output value and N is the total number of data sets, the objective is to establish a function that indicates the degree of independence of y_i from the input x_i.

In SVMs, this regression function is approximated using the following function:

$$f(x)=\omega.\varphi(x)+b \tag{10}$$

where ω is a weight vector, b is a bias (scalar value) and $\varphi(x)$ is the high-dimensional feature space which is nonlinearly mapped from the input space x. The coefficients b and ω are calculated by minimizing the following regularized risk function:

$$C\frac{1}{n}\sum_{i=1}^{n} L_\varepsilon(f(x_i), y_i) + \frac{1}{2}\|\omega\|^2 \tag{11}$$

In the regularized risk function, the term $\frac{1}{n}\sum_{i=1}^{n} L_\varepsilon(f(x_i), y_i)$ is empirical error (risk), and measured by function L_ε given below:

$$L_\varepsilon(f(x_i), y_i) = \begin{cases} 0, & |f(x_i) - y_i| < \varepsilon \\ |f(x_i) - y_i| - \varepsilon, & |f(x_i) - y_i| \geq \varepsilon \end{cases} \tag{12}$$

The term $\frac{1}{2}\|\omega\|^2$ is the regularization term, which represents the Euclidean norm, C is a positive trade-off parameter that regulates the degree of the empirical error in the optimization problem that is selected by the user. is called tube size and it is equivalent to the accuracy of the approximation placed on the training data points.

To obtain the estimations of w and b, Eq. (11) is transformed to the primal function given by Eq. (12) by introducing the positive slack variables ξ and ξ* as follows:

Minimize

$$R(\xi, \xi^*, \omega, b) = \frac{1}{2}\|\omega\|^2 + C\sum_{i=1}^{n}(\xi_i + \xi_i^*) \tag{13}$$

$$\text{subjected to } \begin{cases} y_i - \omega\phi(x_i) - b_i \leq \varepsilon + \xi_i \\ \omega\phi(x_i) + b_i - y_i \leq \varepsilon + \xi_i^* \\ \xi_i, \xi_i^* \geq 0, \ \ i = 1, \ldots, l \end{cases}$$

To address the optimization problem, Lagrange multipliers α and α* are added to the condition equations, and the equation can be written in its dual form:

$$R(\alpha, \alpha^*) = \sum_{i=1}^{n} y_i(\alpha_i - \alpha_i^*) - \varepsilon\sum_{i=1}^{n}(\alpha_i - \alpha_i^*) - \\ - \frac{1}{2}\sum_{i=1}^{n}\sum_{j=1}^{n}(\alpha_i - \alpha_i^*)(\alpha_j - \alpha_j^*)K(x_i, x_j) \tag{14}$$

with constraints:

$$\sum_{i=1}^{n}(\alpha_i - \alpha_i^*) = 0 \qquad 0 \leq \alpha_i \leq C, 0 \leq \alpha_i^* \leq C \qquad i = 1, 2, \ldots\ldots, n$$

where α_i and α_{i^*} are Lagrange multipliers to be solved, and $K(x_i,x_j)$ is the so-called kernel function and calculated by $K(x_i,x_j)=\varphi(x_i).\varphi(x_j)$ on the feature space. The kernel allows SVMs to form nonlinear boundaries; in other words, it gives the SVM the capacity to model complicated separating hyperplanes. In this study, after a number of trial-and-error processes, the radial basis function (RBF) was chosen as the kernel function. The RBF is defined as follows:

$$(x_i,x_j)=\exp(\gamma\|x_i - x_j\|^2), \qquad \gamma>0 \tag{15}$$

where x_i and x_j are vectors in the input space and γ is the kernel parameter.

After calculating Lagrange multipliers, an optimal desired weights vector of the regression hyperplane is found as follows:

$$\omega = \sum_{i=1}^{n}(\alpha_i - \alpha_i^*)\,\varphi(x) \tag{16}$$

and Eq. (10) can be rewritten as follows:

$$f(x, \alpha, \alpha^*) = \sum_{i=1}^{n}(\alpha_i - \alpha_i^*)\cdot K(x_i, x_j) + b \tag{17}$$

where n is the number of support vectors, $(\alpha_i - \alpha_i^*)$ are their Lagrange multipliers, the term $K(x_i,x_j)$ is the kernel function in the input space and the bias b is calculated from training samples.

There are three free parameters while using the RBF kernel: C (cost), ε (epsilon) and γ (gamma) should be determined to find the optimal solutions. In this study we have used the genetic algorithm (*GA*) technique with a ten-fold cross-validation procedure to optimize these parameters (Saud et al., 2020) and varying the parameters ε = 0.002 to ε = 2, C = 0.0001 to C = 10, and γ = 0.0001 to γ = 2. A GA is an intelligent optimization method based on the principles of genetics and natural selection. Further details of this technique can be found in Antonanzas-Torres et al. (2015) and Zhang et al. (2015).

2.5. CatBoost

CatBoost is a decision-tree machine learning algorithm based on gradient boosting decision tree (GBDT), developed by researchers from the Russian internet company Yandex (Prokhorenkova et al., 2018). It is capable of solving problems with heterogeneous characteristics, noisy data and complex dependencies compared to other algorithms based on decision trees. Among the advantages of using CatBoost is that it requires the configuration of few hyperparameters, thus avoiding overfitting

and obtaining more generalized models. Decision trees are used for regression, and each tree corresponds to a partition of the feature space and the output value.

This model has several advantages compared with traditional GBDT algorithms, which generally cope with categorical features by a method named Greedy Target Statistics (Greedy *TS*). To deal with categorical features during training rather than the preprocessing phase to estimate the expected and category driven target, CatBoost allows the use of a complete data set for training. According to (Prokhorenkova et al., 2018), the Greedy *TS* strategy manages categorical features with minimum information loss. This is useful for minimizing information loss and overfitting. Given a data set D={X_i} i= *1,…,n,* where $X_i=(x_i,1,\cdots,x_i,m)$ is a vector of *m* characteristics, the category of *the k-th* training example can be replaced by a numerical characteristic expressed in (Eq. 20) according to the requested *TS*. The substitution of a given categorical example $x\sigma_{p,k}$, *k* can be obtained by calculating its average value with the same category value placed before in a random permutation of data set $\sigma=(\sigma_1,\cdots,\sigma_n)$. Also, CatBoost is able to combine various categorical features into a new one in a greedy way by establishing a new tree split.

$$\hat{x}\sigma_{p,k} = \mathbb{E}\left(y \middle| x\sigma_p = x\sigma_{p,k}\right) = \frac{\sum_{j=1}^{p-1}[x\sigma_{j,k}=x\sigma_{p,k}]+y\sigma_j+aP}{\sum_{j=1}^{p-1}[x\sigma_{j,k}=x\sigma_{p,k}]+a} \quad (20)$$

where *y* is the objective function, *P* is a previous value, is the weight of the previous value, and $[x\sigma_{j,k}=x\sigma_{p,k}]$ is equal to one when $x\sigma_{j,k}=x\sigma_{p,k}$, otherwise it is equal to zero, since $\alpha>0$ represents the P weight. This method contributes to reducing the noise obtained from the low frequency category.

On the other hand, CatBoost combines multiple categorical features, using a greedy way of combining all the categorical characteristics and their combinations in the current tree with all the categorical characteristics in the data set, so that CatBoost overcomes the gradient bias.

The classic GBDT procedure generates a weak learner in each iteration and each learner is trained based on the gradient of the previous learner. The accumulation of the classified results of all learners provides the result (Friedman, 2002). However, it will lead to a punctual and biased gradient estimation, causing the final learned model to overfit. CatBoost uses a new method to change the gradient estimation method in the classic algorithm, called gradient augmentation. This method can overcome the prediction change caused by gradient bias and further improve model generalizability.

To obtain an unbiased gradient estimate, CatBoost trains a separate M_i model for each x_i sample, and the M_i model is trained with a data set that does not contain the X_i sample. In this case, M_i is used to obtain a gradient estimate of the sample. Also, this gradient will be used to train the base learner for the final model.

In the present study, in the implementation of the CatBoost model, some of its main parameters that affect the precision and model stability were adjusted using the cross-validation (fold = 5) technique (Saud et al., 2020); the number of iterations varied between 200 and 800 at 100 intervals, the maximum depth of tree ranged from 2 to 10 at intervals of 2, and the proportion of subsets varied from 0.5 to 1 at intervals of 0.05.

2.6. Hargreaves and Samani equation

The HS model (Hargreaves and Samani, 1985) is considered an alternative for estimating ET_0 when only temperature records are available. The HS model is structured as follows:

$$ET_{HS}=K_{coef}*0.408*H_0*(T_{mean}+17.8)*(T_{max}-T_{min})^{0.5} \quad (21)$$

where ET_{HS} is the reference evapotranspiration estimated (mm day^{-1}); K_{coef} is an empirical coefficient, which was initially established at 0.0023 but has been recalibrated according to the place used; T_{mean}, T_{max}, and T_{min} are the average, maximum and minimum daily air temperature respectively; H_0 is the extraterrestrial solar radiation (MJ m^{-2} day^{-1}); and the coefficient 0.048 is for converting MJm^{-2} day^{-1} to mm day^{-1}.

In this study, the K_{coef} was obtained by the nonlinear least squares fitting technique.

2.7. Inputs considered and model scenarios

In the present study, three input combinations of the daily minimum air temperature (T_{min}; °C), maximum air temperature (T_{max}; °C), mean relative humidity (RH; %), extraterrestrial radiation (H_0; MJ m^{-2} day^{-1}), and rainy days (RT) as binary number [(W), rainfall > 0, W = 1; rainfall = 0, W = 0] were used to estimate the daily reference evapotranspiration. To identify the influence of the parameters considered on the accurate prediction of ET_0, the Pearson correlation coefficients between the ET_0 and independent parameters (inputs) were calculated. Tab. 2 presents the Pearson correlation coefficients obtained. According to Tab. 2, all inputs considered were observed to have favorable correlations with ET_0. However, the highest correlation was obtained for T_{max} and RH, while the lowest correlation was obtained for the RT variable. In this study, three scenarios were considered

Table 2. Pearson correlations between ET_0 and input variables used in this study.

Station/Variable	H_0	T_{max}	T_{min}	RH	RT
Calakmul	0.660**	0.800**	0.403**	-0.748**	-0.250**
Campeche	0.735**	0.746**	0.490**	-0.662**	-0.266**
Efraín Hernández	0.610**	0.738**	0.371**	-0.688**	-0.372**
Mérida	0.646**	0.776**	0.411**	-0.698**	-0.272**
Tantakín	0.655**	0.784**	0.247**	-0.712**	-0.265**

** Correlation is significant at the 0.05 level (2-tailed).

to evaluate the effect of relative humidity, rainfall and temperature, namely:
(1) Relative humidity-based: T_{min}, T_{max}, RH and H_0 (SVM1, ANFIS1, CatBoost1),
(2) Rainfall-based: T_{min}, T_{max}, RT and H_0 (SVM2, ANFIS2, CatBoost2),
(3) Temperature-based: T_{min}, T_{max} and H_0 (SVM3, ANFIS3, CatBoost3),
H_0 was calculated as a function of the day of year, site latitude and solar angle, according to the equation proposed by Allen et al. (1998).

As a normal practice for developing predictive models and to avoid problems in the training and testing stages due to the different orders of magnitude and large-scale fluctuations of the inputs that generate numerical issues while producing the forecast, the dataset was normalized to the range from zero to one using the following equation (Feng et al., 2016):

$$x_n = \frac{x_0 - x_{min}}{x_{max} - x_{min}} \tag{22}$$

where x_n, x_0, x_{min} and x_{max} are the normalized value, real value, minimum value and maximum value respectively.

Moreover, to ensure the representativeness of the dataset, the database was randomly split into two subsets, using 70% for training and the remaining 30% to test the model. The training dataset was used to train all the models, while the testing data was used to verify the accuracy and the performance of the trained model. Despite the fact that a k-fold validation might be desirable, a simple holdout assessment was applied, i.e., a single data set assignment was considered for evaluating the models. Given the size of the data series, the test set sample was considered representative enough. Further, in light of the different modeling approaches considered, the application of the k-fold assessment might have involved too high computational costs.

A script file written in MATLAB 2019b software version was used to carry out the computer simulation of the ANFIS models. For the SVM and CatBoost models, two open-source software packages named 'LIBSVM 3.2' (Chang et al., 2013) and 'Catboost' respectively were implemented using the R computing environment (Meyer and Wien, 2014; RDevelopment, 2009).

2.8. Model performance evaluation

The performance and accuracy of the proposed models for estimating daily ET_0 were evaluated using five common statistical tests (Despotovic et al., 2015; Teke et al., 2015): root mean square error (RMSE; Eq. 23), mean absolute error (MAE; Eq. 24), mean bias error (MBE; Eq. 25), coefficient of determination (R^2; Eq. 26) and the Nash–Sutcliffe model efficiency coefficient (NSE; Eq. 27). The five criteria adopted are sufficient to fully characterize the efficiency of the models.

$$RMSE = \sqrt{\frac{1}{n}\sum_{i=1}^{n}(x-y)^2} \quad (mm\ day^{-1}) \tag{23}$$

$$MAE = \frac{1}{n}\sum_{i=1}^{n}(|y-x|) \quad (mm\ day^{-1}) \tag{24}$$

$$MBE = \frac{1}{n}\sum_{i=1}^{n}(y-x) \quad (mm\ day^{-1}) \tag{25}$$

$$R^2 = \frac{\left[\sum_{i=1}^{n}(x-x_{avg})(y-y_{avg})\right]^2}{\sum_{i=1}^{n}(x-x_{avg})^2 \sum_{i=1}^{n}(y-y_{avg})^2} \quad \text{(unitless)} \tag{26}$$

$$NSE = 1 - \frac{\sum_{i=1}^{n}(y-x)^2}{\sum_{i=1}^{n}(y-y_{avg})^2} \quad \text{(unitless)} \tag{27}$$

where n and avg represent the total number of evaluated data and the average of the variable, and x and y are the ET_0 values predicted by the models and ET_0-FAO56PM respectively.

Smaller RMSE and MAE values imply a closer approximation of the values measured by the models. Larger R^2 values indicate a closer match of measured data trends with the model results. Mean Bias Error (MBE) captures the average bias in the prediction. MBE is primarily used to estimate the average bias in the model and to decide if any steps need to be taken to correct the model bias. Positive values of MBE indicate the overestimation of daily ET_0 by a model and negative values indicate underestimation. The NSE values can range from -∞ to 1, and a perfect fit between the simulated and observed data is reached when NSE value is close to 1 (Krause et al., 2005).

3. RESULTS AND DISCUSSION

In this study, the capabilities of three artificial intelligence techniques (i.e., CatBoost, ANFIS and SVMs) for predicting ET_0 with the daily meteorological variables T_{max}, T_{min}, RH, R_s and u_2 were examined. The type of input parameters plays an important role in the accuracy of AI models in predicting daily ET_0. Fig. 3 shows the scatter plots of the ET_0 values estimated by the best AI technique and calibrated HS model in each scenario during the testing phase and measured values at the five meteorological stations. According to R^2 values, the plots clearly reveal that relative humidity might be the most influential input for estimating ET_0, and it is also noted that the SVM method was the best in the three scenarios evaluated. In addition, it is observed that the empirical HS equation commonly used when temperature data are available performed worse compared to the temperature-based AI models. Tab. 4 gives the R^2, NSE, RMSE, MAE and MBE values for ANFIS, SVM and CatBoost models during the training and testing phase. In the first scenario, the effect of relative humidity on the model's prediction accuracy was evaluated in a sub-humid tropical region. The SVM1 model had the best performance for all evaluated stations, with an RMSE of 0.37 –0.479 mm day^{-1}, MAE of 0.285–0.372 mm day^{-1}, R^2 of 0.937–0.862 and NSE of 0.936–0.861. The CatBoost1 and ANFIS1 models were ranked second and third respectively. For the second scenario, the effect of rainfall on the performance of the models was investigated, since it is usually measured and can be used to improve ET_0 estimation. The SVM2 models outperform the CatBoost2 and ANFIS2 models for all locations with an RMSE of 0.494–0.700 mm day^{-1}, MAE of 0.379–0.534 mm day^{-1}, R^2 of 0.834–0.758 and NSE of 0.833–0.752. On the other hand, the ANFIS2 and CatBoost2 models based on rainfall data presented similar performance criteria (RMSE, MAE, R^2 and NSE). In the third scenario, considering that relative humidity and rainfall data are not always readily available, a temperature-based model may be helpful. The SVM3 model provided the best performance at four of the five stations evaluated with RMSE values of 0.548–0.731 mm day^{-1}, MAE of 0.418–0.563 mm day^{-1}, R^2 of 0.779–0.738 and NSE of 0.778–0.731, with the CatBoost3 model showing higher accuracy at the Mérida station. Overall, the SVM technique offers better performance for all evaluated scenarios with a RMSE = 0.552 mm day^{-1}, MAE = 0.425 mm day^{-1}, R^2 = 0.811 and NSE = 0.806, followed by the CatBoost model with a RMSE = 0.561 mm day^{-1}, MAE = 0.434 mm day^{-1}, R^2 = 0.799 and NSE = 0.737. As seen in scenario 1, the inclusion of relative humidity significantly improved all evaluated techniques.

In general, during the test phase, it should be noted that the consideration of relative humidity as an input in the SVM1 model significantly increased the estimation accuracy through a decrease in MAE and RMSE values of 32.73 and 32.71% respectively, and an increase in R^2 of 14.5%. Meanwhile, when W data were added to the SVM2 model, it showed a slight reduction in MAE and RMSE of 9.06 and 8.87% respectively, while R^2 increased by 4.4%. As demonstrated in several studies, the combination of bio-inspired algorithms improves the accuracy of artificial intelligence models (Mohammadi and Mehdizadeh, 2020; Yin et al., 2017). In the present study the parameters of the SVM-based models (C, g, and e) were optimized using the genetic algorithm (Tab. 3).

One of the main drawbacks of AI-based techniques is overfitting (Fathian et al., 2019). However, in the case of the SVM method, one of its main advantages over other AI methods lies in the fact that the non-linear problem always converges to a global minimum. In most studies, model accuracy has been shown to increase in ET_0 prediction as the number of meteorological parameters increase. A study conducted by Chen et al. (2020) showed that the performance of SVM models was better than LSTM and DNN models when relative humidity features were available. Tab. 4 also shows the performance indicators for the data set during the training

Table 3. The SVM parameters optimized by the GA.

Station/Model	Optimum values		
	Cost (C)	Gamma (γ)	Epsilon (ε)
Calakmul			
SVM1	1.957	0.196	0.318
SVM2	2.170	0.452	0.305
SVM3	1.135	0.668	0.350
Campeche			
SVM1	4.774	0.334	0.299
SVM2	2.911	0.114	0.420
SVM3	5.412	0.136	0.472
Efraín Hernández			
SVM1	1.488	0.381	0.244
SVM2	3.617	0.422	0.356
SVM3	1.963	0.551	0.299
Mérida			
SVM1	4.585	0.108	0.291
SVM2	2.263	0.227	0.413
SVM3	7.250	0.598	0.402
Tantakín			
SVM1	9.315	0.148	0.252
SVM2	5.835	0.110	0.404
SVM3	5.966	0.200	0.509

Table 4. Training and test performance indicators by station.

Station/model	Training data					Test data				
	R^2	NSE	RMSE (mm day^{-1})	MAE (mm day^{-1})	MBE (mm day^{-1})	R^2	NSE	RMSE (mm day^{-1})	MAE (mm day^{-1})	MBE (mm day^{-1})
Calakmul										
CatBoost1	0.859	0.824	0.444	0.334	-0.025	0.851	0.823	0.459	0.348	-0.035
SVM1	0.848	0.849	0.455	0.341	-0.006	**0.862**	**0.862**	**0.447**	**0.340**	**0.008**
ANFIS1	0.824	0.824	0.475	0.359	0.000	0.86	0.836	0.473	0.355	0.135
CatBoost2	0.760	0.657	0.578	0.441	-0.025	0.763	0.662	0.581	0.447	-0.032
SVM2	0.764	0.763	0.576	0.434	0.009	**0.767**	**0.765**	**0.569**	**0.435**	**0.042**
ANFIS2	0.766	0.766	0.547	0.415	0.000	0.759	0.697	0.707	0.538	0.254
CatBoost3	0.736	0.609	0.606	0.462	-0.026	0.732	0.601	0.619	0.475	-0.045
SVM3	0.7211	0.720	0.621	0.474	0.016	**0.746**	**0.742**	**0.607**	**0.461**	**0.029**
ANFIS3	0.732	0.732	0.586	0.445	0.000	0.695	0.646	0.765	0.580	0.240
Campeche										
CatBoost1	0.861	0.824	0.475	0.365	-0.032	0.860	0.820	0.482	0.370	-0.028
SVM1	0.845	0.846	0.498	0.376	0.003	**0.862**	**0.861**	**0.479**	**0.372**	**0.036**
ANFIS1	0.858	0.858	0.477	0.359	0.000	0.807	0.800	0.569	0.422	-0.082
CatBoost2	0.791	0.716	0.582	0.448	-0.031	0.780	0.703	0.602	0.463	-0.017
SVM2	0.782	0.782	0.592	0.451	-0.011	**0.793**	**0.792**	**0.584**	**0.455**	**0.006**
ANFIS2	0.803	0.803	0.562	0.424	0.000	0.765	0.732	0.659	0.529	0.231
CatBoost3	0.743	0.626	0.645	0.494	-0.032	0.723	0.598	0.675	0.520	-0.022
SVM3	0.716	0.715	0.676	0.512	-0.034	**0.745**	**0.744**	**0.652**	**0.508**	**-0.009**
ANFIS3	0.746	0.746	0.638	0.481	0.000	0.683	0.654	0.749	0.598	0.212
Efraín Hernández										
CatBoost1	0.871	0.837	0.406	0.311	-0.030	0.851	0.822	0.432	0.333	-0.029
SVM1	0.862	0.863	0.417	0.314	-0.008	**0.864**	**0.864**	**0.411**	**0.315**	**-0.001**
ANFIS1	0.862	0.862	0.415	0.312	0.000	0.846	0.828	0.451	0.338	-0.118
CatBoost2	0.821	0.772	0.474	0.361	0.000	0.800	0.744	0.506	0.387	0.013
SVM2	0.806	0.806	0.496	0.38	0.000	**0.805**	**0.804**	**0.494**	**0.379**	**0.029**
ANFIS2	0.8	0.801	0.497	0.379	0.000	0.801	0.779	0.512	0.385	-0.147
CatBoost3	0.782	0.698	0.523	0.400	0.000	0.741	0.663	0.578	0.445	-0.029
SVM3	0.757	0.757	0.547	0.417	-0.018	**0.774**	**0.772**	**0.548**	**0.418**	**-0.007**
ANFIS3	0.736	0.737	0.572	0.442	0.000	0.738	0.712	0.583	0.450	-0.142
Mérida										
CatBoost1	0.934	0.927	0.374	0.280	0.000	0.924	0.918	0.381	0.289	-0.024
SVM1	0.923	0.924	0.394	0.300	0.017	**0.937**	**0.936**	**0.371**	**0.285**	**0.035**
ANFIS1	0.932	0.932	0.379	0.282	0.000	0.921	0.920	0.391	0.300	0.007
CatBoost2	0.847	0.811	0.569	0.438	0.000	0.839	0.807	0.556	0.442	-0.029
SVM2	0.834	0.834	0.574	0.449	0.006	**0.834**	**0.833**	**0.580**	**0.450**	**0.015**
ANFIS2	0.837	0.837	0.588	0.455	0.000	0.828	0.825	0.611	0.467	-0.035
CatBoost3	0.791	0.716	0.667	0.513	0.000	0.786	0.712	0.643	0.500	-0.050
SVM3	0.783	0.783	0.670	0.519	0.010	**0.779**	**0.778**	**0.678**	**0.521**	**0.011**
ANFIS3	0.765	0.765	0.706	0.551	0.000	0.749	0.741	0.705	0.537	-0.041
Tantakín										
CatBoost1	0.906	0.892	0.428	0.321	-0.001	0.866	0.849	0.499	0.367	0.033
SVM1	0.887	0.887	0.467	0.346	-0.011	**0.901**	**0.900**	**0.437**	**0.333**	**0.004**
ANFIS1	0.896	0.897	0.458	0.340	0.000	0.861	0.858	0.485	0.357	-0.058
CatBoost2	0.778	0.700	0.659	0.507	-0.001	0.756	0.677	0.672	0.522	-0.004
SVM2	0.749	0.749	0.691	0.532	0.017	**0.758**	**0.752**	**0.700**	**0.534**	**0.061**
ANFIS2	0.797	0.798	0.640	0.489	0.000	0.736	0.536	0.877	0.730	-0.531
CatBoost3	0.751	0.644	0.699	0.536	-0.001	0.715	0.598	0.725	0.562	0.004
SVM3	0.705	0.705	0.745	0.574	0.000	**0.738**	**0.737**	**0.731**	**0.563**	**0.008**
ANFIS3	0.762	0.762	0.695	0.524	0.000	0.695	0.454	0.952	0.785	-0.571

Note: Models with the best fit during the test phase are shown in bold.

Table 5. Performance statistics of the Hargreaves–Samani model.

Station/model	R^2	NSE	RMSE (mm day^{-1})	MAE (mm day^{-1})	MBE (mm day^{-1})	K_{coef}
Calibrated						
Calakmul	0.692	0.582	0.826	0.614	0.241	0.0015
Campeche	0.653	0.623	0.775	0.615	0.217	0.0020
Efraín Hernández	0.678	0.634	0.653	0.507	-0.220	0.0019
Mérida	0.702	0.701	0.754	0.590	-0.012	0.0021
Tantakín	0.668	0.577	0.831	0.680	-0.373	0.0018
Uncalibrated						
Calakmul	0.692	0.534	1.681	1.540	-1.524	0.0023
Campeche	0.653	0.569	0.827	0.644	-0.346	0.0023
Efraín Hernández	0.678	0.342	1.250	1.101	-1.080	0.0023
Mérida	0.702	0.637	0.830	0.642	-0.346	0.0023
Tantakín	0.668	0.459	1.841	1.702	-1.677	0.0023

phase. It should be noted that the R^2, NSE, RMSE and MAE values are similar to those reached during the test phase; these values denote the absence of overfitting during training, due to the previous adjustment of the model's parameters.

Tab. 5 shows the performance results of the HS model, as well as its calibrated empirical coefficient (K_{coef}). On comparing these results with the AI-based models of scenario 3 (temperature-based), it is clearly observed that in general the AI-based models outperformed the HS method. In fact, many studies have shown the superiority of AI-based methods over the HS equation (Reis et al., 2019; Chen et al., 2020; Zhu et al., 2020). In addition, the calibration of the Ks coefficient considerably improved the performance of the HS models compared to the uncalibrated ones. On the other hand, the temperature- and extraterrestrial radiation-based HS equation tended to overestimate ET_0 in humid and sub-humid regions (Allen et al., 1998), with estimates improving when calibrated in local climate conditions (Almorox et al., 2015). However, the uncalibrated HS equation was found to underestimate ET_0 under the warm sub-humid climate of the Yucatán Peninsula, according to the MBE statistic in Tab. 5.

Overall, SVM showed the best performance among the three AI models, and comparing the CatBoost and ANFIS models, the CatBoost model showed better performance than the ANFIS model for all three scenarios evaluated. These results agreed with the result obtained by Raza et al. (2020), who evaluated five AI-based methods, finding that the SVM method improves the accuracy of estimates in both hyper-arid and high-humidity climates. Similar results were obtained by Huang et al. (2019b) in humid regions of China when they evaluated the SVM, CatBoost and RF methods, finding that, of the three methods, SVMs offered the best prediction accuracy and stability with incomplete combinations of meteorological parameters as inputs (T_{min}, T_{max}, RH) with a RMSE value of 0.640 mm day^{-1}, while CatBoost performed best with the complete combination of parameters (T_{min}, T_{max}, RH, U_2 and R_s) with a RMSE value of 0.220 mm day^{-1}.

Regarding the bias of the AI-based models, Tab. 4 shows that the SVM model had small positive MBE values during the test phase, suggesting that the SVM model slightly overestimates ET_0 values at the study site, the exception being at the Campeche station when only temperature data were used. Overall, the CatBoost method had a tendency to slightly underestimate the values of ET_0, according to the negative MBE values. In the case of the ANFIS models, according to the MBE indicator, the model overestimated ET_0 values at the Campeche and Calakmul stations, and underestimated ET_0 values at the Efraín Hernández, Mérida and Tantakín stations.

One of the main advantages of AI-based models over traditional methods is that overfitting problems can be avoided by selecting an appropriate structure, such as in the case of ANFIS method, or by adjusting internal parameters through cross-validation in CatBoost or using algorithms in the case of SVM models.

The main advantage of the use of AI models is their capacity to model large amounts of noisy data from dynamic and non-linear systems. One of the main disadvantages of using AI-based models is that the trained algorithm to be used requires the use of specialized software (i.e., MATLAB, R or Python) or, where appropriate, it must be embedded as a module on an Arduino or Raspberry Pi board.

4. CONCLUSIONS

In the present study, the performance of SVM, ANFIS and CatBoost models was assessed for estimating daily ET_0, considering climatic data from five weather stations located in the Yucatán Peninsula, Mexico.

Overall, the SVM approach showed the best performance for all evaluated scenarios for estimating ET_0, which is helpful for irrigation scheduling in a warm sub-humid region of the Yucatán Peninsula, Mexico and possibly elsewhere with similar climate. In the present study, it has been shown that the use of the GA algorithm combined with SVM-based models improves the accuracy of daily ET_0 estimation.

Most of the previous works carried out in warm sub-humid climates include the relative humidity vari-

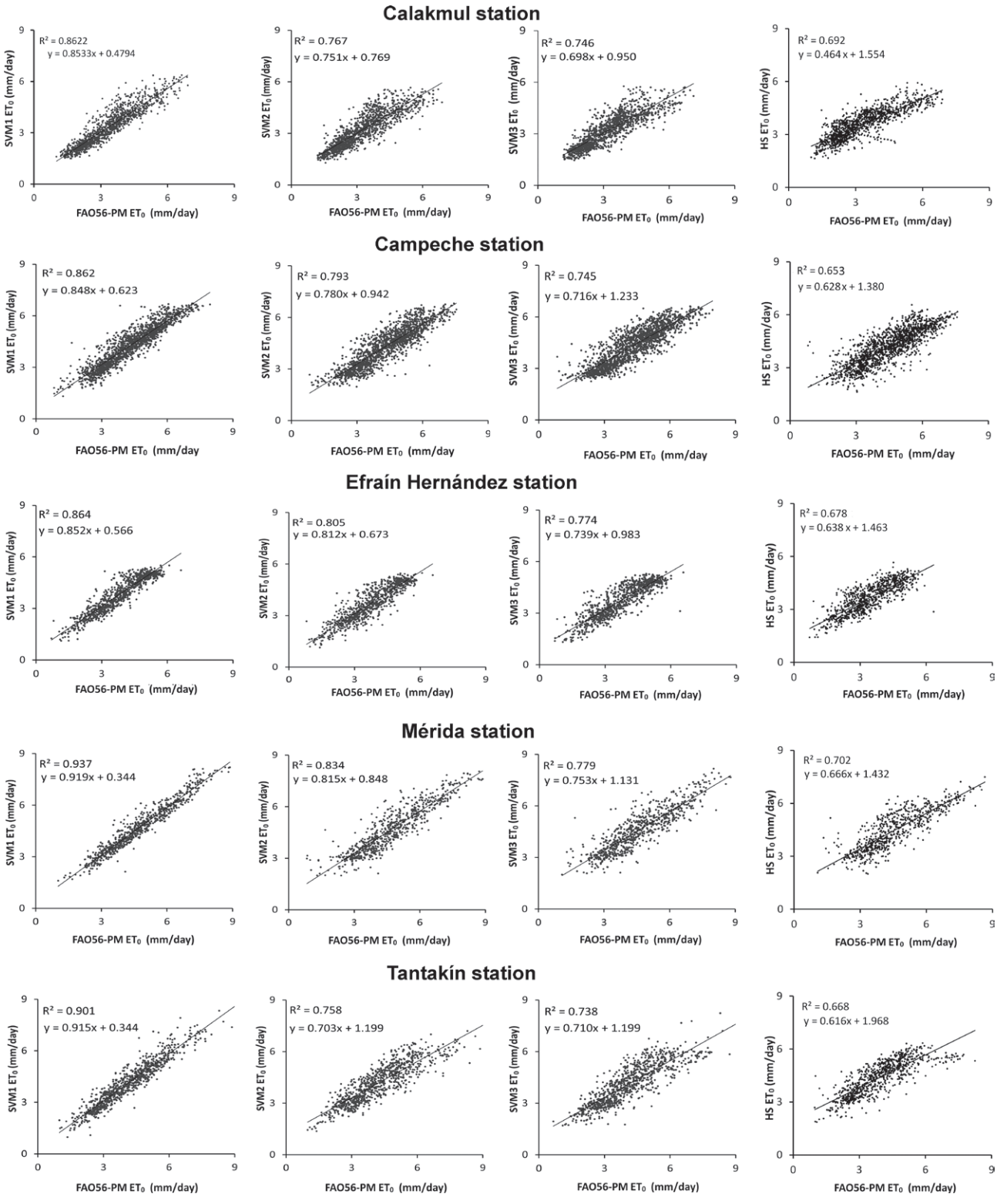

Fig. 3. The FAO56-PM ET_0 and estimated ET_0 values obtained by the best AI model and calibrated HS model in each scenario during the testing phase.

able in the model. In this study, the precipitation variable was considered because the variability of temperature in the rainy season in the Yucatán region is strongly modulated by precipitation events. This way, adding precipitation data as a binary number in the rainfall-based scenario slightly increased model performance. However, the inclusion of RH values into the relative humidity-based scenario significantly improved estimation accuracy. A major disadvantage of this scenario is the unavailability of RH data in some regions, while temperature and rainfall data are generally measured at all weather stations. This suggests that, if RH data are available, the SVM1 model should be used to obtain better results. Finally, a comparative analysis of model performance showed that the AI models have better ability than the HS model for ET_0 modelling when only temperature records are available, although the HS model presents the advantage of using an algebraic equation, facilitating its application.

AI-based models can be a suitable alternative to conventional models for ET_0 modelling; however, prior adjustment of their internal parameters by using a cross-validation test is necessary to avoid overfitting. In the future, in order to improve the present study, it would be convenient to analyze the performance of the models under a seasonal analysis scheme, as well as the performance of the models in the dry and rainy seasons.

Thus, the results of this study indicate that SVMs increase the prediction accuracies of ET_0 estimates in warm sub-humid tropical climates such as the Yucatán in Mexico, especially when air humidity is included in the model.

ACKNOWLEDGEMENTS

This research did not receive any specific grant from funding agencies in the public, commercial, or not-for-profit sectors.

REFERENCES

Alizamir, M., Kisi, O., Adnan, R. M., Kuriqi, A. 2020. Modelling reference evapotranspiration by combining neuro-fuzzy and evolutionary strategies. Acta Geophysica, 68, 1113–1126. DOI: 10.1007/s11600-020-00446-9

Allen, R. G., Pereira, L. S., Raes, D., Smith, M. 1998. Crop evapotranspiration–Guidelines for computing crop water requirements–FAO Irrigation and drainage paper 56. Irrig. Drain, 300(9), D05109.

Almorox, J., Quej, V. H., Martí, P. 2015. Global performance ranking of temperature-based approaches for evapotranspiration estimation considering Köppen climate classes. Journal of Hydrology, 528, 514–522. DOI: 10.1016/j.jhydrol.2015.06.057

Antonanzas-Torres, F., Urraca, R., Antonanzas, J., Fernandez-Ceniceros, J., Martinez-De-Pison, F. J. 2015. Generation of daily global solar irradiation with support vector machines for regression. Energy Conversion and Management, 96, 277–286. DOI: 10.1016/j.enconman.2015.02.086

Chang, C., Lin, C., Tieleman, T. 2013. LIBSVM: A Library for Support Vector Machines. ACM Transactions on Intelligent Systems and Technology (TIST), 307, 1–39. DOI: 10.1145/1961189.1961199

Chen, Z., Zhu, Z., Jiang, H., Sun, S. 2020. Estimating daily reference evapotranspiration based on limited meteorological data using deep learning and classical machine learning methods. Journal of Hydrology, 591(125286), 1–12. DOI: j.jhydrol.2020.125286

Cobaner, M. 2011. Evapotranspiration estimation by two different neuro-fuzzy inference systems. Journal of Hydrology, 398(3–4), 292–302. DOI: 10.1016/j.jhydrol.2010.12.030

Despotovic, M., Nedic, V., Despotovic, D., Cvetanovic, S. 2015. Review and statistical analysis of different global solar radiation sunshine models. Renewable and Sustainable Energy Reviews, 52, 1869-1880. DOI: 10.1016/j.rser.2015.08-035

Dorogush, A. V., Ershov, V., Gulin, A. (2018). CatBoost: gradient boosting with categorical features support. arXiv preprint arXiv:1810.11363.

Fathian, F., Mehdizadeh, S., Sales, A., Safari, M. 2019. Hybrid models to improve the monthly river flow prediction: Integrating artificial intelligence and nonlinear time series models. Journal of Hydrology, 575, 1200–1213. DOI: 10.1016/j.jhydrol.2019.06.025

Feng, Y., Cui, N., Zhao, L., Hu, X., Gong, D. 2016. Comparison of ELM, GANN, WNN and empirical models for estimating reference evapotranspiration in humid region of Southwest China. Journal of Hydrology, 536, 376–383. DOI: 10.1016/j.jhydrol.2016.02.053

Friedman, J. H. 2002. Stochastic gradient boosting. Computational statistics & data analysis, 38(4), 367–378. DOI: 10.1016/S0167-9473(01)00065-2

Fritsch, F. N., Carlson, R. E. 1980. Monotone piecewise cubic interpolation. SIAM Journal on Numerical Analysis, 17(2), 238–246. DOI: 10.1137/0717021

Gocić, M., Motamedi, S., Shamshirband, S., Petković, D., Ch, S., Hashim, R., Arif, M. 2015. Soft computing approaches for forecasting reference evapotranspira-

tion. Computers and Electronics in Agriculture, 113, 164–173. DOI: 10.1016/j.compag.2015.02.010

Granata, F., Di, N. 2021. Forecasting evapotranspiration in different climates using ensembles of recurrent neural networks. Agricultural Water Management, 255(107040), 1–19. DOI: j.agwat.2021.107040

Hargreaves, G. H., & Samani, Z. A. (1985). Reference Crop Evapotranspiration from Ambient Air Temperature; American Society of Agricultural Engineers: St. Joseph, MI, USA, 85

Huang, G., Wu, L., Ma, X., Zhang, W., Fan, J., Yu, X., Zeng, W., Zhou, H. 2019b. Evaluation of CatBoost method for prediction of reference evapotranspiration in humid regions. Journal of Hydrology. 574, 1029–1041. DOI: 10.1016/j.jhydrol.2019.04.085

Jang, J.S.R. 1993. ANFIS: adaptive-network-based fuzzy inference system, IEEE transactions on systems, man, and cybernetics, 23(3), 665-685. DOI: 10.1109/21.256541

Jang, J.S.R., Sun, C.T., Mizutani, E. 1997. Neuro-fuzzy and Soft Computing: A Computational Approach to Learning and Machine Intelligence, Prentice Hall, New Jersey.

Jensen, M. E., Burman, R. D., Allen, R. G. 1990. Evapotranspiration and irrigation water requirements: a manual. ASCE manuals and reports on engineering practice (USA). no.70.

Krause, P., Boyle, D. P., Bäse, F. 2005. Comparison of different efficiency criteria for hydrological model assessment. Advances in geosciences, 5, 89-97. DOI: 10.5194/adgeo-5-89-2005

Kisi, O. 2013. Least squares support vector machine for modeling daily reference evapotranspiration. Irrigation Science, 31(4), 611–619. DOI: 10.1007/s00271-012-0336-2

Köppen, W. 1936. Das geographisca System der Klimate In: W. Köppen and G.Geiger, ed.Handbuch der Klimatologie (Handbuch der Klimatologie, vol.1: C.Gebr, Borntraeger).

Meyer, D., Wien, F. H. T. 2014. Support vector machines. The Interface to libsvm in package e1071.

Midleton N, Thomas D. 1997. World atlas of desertification, 2nd edition. Oxford Univ. Press

Mohammadi, B., Mehdizadeh, S. 2020. Modeling daily reference evapotranspiration via a novel approach based on support vector regression coupled with whale optimization algorithm, Agricultural Water Management, 237(106145), 1–14. DOI: 10.1016/j.agwat.2020.106145

Petković, D., Gocic, M., Trajkovic, S., Shamshirband, S., Motamedi, S., Hashim, R., Bonakdari, H. 2015. Determination of the most influential weather parameters on reference evapotranspiration by adaptive neuro-fuzzy methodology. Computers and Electronics in Agriculture, 114, 277–284. DOI: 10.1016/j.compag.2015.04.012

Prokhorenkova, L., Gusev, G., Vorobev, A., Dorogush, A. v., Gulin, A. 2018. CatBoost: unbiased boosting with categorical features. In Advances in neural information processing systems, 6638–6648. https://github.com/catboost/catboost

Raza, A., Shoaib, M., Faiz, M. A., Baig, F., Khan, M. M., Ullah, M. K., Zubair, M. 2020. Comparative Assessment of Reference Evapotranspiration Estimation Using Conventional Method and Machine Learning Algorithms in Four Climatic Regions. Pure and Applied Geophysics, 177(9), 4479–4508. DOI: 10.1007/S00024-020-02473-5

RDevelopment, C. 2009. TEAM 2009: R: A Language and Environment for Statistical Computing. Vienna, Austria.

Reis, M., Silva, A. da, Junior, J., Santos, L., Azevedo, A., Lopes, E. 2019. Empirical and learning machine approaches to estimating reference evapotranspiration based on temperature data. Computers and Electronics in Agriculture, 165(104937), 1–10. DOI: 10.1016/j.compag.2019.104937

Rezaabad, M. Z., Ghazanfari, S., Salajegheh, M. 2020. ANFIS Modeling with ICA, BBO, TLBO, and IWO Optimization Algorithms and Sensitivity Analysis for Predicting Daily Reference Evapotranspiration. Journal of Hydrologic Engineering, 25(8), 04020038. DOI: 10.1061/(ASCE)HE.1943-5584.0001963

Roy, D. K., Barzegar, R., Quilty, J., Adamowski, J. 2020. Using ensembles of adaptive neuro-fuzzy inference system and optimization algorithms to predict reference evapotranspiration in subtropical climatic zones. Journal of Hydrology, 591, 125509. 10.1016/J.JHYDROL.2020.125509

Saud, S., Jamil, B., Upadhyay, Y., Irshad, K. 2020. Performance improvement of empirical models for estimation of global solar radiation in India: A k-fold cross-validation approach. Sustainable Energy Technologies and Assessments, 40, 100768. DOI: 10.1016/j.seta.2020.100768

Shiri, J., Kisi, O., Landeras, G., Javier Lopez, J., Nazemi, A. H., Stuyt, L.C.P.M. 2012. Daily reference evapotranspiration modeling by using genetic programming approach in the Basque Country (Northern Spain). Journal of Hydrology, 414, 302–316. DOI: 10.1016/j.jhydrol.2011.11.004.

Teke, A., Yıldırım, H. B., and Çelik, Ö. 2015. Evaluation and performance comparison of different models for the estimation of solar radiation. Renewable and

Sustainable Energy Reviews, 50, 1097–1107. DOI: 10.1016/j.rser.2015.05.049

Tikhamarine, Y., Malik, A., Kumar, A., Souag-Gamane, D., and Kisi, O. 2019. Estimation of monthly reference evapotranspiration using novel hybrid machine learning approaches. Hydrological Sciences Journal, 64(15), 1824–1842. DOI: 10.1080/02626667.2019.1678750

Tikhamarine, Y., Malik, A., Pandey, K., Sammen, S., Souag-Gamane, D., Heddam, S., Kisi, O. 2020. Monthly evapotranspiration estimation using optimal climatic parameters: efficacy of hybrid support vector regression integrated with whale optimization algorithm. Environmental Monitoring and Assessment, 192(11). DOI: 10.1007/S10661-020-08659-7

Torrente Cantó, L. 2018. Reconstrucción basada en interpolación de Hermite aplicada a funciones discontinuas. http://hdl.handle.net/10317/7584

Vapnik, V. 2013. The nature of statistical learning theory. Springer Science & Business Media. DOI: 10.1007/978-1-4757-3264-1

Wang, Z., Wu, P., Zhao, X., Cao, X., Gao, Y. 2014. GANN models for reference evapotranspiration estimation developed with weather data from different climatic regions. Theoretical and Applied Climatology, 116(3–4), 481–489. DOI: 10.1007/s00704-013-0967-0

Yin, Z., Wen, X., Feng, Q., He, Z., Zou, S., Yang, L. 2017. Integrating genetic algorithm and support vector machine for modeling daily reference evapotranspiration in a semi-arid mountain area. Hydrology Research, 48(5), 1177–1191. DOI: 10.2166/nh.2016.205

Zhang, L., Juyang, L. E. I., Qilin, Z., Yudong, W. 2015. Using Genetic Algorithm to Optimize Parameters of Support Vector Machine and Its Application in Material Fatigue Life Prediction. Advances in Natural Science, 8(1). DOI: 10.3968/6404

Zhang, Y., Zhao, Z., Zheng, J. 2020. CatBoost: A new approach for estimating daily reference crop evapotranspiration in arid and semi-arid regions of Northern China. Journal of Hydrology, 588, 125087. DOI: j. jhydrol.2020.125087.

Zhu, B., Feng, Y., Gong, D., Jiang, S., Zhao, L., Cui, N. 2020. Hybrid particle swarm optimization with extreme learning machine for daily reference evapotranspiration prediction from limited climatic data. Computers and Electronics in Agriculture, 173, 105430. DOI: j.jhydrol.2020.125286

Italian Journal of Agrometeorology
Rivista Italiana di Agrometeorologia

Firenze University Press
www.fupress.com/ijam

Citation: S. Gounari, N. Proutsos, G. Goras (2022) How does weather impact on beehive productivity in a Mediterranean island?. *Italian Journal of Agrometeorology* (1): 65-81. doi: 10.36253/ijam-1195

Received: January 24, 2021

Accepted: January 24, 2022

Published: July 19, 2022

Data Availability Statement: All relevant data are within the paper and its Supporting Information files.

Competing Interests: The Author(s) declare(s) no conflict of interest.

ORCID:
SG: 0000-0003-3417-7800
NP: 0000-0002-8270-2991
GG: 0000-0003-0740-3454

How does weather impact on beehive productivity in a Mediterranean island?

Sofia Gounari[1], Nikolaos Proutsos[1,*], Georgios Goras[2]

[1] *Institute of Mediterranean Forest Ecosystems, Hellenic Agricultural Organization "DEMETER", Greece*
[2] *Faculty of Crop Science, Agricultural University of Athens, Greece*
*Corresponding author. E-mail: np@fria.gr

Abstract. Bee productivity is an essential factor affecting, not only the production of honey or other beehive products but also food security due to the very important role of bees as pollinators. The behavior of the bees and thus their productivity is highly affected by the weather fluctuations. In the present study, five years (2015-2019) of beehive weight data were analyzedto assess the impact of the prevailing weather conditions at an east Mediterranean island, on the productivity of bees. The results indicate that temperature and water-related parameters, significantly affect beehive productivity. Specifically, temperature optimum values of 17°C in spring and 26°C in summer, are associated with higher daily relative changes of the beehive weight, while bee productivity enhances at daily temperatures between 14 and 28°C, presenting negative values beyond this range. The effects of temperature, windspeed, diurnal temperature range, vapor pressure deficit, saturation vapor pressure, and the duration of hot and dry periods, on beehive productivity are strong and negative, whereas the effect of relative humidity is also significant but positive. The results of the study enhance the knowledge of the weather impacts on beehive production especially under the climatic conditions of a small east Mediterranean island, with applications in beekeepers scheduling and hive designing, to maximize beehive productivity.

Keywords: temperature, vapor pressure, diurnal temperature range DTR, vapor pressure deficit VPD, relative humidity, weather, beehive productivity, Greece, Mediterranean island.

1. INTRODUCTION

Honey production is an important sector for the world's economy (Ciesla, 2002; Gallai et al., 2009), rapidly growing in the last decades (Aizen and Harder, 2009). Even though the main role of beekeeping is honey production (Aizen and Harder, 2009; Morse and Calderone, 2000), the maintenance of honey bees significantly contributes to pollination activity. Honeybees as pollinators, provide valuable services to agricultural (Freitas and Paxton, 1996; Ricketts et al., 2004; Roubik, 1995, 2002) and natural ecosystems with significant impact on biodiversity and food security (Allen-Wardell et al., 1998; Ortiz-Caraballo, 2007).

Climate change is considered a major factor affecting honeybees' behavior and productivity with major consequences in both honey and agricultural production (Łangowska et al., 2017). Many research studies express serious concerns about the mass losses of bee colonies and the role of bees as pollinators (Cressey, 2014; Polce et al., 2014; Potts et al., 2010), while others underline important issues for the impact of climate change on honeybee abundance and honey yields (Crane, 1990; Le Conte and Navajas, 2008; van Engelsdorp et al., 2008). The impact of the changing climate is anticipated to be serious in the region of East Mediterranean and the Middle East since positive warming trends and increasing aridity is identified by many research studies (Proutsos et al., 2010; 2020; Tanarhte et al., 2012; Tsiros et al., 2020). Small islands are even more vulnerable regarding agricultural production and trade under the current climate change scenarios (Poonyth and Ford, 2004).

Even though the impacts of the warming climate and the weather conditions on honeybees are generally acknowledged, there islimited research on the connection of honeybees biology, behavior, and productivity with the climatic or weather changes (Gordo and Sanz, 2006; Henneken et al., 2012; Łangowska et al., 2017; Scheifinger et al., 2005; Sparks et al., 2010), whereas data from field experiments (apiaries) are also quite rare.

Bees' activity and honey yields are highly affected by climate and weather at different spatial scales, as shown by the effects of geographical attributes such as latitude (Crane, 1990; Gerlach, 1985; Holmes, 2002; Spivak, 1992) and elevation (Spivak, 1992) on honey yields and bee activity. Temperature, solar radiation or sunshine, wind, and precipitation, are considered as most influential for bee's productivity (Delgado et al., 2012; Łangowska et al., 2017; Puškadija et al., 2007; Vicens and Bosch, 2000) and are used as predictors for honey production, at specific geographical and time-frame scales (Rocha and Dias, 2017).

The precise relations of the meteorological factors with honeybees' behavior and productivity are still not thoroughly investigated. Despite the many negative reports and the documented climate change impacts on honeybees, there are many research studies indicating the opposite effect, when meteorological factors are analyzed under specific timesteps and regions. Łangowska et al. (2017) found strong negative relationships between honey bee spring activity (dates of first cleansing flight and first hive inspection) and temperature, with, however, high variability in timing from year to year. However, in the same study, the authors investigated the temperature influence on honey production, considering annual hive yields for more than 40 years (1965-2010) in southern Poland and the southern UK and found a significant positive relation between annual yield and April-August temperature, suggesting that an increase of 1°C is associated with 8.97 kg and 8.71 kg increases in yields in southern Poland and the southern UK, respectively. They, also mention a positive relationship between June temperature and yield, suggesting that an increase of 1°C is associated with a 3.7 kg increase in yield. Clarke and Robert (2018) investigated the relationship between honeybee foraging activity and local weather conditions and found a strong connection of bees' activity with temperature and solar radiation. Burrill and Dietz (1981) also studied the effect of meteorological variables of temperature and solar radiation on bee foraging effort and found a positive correlation with temperature. They also found a positive correlation with solar radiation, but only up to a certain threshold of 460 W m^{-2}, since at higher radiation flux densities the correlation was negative.

Relative humidity is also considered as an influential factor for honey productivity and bees' survival since its values inside the hive affect honey maturation and define egg hatching (Doull, 1976; Li et al., 2016). Joshi and Joshi (2010), however, found a weak impact of RH on flight activity. In an interesting work by Abou-Shaara et al. (2017), the authors reviewed the impacts of both temperature and relative humidity on the honeybees' activities, presenting also specific thresholds and optimum values.

Precipitation may have an impact on beebehavior. de Mattos et al. (2018) in Southeastern Brazil, detected that summer rainfall and cloud cover is strongly and positively related to pollen foraging, whereas bees enhance the foraging effort the day before a heavy rainfall (He et al., 2016).

Relevant research studies assessing the impact of small islands climate on bees' productivity arevery rare. Delgado et al. (2012) performed a comparison between contemporary (1998-2005) and historical (1910-1974) honey yield data in the island of Puerto Rico in the Caribbean and found that suitable areas for honey production and honey yields are anticipated to decrease in the future, considering the scenarios of climate change. They also assessed the effect of bioclimatic parameters on honey production concluding that temperature seasonality and mean temperature of the wettest quarter of the year have a negative effect, whereas precipitation of the wettest month and minimum temperature of the coldest month were positively correlated.

Additionally to the effects of weather on honeybee behavior, meteorological factors can affect honey yields, by impacting on vegetation dynamics or even on other insects that control honey production. The availability

of food (pollen, nectar, or honeydew produced by other insects) for the bees is critical and highly influenced by climate and weather. Pollen and nectar availability is sensitive to drought (Waser and Price, 2016) and other abiotic and biotic factors as temperature, water availability, nutrients, herbivory of leaves etc (Kenoyer, 1917; Huber, 1956; Shuel, 1967; Pleasants and Chaplin, 1983; Vasek et al., 1987; Devlin, 1988; Stephenson et al., 1992; Turner, 1993; Lau and Stephenson, 1994; Quesada et al., 1995; Petanidou et al., 1999). Corbet (1990) identified that weather affects pollinator activity, by altering the quantity and sugar concentration of nectar in flowers. Also, Petanidou et al. (1999) found that nutrient and water availability affected nectar production and nectary structure in Labiate species, whereas Devlin (1988) suggested that reduced light availability induced decrease in the amount of nectar of flowers, but not affected the pollen grain number. Quesada et al. (1995) identified the natural herbivory by beetles as a significant factor affecting negatively the production of staminate flowers and pollen grains per flower. Additionally, Vasek et al. (1987) suggested that higher nutrient levels in the soil resulted in the development of higher number of flowers and also advanced the flowering period of the plants.

Apart from the impact of weather on the availability of pollen and nectar, critical is its influence on the honeydew-producing insects, since honeydew is a significant food source for honeybees, highly affecting honey production. The honeydew producers, mainly Coccoidea or Aphidoidea, are insects with highly modified mouthparts and digestive system (Kunkel, 1997). They produce droplets of honeydew asthey feed from the phloem sap of mainly forest trees. Specifically, for pines (*Pinus* spp.), the main honeydew producing insect is *Marchalina hellenica* (Hemiptera: Coccoidea, Marchalinidae). Honeydew honey is the final product of a biological system, elements of which are: the tree, the honeydew insect, the honeybee, the beekeeper and the unpredictable factor, which affects all previous i.e. the weather conditions (Gounari, 2010). In Greece, honeydew pinehoney represents more than 60% of the country's annual honey production (Thrasyvoulou and Manikis, 1995). More specifically, the honey production of the island of Rhodesis characterized as pine honeydew honey with a percentage of about 20-30% nectar honey, depending of the year (Moschidis et al., 2019). Consequently, adverse weather conditions are expected to impact honey production by affecting honeybees' behavior, the phenology and the sap flow of trees, and the behavior and phenology of the honeydew-producing insects.

Aim of the present work is to study the impact of the weather in a small island in the eastern Mediterranean basin, on the honeybees' productivity, be assessing a great number of temperature, humidity, wind, and other related biometeorological variables. Such results would be useful for honey production weather-based prediction models and also for assessing the impacts of climate change in the highly vulnerable regions, as are the small islands or the eastern part of the Mediterranean basin.

2. MATERIALS AND METHODS

2.1 Sites description

The island of Rhodes is located in southeastern Greece and is surrounded by the Aegean Sea, part of the east Mediterranean basin. It covers an area of about 1400 km^2 with altitudes ranging from 0 to 1215 m a.s.l. and a coastline of 220 km. In the north-east and central west part of the island two experimental apiaries were established in the areas of Sianna (36° 9' 58.88" N, 27° 45' 9.02" E) and Kallithies (36° 20' 47.53" N, 28° 10' 23.92" E) depicted in Fig. 1 and an aspect of each site is presented in Fig. 2. The sites are located either inside (Sianna) or quite near (Kallithies) to protected areas of the Natura 2000 network (sites codes: GR4210029, GR4210005, GR4210030). The sites selection was performed considering their importance for beekeeping, due to the enhanced biodiversity and the increased flora richness concerning important plant species in beekeeping, as *Pinus brutia*, *Pistacia lentiscus Coridothymus capitatus*, *Cistus* spp, *Erica verticillata*, *Ceratonia siliqua*, *Satureja Cf thymbra*, *Smilax aspera* L, *Eucalyptus* spp., *Myrtus communis, Echium* spp, etc. The nectar produced by these plants along with the honeydew from thepines trees determine both the qualitative and quantitative characteristics of local honey production which, on an annual basis ranges from 200 to 250 tons of exceptional honey, mainly honeydew pine honey with 20-30% of polyflora honey, with distinctive organoleptic characteristics (Moschidis et al, 2019).

The flowering period of the plants and the life-cycle of the honeydew producing insects, control the honey production in the region. In Table 1, the flowering period of the main plant species for honey production in the island of Rhodes is presented (Moschidis et al., 2013). During the cold winter period December-February, the food availability for the bees is reduced, whereas nectar and pollen are abundant in spring and remain available, in smaller quantities in summer and autumn.

The insect *Marchalina hellenica* produces honeydew secretions from late June to late March or April of the next year. The period which honey bees can store honey is from August to November with two pauses, one at the

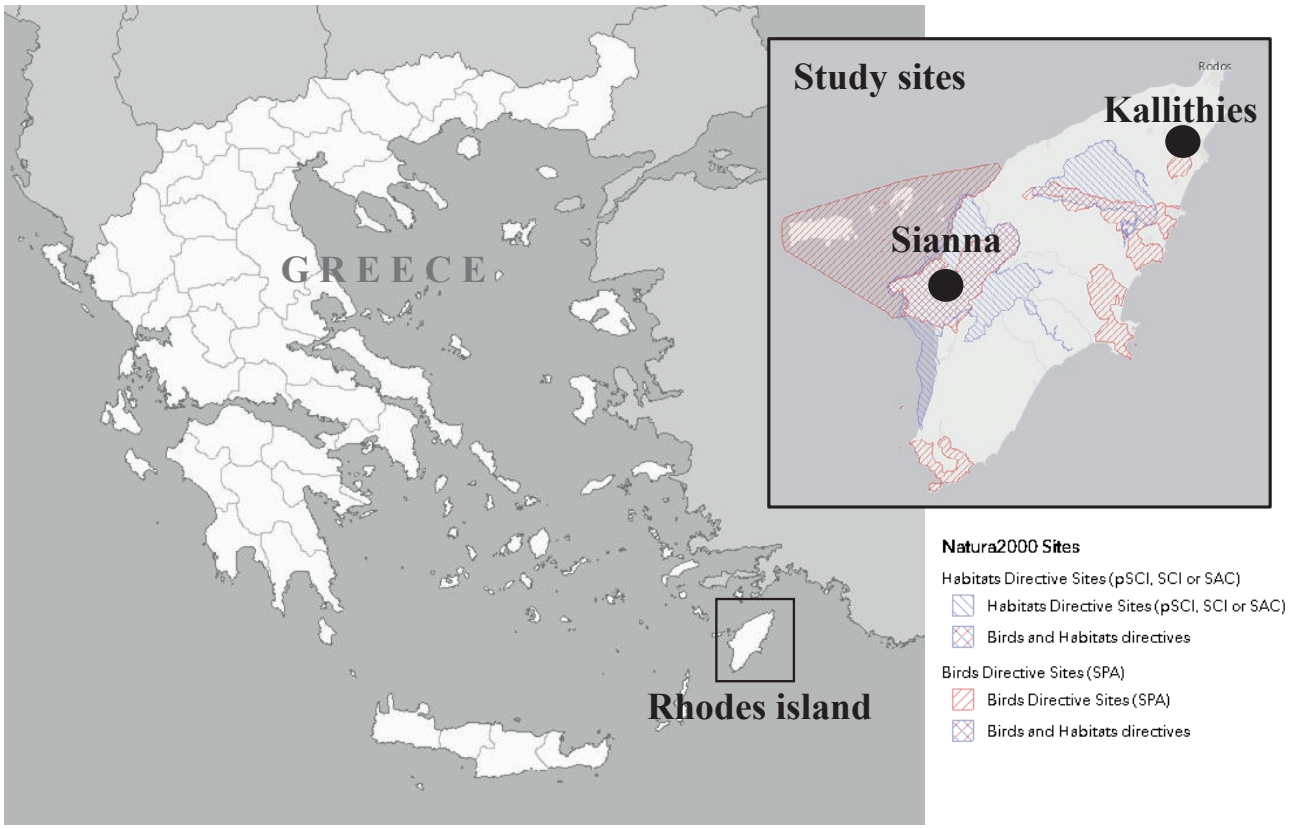

Fig. 1. Sites where apiaries were established on the island of Rhodes. The hives were placed in forest openings inside (Sianna) or near (Kallithies) sites of the Natura 2000 network.

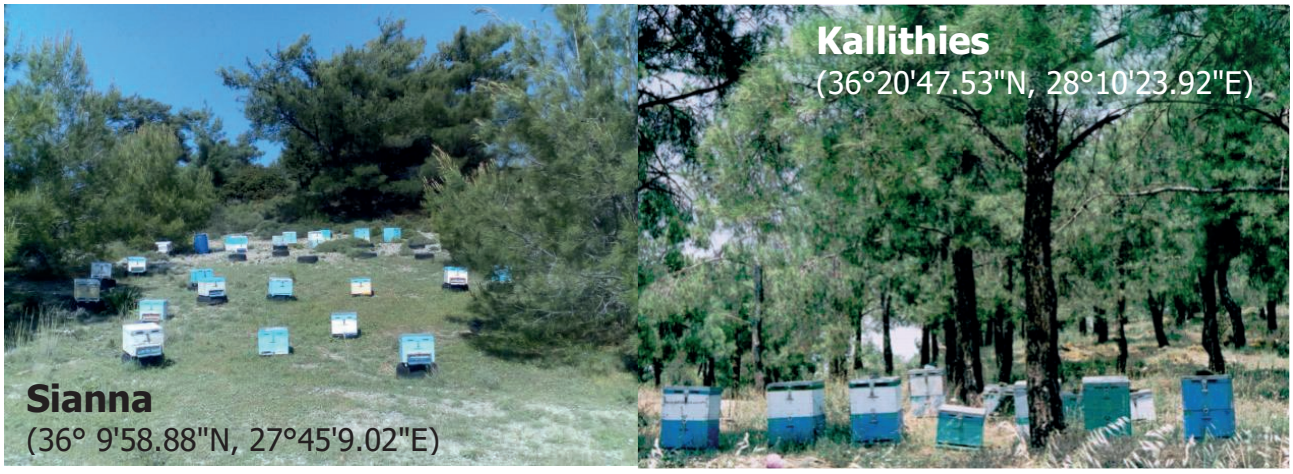

Fig. 2. Aspects of the experimental apiaries in Sianna and Kallithies sites.

end of August and the other at the beginning of October and in spring from late February to the end of March or until the female adult appears. In general, insects' adult appearance and the ovulation time occur from 25 March – 25 April, depending on the weather conditions. By mid-June all the first stage nymphs are attached to the branches of the pine trees, under the scales, they form colonies and the first honeydew drops appear. The insect

Table 1. Flowering period of the main plant species for honey production in Rhodes island. The period of honeydew production on pines by the insect Marchalina hellenica is also presented.

	Flowering period (Month)											
Plant Species	1	2	3	4	5	6	7	8	9	10	11	12
Ceratonia siliqua								■	■	■		
Cistus spp.			■	■								
Coridothymus capitatus					■	■	■					
Echium spp.			■	■	■	■						
Erica verticillata								■	■	■		
Eryngium campestre					■	■	■					
Eucalyptus spp.					■	■	■					
Inula viscoza								■	■	■		
Lavandula stoechas			■	■								
Lithodora hispidula			■	■								
Myrtus communis					■	■	■					
Oxalis pes-caprae	■	■										
Pistacia lentiscus			■	■								
Satureja Cf thymbra			■	■								
Salvia officinalis			■	■								
Sinapis arvensis	■	■										
Smilax aspera								■	■	■		
Trifolium repens			■	■								
Urginea maritima								■	■	■		
Vitex agnus-castus					■	■	■					
Insect	Honeydew production period											
Marchalina hellenica	■	■	■	■		■	■	■	■	■	■	■

hibernates as a 3rd stage nymph, producing honeydew secretions, which honeybees cannot collect during the winter due to bad weather conditions.

The climate of the region is Mediterranean type. Considering the available climatic data, obtained from the local meteorological station which was installed by the Hellenic Meteorological Service (lat. 36º 40' N, long 28º 28' E, alt. 35m), the area belongs to the humid (H) climate zone according to Climatic Zone Classification of UNEP (UNEP, 1992), with Thornthwaite's Aridity Index (AI) values presenting to decrease from 0.77 (during the period 1930-1960) to 0.74 (for the period 1960-1997), indicating that more arid conditions persist nowadays compared to the past (Tsiros et al., 2020). The annual precipitation is 703 mm, unevenly distributed mainly in winter (58.7%) and autumn (23.5%) and less in summer (only 0.4%) and spring (17.4%). In general, the summer months in Rhodes are extremely dry, with August and July being the driest (0.2 and 0.4 mm, respectively).

The annual temperature in the region is 19.1ºC, while its average minimum and maximum values are

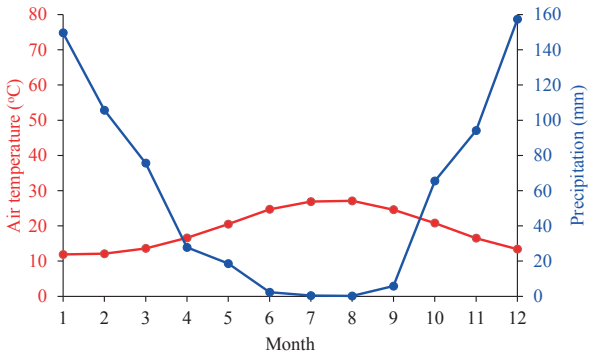

Fig. 3. The Pluvio Diagram for the city of Rhodes derived from meteorological data of the period 1955-2017.

22.5 and 15.2ºC, respectively. The seasonal temperature averages vary from 12.5ºC in winter to 26.2ºC in summer, with intermediate values of 16.9ºC and 20.6ºC in spring and summer, respectively. The warmer month is August (27.1ºC) and the cooler is January (11.9ºC). According to the pluvio diagram (Fig. 3), the dry season occurs from mid-April until September.

2.2 Hive productivity data

According to Meikle et al. (2008), the weight of the hive indicates colony size and food reserves. The beehive productivity in the present study was assessed by studying the relative daily mass changes, expressed as percentages of the change of each hive's mass (% or hive's mass daily change per total mass of the hive), of two hives placed in different sites at the north and southwest parts of the Rhodes island. The field experiment was conducted during years 2015 (March to December), 2016 (February to November), 2017 (February to July), 2018 (March to December) and 2019 (January to September). A total number of 894 daily mass records from the first hive and 693 from the second were recorded during the 5-year period, distributed mainly in summer (38.7%) and spring (34.9%) and less in autumn (21.0%) and winter (5.4%). The analysis was performed for the first hive and the second was used for crosschecking the results. From the dataset, all values recorded during hive maintenance for honey extraction works were excluded to avoid inconsistencies.

Commonly in the region, beekeepers transport their beehives into pine forests for pine honey harvest twice a year, in spring (March) and summer (late August). However, for the needs of this study, the hives remained in the same sites throughout the year. In order to ensure that our data are representative, all hives used in this

work had sisters queens and similar brood and population growth characteristics. The usual seasonal manipulations were carried out in the beehives, while the rate of infestation by Varroa and Nosema, the main diseases of bees in Greece, was also monitored. All beehives were maintained by the same beekeeper, under the supervision of the authors.

2.3 Meteorological data and analysis

Weather data were obtained from the local meteorological station of the Athens National Observatory (36° 24' N, 28° 12' E, elev. 95 m a.s.l., https://meteosearch.meteo.gr) which operates on the island of Rhodes since 2012. Specifically, daily values of air temperature T and relative humidity RH attributes (daily average, minimum and maximum), wind speed WS and daily wind gust WSgust, wind direction WD, and precipitation P were used in this study for the years 2015 to 2019. Air humidity-related parameters were also estimated: vapor pressure at saturation e_s, by employing Tetens' (1930) formula (Eq. 1), actual vapor pressure e_a (Eq. 2), and vapor pressure deficit VPD, which is an index for evaluating atmospheric dryness estimated by Eq. 3.

$$e_s = 0.61078\, e^{\frac{17.27\,T}{237.3+T}} \text{ in kPa} \quad (1)$$

$$e_a = \frac{RH}{100} 0.61078\, e^{\frac{17.27\,T}{237.3+T}} \text{ in kPa} \quad (2)$$

$$VPD = e_s - e_a \quad (3)$$

Additionally, the diurnal temperature range $DTR = T_{max} - T_{min}$, expressing mainly the temperature range on a daily basis, was also employed.

For assessing the effect weather parameters on the hive productivity, post-processing analysis was performed by grouping the data according to the meteorological parameter each time examined. The values of weather parameters were grouped in appropriate bin classes per 1°C for the temperature T attributes (T_{mean}, T_{min} and T_{max}) and DTR, per 10% for the RH attributes (RH_{mean}, RH_{min} and RH_{max}), per 0.2 kPa for the e_s, e_a and VPD, per 1 km/h for average wind speed (WS), per 5 km/h for gust windspeed (WSgust) and 16 wind direction classes (WD).

Correlation analysis was additionally performedto identify the relations between beehive productivity and weather variables. For this purpose, the Pearson'scorrelation coefficient was calculated and the significance levels were determined. Pearson's correlation coefficient is a parametric measure of the strength and direction of the linear relationship between paired values of continuous variables. Its values are dimensionless and range between -1 and +1. The negative or positive values of the coefficient indicate respectively a negative or positive relationship between the examined variables, whereas its absolute magnitude shows the strength of the linear relationship (Yeager, 2021). The IBM SPSS Statistics software package was used for conducting the statistical analysis (https://www.ibm.com/analytics/spss-statistics-software).

3. RESULTS

3.1 Prevailing weather conditions

From the analysis of the meteorological data for the period 2015-2019, year 2017 was the cooler and 2019 the warmer in terms of mean, maximum and minimum temperature. Also, 2019 was the wetter year with higher values of mean and maximum relative humidity, less days without rain and extremely higher annual precipitation, though 2018 presented higher minimum relative humidity and actual vapor pressure and lower vapor pressure deficit. The drier year was 2016 with less annual precipitation, increased days without rain and vapor pressure deficit values and reduced relative humidity values (mean, minimum and maximum). However, 2017 presented the lower actual vapor pressure values. Specific annual values of various meteorological and biometeorological parameters for the study years are presented in Table 2.

The meteorological data analysis forthe period from April to June, which is the common period with available beehive productivity data among the years of this study, indicates that 2018 (April to June) presented the higher temperatures (22.1°C for T_{mean}, 25.3°C for T_{max} and 19.5°C for T_{min}), vapor pressure deficit (0.785 kPa) and number of dry days (82) and lower precipitation (22.8mm) as well, while in 2015 were recorded the lowest temperatures (19.9°C for T_{mean}, 23.3°C for T_{max} and 17.3°C for T_{min}) but also the lowest mean and minimum relative humidity (69.3% and 54.2%, respectively) and actual vapor pressure (1.65 kPa) values. Year 2019 could be considered as the wetter for the specific period of the year, since it has the higher RH mean and minimum values (71.6% and 57.3% respectively), higher precipitation (94.6mm) and lowest vapor pressure deficit (0.712 kPa) and number or dry days (75).

3.2 Beehive productivity rates and yields

The relative beehive weight changes, in the island of Rhodes, are presented per year and season in Fig. 4.

Table 2. Mean values and standard deviations SD for the meteorological parameters and attributes during years 2015 -2019.

Parameter	2015		2016		2017		2018		2019	
	mean	SD	mean	SD	mean	SD	mean	SD	mean	SD
T_{mean} (°C)	19.5	5.6	19.5	5.6	19.2	5.6	20.2	5.2	19.7	5.4
T_{max} (°C)	22.5	6.1	22.4	6.0	22.0	6.0	22.8	5.6	22.5	5.8
T_{min} (°C)	17.2	5.5	17.2	5.5	17.0	5.4	18.0	5.1	17.4	5.2
DTR (°C)	5.3	1.5	5.2	1.4	5.0	1.3	4.8	1.3	5.1	1.4
RH_{mean} (%)	69.6	9.1	68.9	9.5	70.0	9.4	72.2	8.4	72.3	8.2
RH_{max} (%)	82.6	8.4	82.2	9.2	82.6	8.7	84.4	7.3	85.0	7.0
RH_{min} (%)	56.6	11.5	55.6	11.7	57.5	11.7	60.0	11.2	59.7	11.2
e_s (kPa)	2.39	0.80	2.39	0.79	2.35	0.81	2.47	0.77	2.41	0.79
e_a (kPa)	1.67	0.59	1.66	0.59	1.63	0.55	1.77	0.54	1.73	0.54
VPD (kPa)	0.72	0.33	0.73	0.32	0.71	0.36	0.70	0.34	0.68	0.35
WS (km/h)	7.6	3.4	8.0	3.3	7.9	3.3	8.1	3.3	7.8	3.5
WSgust (km/h)	31.8	10.5	32.8	10.0	31.2	9.5	32.6	10.2	32.2	11.6
Precipitation (mm)	568		316		479		631		1198	
Spring T_{mean} (°C)	16.9	3.2	17.9	2.6	17.1	2.7	19.1	3.3	17.1	2.9
Spring WS (km/h)	7.43	3.30	8.09	3.47	7.51	2.79	8.08	3.36	7.53	3.38
Spring e_s (kPa)	1.95		2.07		1.97		2.25		1.98	
Spring e_a (kPa)	1.36		1.43		1.43		1.61		1.41	
Spring VPD (kPa)	0.59		0.64		0.54		0.64		0.56	
Spring DTR	5.51		5.55		5.33		5.26		5.33	
No of spring days with T_{mean}>20°C	20		19		13		38		16	
No of summer days with T_{mean}>25°C	59		75		71		69		68	
No of summer days with WS>10 km/h	23		44		41		40		27	
No of spring days without rain	67		70		74		79		68	
No of days without rain	287		308		295		287		266	

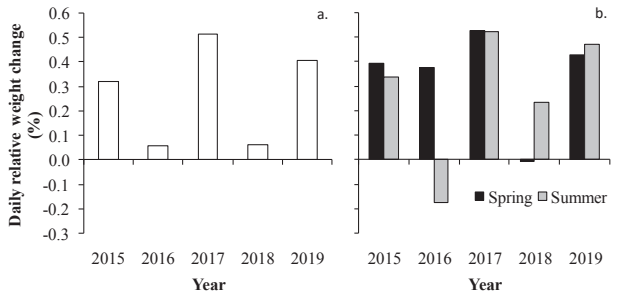

Fig. 4. Relative changes of diurnal beehive productivity (%) during the experimental periods of years 2015, 2016, 2017, 2018 and 2019, derived from (a) all data and (b) spring and summer values.

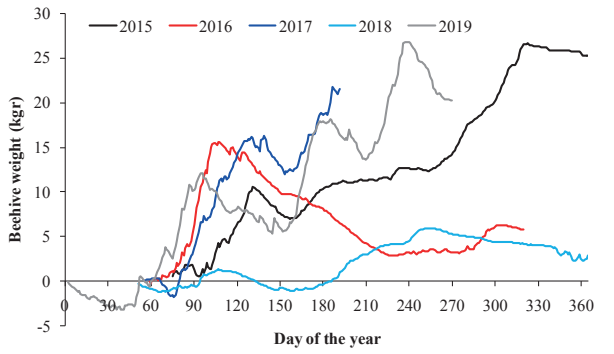

Fig. 5. Cumulative beehive production per day in kgr during the years 2015, 2016, 2017, 2018 and 2019.

The productivity in years 2016 and 2018 is reduced and in years 2019 and 2017 increased. Specifically, year 2016 present an intermediate weight gainin spring, whereas in summer it was very low presenting negative average values. On the other hand, year 2018 had a relatively small productivity in summer and it even smaller in spring, presenting almost zero average weight change.

The day by day changes of the beehive weight is presented per year in Fig. 5, appear negative rates in winter, starting to increasein early spring. Beehive weight reaches its maximum in spring, at dates that differ from year to year. Thereafter, productivity starts decreasing, until the end of spring or the beginning of summer. During

summer, an increasing rate persists with duration that also depends on the year. The above pattern, generally describes the beehive weight changes for most years. However, it appears that in 2016, the summer increase in productivity was not accomplished. Also, during the spring season of the year 2018, the maximization of beehive productivity didn't reach satisfactory values.

The relatively low productivity, recorded in 2016 is probably associated with thestronger winds prevailing this specific year, during most of the days of the summer period. Compared to the other years, the number of summer days with average windspeeds greater than 10 km/h is much higher, i.e. 44 days, while in other years the respective numbers vary between 23 days (2015) and 41 days (2017). Additionally, during the summer of 2016, the persistence of relative hot days was more common compared to the other years of the study. Specifically, a number of 75 days with daily temperatures greater than 25ºC was recorded during the summer of 2016, when the respective values for the other years were much lower ranging from 59 days (2015) to 69 days (2018). It should be also noted that the year 2016 has also the greater number (308 days) of dry days i.e. days without rainfall, while all other years have smaller respective numbers (266-295 days).

The small productivity during the spring of 2018 is probably due to the prevailing warmer weather conditions. More specifically, in the summer of 2018, the average temperature is much higher (19.1ºC) compared to the other years (ranging from 16.9ºC in 2015 to 17.9ºC in 2016). These hot conditions persisted during most of the days of the spring season, since the number of days with T_{mean}>20ºC was 38 in 2018, much increased compared to the other years (range from 13 days in 2017 to 20 days in 2015). Additionally, in spring 2018,e_s and VPD were increased (2.25 and 0.64 kPa, respectively) and DTR decreased (5.26ºC), whereas the number of days without rain was the highest (79 days).

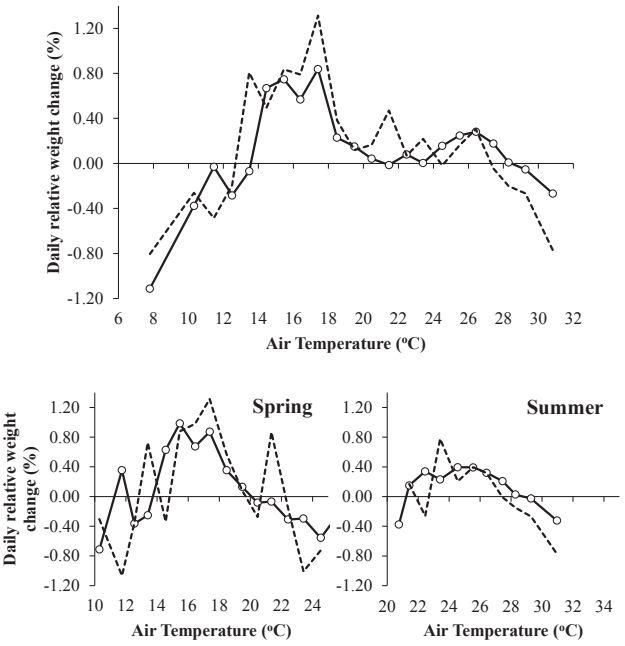

Fig. 6. Relative changes of diurnal beehiveproductivity (%) under different daily air temperature T values grouped in 1ºC bin classes, using annual and seasonal (spring and summer) data. The dashed line presents the respective changes of a second beehivefor cross-checking.

3.3 Assessing the impact of meteorological factors on beehive productivity

3.3.1 Effect of air temperature and temperature-related attributes

Air temperature appears to affect beehive productivity presenting two optimum values as clearly depicted in Fig. 6. At low temperatures, the diurnal hive production rate takes negative values indicating that the bees consume more honey inside the hive compared to the food collection from outside. The rates remain negative though increasing to about 14ºC. Thereafter, the increasing pace is sustained and the beehive productivity becomes positive and maximizes (+0.838%) when the daily temperature reaches about 17ºC. An additional temperature increase results in productivity reduction, which reaches zero valuesat about 21ºC. As temperatures increase further, the productivity rates remain positive but low, presenting however a minor positive increasing trend. This, results in a second though lower maximum (+0.304%) at temperatures around 26ºC. The slightly increasing productivity cannot be sustained in warmer weather conditions. The productivity rates start reducing at temperatures higher than 26ºC. For extremely warm conditions (temperatures above 28ºC) the productivity becomes negative.

The two optimum values of air temperature for the highest rates in beehive productivity described above appear to have a seasonal connection as also depicted in Fig. 5, where spring and summer changes of beehive productivity are examined in conjunction with the respective daily temperatures. Considering that the double optimum temperatures are related to different seasons (mainly spring and summer), the higher hive productivity appears to be associated with the food availability and more specifically with the availability of nectar and pollen produced by the plants mainly during the

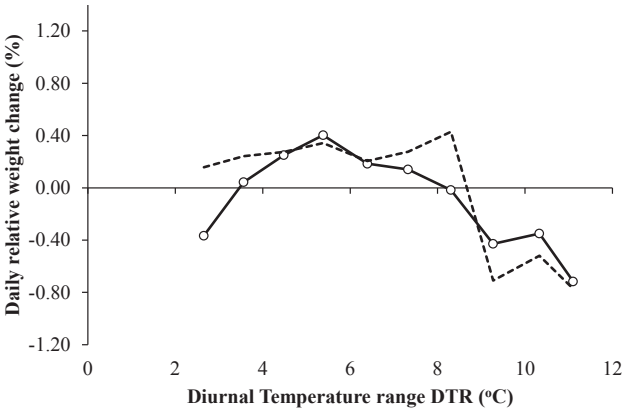

Fig. 7. Changes of diurnal beehive productivity (in kgr/d) under different diurnal temperature range DTR values grouped in 1ºC bin classes. The dashed line presents the respective changes of a second beehive used for crosschecking.

spring period and with the availability of honeydew produced by the insect *Marchalina hellenica*. This is in line with the flowering periods of the plants in the region and also with the phenological stages of the insect since in spring most of the plant species on the island are in their flowering stage and also in spring *Marchalina hellenica* adults dominate and produce high quantities of honeydew (Gounari, 2006).

The impact of the diurnal temperature range DTR on the beehive daily production is presented in Fig. 7. In general, DTR expresses the diurnal changes of temperature i.e. the difference between daytime and night temperatures. In many studies, DTR is associated with atmospheric cloudiness, with its higher values indicating clear skies and the lower overcast sky conditions. As depicted in Fig. 7, very low values of DTR (around 3ºC) are connected with negative or low positive productivity rates of the hive. As DTR increases, reaching intermediate values (greater than 3ºC but lower than 5ºC), the beehive productivity becomes positive and increasing, reaching a maximum at DTR=5ºC.

At the optimum DTR value of about 5ºC, the relative diurnal beehive weight change is maximized to +0.342%. Higher DTR results in diminished but positive productivity rates, which become negative at DTR values greater than 8ºC. The negative productivity rates can reach -0.772% when DTR becomes equal to about 11ºC.

The pattern mentionedabove can be explained by considering DTR as an indirect index of the sky clearness, suggesting that at lower or higher DTR values (overcast or clear skies, respectively), the beehive productivity is reduced, reaching negative to low positive productivity rates.

It should be noted, that the above-mentioned DTR values are rather small compared to other regions, even of the Greek peninsula. This is rather expected for a Mediterranean island, where hot and dry conditions generally persist both during daytime and nighttime. Thus the above thresholds may differ to other e.g. mountainous regions.

3.3.2 Effect of air humidity and other water-related attributes

Relative humidity RH presents a more sound effect on the beehive productivity daily rates, presenting to increase with RH by an average rate of +0.237% change per 10% increase of RH_{mean}. Similar patterns also present the RH_{min} and RH_{max} values but with different changing rates (+0.137% per 10% increase of RH_{min} and +0.242% per 10% increase of RH_{max}), as illustrated in Fig. 8a.

Since RH is an indirect (relative) measure of the humidity content of the air, the actual vapor pressure e_a and the vapor pressure at saturation e_s were also employed to detect the effect of air humidity on beehive productivity (Fig. 8c and d). The hive productivity increases with e_a for values lower than 1.3 kPa present-

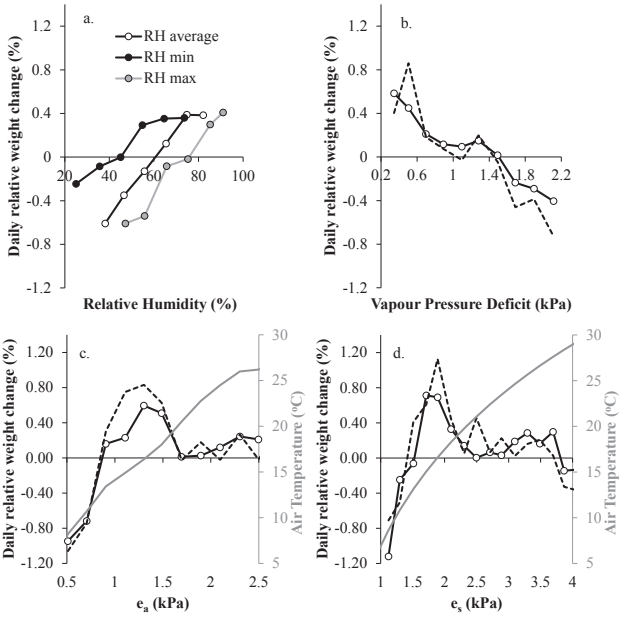

Fig. 8. Relative changes of diurnal beehive production (%) under different daily values of (a) mean, maximum, and minimum relative humidity RH, grouped in 10% bin classes, (b) vapor pressure deficit VPD, (c) actual vapor pressure e_a and (d) saturation vapor pressure e_s, grouped in 0.2 kPa bin classes. The dashed line presents the respective changes of a second beehive and the respective air temperature values are also presented (grey line).

ing, however, negative values at e_a less than 0.8 kPa. The e_a value of 1.3 kPa can be considered as an optimum for beehive productivity rate since at higher e_a values the daily hive production reduces becoming almost zero at very humid weather conditions i.e. for e_a greater than 1.7 kPa. The reduction of the productivity when e_a increases more than 1.3 kPa may be attributed to the higher temperatures (about 17°C) which, as reported above, are connected with decreasing hive productivity.

The pattern mentioned above refers to spring, whereas the respective distribution for all-season data indicates that for e_a values greater than 1.7 (mainly prevailing in summer), does not result in negative productivity rates. This indicates that in summer, other parameters, beyond e_a, may also affect the beehive productivity.

The pattern of e_a is also similar to the respective pattern of e_s as depicted in Fig. 8c, but with different thresholds. Here the optimum e_s value for maximum beehive productivity rates is 1.9 kPa.

A significant variable for assessing atmospheric dryness is the vapor pressure deficit VPD, which expresses the demand of the atmosphere for water vapor and combines the effects of e_a and e_s, (i.e. RH and T). Its effect on the beehive productivity is sound as presented in Fig. 8b. As VPD increases i.e. the atmosphere becomes drier, the diurnal beehive productivity reduces. The reduction occurs with an average rate of +0.507% per kPa. Negative productivity is identified at VPD values greater than 1.5 kPa.

In order to assess the impact of air dryness on beehive productivity, the length of the periods with extremely dry conditions (consecutive days with VPD greater than 1.5 kPa) was also investigated. The results shown in Table 3, indicate that the impact of the persistence of extremely dry days with VPD greater than 1.5 kPa, on beehive productivity, is rapid resulting in negative production rates even if the length of the dry period is only one day.

Table 3. Relative diurnal beehive production changes (%) for different duration of extremely dry periods (number of consecutive days with VPD>1.5 kPa).

Consecutive days with VPD>1.5 kPa	Relative diurnal beehive production (%)					
	Colony 1			Colony 2		
	N	mean	SD	N	mean	SD
1	11	-0.032	0.565	8	-0.160	0.545
2	13	-0.127	0.606	10	-0.123	0.571
3	7	-0.483	0.428	5	-0.623	0.406
4	1	-0.139	0.294			

3.3.3 Wind effect

The wind, in terms of its speed, also appears to affect beehive productivity (Fig. 9), probably because strong winds can affect the bees' flights. Daily average windspeed values lower than 7 km/h seems to favor the productivity of the hive. At such wind conditions the productivity rates are maximized (average rate +0.372%). As winds become stronger, the productivity rates appear to reduce with a pace of -0.080% per 1 km/h increase of the daily average windspeed values. Notably, beehive productivity becomes negative only at very high windspeeds (above 14 km/h), suggesting that only under extremely strong winds, the bees stop flying and remain inside the hive. Similarly, is the pattern for the maximum daily windspeed (Fig. 9b). Wind gust greater than 40 km/h is associated with zero productivity, which becomes negative as maximum windspeed increases.

Wind direction does not appear to have a direct effect on beehive production (Fig. 10). Its rather increased values, identified under NNE and SSE winds, whereas at NNW and E winds the productivity is minimized.

3.4 Correlations between beehive productivity and meteorological variables

To further the significance and the impact of the temperature and temperature-related parameters, a correlation analysis was performed by employing Pearson correlation coefficient r. The respective r values and their significance from the correlation between the relative daily weight changes of the two beehives and the different meteorological temperature-related variables are presented in Table 4.

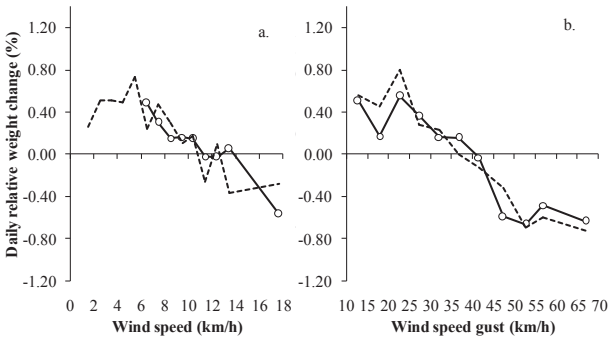

Fig. 9. Relative changes of diurnal beehive production (%) under different daily average (a) and gust (b) wind speed WS values grouped in 1 km/h and 5 km/h bin classes, respectively. The dashed line presents the respective changes of a second beehive for cross-checking.

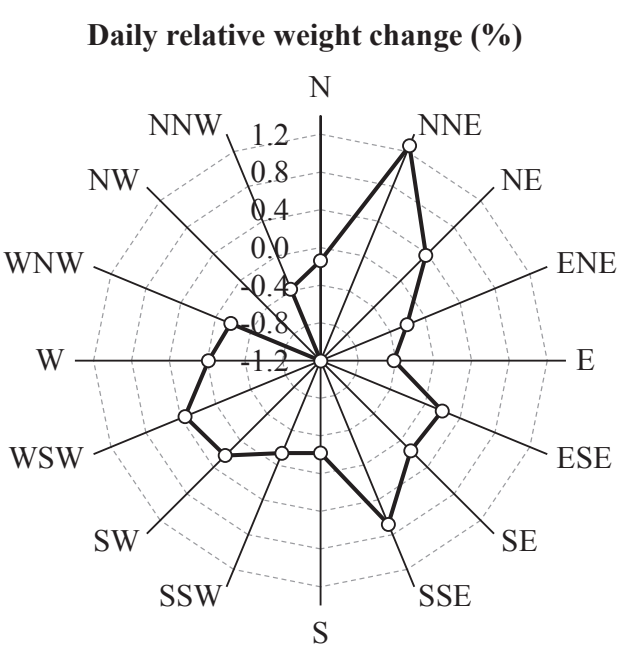

Fig. 10. Changes of diurnal honey production (in kgr/d) under different wind directions.

From the analysis of data from the two hives, significant negative correlations are identified between beehive productivity and all temperature attributes (T_{mean}, T_{max}, and T_{min}), indicating the strong influence of temperature. More specifically T_{mean} is significantly related to hive productivity both on an annual basis (r=-0.135, p<0.01) and for all seasons (r=-0.232, p<0.01 for spring, r=-0.118, p<0.05 for summer; r=-0.253, p<0.01), except winter. T_{max} plays a significant role mainly in spring (r=-0.212, p<0.01) and summer (r=-0.146, p<0.01), negatively affecting annual production (r=-0.130, p<0.01), whereas T_{min} effect is significant and negative only is spring (r=-0.229, p<0.01), affecting also the annual productivity (r=-0.128, p<0.01). DTR effect on beehive productivity is negative and strong (r=-0.169, p<0.01) during summer, however not affecting annual productivity.

The duration of hot conditions, expressed by the number of consecutive days with temperatures greater than 20ºC, present a strong negative correlation with beehive productivity during the transitional seasons of spring (r=-0.194, p<0.01) and autumn (r=-0.242, p<0.01), affecting also the total annual production (r=-0.119, p<0.01).

Relative humidity (RH) mean, maximum and minimum attributes are positively related to beehive productivity on an annual basis with high significant levels (p<0.01) as presented in Table 5. The seasonal values show strong positive correlations in spring and summer. The e_s values present a strong negative correlation with the beehive productivity for all seasons, except winter, whereas VPD presents similar results. The e_a is negatively correlated with productivity in autumn but positively

Table 4. Pearson correlation coefficients (r), number of values (N), and significance levels from the correlation between the relative daily weight changes of the two beehives and the meteorological variables of the mean (T_{mean}), maximum (T_{max}), and minimum (T_{min}) temperature, diurnal temperature range (DTR), and number of cold days with T_{mean}>20 ºC, on an annual and seasonal basis.

Variable	Hive No	Annual		Spring		Summer		Autumn		Winter	
		N	r	N	r	N	r	N	r	N	r
T_{mean} (ºC)	all	894	**-0.135****	312	**-0.232****	346	**-0.118***	188	**-0.253****	48	0.207
	1	807	**-0.086***	289	**-0.232****	302	-0.066	171	-0.119	45	0.262
	2	452	**-0.147****	150	**-0.145**	184	**-0.181***	86	**-0.321****	32	0.331
T_{max} (ºC)	all	894	**-0.130****	312	**-0.212****	346	**-0.146****	188	**-0.227****	48	0.226
	1	807	**-0.085***	289	**-0.222****	302	-0.096	171	-0.098	45	**0.318***
	2	452	**-0.138****	150	-0.118	184	**-0.174***	86	**-0.302****	32	0.335
T_{min} (ºC)	all	894	**-0.128****	312	**-0.229****	346	-0.056	188	**-0.239****	48	0.188
	1	807	**-0.079***	289	**-0.227****	302	-0.003	171	-0.113	45	0.223
	2	452	**-0.139****	150	-0.126	184	**-0.155***	86	**-0.290****	32	0.329
DTR (ºC)	all	894	-0.052	312	-0.059	346	**-0.169****	188	-0.042	48	0.144
	1	807	-0.050	289	-0.087	302	**-0.158****	171	0.007	45	**0.302***
	2	452	-0.051	150	-0.045	184	-0.094	86	-0.163	32	0.052
No c.d. T>20ºC (days)	all	894	**-0.119****	312	**-0.194****	346	-0.011	188	**-0.242****	na	na
	1	807	**-0.085***	289	**-0.173****	302	0.002	171	**-0.171***	na	na
	2	452	**-0.118***	150	**-0.168***	184	-0.007	86	-0.133	na	na

*Correlation is significant at the 0.05 level. **Correlation is significant at the 0.01 level.

Table 5. Pearson correlation coefficients (r), number of values (N), and significance levels from the correlation between the relative daily weight changes of the two beehives and the meteorological variables of the mean (RH_{mean}), maximum (RH_{max}), and minimum (RH_{min}) relative humidity, actual (e_a), and saturation (e_s) vapor pressure, and vapor pressure deficit (VPD), on an annual and seasonal basis.

Variable	Hive No	Annual		Spring		Summer		Autumn		Winter	
		N	r	N	r	N	r	N	r	N	r
RH_{mean} (%)	all	894	**0.186****	312	**0.212****	346	**0.227****	188	0.044	48	0.192
	1	807	**0.201****	289	**0.259****	302	**0.174****	171	0.026	45	0.241
	2	452	**0.182****	150	**0.194***	184	**0.236****	86	0.073	32	0.262
RH_{max} (%)	all	894	**0.196****	312	**0.239****	346	**0.174****	188	0.048	48	0.199
	1	807	**0.204****	289	**0.255****	302	**0.150****	171	0.036	45	0.241
	2	452	**0.195****	150	**0.227****	184	**0.203****	86	0.078	32	0.243
RH_{min} (%)	all	894	**0.148****	312	**0.158****	346	**0.226****	188	0.035	48	0.156
	1	807	**0.166****	289	**0.218****	302	**0.163****	171	0.015	45	0.215
	2	452	**0.139****	150	0.129	184	**0.221****	86	0.060	32	0.233
e_s (kPa)	all	894	**-0.139****	312	**-0.250****	346	**-0.125***	188	**-0.263****	48	0.186
	1	807	**-0.090***	289	**-0.250****	302	-0.075	171	-0.125	45	0.244
	2	452	**-0.160****	150	**-0.166***	184	**-0.187***	86	**-0.335****	32	0.315
e_a (kPa)	all	894	-0.055	312	-0.102	346	**0.110***	188	**-0.166***	48	0.200
	1	807	-0.005	289	-0.078	302	0.105	171	-0.072	45	0.267
	2	452	-0.079	150	-0.029	184	**0.061**	86	-0.189	32	0.309
VPD (kPa)	all	894	**-0.207****	312	**-0.292****	346	**-0.221****	188	**-0.199****	48	-0.070
	1	807	**-0.181****	289	**-0.325****	302	**-0.169****	171	-0.107	45	-0.102
	2	452	**-0.221****	150	**-0.252****	184	**-0.241****	86	**-0.237***	32	-0.092

*Correlation is significant at the 0.05 level. **Correlation is significant at the 0.01 level.

Table 6. Pearson correlation coefficients (r), number of values (N), and significance levels from the correlation between the relative daily weight changes of the two beehives and the meteorological variables of average (WS) and maximum (WSgust) windspeed, on an annual and seasonal basis.

Variable	Hive No	Annual		Spring		Summer		Autumn		Winter	
		N	r	N	r	N	r	N	r	N	r
WS	all	894	**-0.162****	312	**-0.250****	346	-0.031	188	-0.131	48	**-0.295***
	1	807	**-0.179****	289	**-0.319****	302	-0.047	171	-0.095	45	**-0.316***
	2	452	**-0.168****	150	**-0.177***	184	-0.086	86	-0.047	32	**-0.383***
WSgust	all	894	**-0.174****	312	**-0.244****	346	0.005	188	**-0.193****	48	**-0.313***
	1	807	**-0.199****	289	**-0.302****	302	0.009	171	**-0.179***	45	**-0.400****
	2	452	**-0.176****	150	**-0.187***	184	-0.105	86	-0.038	32	**-0.407***

*Correlation is significant at the 0.05 level. **Correlation is significant at the 0.01 level.

in summer, indicating that increased water content in the atmosphere results in increased productivity in summer and decreased productivity in autumn.

Spring and winter average and maximum windspeeds are strongly and negatively correlated with beehive productivity, affecting also the annual production of the hives as indicated by the respective values of the Pearson correlation factor (Table 6).

4. DISCUSSION

The microenvironment inside the beehive is strictly regulated. This implies that the honeybees dedicate much of their effort and energy to regulate beehive's narrow-ranged micrometeorological conditions (Ellis, 2009). Outside the hive, foraging can occur between a wide temperature range from 10 to 40ºC (Abou-Shaara,

2014). At lower temperatures, bees reduce the foraging trips (Joshi and Joshi, 2010), which in general start when the average temperature reaches 6.57ºC and are maximized at 20ºC (Tan et al., 2012). It is also worth noting that honeybees at high altitudes (above 1,000 m a.s.l.) perform foraging flights to harvest water or pollen, even at ambient temperatures lower than 5ºC, according to authors' unpublished research data and field observations in Greece. However, Woyke et al. (2003) mention that 10ºC is the threshold for foraging initiation, and the number of foragers increases 10fold at 12ºC. Blažytė-Čereškienė et al. (2010) observed the minimum forage activity at 43ºC. In the present work, we found an optimum value of the ambient temperature of about 17ºC where beehive productivity reaches its maximum rates. On a seasonal basis, average daily temperatures between 14 and 18ºC are associated with the highest rates of bee productivity, which is maximized at 17ºC. In summer, the respective range is between 22 and 27ºC and the optimum summer temperature is 25ºC.

The impact of temperature is associated with the food availability and bees' phenology. At low daily temperatures, mainly recorded in winter, early spring and late autumn, the available nectar sources are minimum and used for the development of the brood and for the regulation of the inside beehive temperature in the broodnest. As temperatures increase (during spring) the availability of nectar and pollen enhances, and is mainly used for strengthening thecolony. If the weather conditions are not favorable during the spring season, the hive will not be able to exploit the available food (nectar, pollen or honeydew). For example in year 2016, strong winds and dry conditions (reduced precipitation during spring) prevented the increase of the beehive productivity, byshortening theflowering period (diminished pollen and nectar production) and reducing sap flows of pine trees (reduced honeydew production). Similarly, in 2018, the very warm spring had similar effects. At high temperatures (above 17ºC), occurring mainly in late spring, summer and early autumn, the availability of food (nectar and pollen production) is diminished since the flowering stages of many plants is completed, whereas the pines sap-flow (honeydew production) is also diminished. Under such conditions and as temperatures increase further (mid-summer), food availability and thus beehive productivity reduces. Short flowering periods of few species are available for the bees, allowing a small increase of the hive productivity at daily temperatures around 25ºC (second optimum value).

In our study, the correlation of beehive productivity and temperature is generally, negative and strong on an annual basis and for almost all seasons (except winter) for all temperature attributes examined (average, minimum or maximum daily temperature). It should be stated, however, that, regardless of the general trends, at daily average temperatures lower than 17ºC (optimum value) the trends are positive, becoming negative for warmer conditions, indicating the non-linear relationship between temperature and beehive productivity. The negative effect of high temperature is attributed to both the reduction of food (nectar, pollen, honeydew availability) and to changes in the colony phenology and bees' behavior. Łangowska et al. (2017), mention also a strong negative relationship between honey bee spring phenology and temperature, stating also that rising temperatures especially in summer can decrease the first harvest production. Delgado et al. (2012) in the island of Puerto Rico found that temperature seasonality and mean temperature of the wettest quarter of the year have negative effects, whereas precipitation of the wettest month and minimum temperature of the coldest month were positively correlated.

DTR appears to have a strong ($p<0.01$) negative correlation with beehive productivity and can be explained considering that DTR is related to atmospheric cloudiness and solar radiation fluxes, both acknowledged as significant parameters affecting the photosynthetic activity of the plants and their growth (Gimeno et al., 2012; Gu et al., 2003; Proutsos et al., 2019; Proutsos and Tigkas, 2020). High DTR values (clear sky conditions) usually prevailing in summer are also associated with increased temperatures and VPD values. Under such hot and dry conditions, the honey production is negatively affected probably because the bees will either remain in the hive to regulate its temperature by fanningor have to cope with a food deficit. The low food availability is probably due to the diminished nectar outflow from plants, the reduced activity of the honeydew-producing insects (due to the reduction of the sap flow of the trees) or the inability of bees to collect the honeydew droplets (due to the droplets' dehydration which makes them more compact and not easy to be collected). Lower DTR values (partly overcast skies) are associated with higher precipitation and lower evapotranspiration rates (Easterling et al., 1997) and according to the results of this study, also with increased productivity of the beehive, indicating that cloudy and wet weather enhances bees productivity.

Research studies are indicating that RH has a very weak (Joshi and Joshi, 2010) or negative impact on bees flight activity. Vicens and Bosch (2000) found that the activity of the Africanized honeybees was more intense at relatively low RH (around 43.6%) when associated with hot conditions (air temperatures of about 29.4

± 4.9°C). In our study, RH (all attributes i.e. average, maximum, and minimum daily values) appears to affect beehive productivity and has a strong positive influence, especially during the productive seasons of spring and summer. This is probably because on Rhodes island the honey productivity is highly influenced by the availability of food and especially honeydew, which is more easily collected by honeybees when RH is increased. Similarly, VPD and e_s, which can also be used as atmospheric dryness indices, also present a strong negative correlation with beehive productivity especially during spring, summer, and autumn.

Windspeed (WS) effect on bee productivity is also evident, presenting a negative correlation, especially in spring. Hive productivity is zero when the daily average (or maximum) WS reaches 14 km/h (or 40 km/h) and becomes negative for even higher values. This may be attributed to the wind effect on bees flying ability or the dehydration of honeydew droplets (that cannot be exploited by the bees), contributing to negative impacts on honey yields. Additionally, when strong winds are associated with increased temperatures (as often recorded in the islands of east Mediterranean), plants as pines reduce their sap-flows (reduction in honeydew production), while others, as thyme, stop the production of nectar. The negative wind effect is also assessed by Lundie (1925), who found a negative linear relationship between wind speed and the number of forages. According to the author, honeybees normally fly with windspeeds 29 and 26 km/h, without and with load respectively and their flying speed can reach 32-34 km/h when agitated (without load), but they cannot carry loads upwind against strong winds (greater than 26 km/h).

5. CONCLUDING REMARKS

Weather conditions impact beehive productivity. In the small Mediterranean island, where the present study was conducted, the daily relative weight changes of the beehive were used as an index for assessing bees' productivity. Temperature and its attributes (i.e. T_{mean}, T_{max}, T_{min}, and DTR) are, in general, negatively related to beehive productivity, presenting strong correlations, especially during summer. T_{mean} and T_{max} have a significant negative influence on the hive weight changes in all seasons except winter, while T_{min} only in spring and autumn.

Beehive positive production rates are recorded for average daily temperatures higher than 14°C. The T_{mean} optimum value is 17°C and is associated with an average daily hives change of +0.838%, achieved mainly in spring. The summer T_{mean} optimum is 26°C and is associated with an average productivity rate of +0.303%. Very high daily temperatures (above 28°C) are connected with negative hive weight changes. The duration of hot periods (i.e. consecutive days with T_{mean}>20°C) present also a significant and negative correlation with bees' productivity in spring and autumn.

In summer, the effect of DTR is also strong and negative. High DTR (usually associated with hot and clear sky conditions) reduces the productivity rates, whereas intermediate DTR (usually representing partly overcast days) enhances it. A maximum rate of +0.342% is achieved when DTR is about 5°C.

RH attributes (RH_{mean}, RH_{max}, and RH_{min}) have a positive strong influence on the hive productivity rates, especially in spring and summer. Also, VPD and e_s have significant negative influence in all seasons except winter. For VPD greater than 1.5 kPa the daily changing rates of beehive weight become negative, while as the length of dry periods (consecutive days with VPD>1.5 kPa) increases, the productivity rates decrease. Additionally, the productivity rates decrease with windspeed, and present strong correlation is spring and summer.

The general findings of this work can be used to enhance existing knowledge concerning the impact of weather variables on bees' behavior and productivity especially at the microenvironment of a relatively small Mediterranean island, with potential applications to beekeepers scheduling for moving apiaries in order to achieve higher beehive product yields. Also, such information can be meaningful in beehive designing. However, further research is necessary to identify the critical weather variables affecting honey production atlocal level either directly (honeybees' behavior) or indirectly (vegetation dynamics or behavior of honeydew-producing insects). Additionally, it should be noted that theavailable data presented in this work (5 years) may be considered sufficient to draw some initial conclusions concerning the short-term impact of the meteorological variables on beehive productivity but longer timeseries are necessary in order to assess the impact of climate on bees behavior, activity and honey production. Within this framework, the findings of this paper are part of an ongoing research project aiming to better understand the impact of critical factors (climate, beekeeping manipulations, honeydew-producing insects bioecology) on honey productivity in Greece. Future research may concern the integration of the present work's results in a forecasting honey production model based on the honeydew harvest, to be used as a tool from beekeepers for increasing honey yields and decreasing beekeeping costs.

ACKNOWLEDGMENTS

The present research was implemented within the framework of the Emblematic Research Action "The Honeybee Roads" (subaction Practical Beekeeping-Beekeeping Flora) of the Project 2018SE01300000, Subproject 1: "Establishment of national research networks in the value chains of "olive", "grapevine", "honey" and "livestock"" and was financed by the Greek national funds through the Public Investments Program of the General Secretariat for Research and Innovation (GSRI)-Hellenic Ministry of Education, Research and Religious Affairs.

The weight data used in this work were obtained within the implementation of the Project "Improving the conditions for the production and marketing of beekeeping products- Regulations (EC) 1234/2007, 797/2004 and 917/2004", co-financed by the Hellenic Ministry of Rural Development and Foods and the European Union.

REFERENCES

Abou-Shaara, H., 2014. The foraging behaviour of honey bees, *Apis mellifera*: a review. Veterinarni Medicina, 59(1).

Abou-Shaara, H., Owayss, A.A., Ibrahim, Y. and Basuny, N., 2017. A review of impacts of temperature and relative humidity on various activities of honey bees. Insectes Sociaux, 64(4): 455-463.

Aizen, M.A. and Harder, L.D., 2009. The global stock of domesticated honey bees is growing slower than agricultural demand for pollination. Current biology, 19(11): 915-918.

Allen-Wardell, G. et al., 1998. The potential consequences of pollinator declines on the conservation of biodiversity and stability of food crop yields. Conservation biology: 8-17.

Blažytė-Čereškienė, L., Vaitkevičienė, G., Venskutonytė, S. and Būda, V., 2010. Honey bee foraging in spring oilseed rape crops under high ambient temperature conditions. Žemdirb.(Agric.), 97: 61-70.

Burrill, R.M. and Dietz, A., 1981. The response of honey bees to variations in solar radiation and temperature. Apidologie, 12(4): 319-328.

Ciesla, W.M., 2002. Non-wood forest products from temperate broad-leaved trees, 15. Food & Agriculture Org.

Clarke, D. and Robert, D., 2018. Predictive modelling of honey bee foraging activity using local weather conditions. Apidologie, 49(3): 386-396.

Corbet, S.A., 1990. Pollination and the weather. Israel Journal of Plant Sciences, 39 (1-2): 13-30.

Crane, E., 1990. Bees and beekeeping: science, practice and world resources. Heinemann Newnes.

Cressey, D., 2014. EU states lose up to one-third of honeybees per year. Nature News.

deMattos, I., Souza, J. and Soares, A., 2018. Analysis of the effects of climate variables on *Apis mellifera* pollen foraging performance. Arquivo Brasileiro de Medicina Veterinária e Zootecnia, 70(4): 1301-1308.

Delgado, D.L., Pérez, M.E., Galindo-Cardona, A., Giray, T. and Restrepo, C., 2012. Forecasting the influence of climate change on agroecosystem services: potential impacts on honey yields in a small-island developing state. Psyche, 2012.

Devlin, B., 1988. The effects of stress on reproductive characters of *Lobelia cardinalis*. Ecology, 69(6), 1716-1720.

Doull, K.M., 1976. The effects of different humidities on the hatching of the eggs of honeybees. Apidologie, 7(1): 61-66.

Easterling, D.R., Horton, B., Jones, P.D., Peterson, T.C., Karl, T.R., Parker, D.E., Salinger, M.J., Razuvayev, V., Plummer, N., Jamason, P and Folland, C.K., 1997. Maximum and minimum temperature trends for the globe. Science, 277(5324), 364-367.

Ellis, M.B., 2009. Homeostasis: humidity and water relations in honeybee colonies (*Apis mellifera*). Doctoral dissertation, University of Pretoria. https://repository.up.ac.za/handle/2263/28357

Freitas, B. and Paxton, R., 1996. The role of wind and insects in cashew (*Anacardium occidentale*) pollination in NE Brazil. Journal of Agricultural Science-Cambridge-, 126: 319-326.

Gallai, N., Salles, J.-M., Settele, J. and Vaissière, B.E., 2009. Economic valuation of the vulnerability of world agriculture confronted with pollinator decline. Ecological economics, 68(3): 810-821.

Gerlach, J., 1985. The dependence of honey-bee behaviour on weather—shown by the results of weighing bee-hives in the period of 1969 to 1978 in the region of the Beekeepers Association of Hannover. International journal of biometeorology, 29(1): 67-85.

Gimeno, T.E., Camarero, J.J., Granda, E., Pías, B. and Valladares, F., 2012. Enhanced growth of *Juniperus thurifera* under a warmer climate is explained by a positive carbon gain under cold and drought. Tree physiology, 32(3): 326-336.

Gordo, O. and Sanz, J.J., 2006. Temporal trends in phenology of the honey bee *Apis mellifera* (L.) and the small white *Pieris rapae* (L.) in the Iberian Peninsula (1952–2004). Ecological Entomology, 31(3): 261-268.

Gounari, S., 2006. Studies on the phenology of *Marchalina hellenica* (gen.) (Hemiptera: Coccoidea, Margaro-

didae) in relation to honeydew flow. Journal of Apicultural Research, 45(1), 8-12.

Gounari, S., 2010. Biology and Phenology of *Marchalina hellenica* Genn. (Hemiptera: Marchalinidae) in Greece. Proceedings of the XII International Symposium on Scale Insects Studies, Greece.

Gu, L., Baldocchi, D.D., Wofsy, S.C., Munger, J.W., Michalsky, J.J., Urbanski, S.P. and Boden, T.A., 2003. Response of a deciduous forest to the Mount Pinatubo eruption: Enhanced photosynthesis. Science, 299(5615), 2035-2038.

He, X.J., Tian, L.Q., Wu, X.B. and Zeng, Z.J., 2016. RFID monitoring indicates honeybees work harder before a rainy day. Insect science, 23(1): 157-159.

Henneken, R., Helm, S. and Menzel, A., 2012. Meteorological influences on swarm emergence in honey bees (hymenoptera: Apidae) as detected by crowdsourcing. Environmental entomology, 41(6): 1462-1465.

Holmes, W., 2002. The influence of weather on annual yields of honey. The Journal of Agricultural Science, 139(1): 95.

Huber, H., 1956. Die Abhängigkeit der Nektarsekretion von Temperatur, Luft und Bodenfeuchtigkeit. Planta 48: 47–98.

Joshi, N.C. and Joshi, P., 2010. Foraging behaviour of *Apis* spp. on apple flowers in a subtropical environment. New York Science Journal, 3(3): 71-76.

Kenoyer, L.A., 1917. Environmental influences on nectar secretion. Botanical Gazette 63:249–265.

Kunkel, H., 1997. Scale insect honeydew as forage for honey production. In Ben-Dov, Y. and Hodgson, C.J., Soft Scale Insects, their Biology, Natural Enemies and Control. World Crop Pests, Vol 7A, pp. 291- 302, Elsevier, Amsterdam.

Łangowska, A. Zawilak, M., Sparks, T.H., Glazaczow, A., Tomkins, P.W., and Tryjanowski, P., 2017. Long-term effect of temperature on honey yield and honeybee phenology. International journal of biometeorology, 61(6): 1125-1132.

Lau, T.C., and Stephenson, A.G., 1994. Effects of soil phosphorus on pollen production, pollen size, pollen phosphorus content, and the ability to sire seeds in *Cucurbita pepo* (Cucurbitaceae). Sexual Plant Reproduction 7:215–220.

Le Conte, Y. and Navajas, M., 2008. Climate change: impact on honey bee populations and diseases. Revue Scientifique et Technique-Office International des Epizooties, 27(2): 499-510.

Li, Z. et al., 2016. Drone and worker brood microclimates are regulated differentially in honey bees, *Apis mellifera*. PloS one, 11(2): e0148740.

Lundie, A.E., 1925. The flight activities of the honeybee. United States Department of Agriculture.

Meikle, W.G., Rector, B.G., Mercadier, G. and Holst, N., 2008. Within-day variation in continuous hive weight data as a measure of honey bee colony activity. Apidologie, 39(6): 694-707.

Morse, R.A. and Calderone, N.W., 2000. The value of honey bees as pollinators of US crops in 2000. Bee culture, 128(3): 1-15.

Moschidis, G., Dimou, M., Gounari, S., Pidiakis, C., Diakostamatiou, M., Thrasyvoulou, A. and Tananaki, C., 2019. Microscopic and physicochemical characteristics. Proceedings of the 3rd Pan-Hellenic Conference on Professional Beekeeping, Patras, Greece (in greek).

Moschidis G., Dimou M., Tananaki C. and Thrasyvoulou A., 2013. Pollen atlas of Rhodes island, Greece. XXXXIII International Apimondia Congress, Kyiv, Ukraine.

Ortiz-Caraballo, M.A., 2007. Mating system and fecundity of *Goetzea elegans* (Solanaceae), an endangered tree of Puerto Rico, University of Puerto Rico Rio Piedras.

Petanidou, T., Goethals, V. and Smets, E., 1999. The effect of nutrient and water availability on nectar production and nectary structure of the dominant Labiatae species of phrygana. Systematics and Geography of Plants 68:233–244.

Pleasants, J.M. and S.J. Chaplin, 1983. Nectar production rates of *Asclepias quadrifolia*: causes and consequences of individual variation. Oecologia 59:232–238.

Polce, C. et al., 2014. Climate-driven spatial mismatches between British orchards and their pollinators: increased risks of pollination deficits. Global change biology, 20(9): 2815-2828.

Poonyth, D. and Ford, D., 2004. Small Island Developing States: Agricultural Production and Trade, Preferences and Policy, 7. FAO.

Potts, S.G. et al., 2010. Global pollinator declines: trends, impacts and drivers. Trends in ecology & evolution, 25(6): 345-353.

Proutsos, N., Liakatas, A. and Alexandris, S., 2019. Ratio of photosynthetically active to total incoming radiation above a Mediterranean deciduous oak forest. Theoretical and Applied Climatology, 137(3-4): 2927-2939.

Proutsos, N. and Tigkas, D., 2020. Growth Response of Endemic Black Pine Trees to Meteorological Variations and Drought Episodes in a Mediterranean Region. Atmosphere, 11(6): 554.

Proutsos, N., Tsagari, K., Karetsos, G., Liakatas, A. and Kritikos, T., 2010. Recent temperature trends over mountainous Greece. European Water, 32: 15-23.

Proutsos N., E. Korakaki., A. Bourletsikas, A. Solomou, E. V. Avramidou, C. Georgiadis, A.B. Kontogianni, K. Tsa-

gari, 2020. Urban temperature trends in east Mediterranean: The case of Heraklion-Crete. European Water, Special Issue: "11th Word Congress on Water Resources and Environment" (EWRA2019), 69/70: 3-14, http://www.ewra.net/ew/pdf/EW_2020_69-70_01.pdf

Puškadija, Z. et al., 2007. Influence of weather conditions on honey bee visits (*Apis mellifera carnica*) during sunflower (*Helianthus annuus* L.) blooming period. Poljoprivreda, 13(1): 230-233.

Quesada, M., Bollman, K. and Stephenson, A.G., 1995. Leaf damage decreases pollen production and hinders pollen performance in *Cucurbita texana*. Ecology 76:437–443.

Ricketts, T.H., Daily, G.C., Ehrlich, P.R. and Michener, C.D., 2004. Economic value of tropical forest to coffee production. Proceedings of the National Academy of Sciences, 101(34): 12579-12582.

Rocha, H. and Dias, J., 2017. Honey Yield Forecast Using Radial Basis Functions, International Workshop on Machine Learning, Optimization, and Big Data. Springer, pp. 483-495.

Roubik, D.W., 1995. Pollination of cultivated plants in the tropics, 118. Food & Agriculture Org.

Roubik, D.W., 2002. The value of bees to the coffee harvest. Nature, 417(6890): 708-708.

Scheifinger, H., Koch, E. and Winkler, H., 2005. Results of a first look into the Austrian animal phenological records. Meteorologische Zeitschrift, 14(2): 203-209.

Shuel, R.W., 1967. The influence of external factors on nectar production. American Bee Journal 107:54–56.

Sparks, T.H., Łangowska, A., Glazaczow, A., Wilkaniec, Z., Bienkowska, M., and Tryjanowski, P., 2010. Advances in the timing of spring cleaning by the honeybee *Apis mellifera* in Poland. Ecological Entomology, 35(6): 788-791.

Spivak, M., 1992. The relative success of Africanized and European honey-bees over a range of life-zones in Costa Rica. Journal of Applied Ecology: 150-162.

Stephenson, A.G., Lau, T.-C., Quesada, M. and Winsor, J. A., 1992. Factors that affect pollen performance. In R. Wyatt (ed.) Ecology and evolution of plant reproduction. Chapman and Hall, New York, New York, USA, 119–136 pp.

Tan, K., Yang, S., Wang, Z.-W., Radloff, S.E. and Oldroyd, B.P., 2012. Differences in foraging and broodnest temperature in the honey bees *Apis cerana* and *A. mellifera*. Apidologie, 43(6): 618-623.

Tanarhte, M., Hadjinicolaou, P. and Lelieveld, J., 2012. Intercomparison of temperature and precipitation data sets based on observations in the Mediterranean and the Middle East. Journal of Geophysical Research: Atmospheres, 117(D12).

Tetens, O., 1930. Uber Einige Meteorologische Begriffe. Z. geophys, 6: 297-309.

Thrasyvoulou, A. and Manikis, J., 1995. Some physicochemical and microscopic characteristics of Greek unifloral honeys.

Tsiros, I.X., Nastos, P., Proutsos, N.D. and Tsaousidis, A., 2020. Variability of the aridity index and related drought parameters in Greece using climatological data over the last century (1900–1997). Atmospheric Research, 240: 104914.

Turner, L.B., 1993. The effect of water stress on floral characters, pollination and seed set in white clover (*Trifolium repens* L.). Journal of Experimental Botany 44:1155–1160.

UNEP, 1992. World Atlas of Desertification.

van Engelsdorp, D., Hayes, J., Underwood, R.M. and Pettis, J., 2008. A survey of honey bee colony losses in the US, fall 2007 to spring 2008. PLoS One, 3(12): 1-6.

Vasek, F.C., Weng, V., Beaver, R.J., and Huszar, C.K., 1987. Effects of mineral nutrition on components of reproduction in *Clarkia ungucilata*. Aliso: A Journal of Systematic and Evolutionary Botany, 11(4), 599-618.

Vicens, N. and Bosch, J., 2000. Weather-dependent pollinator activity in an apple orchard, with special reference to *Osmia cornuta* and *Apis mellifera* (Hymenoptera: Megachilidae and Apidae). Environmental entomology, 29(3): 413-420.

Waser, N.M. and Price, M.V., 2016. Drought, pollen and nectar availability, and pollination success. Ecology, 97(6), 1400-1409.

Woyke, J., Wilde, J. and Wilde, M., 2003. Flight activity reaction to temperature changes in *Apis dorsata*, *Apis laboriosa* and *Apis mellifera*. Journal of Apicultural Science, 47(2): 73-80.

Yeager K., 2021. LibGuides: SPSS Tutorials: Pearson Correlation. Available online at https://libguides.library.kent.edu/SPSS/PearsonCorr (accessed in 18/5/2021).

Italian Journal of Agrometeorology
Rivista Italiana di Agrometeorologia

Firenze University Press
www.fupress.com/ijam

OPEN ACCESS

Citation: H. Fatemi Kiyan, M. Tatari, M.R. Tokalo, M. Salehi, K. Hajmohammadnia Ghalibaf (2022) The effect of deficit irrigation and fertilizer on quantitative and qualitative yield of quinoa (*Chenopodium quinoa*). *Italian Journal of Agrometeorology* (1): 83-99. doi: 10.36253/ijam-1136

Received: November 19, 2020

Accepted: November 29, 2021

Published: July 19, 2022

Data Availability Statement: All relevant data are within the paper and its Supporting Information files.

Competing Interests: The Author(s) declare(s) no conflict of interest.

The effect of deficit irrigation and fertilizer on quantitative and qualitative yield of quinoa (*Chenopodium quinoa*)

Hassan Fatemi Kiyan[1], Maryam Tatari[1,*], Mohammad Reza Tokalo[2], Masomeh Salehi[3], Kamal Hajmohammadnia Ghalibaf[4]

[1] *Department of Agronomy, Islamic Azad University, Shirvan Branch, Shirvan, Iran*
[2] *Department of Agronomy, Islamic Azade University, Bojnourd Branch, Bojnourd, Iran*
[3] *National Saline Research Center Agricultural Education and Extension Research Organization, Yazd, Iran*
[4] *Department of Agronomy, Faculty of Agriculture, Ferdowsi University of Mashhad, Iran*
*Corresponding author. E-mail: maryamtatari@yahoo.com

Abstract. In order to investigate the effect of deficit irrigation and chemical fertilizers on yield and some physiological traits of quinoa an experiment was conducted in 2019 as split plot based on a randomized complete block design in two locations (Mashhad and Neishabour). Irrigation included, I0: full irrigation, I1: no irrigation at emergence stage, I2: no irrigation at stem elongation stage, I3: no irrigation at flowering stage, I4: no irrigation at seed setting stage. Fertilizer treatments included control (no fertilizer application); chemical fertilizer application according to local practices; manure application of 10 tons; and manure application of 20 tons per hectare. In general, seed yield, percentage of protein and seed oil in Mashhad was higher than in Neishabour. I2 treatment had the least negative effect on relative leaf water content. Application of chemical fertilizers, 10 tons and 20 tons of animal manure increased the percent of seed protein by 1.43, 1.66 and 2.37 compared to the control, respectively. The highest percentage of seed oil (5.91%) was obtained for treatment I2 in Mashhad and the lowest percentage of seed oil (4.18%) was obtained for treatment I4 in Neishabour. The lowest seed yield due to I1 treatment was observed in Neishabour and the highest seed yield was related to I0 treatment with 20 tons of manure and was observed in Mashhad. The results showed that the yield and water stress tolerance potential of quinoa can be modified by irrigation, fertilizer source and location.

Keywords: quinoa seed quality, irrigation management, organic fertilizer, plant pigment, electrolyte leakage.

INTRODUCTION

Quinoa (*Chenopodium quinoa*) is native to the Andes Mountains in Bolivia, Chile and Peru, and Bolivia, Peru and Ecuador are the most important producers (Vega-Galvez et al., 2010). Quinoa belongs to the Chenopodiaceae family, a genus of Chenopodium, and is considered as similar to cere-

als. Quinoa is rich in protein, iron and calcium and is better than wheat and rice in terms of amino acid balance (James, 2009). It is a very high nutritional value has been compared to dry milk by the FAO, and has been called vegetable caviar (James, 2009). Global interest and attention to this plant are due to its high nutritional value (Garcia et al., 2015; Nowak et al., 2016). In general, quinoa can be less affected by frost (Jacobsen et al., 2005), salinity (Hariadi et al., 2011; Razzaghi et al., 2011; Ruiz-Carrasco et al., 2011), poor soils. (Jacobsen et al., 2009) and drought (Hirich and Choukr-Allah, 2014) than other crop species. It is believed that the presence of several drought resistance mechanisms in quinoa has made it suitable for arid and semi-arid regions (El youssfi et al., 2012; Hirich et al., 2012). In 2018, the cultivation area and production of quinoa in the world were estimated as 178313 hectares and 158920 tons, respectively (FAO, 2020). Quinoa is currently grown in twenty provinces in Iran.

Drought stress is one of the most common and destructive abiotic stresses across the world and limits the growth and yield of plants, especially in arid and semi-arid regions (Wang et al., 2014; Heuberger and Pfeiffer 2013). Drought stress affects a combination of physiological and biochemical processes of plants and negatively impact the growth and yield (Zulkarami et al., 2016). Deficit irrigation strategy is a good way to increase water productivity in crop production under drought conditions. This strategy is very effective in arid and semi-arid regions that suffer from water scarcity (Hirich and Choukr-Allah, 2014). Global warming has affected the climate of different parts of the world, including Iran, which has increased the salinity of the country's arable land. The Quinoa shows a high tolerance to drought, salinity and cold stress, which can be a suitable plant for achieving sustainable agriculture and proper nutrition according to the existing conditions in Iran. Quinoa yield varies according to climatic conditions, planting date and cultivar. Geerts et al. (2008) reported the maximum yield under full irrigation conditions as 2.04 t/ha, under deficit irrigation as 2.01 t/ha, and under rainfed conditions as 1.68 t/ha. Stikic et al. (2011) reported that quinoa has great agronomic and nutritional potential, even in dryland conditions and without fertilizer application. In their study, the grain yield was 1.72 t/ha and the grain quality was good with the protein content of in the range of 15.16 and 17.41 percent.

The Addition of organic matter increases the storage capacity of soil water under water deficit conditions. Studies on the addition of organic fertilizers to the soil in arid and semi-arid regions have shown that organic matter improves soil fertility, soil moisture content and increases soil hydraulic conductivity (Wesseling et al., 2009). Organic matter to soil also has a positive effect on crop growth and yield (Gopinath et al., 2008; Ibrahim et al., 2008). There are few studies examining soil organic management on quinoa yield (Hirich et al., 2014), however other crops in other studies have responded positively to such treatments as well (Hartley et al., 2010; Dadkhah, 2014).

Although quinoa has the potential for growth in harsh environments with fewer resources availability and high stress tolerance compared to other crops, so far not many studies have been performed on the production and quality of quinoa under Iranian agricultural systems. Therefore, this study was conducted to determine the effect of deficit irrigation and organic fertilizer on quantitative and qualitative yield as well as some physiological traits of quinoa about drought stress in Mashhad and Neishabour.

MATERIALS AND METHODS

This experiment was performed in 2019 in two locations, the Agricultural Research Field of Toroq in Mashhad and the Agricultural Research Field of Ayesha in Neishabour. The climatic characteristics of these two locations are presented in (Table 1). The experiment was performed as split plots based on a randomized complete block design with three replications in both locations. The treatments of this experiment included different levels of irrigation allocated as the main plot and fertilizer treatments as the subplots.

Deficit irrigation levels included I0: full irrigation, I1: cessation of irrigation in emergence stage, I2: cessation of irrigation in elongation of the stem stage, I3: cessation of irrigation in the flowering stage, I4: cessation of irrigation in seed setting stage (Sosa-Zuniga et al., 2017). Fertilizer treatments also included control (no fertilizer application), chemical fertilizer based on local management fertilizer recommendation, 10 t/ha of livestock manure and 20 t/ha of livestock manure. It should be noted that the recommendation of quinoa fertilizer in Iran includes 100 kg/ha of phosphate fertilizer, 100 kg of potash fertilizer and 50 kg of nitrogen fertilizer. Before the experiment, the soil sample was randomly taken from a depth of 0-30 cm from the fields in both locations and transferred to the laboratory to determine the soil properties (Table 2).

Sub-plots were 3 m long and 2 m wide. The dimensions of the subplot were 0.6 m^2. The distance between the plots was 1.5 m and the distance between the blocks

Table 1. Physical and chemical characters of soil in two study locations, Neyshabour and Mashhad (Soil depth 0-30 cm).

Location	pH	EC ($dS.m^{-1}$)	SAR	O.C (%)	Total N (%)	Available P (ppm)	Available K (ppm)	Lime (%)	Soil tissue
Neyshabur	7.93	0.899	4.95	0.742	0.07	3.4	217	17.73	Loam
Mashhad	7.74	2.34	8.23	0.362	0.03	3.5	145	13.75	Loam

Table 2. Climate and geographical conditions of two study locations (Neyshabour and Mashhad).

Location	Longitude	Latitude	Altitude above sea level (m)	Average annual rainfall (mm)	Annual mean temperature (°C)	Annual mean daily maximum temperatures (°C)	Annual mean daily minimum temperatures (°C)
Neyshabur	58° 50'E	36°10'N	1250	240	14.7	22.5	6.8
Mashhad	59° 35'E	36°20'N	950	222.3	16.5	23	9.4

Table 3. Summary of information and date of field operations tested at two locations.

Location	Planting date	Rainfall August (mm)	Rainfall September (mm)	Date of chemical fertilizer use *	Date of manure fertilizer use	Irrigation date of emergence stage	Irrigation date Stem elongation stage	Irrigation date of flowering stage	Irrigation date Seedling stage
Neyshabur	27-7-19	0	0	22/06/19	22/06/19	29/07/19	11/08/19	26/08/19	08/09/19
Mashhad	4-8-19	0	0	22/06/19	22/06/19	07/08/19	19/08/19	01/09/19	13/09/19

*Chemical fertilizers including 220 kg of potassium sulfate, 130 kg of triple superphosphate and 200 kg of urea per hectare were applied. Urea was given to two farms during the germination stage.

was 3 m. In order to prepare the ground, first reversible plowing and then disc were used. After leveling and plotting, the manure was spread on the plots based on specified amount and mixed thoroughly with the soil with a shovel. Then 6 rows were created in each plot with a distance of 0.25 m and quinoa seeds were planted. The employed seed in this experiment was Titicaca cultivar which was obtained from Agricultural Research Center of Yazd. After planting, in order to achieve uniformity of emergence, the first irrigation was applied equally for all plots. The second irrigation was applied three days later. Then, after ensuring the establishment of seedlings, deficit irrigation treatments were performed according to the mentioned developmental stages. Surface irrigation was applied to irrigate each plot and irrigation intervals were considered as 14 days. The water requirement of the plant was calculated using Cropwat software. The geographical, climatological characteristics and the date of planting, irrigation and fertilization operations of the two studied locations are presented in (Table 3).

Evaluation was performed by measuring traits including relative leaf water content, soluble sugar content, total chlorophyll, carotenoids, electrolyte leakage of ions, protein percentage, oil percentage and grain yield. For measurement of relative leaf water content, ten leaf discs were collected from the middle leaves of each experimental unit and after weighing with an accuracy of 0.0001 g, they were transferred to double-distilled petri dishes containing water and for 24 hours were stored in dark at 4 °C for complete water absorption. The leaves were then removed and were put between two filter papers to dry extra water and then leaves weight as turgid weight was measured. The leaves were dried in an oven at 70 °C for 48 hours and weighed again as dry weight. Then the relative water content of the fresh leaves was determined using (Equation 1) (Mahmood et al., 2003):

$$RWC = (Fw - Dw) / (Tw - Dw) \times 100 \quad (1)$$

Where Fw is the fresh weight of the leaf, Dw is the dry weight of the leaf and Tw is the turgid weigh t of the leaf. The amount of plant solution sugars was read using the sulfuric phenol method and was read by the UV-2100 model spectrophotometer at 485 nm wavelength (Irigoyen et al., 1992). Porra (2002) method was used to measure chlorophyll content. For this purpose,

500 mg of each selected leaf was homogenized in 5 ml of 80% acetone and after centrifugation at 4 °C for 15 minutes at 13000 rpm, the supernatant was removed and then its volume with 80% acetone was reduced to 10 ml. The concentration of the solution was measured by spectrophotometer at wavelengths of 663 nm for chlorophyll a, 645 nm for chlorophyll b and 470 nm for carotenoids. To measure total chlorophyll, the values of chlorophyll a and b were added together. Flint et al. (1967) method was used to measure ion leakage. The protein content of the samples was determined by a micro-kejldahl UK electrothermal equipment by using half a gram of plant samples after digestion and distillation (Helvich, 1990). In order to extract the oil and determine its percentage, Soxhlet and hexane solvent method was used (Carrillo et al., 2017). Sampling was performed randomly by (1×1) m quadrat from each plot, considering the removal of the margin effect, to determine the final grain yield.

Analysis of variance and comparison of mean data were performed by Duncan's multiple range test with SAS 9.4 software and figures were prepared by MS Excel. Before performing the combined analysis of variance, the homogeneity of variance of experimental errors was tested using Bartlett test.

RESULTS AND DISCUSSION

Relative leaf water content

One of the physiological parameters responding to dehydration is the relative leaf water content, which shows a good correlation with drought tolerance. In other words, changes in leaf moisture content can be used as a short-term response to stress and a measure of the ability to maintain resource strength under drought stress conditions (Ahmadi et al., 2010). According to the analysis of variance, the effects of location, deficit irrigation and fertilizer as well as the interaction of location and fertilizer on the relative water content of the leaves were significant (Table 4). The highest relative water content was observed for full irrigation treatment (80.11%), then no irrigation (I_2) at the growth stage of stem elongation (77.28%) had the highest relative water content with complete irrigation treatment. In other words, among the deficit irrigation levels, no irrigation at stage I_2 had the least negative effect on the relative water content of leaves, so it can be said that by eliminating irrigation at the stage of the stem elongation in addition to saving limited water resources, the leaf moisture content change is not significant. In contrast, no irrigation at the flowering stage (I_3) resulted in the lowest relative water content of leaves (60.84%) (Table 5).

If drought stress persists, the relative water content of the leaf decreases, causing a change in the cell membrane and consequently an increase in electrolyte leakage from the cell (Fu et al., 2004). A similar relationship was observed between the relative leaf water content and ion electrolyte leakage in this study. It seems the plants under water stress, by increasing the osmotic pressure, reduce the spaces between cells and the water content of their tissue, allowing water to move from the soil to the cells, and as a result, their relative amount of water

Table 4. Compound analysis of various quinoa traits under deficit irrigation in different phonological stages and fertilizers (chemical and organic) in Mashhad and Neishbour.

SOV	df	Leaf relative water content	Soluble sugar content	Total chlorophyll content	Carotenoid content	Ion electrolyte leakage	Seed protein (%)	Seed oil (%)	Seed yield
Location	1	9490.79**	23.11**	0.46^{ns}	0.0000^{ns}	5967.26**	25.76**	5.09**	189210.21**
Rep (location)	4	80.89	0.70	0.25	0.1029	66.86	0.33	0.58	35545.08
Deficit irrigation	4	1357.51**	3.81**	5.47**	0.3463**	892.76**	6.28**	3.38**	152903.93**
Location ×Deficit irrigation	4	33.40^{ns}	1.08**	0.21^{ns}	0.1992**	87.32**	6.93**	1.87**	20796.38**
Error a	16	81.43	0.23	0.72	0.0142	128.76	0.63	0.83	10972.53
Fertilizer	3	175.93**	14.41**	16.73**	0.3394**	954.64**	1.00*	0.24*	67648.28**
Fertilizer × Deficit irrigation	12	19.54^{ns}	0.18**	0.22^{ns}	0.0257**	30.96^{ns}	0.07^{ns}	0.21**	10650.94*
Location × Fertilizer	3	71.72*	1.99**	0.59*	0.0517**	89.41**	0.18^{ns}	0.14^{ns}	22080.36**
Fertilizer × Deficit irrigation × Location	12	9.59^{ns}	0.07*	0.16^{ns}	0.0351**	26.85^{ns}	0.01^{ns}	0.11^{ns}	9037.06*
Error b	60	25.56	0.032	0.16	0.0054	18.45	0.035	0.065	4470.06
CV		7.04	9.99	12.86	12.39	13.55	3.21	4.69	21.03

ns, * and **: Non-significant, significant at 5% and 1% probability level, respectively.

Table 5. Mean comparison of different quinoa traits under deficit irrigation in different phonological stages and fertilizer treatments (chemical and organic) in Mashhad and Neishabour.

	Relative leaf water content (%)	Chlorophyll content (mg/g)	Seed yield (g/m^2)		Protein (%)	Seed yield (g/m^2)
I_0: Full Irrigation	80.11 [a*]	3.59 [a]	343.9 [a]	Control	18.12 [b]	253.4 [c]
$I_{1.}$ NO Irrigation at emergence	71.77 [b]	2.33 [d]	176.21 [b]	Chemical fertilizer	18.38 [ab]	322.5 [b]
$I_{2.}$ NO Irrigation at stem elongation	77.28 [a]	3.38 [ab]	357.2 [a]	Manure 10 t/ha	18.42 [ab]	327.9 [b]
I_3 : NO Irrigation at flowering	60.84 [c]	3.16 [bc]	344.6 [a]	Manure 20 t/ha	18.55 [a]	367.8 [a]
I_4 NO:Irrigation at seed setting	69.14 [b]	3.07 [c]	367.7 [a]			

* Means with same letter(s) for each component indicates no significant difference based on Duncan test at 5% probability level.

Table 6. Mean comparison of interaction of location and deficit irrigation treatments effects on quinoa traits.

Location	Deficit irrigation	Electrolyte leakage (%)	Protein (%)	Oil (%)
Neishabour	I_0: Full Irrigation	17.88 [e*]	16.52 [g]	5.62 [cd]
	$I_{1.}$ NO Irrigation at emergence	32.18 [c]	17.59 [f]	5.66 [bc]
	$I_{2.}$ NO Irrigation at stem elongation	19.21 [e]	18.19 [d]	5.42 [de]
	I_3 : NO Irrigation at flowering	27.30 [d]	18.14 [e]	5.31 [e]
	I_4 NO:Irrigation at seed setting	26.65 [d]	19.09 [b]	4.18 f
Mashhad	I_0: Full Irrigation	27.28 [d]	18.59 [cde]	5.83 [ab]
	$I_{1.}$ NO Irrigation at emergence	44.95 [a]	19.63 [a]	5.34 [e]
	$I_{2.}$ NO Irrigation at stem elongation	39.00 [b]	18.63 [bcd]	5.91 [a]
	I_3 : NO Irrigation at flowering	40.60 [b]	18.52 [cde]	5.76 [abc]
	I_4 NO:Irrigation at seed setting	41.90 [ab]	18.79 [bc]	5.40 [e]

*Means with same letter(s) for each component indicates no significant difference based on Duncan test at 5% probability level.

decreases in water shortage conditions. According to (Ma et al., 2006), water stress reduces water potential, relative leaf water content, transpiration, stomatal conductance and ultimately yield.

Comparison of the mean of the interaction of location and fertilizer treatment showed that in general, due to differences in climatic parameters, the relative water content of leaves in Mashhad (62.93%) was lower than Neishabour (80.72%), because according to (Table 1), in Mashhad the average rainfall was lower and the average temperature was higher than Neishabour, which causes a higher evaporative demand of the atmosphere. In addition, the fertilizer treatments showed significantly different results at the two locations. In Neishabour, application of chemical fertilizer treatments, 10 tons and 20 tons of livestock manure increased the relative water content by 3.7%, 5.2% and 2.1% percent, respectively, while in Mashhad, the values of increasing the relative water content but 2% is lower, were higher by 11.4 percent for the organic fertilizer treatments, respectively. (Table 6).

Soluble sugar content

Soluble sugars have assimilated that increase under stress conditions and their accumulation causes osmotic regulation and cell turgescence, and on the other hand, protects and stabilizes membranes and proteins under stress conditions. According to the results of analysis of variance, all single effects, dual interactions as well as triple interactions of location, irrigation and fertilizer on the content of soluble sugars were significant (Table 4). Comparison of the mean of the interaction of location, irrigation and fertilizer in (Figure 1) showed that in general the amount of soluble sugars in Neishabour was higher than in Mashhad. But the response of this trait to fertilizer and deficit irrigation treatments in two study locations was not similar. In general, fertilizer treatments in all conditions increased the amount of soluble sugars. The highest increase in soluble sugars under no irrigation treatment was observed at the flowering stage (I_3) along with the application of 20 tons of manure in Neishabour and the lowest increase under no irrigation treatment was observed in stage (I_2) of stem elonga-

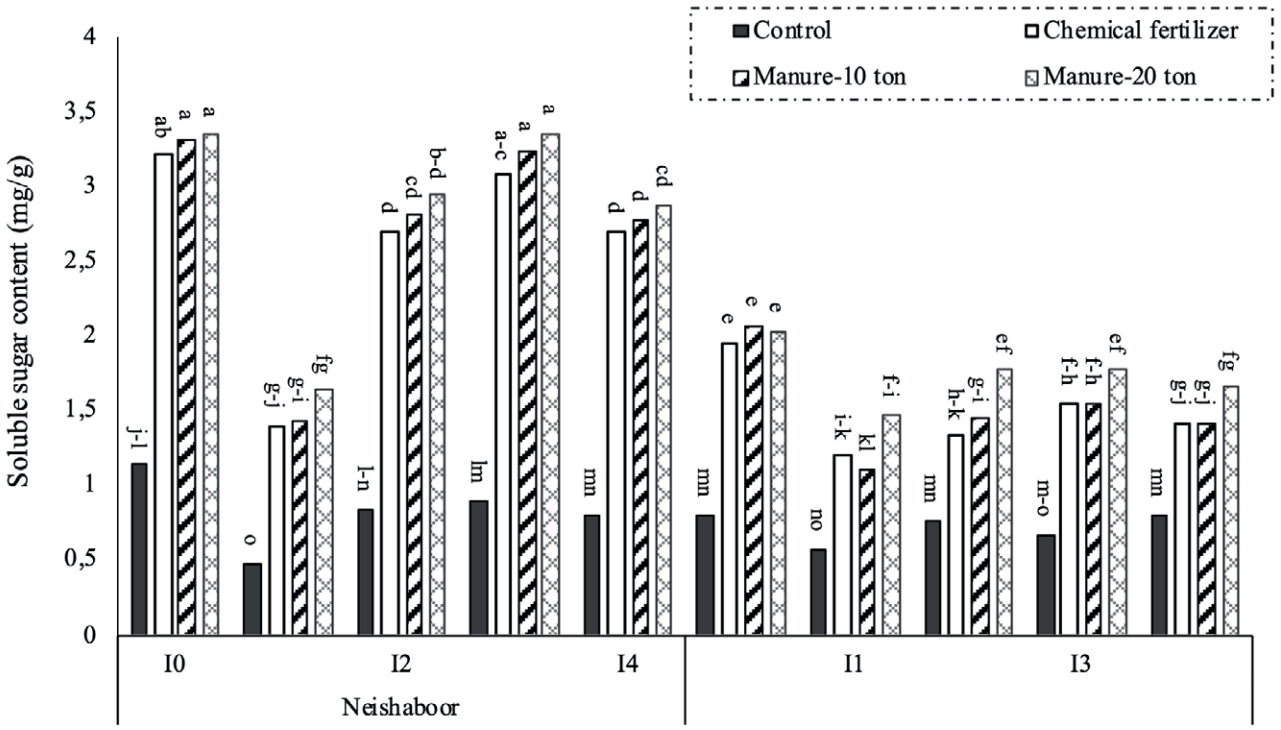

Fig. 1. Mean comparison of triple interaction of location, deficit irrigation and fertilizer effects on soluble sugars content. I_1: no irrigation at emergence stage, I_2: no irrigation at stem elongation stage, I_3: no irrigation at flowering stage, I_4: no irrigation at seed setting stage.

tion and application of chemical fertilizer in Mashhad (Figure 1). The lowest soluble sugars of 0.46 mg/g were observed under no irrigation treatment at emergence stage (I_1) and no fertilizer application in Neishabour and the highest soluble sugars were observed in treatments of 10 and 20 tons of manure and no irrigation levels of I_0 and I_3 in Neishabour (Figure 1). The increase of soluble sugar the cell, which creates an increasing osmotic pressure gradient between soil and plant and thus enables more water absorption from the soil. Accumulation of soluble sugars inside the cells plays an important role in osmotic regulation. It helps reduce cell water potential and keeps more water in the cell to maintain turbulence under dehydration (Turner, 2018). This mechanism promotes biological membrane stability, proteins, increased photosynthesis, and drought resistance. In tolerant plants compatible osmolytes attach to protein surfaces and maintain their natural structure under stress conditions, while in susceptible plants proteins are degraded (Hoekstra et al., 2001). Increased accumulation of soluble sugars in the cell under drought stress would regulate osmotic pressure in quinoa (Bascuñán-Godoy et al., 2016; González et al., 2009; Muscolo et al., 2016) and corn (Johari, 2010). However, (Gámez et al., 2019) reported that some genotypes showed an increase and others showed a decrease of soluble sugars under drought stress, which indicated the difference between genotypes in terms of response to drought stress.

Total chlorophyll content

One of the methods for evaluating and predicting crop tolerance to water stress is to study the amount of changes that occur in chlorophyll (a+b) leaf synthesis due to water scarcity. Decreased chlorophyll synthesis is one of the general reactions of plants to water deficiency (Gardner et al., 2017; Sadak, 2016). Analysis of variance showed that the single effects of irrigation and fertilizer as well as the interaction of location and fertilizer were significant on total chlorophyll content (Table 4). Comparison of the mean of the single effect of deficit irrigation treatment showed that the highest amount of leaf chlorophyll after control (full irrigation) was through the no irrigation (I_2) at the stage of stem elongation (Table 5). No irrigation (I_3) at the flowering stage showed the lowest chlorophyll content of leaves (Table 6). Chlorophyll content in living plants is one of the important factors for photosynthesis. Based on the severity, duration and crop growth stage, the drought effect on each of the chlorophyll levels in plants is different. In fact,

the decrease in chlorophyll due to water stress is related to the increase in the production of oxygen radicals in the cell, because these radicals cause peroxidation and thus decomposition of this pigment (Sheteawi and Tawfik, 2007). Water stress has a direct effect on reducing the chlorophyll index of plant leaves (Adebayo et al., 2014; Elewa et al., 2017). Reduction of photosynthetic pigments can be due to reduced synthesis of the main complex of chlorophyll pigments, optical degradation of the b-pigment protein complex that protects the photosynthetic apparatus, oxidative damage of chloroplast lipids of pigments and proteins or higher chlorophyllase enzyme activity and hormonal disorders (Pandey et al., 2012; Anjum et al., 2011). In addition, stress interferes with the absorption of some essential elements such as iron and magnesium, which are essential for chlorophyll synthesis (Neocleous and Vasilakakis, 2007). Lipoxygenase has also been reported to be one of the enzymes involved in chlorophyll catabolism. This enzyme is one of the enzymes involved in lipid peroxidation during stress (Farooq et al., 2009). Schmidhalter et al. (2006) reported that drought stress disrupts the chlorophyll-making process by limiting the plant's ability to absorb nitrogen. On the other hand, plant uptake and assimilation under drought stress conditions are largely controlled by the two main factors of leaf area and photosynthesis per unit of leaf area. Cell wall solubility, which is required for leaf elongation, prevents an increase in leaf and in turn strongly reduces the number of leaf chloroplasts (Bänziger et al., 2000). In the general reduction of photosynthesis pigments can be mainly due to chloroplast structure disruption and photosynthesis apparatus, photo oxidation of chlorophyll, pigments reaction with singlet oxygen, disruption of required materials for chlorophyll synthesis, prevention of biosynthesis of new chlorophyll, activating the chlorophyll degradation enzymes, and hormonal disorders.

Comparison of the mean of interaction of location and fertilizer treatment showed that 20 tons of livestock manure in Mashhad was associated with the highest chlorophyll content (3.81 mg/g) and non-fertilizer application in Mashhad had the lowest chlorophyll content (1.78 mg/g) (Table 6). Fertilizer application increased the total chlorophyll content of the leaves however the rate of increase was not the same in the two study locations. Treatment of 20 tons of manure in Mashhad had the highest increase and chemical fertilizer treatment in Neishabour had the lowest increase in total chlorophyll (Table 6). Because fertilizer treatments contain nitrogen and nitrogen is the main constituent of chlorophyll in the plant, the application of fertilizers increases the amount of chlorophyll. Livestock manure had a more positive effect on chlorophyll content, probably due to the more gradual release of nutrients in the soil.

Carotenoid content

According to the results of analysis of variance, the single effects of irrigation and fertilizer, dual interactions as well as triple interaction of location, irrigation and fertilizer on carotenoid content were significant (Table 4). Comparison of the mean of the triple interaction showed that the levels of carotenoids in Neishabour were higher than in Mashhad (Figure 2). Because photosynthetic pigments strongly respond to water stress and radiation, there is a difference between the two study locations in this respect. Irrigation and fertilizer treatments showed different effects on carotenoid content. The highest amount of carotenoids (1.067 mg/g) was observed for 10 tons of manure and complete irrigation in Neishabour. The lowest amount of carotenoids as 0.187 mg/g, was obtained for no irrigation treatment at the emergence stage and no fertilizer application in Mashhad (Figure 2). For most of the fertilizer treatment, carotenoids increased, the only exceptions were the application of chemical fertilizers and 10 tons of livestock manure in Neishabour and no irrigation (I_4) at the grain setting stage. When 20 tons of livestock manure and no irrigation (I_1) at the emergence stage were applied, in Mashhad, the highest increase in carotenoid content was achieved (Figure 2). Elewa et al. (2017) also reported a decrease in carotenoid content in quinoa under water stress conditions. Animal manure application increased the carotenoid content in onions (Singh and Sharma, 2018) and cabbage leaves (Qureshi et al., 2014). Increasing the content of carotenoids as auxiliary pigments due to the application of animal manure can be due to increasing the amount and activity of chlorophyll (Qureshi et al., 2014). Carotenoids can transfer energy to chlorophyll a and increase the amplitude of wavelengths that affect photosynthesis, as well as reduce the number of ions. Carotenoids release a lot of energy from photosystems I and II in the form of heat, or harmless chemical reactions, and can maintain chloroplast membranes (Juan et al., 2005). Water stress by reducing the biosynthesis of photosynthetic pigments reduces the concentration of pigments and reduces the potential of photosynthesis and limits the initial production. Water stress, on the other hand, disrupts enzymatic systems that reduce the activity of reactive oxygen species and increases lipid peroxidation, resulting in damage to cell membranes and pigment degradation (Ruíz-Sánchez et al., 2011).

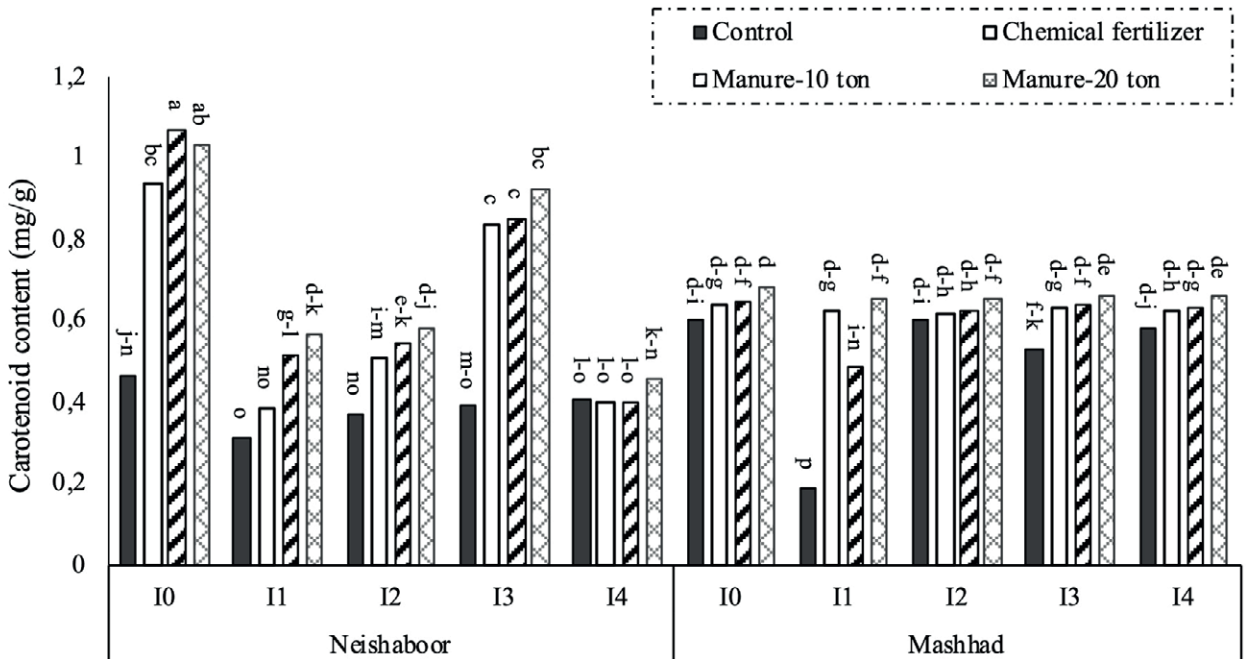

Fig. 2. Mean comparison of triple interaction of location, deficit irrigation and fertilizer on carotenoid content of quinoa crop. I_1: no irrigation at emergence stage, I_2: no irrigation at stem elongation stage, I_3: no irrigation at flowering stage, I_4: no irrigation at seed setting stage.

Electrolytic leakage of ions

The cell membrane is one of the first organs to be damaged under stress and its permeability is increased and electrolyte leakage from the cell eventually causes its death. Therefore, the stability of the membrane is assessed by evaluating the ion permeability (Sairam et al., 2002). According to the results of the analysis of variance, all single effects and dual interactions of applied treatments were significant on the rate of ion electrolyte leakage (Table 4). A comparison of the mean interaction of location and fertilizer treatment and the interaction of location and deficit irrigation is presented in (Tables 6 and 7). In general, the percentage of ion leakage in Mashhad was higher than Neishabour and no irrigation at the flowering and seeding stages showed the highest percentage of ion leakage (Table 7).

Due to the sensitivity of the flowering stage and seed setting to water stress, increasing ion electrolyte leakage at these stages also confirms the sensitivity of these stages to deficit irrigation. However, in no irrigation at the stem elongation stage, no increase in ion electrolyte leakage was observed. The response to fertilizer treatments was not similar in the two locations. Application of fertilizer treatments increased the percentage of electrolyte leakage of ions (Table 6), but the rate of increase was not the same in two locations and at deficit irrigation levels (Table 7). Application of fertilizer treatments at all levels of irrigation increased the electrolyte leakage of ions. The highest increase in ion leakage (118.7%) was obtained in the treatment of 20 tons of manure and complete irrigation and the lowest increase (10.06%) was observed in the treatment of chemical fertilizer and no irrigation at the stem elongation stage (Figure 3). Application of manure increased the relative water content of leaves thus internal cell turgescence required for cell growth. Such a situation decreases the cell membrane stability to enable the cell growth conditions. As cell growth is conditioned to maximum turgor pressure, loosening of the cell wall, and sedimentation of at cell wall so it seems that by increasing the application of manure and soil physical and chemical improvement including water holding capacity, plants less face the drought and reduce investment to increase the membrane stability (Saneoka et al., 2004).

Percentage of grain protein

Analysis of variance showed that the single effects of location, deficit irrigation and fertilizer as well as the dual interaction of location and deficit irrigation on the percentage of quinoa seed protein were significant (Table 4). Comparison of the average effect of single fertilizer treatment showed that the use of chemical fertilizers, 10 tons and 20 tons of animal manure, increased the

Table 7. Mean comparison of interaction of location and fertilizer (chemical and organic) on quinoa traits.

Location	Fertilizer treatment	Relative leaf water content (%)	Chlorophyll content (mg/g)	Electrolyte leakage (%)
Neishabour	Control	78.55 ^{b*}	2.25 ^{d}	18.98 ^{e}
	Chemical fertilizer	81.46 ^{ab}	3.36 ^{bc}	24.96 ^{d}
	Manure 10 t/ha	82.66 ^{a}	3.48 ^{bc}	26.52 ^{cd}
	Manure 20 t/ha	80.22 ^{ab}	3.59 ^{ab}	28.11 ^{c}
Mashhad	Control	59.20 ^{d}	1.78 ^{e}	28.24 ^{c}
	Chemical fertilizer	60.39 ^{d}	3.26 ^{c}	40.72 ^{b}
	Manure 10 t/ha	65.93 ^{c}	3.33 ^{bc}	40.72 ^{b}
	Manure 20 t/ha	66.22 ^{c}	3.81 ^{a}	45.30 ^{a}

* Means with same letter(s) for each component indicates no significant difference based on Duncan test at 5% probability level.

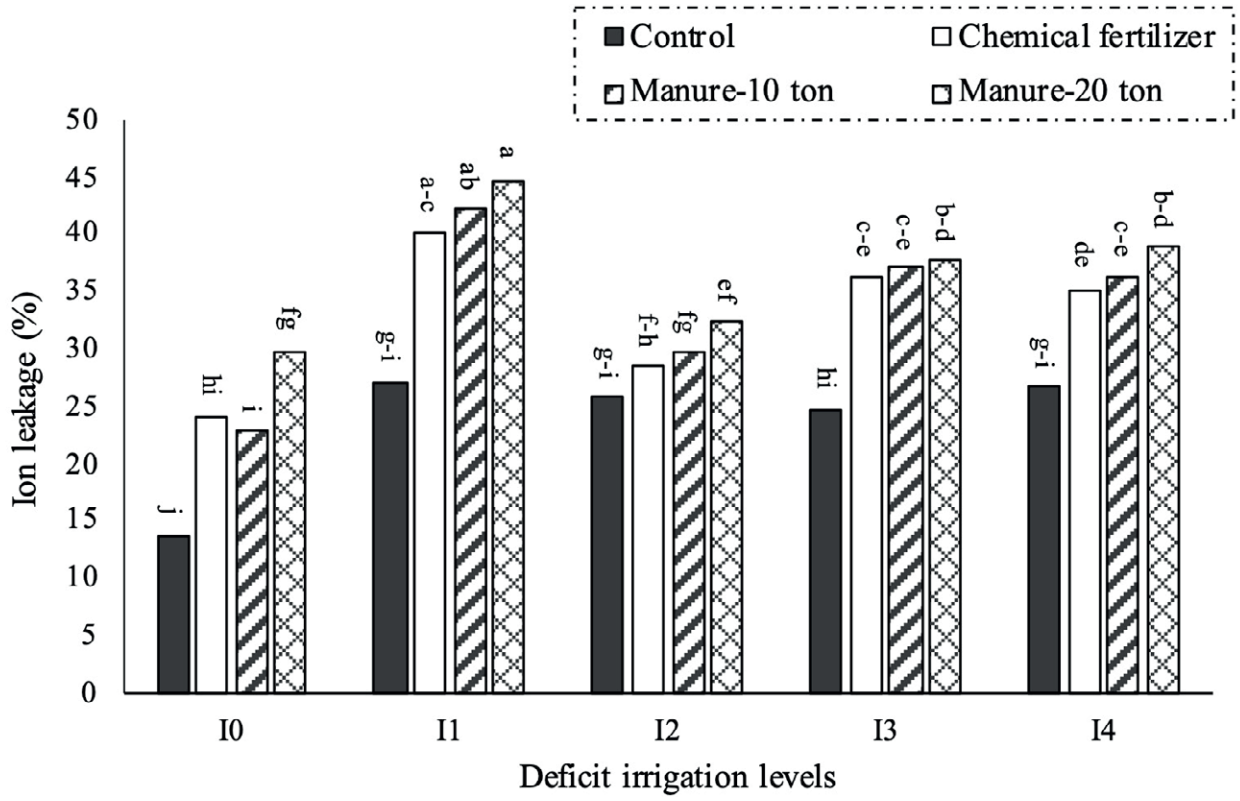

Fig. 3. Mean comparison of interaction of deficit irrigation and fertilizer on ion leakage of quinoa crop. I_1: no irrigation at emergence stage, I_2: no irrigation at stem elongation stage, I_3: no irrigation at flowering stage, I_4: no irrigation at seed setting stage. (This analysis comprises both locations together).

grain protein compared to the control (18.12%) by 1.43%, 1.66% and 2.37% (Table 5). Quinoa seed protein content has been reported to be between 8% and 22% (Jancurová et al., 2009). Studies have indicated that the application of nitrogen fertilizer not only increases the growth and yield of quinoa, but also increases grain quality (Geren, 2015). Thanapornpoonpong (2004) reported the positive effect of nitrogen fertilizer on grain yield, grain protein content and amino acid profile of quinoa. Kakabouki et al. (2014) showed that manure and nitrogen fertilizer treatments had higher values of crude protein content compared to the control treatment. Animal manure can provide the conditions for further growth and expansion of the root system by enhancing the soil structure, soil

temperature and aeration, and as a result, the expansion and distribution of the root system increases the likelihood of nitrogen uptake (Mirzakhani et al., 2009). In fact, nitrogen availability determines the grain protein content and quinoa responds strongly to nitrogen fertilizer (Iqbal and Afzal, 2014). Most of nitrogen uptake would be used to produce the amino acids, amides, enzymes including those enzymes that are involved in photosynthesis. Nitrogen fertilizer increases the amount of nitrogen entering the seed from vegetative parts compared to carbohydrates, thus increases the concentration of nitrogen in the grain and its protein percentage (El Gendy et al., 2015). Other studies have shown that application of nitrogen fertilizer has increased the amount of nitrogen in the soil and therefore the total nitrogen in the grain and consequently the percentage of grain protein in wheat (Limon-Ortega et al., 2008) and soybeans (Devi et al., 2013) increased.

Average percentage of grain protein in Mashhad was higher than Neishabour, but different levels of deficit irrigation showed different effects on grain protein (Table 7). As mentioned earlier, the average rainfall was lower and the average temperature was higher in Mashhad than Neishabour, which indicates that the plant faced more water stress in Mashhad. In Neishabour, the highest percentage of grain protein was recorded under no irrigation treatment at seed setting stage (I_4) and in Mashhad, no irrigation (I_1) at the emergence stage showed the highest percentage of grain protein (Table 7). Protein accumulation changes in response to environmental stresses. In addition to proteins that play an active role in biosynthesis and metabolism, stored proteins and proteins that play a protective role against biotic and abiotic stresses accumulate in the grain, as well (Balla et al., 2011). For example, according to (Esmaeilian et al., 2012), water stress at the flowering stage of sunflower increased the percentage of grain protein. Some studies have also reported an increase in wheat grain protein under late-season heat stress (Labuschagne et al., 2009).

Percentage of seed oil

Analysis of variance showed that the single effects of location and deficit irrigation as well as the dual interaction effects of location and deficit irrigation interaction between location and fertilizer showed a significant effect on the percentage of quinoa seed oil (Table 4). Application of deficit irrigation reduced the percentage of seed oil, although no similar responses were observed at different levels of deficit irrigation in two locations (Table 7). No irrigation at the seedling stage in Neishabour showed the highest decrease in the percentage of seed oil, while no irrigation treatment at the stem elongation stage (I2) showed an increase in the percentage of seed oil compared to the control (full irrigation) (Table 7). The highest percentage of seed oil (5.91%) under deficit irrigation treatment at the stem elongation stage (I_2) was obtained in Mashhad and the lowest percentage of seed oil (4.18%) was obtained in Neishabour under no irrigation treatment at the seed setting stage (I_4) (Table 7). The comparison of the mean interaction of low irrigation and fertilizer treatment showed that in general, deficit irrigation treatments reduced the percentage of seed oil compared to full irrigation treatment (Figure 4). Studies have shown that quinoa seed oil is between 2% to 10% and is similar to soybean oil in terms of fatty acid composition (Jancurová et al., 2009; Altuna et al., 2018). Elewa et al. (2017) also reported a decrease in the percentage of quinoa seed oil under water stress conditions.

Application of fertilizer treatments only in full and no irrigation treatments at stem elongation stage increased the percentage of seed oil, but in other levels of deficit irrigation such a positive response was not observed and even a decrease in oil percentage was recorded due to fertilizer application (Figure 4). In this study, there was an inverse relationship between the percentage of seed oil and the percentage of seed protein. Other studies also found that with increasing nitrogen, grain yield increased but grain oil content decreased. Because with increasing nitrogen, nitrogenous substances increase and the materials available for fatty acid synthesis decrease and thus the percentage of oil decreases (Khan et al., 2002). Nitrogen fertilizers also delay the maturation of the plant and lead to longer seed development, as a result of which the seed does not reach full maturity and the oil content decreases.

Seed yield

Water stress and fertilizer and their dual interactions as well as triple interaction of location, water stress and fertilizer on seed yield were significant (Table 4). The response of quinoa seed yield to deficit irrigation and different levels of fertilizer applied at the two study locations was not similar. Comparison of the mean simple effect of low irrigation levels showed that grain yield had the greatest decrease only in treatment I1 (cessation of irrigation in the emergence stage). At other levels, no significant difference was observed between treatments in terms of response to irrigation deficiency (Table 5). Also, the comparison of the mean of the simple effect of fertilizer treatments showed that the treatment of 20 tons of manure per hectare had the highest grain yield

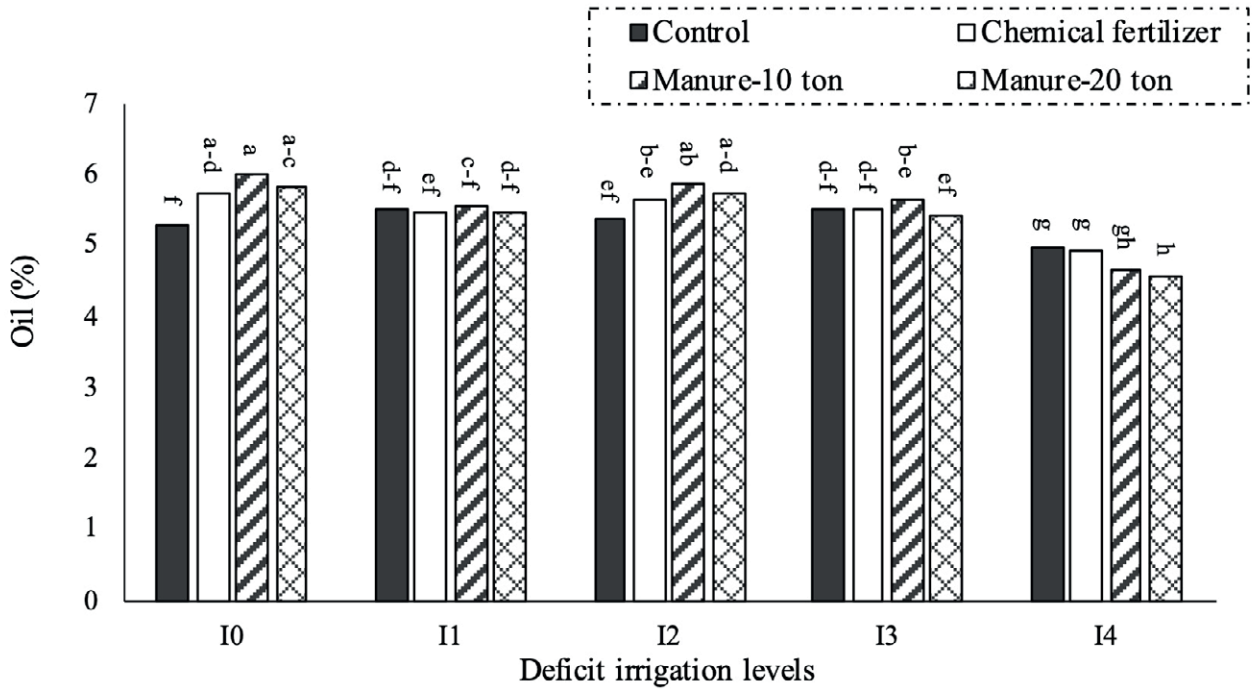

Fig. 4. Mean comparison of interaction of deficit irrigation and fertilizer on oil percentage of quinoa crop. I_1: no irrigation at emergence stage, I_2: no irrigation at stem elongation stage, I_3: no irrigation at flowering stage, I_4: no irrigation at seed setting stage. (This analysis comprises both locations together).

and the control treatment had the lowest grain yield (Table 5). The mean of the triple interaction indicated that the lowest seed yield was achieved for the no irrigation treatment at the emergence stage (I_1) in Neishabour and the highest seed yield was observed for the full irrigation treatment using 20 tons of manure in Mashhad (Figure 5). Deficit irrigation treatments reduced seed yield, but the rate of reduction was not the same at all levels. The highest decrease in seed yield (71.7%) compared to full irrigation was observed in no irrigation treatment at the emergence stage in Neishabour (Figure 5). Studies have shown that high photosynthesis and a specific quinoa leaf area in the early stages of growth allow water to be absorbed by the larger root system and help the plant to avoid water stress at later growth stages (Geerts et al., 2008). Therefore, no irrigation at the emergence stage was not able to prevent the reduction of seed yield and resulted in the lowest yield compare to other levels of deficit irrigation. According to (Hirich et al., 2014), the yield potential of quinoa varies under optimal conditions and depends on climate, soil, planting date and cultivar. In this study, performance fluctuations in the two test sites and between the applied treatments were relatively high (Figure 5). One of the reasons for quinoa response can be the difference in soil salinity in the two places tested. In agricultural systems of arid and semi-arid regions, water and salinity stress are among the main abiotic stresses that affect potential yield and cause yield instability in quinoa (Fuentes and Bhargava, 2011; Razzaghi et al., 2012). Geerts et al. (2008) reported the maximum yield of quinoa in full irrigation conditions of 2.04 t/ha and in low irrigation conditions of 2.01 t/ha, while in dryland conditions quinoa seed yield decreased to 1.68 t/ha. Razzaghi (2011) also reported quinoa seed yield under optimal conditions of 2.3 tons per hectare. Lack of irrigation and water stress reduced quinoa seed yield shoot dry weight and harvest index (Razzaghi et al., 2012; González et al., 2009; Hirich et al., 2014). During seed filling, water deficiency reduces seed yield per unit area by reducing photosynthesis. Water stress in the seed filling stage, especially if accompanied by an increase in temperature, accelerates leaf aging, reduces the seed filling period, average seed weight and yield. This is done by reducing the transfer of photosynthetic material to the developing seeds (Saeidi et al., 2017).

Fertilizer treatments also had different responses. Under no irrigation treatment at the emergence stage in Neishabour, the use of chemical and livestock fertilizers reduced seed yield compared to no fertilizer application.

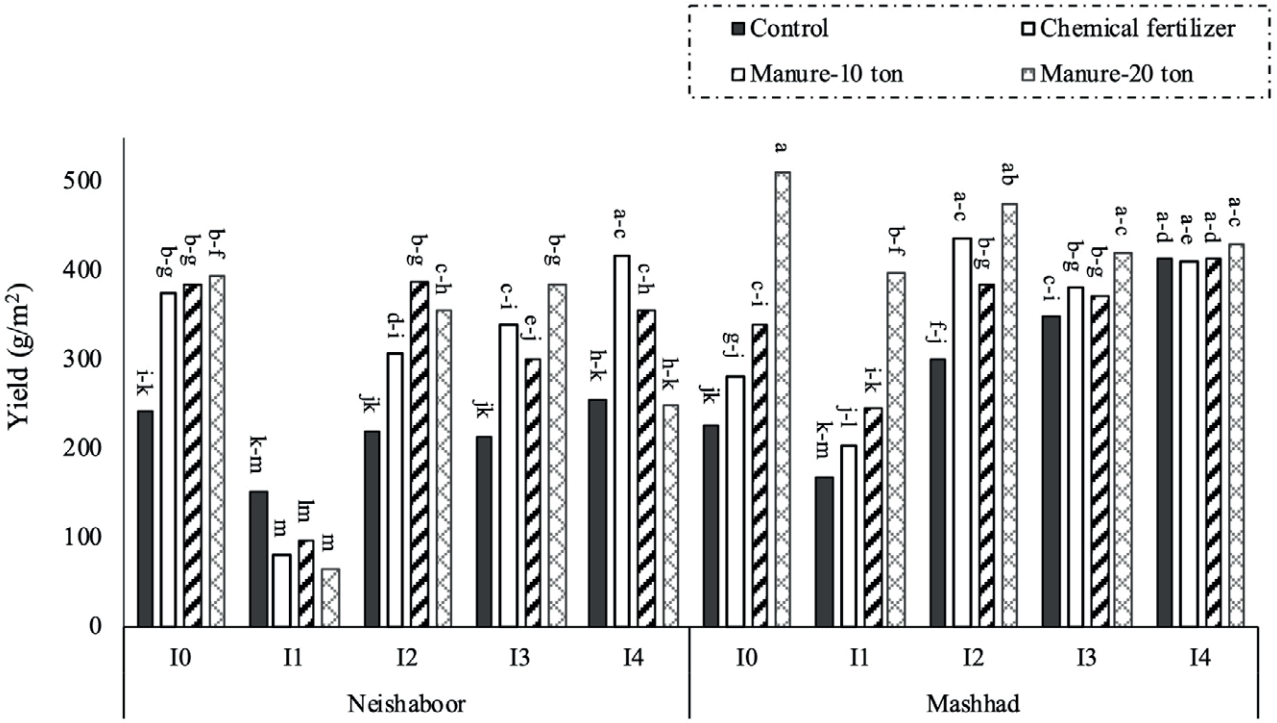

Fig. 5. Mean comparison of triple interaction of location, deficit irrigation and fertilizer on seed yield of quinoa crop. I_1: no irrigation at emergence stage, I_2: no irrigation at stem elongation stage, I_3: no irrigation at flowering stage, I_4: no irrigation at seed setting stage.

It may be the effect of too high salinity at the beginning due to reduced leaching at that site. In Mashhad, under no irrigation at the seed setting stage, the application of fertilizer treatments had no significant effect on seed yield. However, in other deficit irrigation treatments in both locations, the use of chemical and livestock fertilizers increased seed yield (Figure 5). Because the use of animal manure can increase the amount of available nitrogen and because nitrogen is an important component of the chlorophyll molecule, the more it is supplied, the larger the leaves and higher the level of carbonation so increasing the production of hydrocarbons leads to higher yields. Kaul et al. (2005) reported that quinoa strongly reacts to nitrogen fertilizer application. Nitrogen fertilizer increases vegetative growth, plant metabolism and dry matter accumulation (Gomaa, 2013). Shams (2012) pointed to the role of nitrogen in stimulating the metabolic activity of plants and reported that nitrogen increases the amount of metabolites that play an essential role in yield and yield components (Shams, 2012). Shams (2012) also reported an increase in grain yield and biological yield of quinoa using nitrogen fertilizer. The study of the effect of organic matter on soil water holding capacity, especially in arid and semi-arid conditions, on several crops showed that the addition of organic fertilizers increases field capacity, soil water content and soil hydraulic conductivity (Wesseling et al., 2009; Hirich et al., 2014). Adding organic fertilizer to the soil also has a positive effect on growth, and yield (Gopinath et al., 2008; Ibrahim et al., 2008). Manure in the soil after mineralization of organic matter, improves the soil in terms of nutrients and increase the availability of nutrients as a result, nutrient uptake, plant growth and production would be improved (Hartley et al., 2010).

CONCLUSION

The quantitative and qualitative yield potential of quinoa seeds was affected by irrigation, fertilizer source and climatic conditions of study location. In this study, although the average rainfall was lower in Mashhad, overall, the yield of quinoa in Mashhad was higher than Neishabour. This may be the inherent potential of quinoa to tolerate water stress. This feature makes it possible to adopt a deficit irrigation strategy to save water. Application of deficit irrigation at different crop growth stages induced water stress to the crop and negatively impacted the seed quality and physiological traits of quinoa including chlorophyll, carotenoids, ion electrolyte leakage and

relative leaf water content. However, water stress induced by no irrigation at the stem elongation stage was less effective than other levels of deficit irrigation. Because it seems that at this stage the plant has a higher tolerance to water stress. Also, the application of manure compared to chemical fertilizers, increased the water holding capacity in the soil and provided more water to the plant due to the modification of soil organic matter. As a result, seed yield and quality traits did not show a sharp decrease with deficit irrigation. Finally, it can be said that the combination of deficit irrigation, because it seems treatment at the stem elongation stage along with the treatment of 10 tons of manure in both locations, in addition to saving water, showed high performance.

REFERENCES

Adebayo, M. A., Menkir, A., Blay, E., Gracen, V., Danquah, E., & Hearne, S. (2014). Genetic analysis of drought tolerance in adapted× exotic crosses of maize inbred lines under managed stress conditions. *Euphytica*, *196*(2), 261-270. https://doi.org/10.1007/s10681-013-1029-5.

Ahmadi, A., Emam, Y., & Pessarakli, M. (2010). Biochemical changes in maize seedlings exposed to drought stress conditions at different nitrogen levels. *Journal of Plant Nutrition*, *33*(4), 541-556. https://doi.org/10.1080/01904160903506274.

Altuna, J. L., Silva, M., Alvarez, M., Quinteros, M. F., Morales, D., & Carrillo, W. (2018). Ecuadorian quinoa (Chenopodium quinoa Willd) fatty acids profile. *Asian J Pharm Clin Res*, *11*, 209-211. 10.22159/ajpcr.2018.v11i11.24889

Anjum, S. A., Xie, X., Farooq, M., Wang, L., Xue, L. I., Shahbaz, M., & Salhab, J. (2011). Effect of exogenous methyl jasmonate on growth, gas exchange and chlorophyll contents of soybean subjected to drought. *African Journal of Biotechnology*, *10*(47), 9647-9656. https://doi.org/10.5897/AJB10.2641.

Balla, K., Rakszegi, M., Li, Z., Bekes, F., Bencze, S., & Veisz, O. (2011). Quality of winter wheat in relation to heat and drought shock after anthesis. *Czech Journal of Food Sciences*, *29*(2), 117-128. https://doi.org/10.17221/227/2010-CJFS.

Bänziger, M., Edmeades, G. O., Beck, D., & Bellon, M. (2000). *Breeding for drought and nitrogen stress tolerance in maize: from theory to practice. (CIMMYT, Mexico DF, Mexico)*. ISBN 970-648-46-3. https://repository.cimmyt.org/handle/10883/765.

Bascuñán-Godoy, L., Reguera, M., Abdel-Tawab, Y. M., & Blumwald, E. (2016). Water deficit stress-induced changes in carbon and nitrogen partitioning in Chenopodium quinoa Willd. *Planta*, *243*(3), 591-603. https://doi.org/10.1007/s00425-015-2424-z.

Carrillo, W., Carpio, C., Morales, D., Vilcacundo, E., & Alvarez, M. (2017). Fatty acids composition in macadamia seed oil (Macadamia integrifolia) from Ecuador. *Asian Journal of Pharmaceutical and Clinical Research*, *10*, 303-306. http://orcid.org/0000-0002-7609-2939.

Dadkhah, A. (2014). Effect of some plant growth promoting rhizobacteria and chemical fertilizer on growth parameters, yield and essential oil of fennel (Foeniculum vulgare Mill). Zeitschrift für Arznei-& Gewürzpflanzen, 19(3), 118-122.
http://www.zag-info.com/journalarchive.php?subid=3866

Dawood, M. G. (2018). Improving drought tolerance of quinoa plant by foliar treatment of trehalose. *Agricultural Engineering International: CIGR Journal*, *19*(5), 245-254. https://doi.org/10.33472/AFJBS.2.1.2020.39-46.

Devi, K. N., Singh, T. B., Athokpam, H. S., Singh, N. B., & Shamurailatpam, D. (2013). Influence of inorganic, biological and organic manures on nodulation and yield of soybean ('Glycine max Merril'L.) and soil properties. *Australian journal of crop science*, *7*(9), 1407. http://www.cropj.com/nadini_7_9_2013_1407_1415.pdf.

El Gendy, A. G., El Gohary, A. E., Omer, E. A., Hendawy, S. F., Hussein, M. S., Petrova, V., & Stancheva, I. (2015). Effect of nitrogen and potassium fertilizer on herbage and oil yield of chervil plant (Anthriscus cerefolium L.). *Industrial Crops and Products*, *69*, 167-174. https://doi.org/10.1016/j.indcrop.2015.02.023.

El Youssfi, L., Choukr-Allah, R., Zaafrani, M., Mediouni, T., & Hirich, A. (2012). Effect of domestic treated wastewater use on three varieties of Quinoa (Chenopodium quinoa) under semi arid conditions. *International Journal of Environmental and Ecological Engineering*, *6*(8), 562-565. https://doi.org/10.5281/zenodo.1071758.

Esmaeilian, Y., Sirousmehr, A., Asgripour, M., & Amiri, E. (2012). Comparison of sole and combined nutrient application on yield and biochemical composition of sunflower under water stress. Intern J App, 2, 214-220. https://www.academia.edu/RegisterToDownload?ssrv=ss#BulkDownload.

FAOSTAT, (2020). http://www.fao.org/faostat/en/#compare.

Farooq, M., Wahid, A., Kobayashi, N., Fujita, D. B. S. M. A., & Basra, S. M. A. (2009). Plant drought stress: effects, mechanisms and management. In *Sustainable*

agriculture (pp. 153-188). Springer, Dordrecht. https://doi.org/10.1007/978-90-481-2666-8_12.

Flint, H. L., Boyce, B. R., & Beattie, D. J. (1967). Index of injury—a useful expression of freezing injury to plant tissues as determined by the electrolytic method. *Canadian Journal of Plant Science*, *47*(2), 229-230. https://doi.org/10.4141/cjps67-043.

Fu, J., Fry, J., & Huang, B. (2004). Minimum water requirements of four turfgrasses in the transition zone. *HortScience*, *39*(7), 1740-1744. https://doi.org/10.21273/HORTSCI.39.7.1740.

Fu, J., Fry, J., & Huang, B. (2004). Minimum water requirements of four turfgrasses in the transition zone. *HortScience*, *39*(7), 1740-1744. https://doi.org/10.21273/HORTSCI.39.7.1740.

Gámez, A. L., Soba, D., Zamarreño, Á. M., García-Mina, J. M., Aranjuelo, I., & Morales, F. (2019). Effect of water stress during grain filling on yield, quality and physiological traits of Illpa and Rainbow quinoa (Chenopodium quinoa Willd.) cultivars. *Plants*, *8*(6), 173. https://doi.org/10.3390/plants8060173

Garcia, M., Condori, B., & Castillo, C. D. (2015). Agro-ecological and agronomic cultural practices of quinoa in South America. *Quinoa: Improvement and Sustainable Production*, 25-46. https://doi.org/10.1002/9781118628041.ch3.

Gardner, F. P., Pearce, R. B., & Mitchell, R. L. (2017). *Physiology of crop plants* (No. Ed. 2). Scientific Publishers. http://www.scientificpub.com/book-details/Physiology-of-Crop-Plants-108.html.

Geerts, S., Raes, D., Garcia, M., Vacher, J., Mamani, R., Mendoza, J., ... & Taboada, C. (2008). Introducing deficit irrigation to stabilize yields of quinoa (Chenopodium quinoa Willd.). *European journal of agronomy*, *28*(3), 427-436. https://doi.org/10.1016/j.eja.2007.11.008.

Geren, H. (2015). Effects of different nitrogen levels on the grain yield and some yield components of quinoa (Chenopodium quinoa Willd.) under Mediterranean climatic conditions. *Turkish Journal of Field Crops*, *20*(1), 59-64. https://doi.org/10.17557/.39586.

Gomaa, E. F. (2013). Effect of nitrogen, phosphorus and biofertilizers on quinoa plant. *Journal of applied sciences research*, *9*(8), 5210-5222. https://doi.org/10.17557/.39586.

González, J. A., Gallardo, M., Hilal, M. B., Rosa, M. D., & Prado, F. E. (2009). Physiological responses of quinoa (Chenopodium quinoa) to drought and waterlogging stresses: dry matter partitioning. https://doi.org/10.1007/s42106-020-00094-5.

Gopinath, K. A., Saha, S., Mina, B. L., Pande, H., Kundu, S., & Gupta, H. S. (2008). Influence of organic amendments on growth, yield and quality of wheat and on soil properties during transition to organic production. *Nutrient Cycling in Agroecosystems*, *82*(1), 51-60. https://doi.org/10.1007/s10705-008-9168-0.

Hariadi, Y., Marandon, K., Tian, Y., Jacobsen, S. E., & Shabala, S. (2011). Ionic and osmotic relations in quinoa (Chenopodium quinoa Willd.) plants grown at various salinity levels. *Journal of experimental botany*, *62*(1), 185-193. https://doi.org/10.1093/jxb/erq257.

Hartley, I. P., Hopkins, D. W., Sommerkorn, M., & Wookey, P. A. (2010). The response of organic matter mineralisation to nutrient and substrate additions in sub-arctic soils. *Soil Biology and Biochemistry*, *42*(1), 92-100. https://doi.org/10.1016/j.soilbio.2009.10.004.

Helvich, K. (1990). *Official methods of analysis* (No. 630.24 A88 1990). Association of Official Analytical Chemists. https://doi.org/10.1007/BF02670789.

Heuberger, H., & Pfeiffer, T. (2013). Herbs cultivation in the land of milk and honey, as long as there is water-a travel report. Zeitschrift für Arznei-& Gewürzpflanzen, 18(4), 181-184. http://www.zag-info.com/journalarchive.php?subid=3758

Hirich, A., & Choukr-Allah, R. (2014). Faba bean (Vicia faba L.) production under deficit irrigation with treated wastewater applied during vegetative stage. *Desalination and Water Treatment*, *52*(10-12), 2214-2219. https://doi.org/10.1080/19443994.2013.804452.

Hirich, A., Allah, R. C., Jacobsen, S. E., El Youssfi, L., & El Homaria, H. (2012). Using deficit irrigation with treated wastewater in the production of quinoa (Chenopodium quinoa Willd.) in Morocco. *Revista Científica UDO Agrícola*, *12*(3), 570-583. https://doi.org/10.1002/ird.2116.

Hirich, A., Choukr-Allah, R., & Jacobsen, S. E. (2014). Deficit irrigation and organic compost improve growth and yield of quinoa and pea. *Journal of Agronomy and Crop Science*, *200*(5), 390-398. https://doi.org/10.1111/jac.12073.

Hirich, A., Choukr-Allah, R., & Jacobsen, S. E. (2014). The combined effect of deficit irrigation by treated wastewater and organic amendment on quinoa (Chenopodium quinoa Willd.) productivity. *Desalination and Water Treatment*, *52*(10-12), 2208-2213. https://doi.org/10.1080/19443994.2013.777944.

Hoekstra, F. A., Golovina, E. A., & Buitink, J. (2001). Mechanisms of plant desiccation tolerance. *Trends in plant science*, *6*(9), 431-438. https://doi.org/10.1016/S1360-1385(01)02052-0. http://www.zag-info.com/journalarchive.php?subid=3866

Ibrahim, M., Hassan, A., Iqbal, M., & Valeem, E. E. (2008). Response of wheat growth and yield to vari-

ous levels of compost and organic manure. *Pak. J. Bot*, *40*(5), 2135-2141. https://doi.org/10.21271/zjpas.v28i5.453.

Iqbal, S. M. B. S., & Afzal, I. (2014). Evaluating the response of nitrogen application on growth development and yield of quinoa genotypes. *International Journal of Agriculture and Biology*, *16*(5). https://doi.org/10.17557/.39586.

Irigoyen, J. J., Einerich, D. W., & Sánchez-Díaz, M. (1992). Water stress induced changes in concentrations of proline and total soluble sugars in nodulated alfalfa (Medicago sativd) plants. *Physiologia plantarum*, *84*(1), 55-60. https://doi.org/10.1111/j.1399-3054.1992.tb08764.x.

Jacobsen, S. E., Liu, F., & Jensen, C. R. (2009). Does root-sourced ABA play a role for regulation of stomata under drought in quinoa (Chenopodium quinoa Willd.). *Scientia Horticulturae*, *122*(2), 281-287. https://doi.org/10.1016/j.scienta.2009.05.019.

Jacobsen, S. E., Monteros, C., Christiansen, J. L., Bravo, L. A., Corcuera, L. J., & Mujica, A. (2005). Plant responses of quinoa (Chenopodium quinoa Willd.) to frost at various phenological stages. *European Journal of Agronomy*, *22*(2), 131-139. https://doi.org/10.1016/j.eja.2004.01.003.

James, L. E. A. (2009). Quinoa (Chenopodium quinoa Willd.): composition, chemistry, nutritional, and functional properties. *Advances in food and nutrition research*, *58*, 1-31. https://doi.org/10.1016/S1043-4526(09)58001-1.

Jancurová, M., Minarovičová, L., & Dandar, A. (2009). Quinoa–a rewiev. *Czech Journal of Food Sciences*, *27*(2), 71-79. 0.15666/aeer/1704_1010510117.

Johari-Pireivatlou, M. (2010). Effect of soil water stress on yield and proline content of four wheat lines. *African Journal of Biotechnology*, *9*(1). https://doi.org/10.5897/AJB09.521.

Juan, M., Rivero, R. M., Romero, L., & Ruiz, J. M. (2005). Evaluation of some nutritional and biochemical indicators in selecting salt-resistant tomato cultivars. *Environmental and Experimental Botany*, *54*(3), 193-201. https://doi.org/10.1016/j.envexpbot.2004.07.004.

Kakabouki, I., Bilalis, D., Karkanis, A., Zervas, G., & Hela, D. (2014). Effects of fertilization and tillage system on growth and crude protein content of quinoa (Chenopodium quinoa Willd.): An alternative forage crop. *Emirates Journal of Food and Agriculture*, 18-24. 10.9755/ejfa.v26i1.16831.

Kaul, H. P., Kruse, M., & Aufhammer, W. (2005). Yield and nitrogen utilization efficiency of the pseudocereals amaranth, quinoa, and buckwheat under differing nitrogen fertilization. *European Journal of Agronomy*, *22*(1), 95-100. https://doi.org/10.1016/j.eja.2003.11.002.

Khan, N., Jan, A., Khan, I. A., & Khan, N. (2002). Response of canola to nitrogen and sulphur nutrition. *Asian Journal of Plant Sciences*. http://dx.doi.org/10.3923/ajps.2002.516.518.

Labuschagne, M. T., Elago, O., & Koen, E. (2009). The influence of temperature extremes on some quality and starch characteristics in bread, biscuit and durum wheat. *Journal of Cereal Science*, *49*(2), 184-189. https://doi.org/10.1016/j.jcs.2008.09.001.

Limon-Ortega, A., Govaerts, B., & Sayre, K. D. (2008). Straw management, crop rotation, and nitrogen source effect on wheat grain yield and nitrogen use efficiency. *European Journal of Agronomy*, *29*(1), 21-28. https://doi.org/10.1016/j.eja.2008.01.008.

Ma, Q. Q., Wang, W., Li, Y. H., Li, D. Q., & Zou, Q. (2006). Alleviation of photoinhibition in drought-stressed wheat (Triticum aestivum) by foliar-applied glycinebetaine. *Journal of Plant Physiology*, *163*(2), 165-175. https://doi.org/10.1016/j.jplph.2005.04.023.

Mahmood, S., Iram, S., & Athar, H. R. (2003). Intra-specific variability in sesame (Sesamun indicum l.) for various quantitative and qualitative attributes under differential salt regimes. *Journal of Research (Science)*, *14*(2), 177. https://inis.iaea.org/search/search.aspx?orig_q=RN:35036964.

Mirzakhani, M., Ardakani, M. R., Band, A. A., Rejali, F., & Rad, A. S. (2009). Response of spring safflower to co-inoculation with Azotobacter chroococum and Glomus intraradices under different levels of nitrogen and phosphorus. *American Journal of Agricultural and Biological Sciences*, *4*(3), 255-261. http://www.scipub.org/fulltext/AJAB/AJAB43255-261.pdf.

Muscolo, A., Panuccio, M. R., Gioffrè, A. M., & Jacobsen, S. E. (2016). Drought and salinity differently affect growth and secondary metabolites of "Chenopodium quinoa Willd" seedlings. In *Halophytes for Food Security in Dry Lands* (pp. 259-275). Academic Press. https://doi.org/10.1016/B978-0-12-801854-5.00016-9.

Nowak, V., Du, J., & Charrondière, U. R. (2016). Assessment of the nutritional composition of quinoa (Chenopodium quinoa Willd.). *Food chemistry*, *193*, 47-54. https://doi.org/10.1016/j.foodchem.2015.02.111.

Pandey, H. C., Baig, M. J., & Bhatt, R. K. (2012). Effect of moisture stress on chlorophyll accumulation and nitrate reductase activity at vegetative and flowering stage in Avena species. http://krishi.icar.gov.in/jspui/handle/123456789/20845

Porra, R. J. (2002). The chequered history of the development and use of simultaneous equations for the

accurate determination of chlorophylls a and b. *Photosynthesis research*, *73*(1-3), 149-156. https://doi.org/10.1023/A:1020470224740.

Qureshi, F., Wani, J. A., Bashir, U., Malik, M. A., & Mir, S. A. (2014). Response of farmyard manure and inorganic nitrogen on vegetative growth, leaf yield and quality of kale (Brassica oleracea var acephala) in temperate region of Kashmir valley. *Biolife*, *2*(3), 786-791. https://doi.org/10.5897/AJPS2018.1639.

Razzaghi, F., Ahmadi, S. H., Adolf, V. I., Jensen, C. R., Jacobsen, S. E., & Andersen, M. N. (2011). Water relations and transpiration of quinoa (Chenopodium quinoa Willd.) under salinity and soil drying. *Journal of agronomy and crop science*, *197*(5), 348-360. https://doi.org/10.1111/j.1439-037X.2011.00473.x.

Razzaghi, F., Ahmadi, S. H., Jacobsen, S. E., Jensen, C. R., & Andersen, M. N. (2012). Effects of salinity and soil–drying on radiation use efficiency, water productivity and yield of quinoa (Chenopodium quinoa Willd.). *Journal of Agronomy and Crop Science*, *198*(3), 173-184. https://doi.org/10.1111/j.1439-037X.2011.00496.x.

Ruiz-Carrasco, K., Antognoni, F., Coulibaly, A. K., Lizardi, S., Covarrubias, A., Martínez, E. A. & Zurita-Silva, A. (2011). Variation in salinity tolerance of four lowland genotypes of quinoa (Chenopodium quinoa Willd.) as assessed by growth, physiological traits, and sodium transporter gene expression. *Plant Physiology and Biochemistry*, *49*(11), 1333-1341. https://doi.org/10.1016/j.plaphy.2011.08.005.

Ruíz-Sánchez, M., Armada, E., Muñoz, Y., de Salamone, I. E. G., Aroca, R., Ruíz-Lozano, J. M., & Azcón, R. (2011). Azospirillum and arbuscular mycorrhizal colonization enhance rice growth and physiological traits under well-watered and drought conditions. *Journal of plant physiology*, *168*(10), 1031-1037. https://doi.org/10.1016/j.jplph.2010.12.019.

Sadak, M. S. (2016). Mitigation of drought stress on fenugreek plant by foliar application of trehalose. *Int J Chemtech Res,* 9(2), 147-155. doi: 10.1111/j.1600-079X.2010.00817.x

Saeidi, M., Moradi, F., & Abdoli, M. (2017). Impact of drought stress on yield, photosynthesis rate, and sugar alcohols contents in wheat after anthesis in semiarid region of Iran. *Arid Land Research and Management*, *31*(2), 204-218. https://doi.org/10.1080/15324982.2016.1260073

Saneoka, H., Moghaieb, R. E., Premachandra, G. S., & Fujita, K. (2004). Nitrogen nutrition and water stress effects on cell membrane stability and leaf water relations in Agrostis palustris Huds. *Environmental and Experimental Botany*, *52*(2), 131-138. https://doi.org/10.1016/j.envexpbot.2004.01.011.

Sairam, R. K., Rao, K. V., & Srivastava, G. C. (2002). Differential response of wheat genotypes to long term salinity stress in relation to oxidative stress, antioxidant activity and osmolyte concentration. *Plant science*, *163*(5), 1037-1046. https://doi.org/10.1016/S0168-9452(02)00278-9.

Schmidhalter, U., Bredemeier, C., Geesing, D., Mistele, B., Selige, T., & Jungert, S. (2006). Precision agriculture: Spatial and temporal variability of soil water nitrogen and plant crop response. *Bibliotheca Fragmenta Agronomica*, *11*(3), 97-106. http://dx.doi.org/10.1016/j.fcr.2007.11.002.

Shams, A. S. (2012, September). Response of quinoa to nitrogen fertilizer rates under sandy soil conditions. In *Proc. 13th International Conf. Agron., Fac. of Agric., Benha Univ., Egypt* (pp. 9-10). http://dx.doi.org/10.3923/ajpp.2017.20.27.

Sheteawi, S. A., & Tawfik, K. M. (2007). Interaction effect of some biofertilizers and irrigation water regime on mung bean (Vigna radiata) growth and yield. *J. Appl. Sci. Res*, *3*(3), 251-262. 10.5897/AJMR11.689.

Singh, S., & Sharma, R. (2018). Efficacy of farmyard manure for growth and yield of onion (Allium cepa L.) cv. N-53. *Journal of Pharmacognosy and Phytochemistry*, *7*(4), 2771-2775. https://dx.doi.org/10.22161/ijhaf.4.3.1.

Sosa-Zuniga, V., Brito, V., Fuentes, F., & Steinfort, U. (2017). Phenological growth stages of quinoa (Chenopodium quinoa) based on the BBCH scale. *Annals of Applied Biology*, *171*(1), 117-124. https://doi.org/10.1111/aab.12358.

Stikic, R., Glamoclija, D., Demin, M., Vucelic-Radovic, B., Jovanovic, Z., Milojkovic-Opsenica, D.& Milovanovic, M. (2012). Agronomical and nutritional evaluation of quinoa seeds (Chenopodium quinoa Willd.) as an ingredient in bread formulations. *Journal of cereal science*, *55*(2), 132-138. https://doi.org/10.1016/j.jcs.2011.10.010.

Thanapornpoonpong, S. N. (2004). *Effect of nitrogen fertilizer on nitrogen assimilation and seed quality of amaranth (Amaranthus spp.) and quinoa (Chenopodium quinoa Willd)*. Niedersächsische Staats-und Universitätsbibliothek. http://hdl.handle.net/11858/00-1735-0000-0006-AB4D-1.

Turner, N. C. (2018). Turgor maintenance by osmotic adjustment: 40 years of progress. *Journal of experimental botany*, *69*(13), 3223-3233. https://doi.org/10.1093/jxb/ery181.

Vega-Gálvez, A., Miranda, M., Vergara, J., Uribe, E., Puente, L., & Martínez, E. A. (2010). Nutrition facts and functional potential of quinoa (Chenopodium quinoa willd.), an ancient Andean grain:

a review. *Journal of the Science of Food and Agriculture*, *90*(15), 2541-2547. https://doi.org/10.1002/jsfa.4158.

Wang, X., Vignjevic, M., Jiang, D., Jacobsen, S., & Wollenweber, B. (2014). Improved tolerance to drought stress after anthesis due to priming before anthesis in wheat (Triticum aestivum L.) var. Vinjett. *Journal of experimental botany*, *65*(22), 6441-6456. https://doi.org/10.1093/jxb/eru362.

Wesseling, J. G., Stoof, C. R., Ritsema, C. J., Oostindie, K., & Dekker, L. W. (2009). The effect of soil texture and organic amendment on the hydrological behaviour of coarse-textured soils. *Soil use and management*, *25*(3), 274-283. https://doi.org/10.1111/j.1475-2743.2009.00224.x.

Zulkarami, B., Husni, O. M., Halimi, M. S., Mondal, M. M. A., Razi, I. M., & Kausar, H. (2016). Foliar application of polyamines to manage water stress for improved grain filling formation and yield in rice plants. In *Plant, Soil and Microbes* (pp. 353-366). https://doi.org/10.1007/978-3-319-27455-3_17.

Finito di stampare da
Logo s.r.l. – Borgoricco (PD) – Italia

RIGOROUS PEER REVIEW
Each submission to IJAm is subject to a rigorous quality control and peer-review evaluation process before receiving a decision. The initial in-house quality control check deals with issues such as competing interests; ethical requirements for studies involving human participants or animals; financial disclosures; full compliance with IJAm's data availability policy, etc.
Submissions may be returned to authors for queries, and will not be seen by our Editorial Board or peer reviewers until they pass this quality control check.
Each paper is subjected to critical evaluation and review by Field Editors with specific expertise in the different areas of interest and by the members of the international Editorial Board.

OPEN ACCESS POLICY
The Italian Journal of Agrometeorology provides immediate open access to its content. Our publisher, Firenze University Press at the University of Florence, complies with the Budapest Open Access Initiative definition of Open Access: By "open access", we mean the free availability on the public internet, the permission for all users to read, download, copy, distribute, print, search, or link to the full text of the articles, crawl them for indexing, pass them as data to software, or use them for any other lawful purpose, without financial, legal, or technical barriers other than those inseparable from gaining access to the internet itself. The only constraint on reproduction and distribution, and the only role for copyright in this domain is to guarantee the original authors with control over the integrity of their work and the right to be properly acknowledged and cited. We support a greater global exchange of knowledge by making the research published in our journal open to the public and reusable under the terms of a Creative Commons Attribution 4.0 International Public License (CC-BY-4.0). Furthermore, we encourage authors to post their pre-publication manuscript in institutional repositories or on their websites prior to and during the submission process and to post the Publisher's final formatted PDF version after publication without embargo. These practices benefit authors with productive exchanges as well as earlier and greater citation of published work.

COPYRIGHT NOTICE
Authors who publish with IJAm agree to the following terms:
Authors retain the copyright and grant the journal right of first publication with the work simultaneously licensed under a Creative Commons Attribution 4.0 International Public License (CC-BY-4.0) that allows others to share the work with an acknowledgment of the work's authorship and initial publication in IJAm.
Authors are able to enter into separate, additional contractual arrangements for the non-exclusive distribution of the journal's published version of the work (e.g., post it to an institutional repository or publish it in a book), with an acknowledgment of its initial publication in this journal.
Authors are allowed and encouraged to post their work online (e.g., in institutional repositories or on their website) prior to and during the submission process, as it can lead to productive exchanges, as well as earlier and greater citation of published work (See The Effect of Open Access).

PUBLICATION FEES
Unlike many open-access journals, the Italian Journal of Agrometeorology does not charge any publication fee.

WAIVER INFORMATION
Fee waivers do not apply at Firenze University Press because our funding does not rely on author charges.

PUBLICATION ETHICS
Responsibilities of IJAm's editors, reviewers, and authors concerning publication ethics and publication malpractice are described in IJAm's Guidelines on Publication Ethics.

CORRECTIONS AND RETRACTIONS
In accordance with the generally accepted standards of scholarly publishing, IJAm does not alter articles after publication: "Articles that have been published should remain extant, exact and unaltered to the maximum extent possible". In cases of serious errors or (suspected) misconduct IJAm publishes corrections and retractions (expressions of concern).

Corrections
In cases of serious errors that affect or significantly impair the reader's understanding or evaluation of the article, IJAm publishes a correction note that is linked to the published article. The published article will be left unchanged.

Retractions
In accordance with the "Retraction Guidelines" by the Committee on Publication Ethics (COPE) IJAm will retract a published article if:
- there is clear evidence that the findings are unreliable, either as a result of misconduct (e.g. data fabrication) or honest error (e.g. miscalculation)
- the findings have previously been published elsewhere without proper crossreferencing, permission or justification (i.e. cases of redundant publication)
- it turns out to be an act of plagiarism
- it reports unethical research.
- An article is retracted by publishing a retraction notice that is linked to or replaces the retracted article. IJAm will make any effort to clearly identify a retracted article as such.

If an investigation is underway that might result in the retraction of an article IJAm may choose to alert readers by publishing an expression of concern.

ARCHIVING
IJAm and Firenze University Press are experimenting a National legal deposition and long-term digital preservation service.

SUBMITTING TO IJAm
Submissions to IJAm are made using FUP website. Registration and access are available at: https://riviste.fupress.net/index.php/IJAm/submission
For more information about the journal and guidance on how to submit, please see https://riviste.fupress.net/index.php/IJAm/index

Principal Contact
Simone Orlandini, University of Florence
simone.orlandini@unifi.it

Support Contact
Alessandro Pierno, Firenze University Press
alessandro.pierno@unifi.it

GUIDE FOR AUTHORS
1. Manuscript should refer to original researches, not yet published except in strictly preliminary form.
2. Articles of original researches findings are published in Italian Journal of Agrometeorology (IJAm), subsequent to critical review and approval by the Editorial Board. External referees could be engaged for particular topics.
3. Three types of paper can be submitted: original paper, review, technical note. Manuscript must be written in English. All pages and lines of the manuscript should be numbered.
4. First Name, Last Name, position, affiliation, mail address, telephone and fax number of all the Co-Authors are required. Corresponding Authors should be clearly identified.
5. The abstract should be no longer than 12 typed lines.
6. Full stop, not comma, must be used as decimal mark (e.g. 4.33 and not 4,33).
7. Figures, tables, graphs, photos and relative captions should be attached in separate files. All images must be vector or at least 300 effective ppi/dpi to ensure quality reproduction.
8. Captions should be written as: Fig. x – Caption title, Tab. x – Caption title. Images should be referred to in the text as (Fig. x), (Tab. x).
9. Proof of the paper (formatted according to the Journal style) will be sent to the Corresponding Author for proof reading just one time. Corrections can be made only to typographical errors.
10. All the references in the text must be reported in the "References" section and vice-versa. In the text, only the Author(s) last name must be present, without the name or the first letter of the name (e.g. "Rossi, 2003" and not "Federico Rossi, 2003" or "F. Rossi, 2003"). If two authors are present, refer to them as: "Bianchi and Rossi, 2003" in the text (do not use "&" between the surnames). If more than two Authors are present, refer to them as: "Bianchi et al., 2003" in the text.
For journals, references must be in the following form:
Bianchi R., Colombo B., Ferretti N., 2003. Title. Journal name, number: pages.
For books:
Bianchi R., Colombo B., Ferretti N., 2003. Book title. Publisher, publishing location, total number of pages pp.
Manuscripts "in press" can be cited.

BECOME A REVIEWER
Peer review is an integral part of the scholarly publishing process. By registering as a reviewer, you are supporting the academic community by providing constructive feedback on new research, helping to ensure both the quality and integrity of published work in your field. Once registered, you may be asked to undertake reviews of scholarly articles that match your research interests. Reviewers always have the option to decline an invitation to review and we take care not to overburden our reviewers with excessive requests.
You must login before you can become a reviewer.
If you don't want to be a reviewer anymore, you can change your roles by editing your profile.

COMPETING INTERESTS
You should not accept a review assignment if you have a potential competing interest, including the following:
- Prior or current collaborations with the author(s)
- You are a direct competitor
- You may have a known history of antipathy with the author(s)
- You might profit financially from the work

Please inform the editors or journal staff and recuse yourself if you feel that you are unable to offer an impartial review.
When submitting your review, you must indicate whether or not you have any competing interests.

Italian Journal of Agrometeorology

Rivista Italiana di Agrometeorologia

n. 1 – 2022

Table of contents